# Synthesis and Characterization of Polycations with Various Structural Features for Nucleic Acid Delivery

A DISSERTATION
SUBMITTED TO THE FACULTY OF
UNIVERSITY OF MINNESOTA
BY

Yaoying Wu

IN PARTIAL FULFILLMENT OF THE REQUIREMENTS
FOR THE DEGREE OF
DOCTOR OF PHILOSOPHY

Theresa M. Reineke, Advisor

July, 2014

**Acknowledgements**

It has been almost half a decade since I first stepped on the American soil. Over the years, so many people have provided me a great amount of help and support in many different ways, all of which makes my pursuit of PhD degree in United States possible. It would be impossible for me to thank all of them in the limited paragraph, but I would like to sincerely express my gratitude to a few individuals here, whom have been essential throughout my graduate school.

It was my advisor, professor Theresa Reineke, who accepted my application for joining her group, which allowed me to pursuit my research interest in biomaterials. She provided me and the group the opportunities and freedom to explore new research areas, and to acquire new knowledge. I really appreciate all the guidance and support that she gave me.

Dr. Adam Smith, who was my mentor for the first year of my graduate school, taught me a lot about research skills and life in graduate school. His generous advice guided me through my early days in Virginia Tech.

I would like to thank all my friends, from both Virginia Tech and University of Minnesota, for their help on daily basis. I am especially grateful to Dr. Ingle Nilesh, Dr. Kevin Anderson, Dr. Antons Sizvos, Dr. Sneha Kelkar, Dr. Ligeng Yin, Dr. Mallory Cortez, Dr. Tushar Navale, Dr. Bharat Wagh, Dr. William Shearouse, Dr. Lian Xue, Swapnil Tale, Dustin Sprouse. With this happy and ambitious group, I had a great time in graduate school.

I would like to extend my gratitude to Dr. Bob Hafner, who instructed me how to perform cryoTEM imaging. His effort and help was essential for my research.

Finally, I am most grateful to my family for their support and encouragement, especially my father Pengbo Wu, my mother Yuli Wang, and my wife, Lin Lin. My parents have been absolutely supportive to me every step along the way. To my wife, without her love, I would not be able to go through many dark times over the years. They have contributed greatly to all my achievements.

**Dedication**

To my father Wu, Pengbo, and my mother Wang, Yuli

## Abstract

Cationic polymers have been widely explored as non-viral nucleic acid delivery vectors for gene therapy, as they are able to complex with nucleic acids, protect genetic materials from degradation, and facilitate the internalization of transgene expression process. To understand how various structural elements impact the nucleic acid delivery, several classes of polycations were synthesized and examined for their in vitro transfection performance.

Reversible addition-fragmentation chain transfer (RAFT) polymerization was employed for the synthesis of several series of diblock glycopolycations with different carbohydrate containing blocks, including poly(2-deoxy-2-methacrylamido glucopyranose) (PMAG) and poly(methacrylamidotrehalose) (PMAT). Amine containing monomers were subsequently polymerized through chain extension to yield cationic blocks for nucleic acid binding, including N-[3-(N, N-dimethylamino) propyl] methacrylamide (DMAPMA), N-(2-aminoethyl) methacrylamide (AEMA), aminoethylmethacrylate (AEMT), *N*-methyl aminoethylmethacrylate (MAEMT), *N,N*-dimethyl aminoethylmethacrylate (DMAEMT), and *N,N,N*-trimethylammoniumethylmethacrylate (TMAEMT).

Initially, it was demonstrated that these polymers were all able to complex plasmid DNA into polyplex structures and prevent colloidal aggregation of polyplexes in physiological salt conditions. More importantly, glycopolymers with PMAT block can prevent polyplexes from aggregation, and exhibit the ability to protect polyplexes through the cycle of lyophilization and reconstitution.

The role of charge type, block length, and cell type on transfection efficiency and toxicity were studied for the *in vitro* transfection in both HeLa (human cervix adenocarcinoma) and HepG2 (human liver hepatocellular carcinoma) cells by comparing the polyplexes formulation created with PMAG-b-PAEMA and PMAG-b-PDMAPMA. The glycopolycation vehicles with primary amine blocks and PAEMA homopolymers revealed much higher transfection efficiency and lower toxicity when compared to analogs created with DMAPMA. Block length was also shown to influence cellular delivery and toxicity; as the block length of DMAPMA increased, polyplex toxicity increased while transfection decreased. While the charge block played a major role in delivery, the MAG block length did not affect these cellular parameters. Cell type played a major role in efficiency, these glycopolymers revealed higher cellular uptake and transfection efficiency in HepG2 cells than in HeLa cells, while homopolycations (PAEMA and PDMAPMA) lacking the MAG blocks exhibited the opposite trend signifying that the MAG block could aid in hepatocyte transfection.

Lastly, a new class of lipophilic polycations were designed, poly(alkylamidoamine) (PAAA) was synthesized to understand the role of lyophilicity in pDNA transfection. PAAAs with various length of lipophilic linker ($C_3$ to $C_6$) were synthesized via step-growth polymerization, and examined for their in-vitro transfection efficiency and cytotoxicity in multiple cell types, including HDFa (human dermal fibroblasts, adult) cells, HeLa (human cervix adenocarcinoma) cells, HMEC (human mammary epithelial cells), and HUVEC (human umbilical vein endothelial cells). The PAAA vehicles exhibited comparable or even superior transfection efficiency to Lipofectamine 2000, a leading lipid-based transfection reagent. It was revealed that, for

the PAAA polymers examined in this study, an increase in lipophilicity leads to higher cytotoxicity, but also raised the transfection efficiency in HeLa cells.

Overall, we demonstrated the great potential of carbohydrate containing polymer block, which has potential to serve as a targeting moiety, stealthy coating, and even lyo-protectant for polyplex formulations. Different amine types were examined for their nucleic acid delivery ability, and we conclude that tertiary amine containing monomer, DMAPMA, exhibits high toxicity along with low transfection efficiency while primary amine block shows relatively lower toxicity and higher transfection efficiency. Finally, the lipophilic polycations, PAAAs, were shown to be important for improving transfection efficiency in multiple cell types.

## Table of Contents

## List of Tables

## List of Figures

## List of Schemes

# Chapter 1 Literature Survey

This Chapter presents a brief introduction for gene therapy, including the mechanisms of several different types of techniques utilized in gene therapy. Various types of synthetic materials for gene delivery are explored in this chapter. Finally, the important obstacles for polymeric nucleic acid delivery systems are discussed.

## 1.1 Introduction

The double-helix molecular structure of DNA was discovered by Watson and Crick in 1953[1], and the concept of gene therapy was developed close to 40 years later and has been widely accepted as a therapeutic technique[2]. Since 1990, the Human Genome Project[3-4] has continued to unveil genetic detail for many acquired and inherited diseases, such as cancer, HIV, and hemophilia. With the help of this valuable information, it is increasingly possible to design specific drugs to introduce nucleic acids into human cells to prevent, halt, or reverse the pathological process at the genetic level.[5] Over the past two decades, gene therapy has overcome many obstacles and some skepticism, and developed significantly as a promising application for treating severe diseases such as cancer.[6] The progress of gene therapy has also lead to a number of breakthroughs in other areas including the potential of cell-based therapy.[7]

### 1.1.1 The Goals of Gene Therapy

Gene therapy is generally defined as "the introduction, using a vector, of nucleic acids into cells with the intention of altering gene expression to prevent, halt or reverse a pathological process."[5] There are several different methods to alter gene expression, including gene addition, gene correction/editing, and gene knockdown.

**Gene addition and gene correction/editing.** Gene addition is utilized to yield the expression of a therapeutic protein or provide the protein that is missing due to genetic mutation.[5] This method is currently the most commonly attempted method in preclinical and clinical studies.

Gene correction/editing has rapidly become a mainstream method used in biological research over the past few years. This technique generally is to alter genomic sequences at specific genomic targets by combining double stranded breaks (DSB) with homology-directed repair (HDR) or nonhomologous end-joining (NHEJ).[8-9] The crucial first step to induce DSB at the genomic locus to be modified can be achieved by several approaches, zinc finger nucleases (ZFNs),[8, 10] transcription activator-like effector nucleases (TALENs)[11-12] and clustered regulatory interspaced short palindromic repeat (CRISPR)/Cas system[9]. ZFNs are mainly composed of the cleavage domain at C-terminal mediated by FokI nuclease, the DNA binding zinc finger domain at the N-terminal, and the peptide linker that connects the binding domain with nuclease.[8] The binding specificity depends upon the zinc finger binding domain, where a short stretch of amino acid on the α-helix of each zinc finger motif could recognize three base pairs (bp). Linking multiple zinc finger motifs could minimize non-specific binding on nucleic acids.[13] However, it is not often possible to link various zinc fingers for target binding due to interfinger dependence. The activity of ZFN could be reduced by linking multiple zinc finger motifs.[14] Moreover, the specificity of ZFN is critically dependent upon the binding affinity of some zinc finger domain.[15] Like ZFN, TALENs use the FokI domain as a DNA cleavage module, but TALE proteins served as DNA binding domain. TALE proteins, naturally secreted by the plant pathogenic bacteria Xanthomonas, are composed of a series of 33–35-amino-acid repeat domains and each specifically recognizes a single base pair.[16] The specificity of TALE is conferred by the two repeat-variable diresidues (RVDs). The single base recognition nature of TALE proteins offers greater flexibility in

the design of specific binding DNA site than ZFN motifs. One of the main limitations of this technique is that the bulky size of TALENs hinders the broader application.[12, 17]

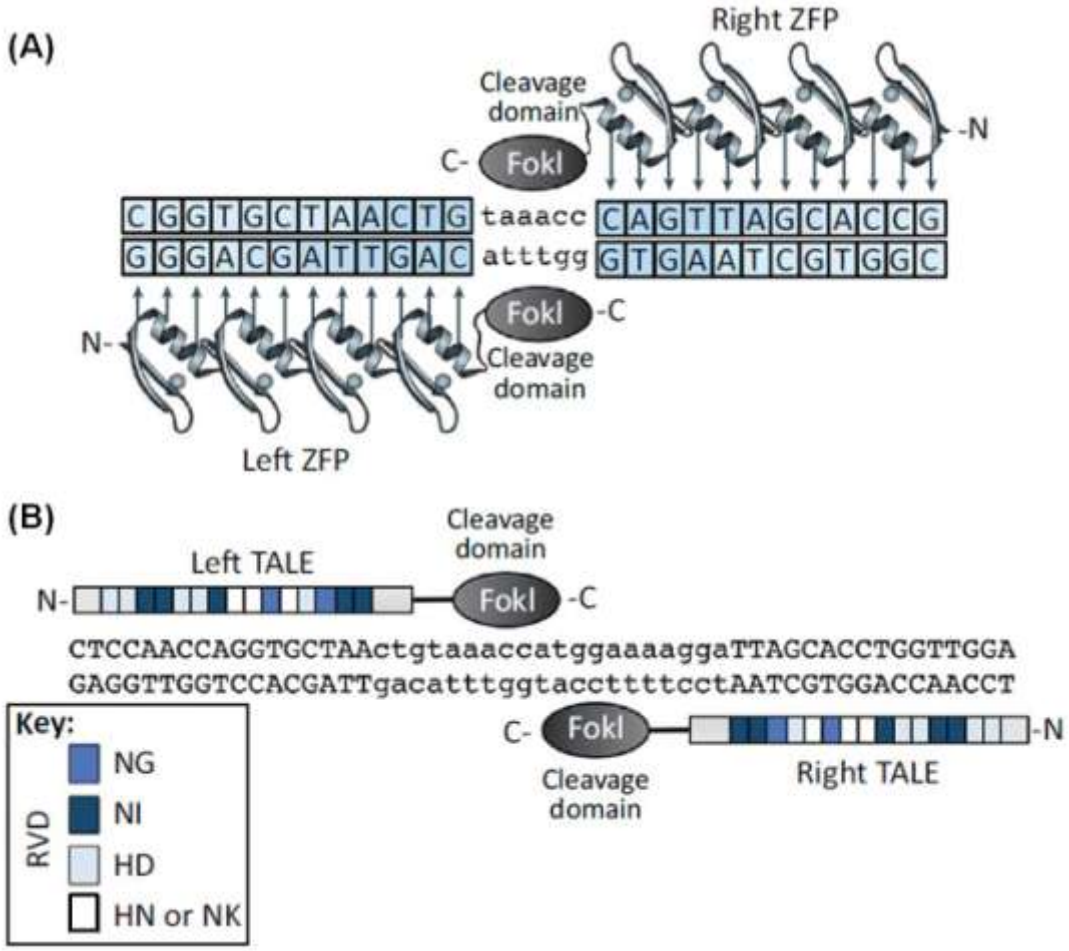


**Figure 1.1** Scheme of zinc-finger nucleases (ZFNs) and transcription activator-like effectors nucleases (TALENs). (Reproduced with permission from reference [Gaj, T.; Gersbach, C. A.; Barbas Iii, C. F. Trends Biotechnol. 2013, 31, 397-405.]. Copyright [2013] Elsevier)

Figure 1.1 (A) demonstrates that a ZFN dimer bound to DNA. ZFN target sites consist of two zinc-finger binding sites separated by a 5–7-bp spacer sequence recognized

by the FokI cleavage domain. Zinc-finger proteins can be designed to recognize unique 'left' and 'right' half-sites. Figure 1.1 (B) shows that a TALE nuclease (TALEN) dimer bound to DNA. TALEN target sites consist of two TALE binding sites separated by a spacer sequence of varying length (12–20 bp). TALEs can be designed to recognize unique left and right half-sites. RVD compositions are indicated.

Unlike ZFN and TALEN using protein-DNA interaction for targeting, recently emerged CRISPR/Cas system utilize RNA moiety to target desired DNA sequence.[9] This RNA-guided system was adapted from a viral immune mechanism.[18] The most widely explored CRISPR/Cas system requires two components to be introduced into cells or organism to realize gene editing, which are Cas9 nuclease and a guide RNA (gRNA) composed of a fusion of a CRISPR RNA (crRNA) and a transactivating CRISPR RNA (tracrRNA). After forming a complex with Cas9 nuclease, gRNA directs Cas9 to target DNA sites using base-paring rules between RNA and DNA, and induce DSB.[9] This technique has shown great promise recently, as it offers significant flexibility in DNA targeting and delivery strategies.[19-21] However, the requirement of protospacer adjacent motif (PAM) sequence upstream of the crRNAbinding region could limit some applications. Besides, the off-target effect and toxicity of this system still needs to be further evaluated.[17]

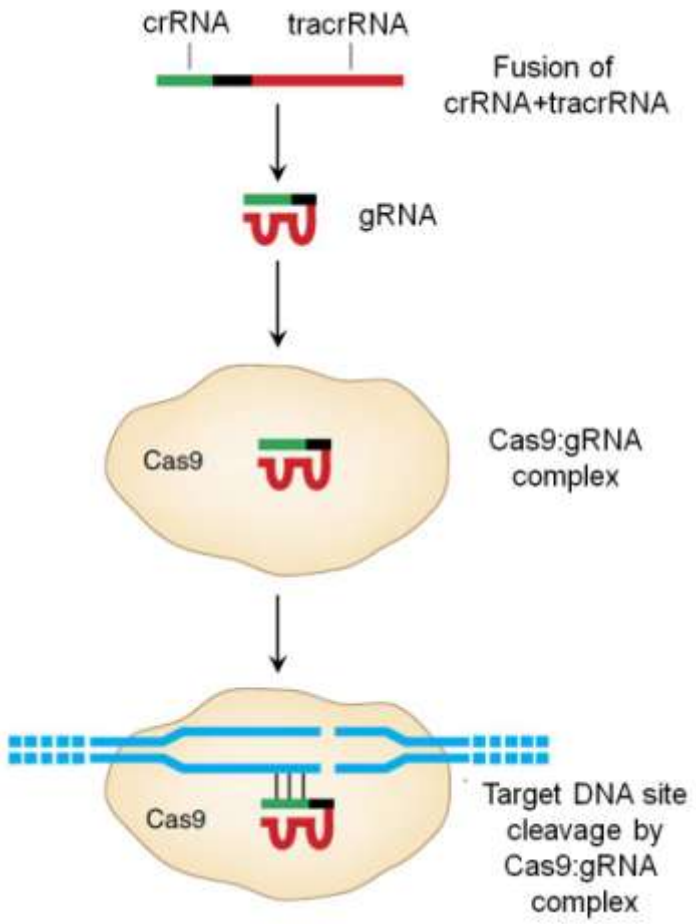


**Figure 1.2** Engineered CRISPR/Cas system. CRISPR/Cas system utilizes a fusion between a crRNA and part of the tracrRNA sequence. (Reproduced with permission from reference [Sander, J. D.; Joung, J. K. Nat Biotech 2014, 32, 347-355.]. Copyright [2014] Nature Publishing Group)

In the Figure 1.2, the single gRNA complexes with Cas9 protein to mediate cleavage of target DNA sites that are complementary to the 5' 20 nt of the gRNA and that lie next to PAM sequence.

**Gene knockdown/silencing.** The discovery of RNA interference (RNAi) has led to a new approach to eliminate a gene expression for therapeutic treatment.[22-23] RNAi is induced by short stretch double strand RNAs (dsRNAs) or short interfering RNAs (siRNAs) that are able to degrade the complementary messenger RNA (mRNA). The mechanism of gene silencing by siRNA is shown in Figure 1.3. In the cytoplasm, long dsRNAs are cleaved by ribonuclease Dicer into short dsRNA or siRNA duplex (19-30 nucleotides). The siRNA duplex is subsequently incorporated into multiprotein RNA-induced silencing complex (RISC). One of the siRNA strands will be released via the cleavage by Argonaute 2 (Ago-2) upon RISC activation, and the other strand (guide siRNA) will direct RISC to specifically bind to the target mRNA that will be subsequently cleaved by RISC.[24] The ability of the RNAi technique to specifically silence target genes has been utilized to treat various therapeutic targets, including viral infections, cancer treatment, etc., and about 22 RNAi-based drugs have been approved for clinical trials.[25] Moreover, several reports have demonstrated the RNAi response in early-phase clinical trials targeting to halt the expression of the M2 subunit of ribonucleotide reductase (RRM2),[26] and vascular endothelial growth factor (VEGF)[27]. Recent development in clinical trials has highlighted the great potential of RNAi therapeutics.

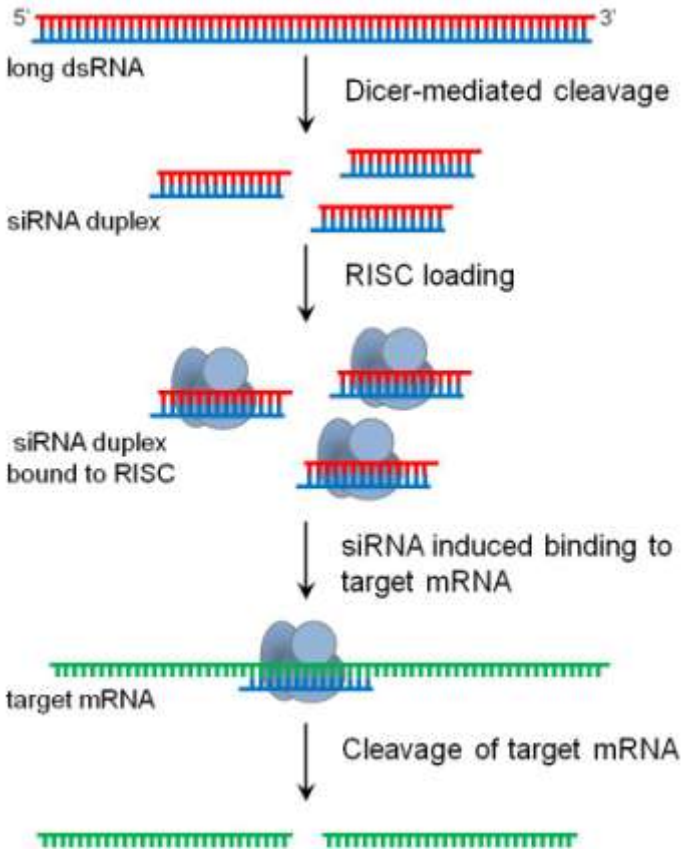


**Figure 1.3** siRNA-mediated gene silencing.

In the cytoplasm, long dsRNAs are cleaved by the endoribonuclease Dicer into short dsRNA duplexes or siRNA. siRNAs are loaded into and activate RISC, which contains Ago-2. Ago-2 cleaves and releases one strand, resulting in an activated form of RISC with a single-strand RNA molecule that directs the specificity of the target mRNA recognition through complementary base pairing. Ago-2 then cleaves the target mRNA, resulting in mRNA degradation and gene silencing.

## 1.2 Non-viral gene delivery

Vectors for gene delivery are usually required to protect genetic materials from enzymatic degradation, and also to facilitate the cellular internalization of the nucleic acid.[28] Initially, various types of genetically modified viruses were used as the vehicles in gene therapies, including retroviral vectors, adenoviral vectors, and adeno-associated viral vectors, owing to their natural ability to facilitate cellular uptake via endocytosis.[29-30] Moreover, viral carriers can directly unload genetic material into the cytoplasm or nucleus without being degraded in the endosomes. However, several fundamental problems of the viral carriers, such as inflammatory and immune responses caused by the viral genome and/or proteins, have hindered the development. Even though deleting viral genes may weaken the immune response, some beneficial attributes from some genes will be removed consequently.[31] Therefore, nonviral gene delivery vehicles based on synthetic materials, are designed currently to offer alternative delivery methods.

The synthetic delivery vectors must have several important features[31-32]: 1) compact the nucleic acids into small complexes to be taken up by cells; 2) prevent the enzymatic degradation of nucleic acids during transport in the cells; 3) avoid the immune response; 4) promote specific cell surface binding, endocytosis, and endosomal escape; 5) release the drug at the proper intracellular location with low toxicity. By well-tailored chemical synthesis, nonviral gene delivery vehicles, including dendrimers, lipids, and polymers, can achieve these positive properties, but potentially avoid the negative aspects of viral delivery vehicles. For many years, polymers have shown their ability to bind nucleic acids, forming polyplexes, through electrostatic interaction and hydrogen

bonding.[33] Polyplexes can be uptaken through endocytic routes and deliver genetic materials into cells. However, most of the polymeric vehicles have low transfection efficiency and/or high cytotoxicity.[34]

Cationic polymers can effectively compact DNA through the electrostatic interaction with polyanionic backbone of DNA.[35] The positive charges along backbone also make polymers highly soluble in water. Meanwhile, the delivery efficiency will be dramatically influenced by very subtle chemical or structural changes to the polymer including molecular weight[36], hydrophobicity[37], charge density[38], and charge type[39-40]. The size of the polyplexes will also be an influencing factor[6]. To achieve optimum therapeutic performance, many different kinds of polymers have been synthesized.

### 1.2.1 Polyethylenimine (PEI)

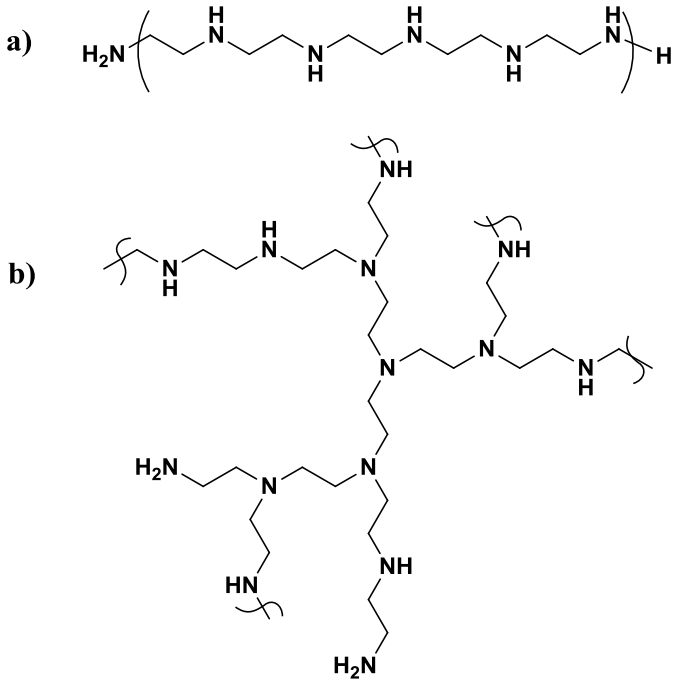


**Figure 1.4** General Structures of Polyethylenimine (PEI): a) linear PEI, a) branched PEI

Polyethylenimine is considered as one of the most efficient delivery vehicles. The first successful example was conducted by Behr et al. in 1995.[41] The structure of PEI could be branched or linear, dependent on the synthetic routes. Acid-catalyzed polymerization of aziridine produces branched structure (bPEI)[42], while hydrolysis after ring opening polymerization of 2-ethyl-2-oxazoline will create a linear structure (lPEI)[43]. Slightly different from the result of theoretical ratio for the branched structure, 1:2:1, experimental measurement proved that the ratio of primary/ secondary/ tertiary amines of commercially available PEIs are close to 1:1:1, indicating the higher degree of branches.[44] This highly branched structure gives PEI high density of amines, which are

easily protonated. Therefore, the charge density of PEI after protonation can vary proportional to the pH of biological environment. At a pH of 7.3, physiological pH, only about 20% of amines are protonated, while over half of amines are protonated at a pH of 5.[45] It has been widely accepted that this high buffering capacity helps PEI to escape from endosomes. This theory proposes that when PEI polyplexes are uptaken via endocytosis, the buffering capacity of PEI will introduce more water, protons, and chloride ions into the endosomal compartment, where the pH drops to 5.0, and finally causes vesicle swelling and rupture. Hence, the polyplexes will be released into cytoplasm.[46] The relationship between transfection efficiency, polymer molecular weight, and the degree of branching has been studied. It has been demonstrated that the transfection efficiency of PEI polyplexes increases with increasing molecular weight[36], while higher molecular weight also produces higher cytotoxicity[47]. The optimal molecular weight of PEI for transfection is reported between 5 and 25kDa.[48] The low molecular weight PEI can more effectively transfect cell lines if high PEI amine/DNA phosphate (N/P) ratios are used. As for the degree of branching of PEI, linear PEI is less effective than branched PEI in transfection if the molecular weights are similar. It has also been shown that the more primary amine PEIs have, the more stable the resulting polyplexes.[6] However, in vivo studies showed that linear structures are very effective despite their relatively poor capacity to form complexes.[49]

To lower toxicity, and increase serum stability of PEI, PEGylation is utilized to modify the structure of this polymer. By introducing a hydrophilic exterior to the polymeric backbone, the interaction of the polyplex with plasma proteins and

erythrocytes is reduced[6]. The length and density of PEG chains influences the transfection efficiency in vitro. For DNA delivery, PEI grafted with short (550 Da) PEG chains is most efficient.[50] For siRNA delivery, a low density of longer (5000 Da) PEG chains conjugated to PEI is preferred.[51] However, in vivo studies of PEI-g-PEG copolymers showed no gene expression with doses of 25μg pDNA in mice.[52] This outcome was due to the low surface charge of copolymers hindering intracellular trafficking of polyplexes and gene transfer after cellular uptake.[6]

As mentioned above, the cytotoxicity of PEI increases with its molecular weight. There are two mechanisms involved in its toxicity. The first is that free PEI can destabilize the cellular membrane and kill cells before cellular internalization. The second is that after releasing DNA, free PEI inside the cell causes cellular stress responses.[53] The first one can be minimized by controlling the N/P ratio and surface change. Modifications of PEI structure are necessary to eliminate the latter process. Biodegradable PEI analogues are also promising, and can be synthesized by incorporating reducible disulfide linkages[54] or acid-labile ester linkages[55].

### 1.2.2 Chitosan

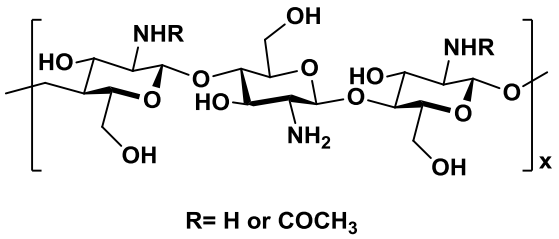


**Figure 1.5** Chemical Structure of Chitosan

Chitosan derived from chitin is a biodegradable, biocompatible material. Along with its cationic potential, chitosan has been accepted one of the most important nonviral delivery vehicles. Chitosan is synthesized through deacetylation of chitin to form a polymer linked by β(1,4) glycosidic bonds. Since chitosan was used as nonviral vector in 1990s[56], researchers have proven that the molecular weight of chitosan plays an important role in its therapeutic performance. Generally, the higher the molecular weight of chitosan, the more stable the resulting polyplex.[57] Longer polymer chains of chitosan can entangle free DNA more effectively after the initial electrostatic interaction. However, it does not mean that the polyplex with the highest molecular weight polymer will transfect the cell most effectively, because DNA is possibly entrapped too tight to be released into cell. The degree of deacetylation will also influence the transfection efficiency of the resulting polyplex. In vitro studies, transfection efficiency is improved as deacetylation increases, resulting from higher charge density and therefore higher stability of the polyplex.[57] However, balance between stability of polyplex and easy release of DNA is a key in vivo, where chitosan with a moderate degree of deacetylation often performs best. Besides, chitosan polyplexes have their highest transfection

efficiency between pH 6.8 and 7.0.[58] If pH is higher than 7.5, DNA will be dissociated from the polyplexes hindering cellular uptake, reducing transfection efficiency in turn. If the pH is lower than 6.5, transfection efficiency will be low due to hindered escape from the endosome. In addition, the transfection efficiency of chitosan polyplexes varies from different cell types used.

In order to enhance chitosan polyplexes' performance, all kinds of structural modifications have been developed. N-quaternization of chitosan terminal amines is utilized to improve chitosan's transfection efficiency, and the resulting increased cytotoxicity is reduced by introducing PEG chains into polymeric structures.[59] Polyethylenimine has been conjugated with chitosan to achieve higher buffering capacity of chitosan polyplex. The resulting derivatives have lower cytotoxicity but the same buffering capacity, compared with PEI.[60] Hydrophobic moieties are also conjugated with chitosan to diminish the aggregation of chitosan polyplexes. The highest transfection efficiency was found for 40kDa deoxycholic acid-chitosan complexes.[61] Further improvements have been achieved by synthesis of chitosan with reducible disulfide linkage[54, 62], design of cross-linked chitosan derivatives,[54] conjugation with various cell-targeting groups.

### 1.2.3 β-Cyclodextrin(β-CD)

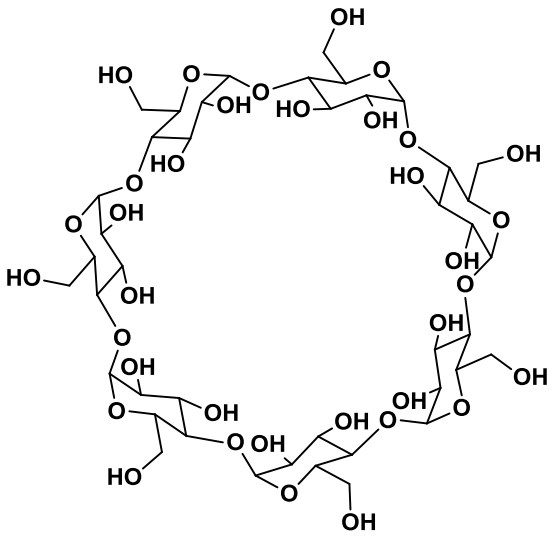

**Figure 1.6** Chemical Structure of β-Cyclodextrin

The β-cyclodextrins can be utilized to overcome the cytotoxicity of nonviral vectors due to its biocompatibility. Linear β-cyclodextrin-based polymers can be obtained through the polymerization of bifunctional β-cyclodextrin monomers with the other cationic bifunctional comonomers.[6] At N/P ratios above 10, the cyclodextrin-based polymers have lower cytotoxicity but similar transfection efficiency compared with PEI. The compounds with n ranging from 4 to 10 have lowest cytotoxicity. But the transfection efficiency will be reduced as well when the alkyl chain is too long, such as 10 methylene units, because the solubility will decrease.[63] It is also noticed that cytotoxicity will increases if the cationic structure is moved further from cyclodextrin[39-40]. Moreover, the mechanism of the endosomal release of cyclodextrin is not always related to buffering capacity.[64] To improve the transfection efficiency in vivo, PEGylation has been utilized to reduce the aggregation of the polyplex.[65]

### 1.2.4 Linear Poly(amido-amine) (PAA)

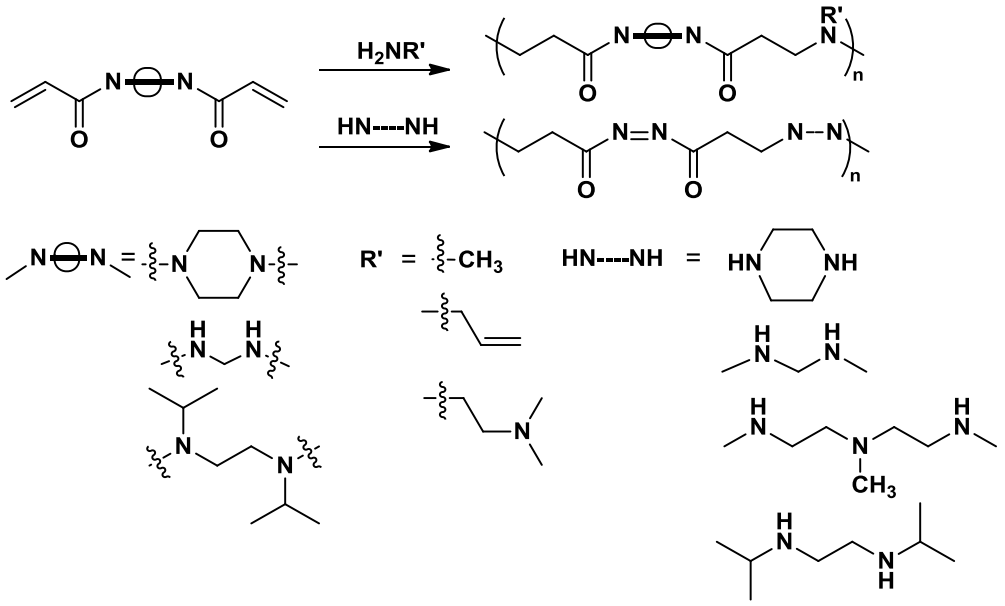


**Scheme 1.1** General synthesis of linear poly(amido-amines) (Reproduced with permission from reference [Mintzer, M. A.; Simanek, E. E. Chem. Rev. 2009, 109, 259-302.]. Copyright [2009] American Chemical Society)

Cationic and amphoteric linear poly(amido-amines) (PAA) are another type of gene delivery vehicle. Hydrogen-transfer polyaddition is utilized to synthesize PAA with amido- and tertiary amino groups. Protonation will reduce the conformational freedom of PAA chains, and hence cause rigid backbone structures, because of the hydrogen binding with carbonyl groups and electrostatic repulsion. This change in conformation of PAA was found to cause hemolytic activity. [66]

The overall negative charge of the amphoteric PAA lowers the in vitro cytotoxicity, and even increases the circulation time of the polyplex in vivo. Hence, PAA polyplexes were mainly accumulated in tumor cells due to the enhanced permeation and

retention (EPR) effect. Gene transfection studies show that amphoteric PAA, Lipofectin, and 70kDa PEI have comparable efficiency, but PAA has low hemolytic activity and cytotoxicity.[67] Many other structural modifications have been explored, including PAA structures with disulfide linkages to improve biodegradability[6].

### 1.2.5 Poly(glycoamidoamine) (PGAA)

Poly(glycoamidoamine)s are a novel library of polymeric gene delivery vehicles designed in our group. As mentioned above, PEI generally has high transfection efficiency but also high cytotoxicity, and chitosan has relatively low transfection efficiency but low cytotoxicity. To combine the advantages of PEI and chitosan, we have designed polymeric delivery vehicles through the step-growth polymerization of carbohydrates and oligoamines. Poly(galactaramidoamine)s (G1-G4), poly(D-glucaramidoamine)s (D1-D4), poly(D-mannaramidoamine)s (M1-M4) and poly(L-tartaramidoamine)s (T1-T4) have been synthesized separately by copolymerization of a mixture of dimethyl meso-galactarate(G), dimethyl D-glucarate(D), D-mannaro-1,4:6,3-dilactone(M), or dimethyl L-tartarate(T) with diethylenetriamine (1), triethylenetetramine (2), tetraethylenepentamine (3), or pentaethylenehexamine (4).[68-69] Previous research showed that these carbohydrate ester and lactone monomers are very reactive towards primary amines. Electron-withdrawing hydroxyl groups adjacent to carbonyl group facilitate the nucleic attack on carbonyls, and protic solvents also accelerate this kind of reaction. Hence, the reaction conditions for this polymerization are mild and catalyst-free.[70-73]

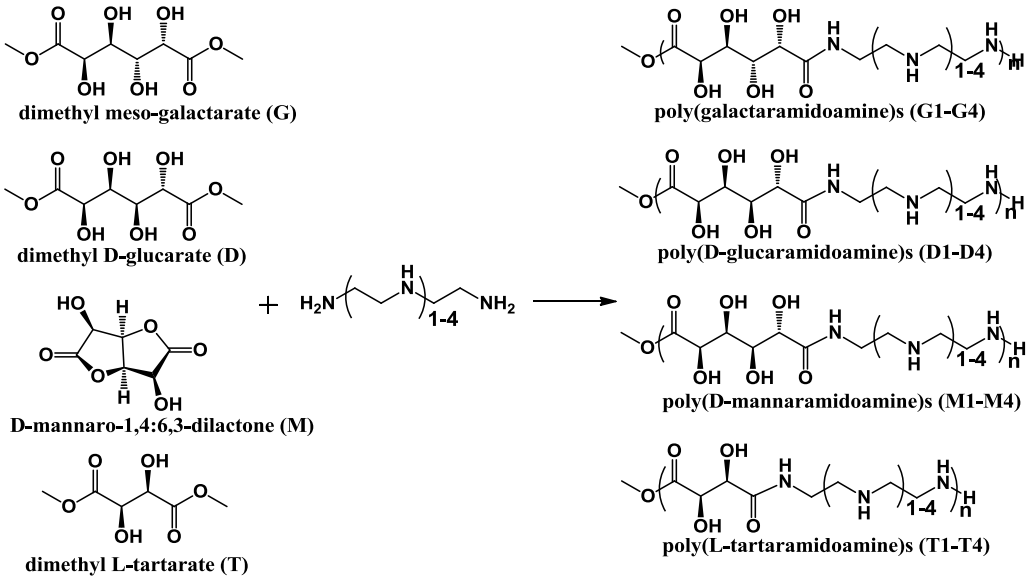


**Scheme 1.2** Synthetic schemes for poly(glycoamidoamine) (PGAA)[68, 74]

Gel electrophoresis studies showed that all the above polymers completely bind with DNA at N/P ratio of about 2. N/P ratio required for binding decreases with the increased number of secondary amines in the PGAA, indicating that secondary amines along the backbone will stabilize the polymer-pDNA complex.[68] The linkage between secondary amine repeat units is much shorter for T4 polymers, so they can bind with pDNA at even lower N/P ratio.[32] The stereochemistry of the hydroxyl groups along the polymeric backbone also plays an important role in binding pDNA. D1 and M1 polymers both will not bind pDNA completely until N/P ratio reaches 5, while typical N/P ratio of binding for G1 is 2. Normally, the strong binding between polymers and pDNA will protect the nucleic acid from degradation, but could hinder the release of pDNA. However, these PGAAs can degrade and release the nucleic acid in cells despite strong binding to pDNA. The hydroxyls along the polymer backbones may facilitate the

degradation through electron-withdrawing effect and hydrogen bonding.[75] In cell culture, PGAA polyplexes showed low cytotoxicity, generally over 80% cell viability. It has been noticed that higher density of secondary amines often leads to higher transfection efficiency, possibly due to enhanced buffering capacity. However, the buffering capacity of the polyplex is not the only factor influencing gene delivery, stereochemistry of the hydroxyl group of repeating units also affect delivery efficiency.[74] In our case, G4 polymers have higher transfection efficiency than D4 and M4 in HeLa cells.[68]

These PGAA polymers synthesized as described above are not completely linear, and they have some degree of branching. Branched PGAAs are found to have a lower toxicity profile and lower gene expression, possibly due to the lower secondary amine density in branched structure.[68] Moreover, it was hypothesized that the degradability of the PGAA polymeric vehicles can help release pDNA and increase the transfection efficiency. PGAA polymers degrade faster at physiological pH than under more acidic conditions. The hydroxyl groups of the PGAA were shown to facilitate the degradation process. PGAA polyplexes could interact with the cell surface glycosaminoglycans, and are internalized via endocytosis.[68, 74] The pathway inhibition experiments revealed that the endocytosis of PGAA polyplexes was mainly through caveolae mediated pathway, while clathrin mediated pathway and macropinocytosis exhibited relatively less impact on the internalization.[76-77] Moreover, it was hypothesized that G4 polymers promote active transport pathway leading to the entry of nucleus, possibly trafficked through the Golgi and endothelial reticulum (ER) according to the confocal microscopy imaging.[78] It was demonstrated that the potential mechanism of cytotoxicity of PGAA was related to

plasma membrane permeabilization in the early stage, and the nuclear membrane permeabilization contributed to the toxic effect after 4 h transfection.[79]

Trehalose is a carbohydrate utilized to develop a related library of PGAA structures. Trehalose conjugated with azides was reacted with dialkynyl oligoethylene amine monomers. The resulting click copolymers have been termed as Tr# (Tr means trehalose, # represents the number of ethylene amines). Trehalose moieties were introduced to prevent the polyplex from aggregating in serum media. Tr3 polyplexes and Tr4 polyplexes are found to be relatively stable in serum, even though Tr1 polyplexes and Tr2 polyplexes aggregate. The explanation is possibly that Tr1 and Tr2 are more protonated than the other two kinds of polymers, so that the electrostatic interaction with pDNA causes aggregation.[33] β-cyclodextrin has also been incorporated into similar polymer structures (CD#, CD means cyclodextrin, # represents the number of ethylene amines) via click reaction.[80] In general, both trehalose and cyclodextrin polymers exhibited low cytotoxicity, and high transfection efficiency.[81] Additionally, the comparison between Tr4 and CD4 polymers with similar degree of polymerization (DP) revealed that Tr4 polymers have higher transfection efficiency for pDNA delivery, while CD4 polymers exhibited higher siRNA delivery efficiency.[82]

### 1.2.6 Polymethacrylate/polymethacrylamide

Various types of cationic polymers have been synthesized from methacrylate or methacrylamide based monomers for gene delivery via radical polymerization. The structures of these monomers are shown in Scheme 3. The initial attempt to synthesize

polymethacrylate polymers, poly(2-(dimethylamino)ethyl methacrylate) (PDMAEMT) for pDNA delivery was performed using radical polymerization initiated by ammonium peroxydisulphate.[83-84] It was demonstrated that PDMAEMT was able to introduce pDNA into cells for expression, and the transfection efficiency of PDMAEMT/pDNA could be improved by using higher polymer/plasmid ratio (20/1, w/w).[84] The molecular weight impact was also observed in this initial pDNA delivery system, which is PDMAEMT with higher molecular weights exhibiting higher transfection efficiency.[84] Van de Wetering et al. have also studied the interaction between pDNA and polymethacrylates and hypothesized that the relative high transfection ability associated with PDMAEMT polymers was related to the buffering capability at physiological pH resulting in the release from endosome.[85] However, the in vivo transfection efficiency of PDMAEMT was shown to be rather negligible, due to the negative effect of some components of the ascites fluid, hyaluornic acid for instance, according to the authors.[86] As the polymerization technique advanced, a number of the methacrylate and methacrylamide based monomers were polymerized via reversible-deactivation radical polymerization (RDRP) techniques[87], including atom transfer radical polymerization (ATRP)[88-89] and reversible addition-fragmentation chain transfer (RAFT) polymerization[90-91]. RDRP provides several advantages in biomaterial design, such as controlled molecular weight growth and polymeric architecture, high compatibility with aqueous polymerization solution, and tolerance to monomers with various functionalities. The synthesis of cationic methacrylamide polymers in aqueous solution has been well established by several groups including ours over the past decade.[92-102] Vasilieva et al. first published

the polymerization of 3-(dimethyamino)propyl methacrylamide (DMAPMA) via aqueous RAFT polymerization to yield cationic polymers.[92] The PDMAPMA block copolymers with folic acid moieties were capable to complex and deliver siRNA relatively efficiently.[93, 95] 2-(dimethylamine)ethyl methacrylate (DMAEMT) were also copolymerized with propylacrylic acid (PAA) via RAFT to yield pH-responsive block copolymers for siRNA delivery.[103-104] The pH-responsive block composed of DMAEMT and PAA (in equal molar ratio) were designed to mediate endosomal release, and facilitate the siRNA delivery into cytosol.[103] As compared to tertiary amine containing monomer, the polymerization of 2-aminoethyl methacrylate (AEMT) often required protected group for primary amine mainly due to the hydrolysis side reactions.[100, 105-107] Smith et al. reported the RAFT polymerization of 2-aminoethyl methacrylamide (AEMA) to yield block copolymers with a glucose amine-containing block and demonstrated that the obtained cationic copolymers were able to form polyplexes with pDNA that is stable even in serum containing medium, and to deliver pDNA for expression.[99] The polyplexes composed of PAEMA copolymers with trehalose containing block have also exhibited excellent siRNA delivery ability even after going through lyophilization.[101] To further understand the impact of amine type on pDNA delivery for methacrylate based polymers, Li et al. prepared a series of cationic block glycopolymers with primary, secondary, tertiary, and quaternary amines and systematically studied the transfection efficiency, cytotoxicity profiles. It was demonstrated that secondary amine bearing polymers, poly[2-(N-methylamino)ethyl methacrylate (MAEMT)], had relatively high transfection

efficiencies compared with other analogues even when transfected in serum containing medium.[100]

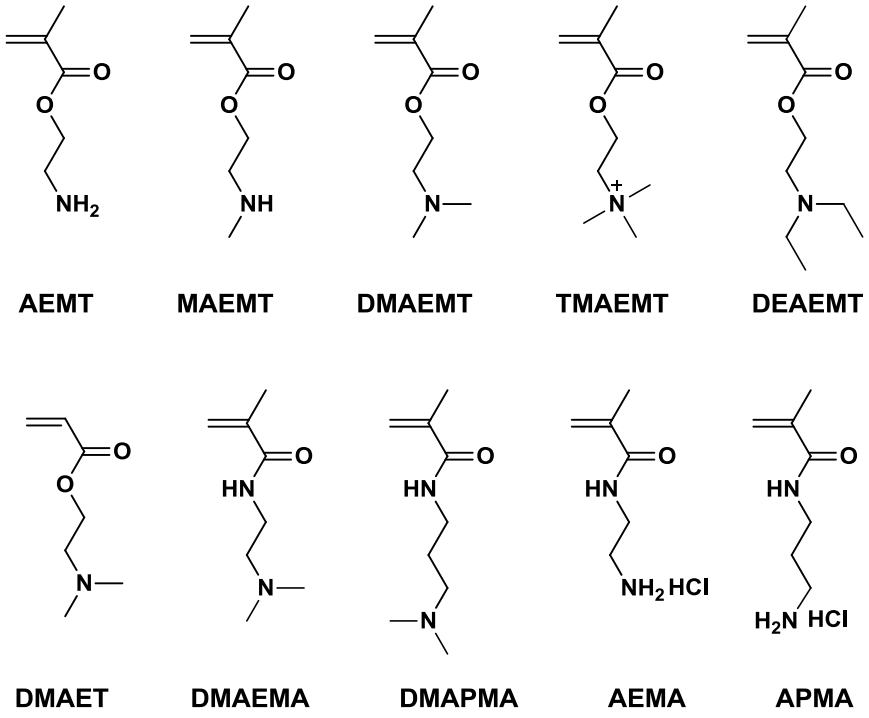


Scheme 1.3 Structures of acrylate or acrylamide based monomers explored for gene delivery

Scheme 1.3 shows the structures of 2-aminoethyl methacrylate (AEMT), 2-(N-methylamino)ethyl methacrylate (MAEMT), 2-(N,N-Dimethylamino)ethyl methacrylate (DMAEMT), 2-(N,N,N-trimethylammonium)ethyl methacrylate (DMAEMT), 2-(N,N-Diethylamino)ethyl methacrylate (DEAEMT), 2-(N,N-Dimethylamino)ethyl acrylate (DMAET), 2-(N,N-Dimethylamino)ethyl methacrylamide (DMAEMA), 2-(N,N-Dimethylamino)propyl methacrylamide (DMAPMA), 2-aminoethyl methacrylamide (AEMA), 3-aminopropyl methacrylamide (APMA)

## 1.3 The barriers to gene delivery with synthetic vehicles

There are a number of potential obstacles that must be overcome for nonviral vectors to achieve successful nucleic acid delivery. Compared with viral vectors, synthetic vectors are still being challenged by one or several of extracellular or intracellular barriers.

### 1.3.1 Packaging of nucleic acid

Cationic polymers could bind to nucleic acids, and form compact nanoparticles spontaneously upon mixing, through electrostatic interactions between the positive charges on the polymers and the negative charges on phosphates along the nucleic acid backbone. This condensation is a entropically driven process.[108] The polyplexes could protect nucleic acid from enzymatic degradation mainly by sterical hindrance. The morphology of the resulting polyplexes were previously observed to be toroidal or spherical structure using atom force microscopy (AFM) and regular transmission electron microscopy (TEM).[99, 109] The size of the polyplexes typically range from about 50 to several hundred nanometers.[110-111] Much research effort has been devoted into understanding the polyplex formation, and the structure of the polycation was shown to greatly affect the formation of polyplexes.[112-114] Prevette and coworkers revealed that polyplex formation process between PGAA polymers and pDNA was not only caused by electrostatic interaction but also facilitated by the hydrogen binding between pDNA and hydroxyl groups on PGAAs according to isothermal titration calorimetry (ITC) and infrared spectroscopy.[112] Ziebarth et al. simulated how the structure of polycations impact

the polyplexes formation, and demonstrated that polyplexes composed of block copolymers could possess "core-corona" structures.[113-114] It should be noted that strong binding ability of polycation may not necessarily result in efficient nucleic acid transfection.[110] Binding to genetic materials should be sufficient for protection and delivery, but binding too strongly could also result in relatively poor transfection efficiency.[99]

### 1.3.2 Prolonged circulation of polyplexes

Upon systemic administration, the polyplexes can form large aggregates under physiological salt conditions, partly due to the absorption of serum albumin and other negatively charged protein. Consequently, the reticuloendoethelial system (RES) can rapidly remove these foreign particles from blood.[115] This significantly reduces the efficacy of polyplexes delivery, especially hampers the delivery to the site of solid tumor through enhanced permeability and retention (EPR) effect. [116]

Many studies demonstrated that modification of polycations with neutral hydrophilic polymers, such as poly(ethylene glycol) (PEG) could improve the serum stability of polyplexes, and thus prolong its blood circulation time.[115, 117-120] PEG polymers could form a flexible shield on the surface of polyplexes, and prevent particles from interacting with each other and/or protein via steric hindrance, which would be affected by the PEG chain molecular weight and density on the surface.[121] Even though optimal PEGylation density varies from systems, it was demonstrated that relatively low PEG density on the surface would lead to "mushroom-like" structure formation,

maximizing surface coverage, while increased density could result in a "brush-like" structure.[115] However, PEGylation could not only prolong the circulation of polyplexes, but also sterically interfere with the interaction between cells and polyplexes and the endosomal escape process.[122] Additionally, Ishida et al. reported that repeated injection of PEG containing system could elicit antibody production and accelerated blood clearance of the nanoparticles.[123]

Various polymeric structures have been explored as an alternative to protect the polyplexes, including poly (N-(2-hydroxypropyl) methacrylamide) (PHPMA)[124], zwitterionic polymers[97, 125-126], and glycopolymers[99-102, 127]. Like PEG, glycopolymers can protect polyplexes from aggregation and degradation, along with some other advantages, such as abundant function group useful for further modification. Moreover, certain glycopolymers were found to provide unique features for polyplex systems.[101-102, 128] Sizovs et al. reported that block glycopolymers synthesized from AEMA and trehalose based monomers could complex with siRNA and form polyplexes with excellent serum stability. Additionally, this particular glycopolymer vehicle was shown to protect the siRNA polyplexes through lyophilization, while the polyplexes composed of PEG analogues lost its activity after reconstitution from dry state.[101] It has also been demonstrated that glycopolymers can enhance the interaction between cells and polyplexes through the "glycocluster effect", which binding between multiple saccharide moieties on polymer backbones and cellular membrane receptors.[102, 129]

### 1.3.3 Targeting delivery

The treatment strategy of gene therapy to treat certain disease, such as cancer, often requires cargo to be delivered to specific site or organ to eliminate target cells. Besides taking advantage of EPR effect,[116] polymeric vectors often lack of the ability to target specific cells. However, targeting moieties can be chemically conjugated with polymeric delivery systems, thus enhancing specific cell uptake mechanism. Folic acid has been widely explored and incorporated into polymeric delivery systems as targeting moiety for nucleic acid and drug delivery for cancer treatment because of the significant up-regulation of the folate receptor on tumor cells.[130-131] Asialoglycoprotein receptors (ASGPR) on hepatocellular membranes are also utilized for nucleic acid delivery as they are able to mediate the endocytosis of hepatocyte.[132-133] Other proteins, including antibodies or antibody fragments, transferrin and epidermal growth factor (EGF), can also provide targeting function for synthetic vectors to enhance the internalization or the accumulation of the polyplexes at specific sites.[134-135]

### 1.3.4 Intracellular trafficking

After being internalized into cells, the polyplexes need to overcome a series of intracellular obstacles. There are several different pathways that polyplexes could be trafficked intracellularly. Many studies have concentrated on two major routes, a clathrin-mediated pathway and a caveolae-mediated pathway.[76, 136-138] (Figure 4) During clathrin-mediated endocytosis, polyplexes will be transported into endosome after loaded into clathrin-coated pits from cell surface, subsequently trafficked into late endosome, and

then lysosomes, the acidic compartment that contain degradative enzymes.[139] In late endosomes, ATPase "proton-pump" enzymes on vesicle membranes help accumulate protons to acidify the vesicles (pH 5-6).[140] It is believed that nucleic acids should escape from endosomes, otherwise it will likely be trapped in the lysosomes and degraded. One hypothesized escape mechanism for polyplexes is that after being trafficked into late endosome, polymers with a number of amines, like PEI, could prevent the vesicles from being acidified through the protonation of amine groups, which forces the ATPase to transport more protons to reach desired pH. The influx of proton and counter ions leads to the rise of osmotic pressure, and ultimately the rupture of vesicles, thus the endosomal content would be released into cytosol.[141]

Although some research groups have achieved certain degree of success in design of polymeric vectors following the aforementioned hypothesis,[103] this mechanism still is being challenged and further studied. Recently, caveolae-mediated endocytosis is proposed to be a favorable pathway for gene delivery.[136] Rejman and coworks investigated both the clathrin-mediated endocytosis and the caveolae-mediated endocytosis for the gene delivery using PEI, and concluded that the latter is more transfection efficient pathway.[137] Fichter et al. also proposed that, instead of being released into cytosol with little or no active transport to nucleus, polyplexes should be trafficked to organelles such as Golgi and endoplasmic reticulum (ER) through caveolae-mediated pathway, which could lead to the entry of nucleus for pDNA.[78]

To enhance the transfection of pDNA, the nuclear localization signals (NLS), short cationic peptide sequences, have been utilized by several groups.[135, 142-143] The NLS

can be recognized by importins, and utilized by many natural proteins to be translocated into nucleus. It is likely that polyplexes conjugated with NLS could take advantage of similar mechanism to enter nucleus, hence enhanced the gene delivery efficiency.[110]

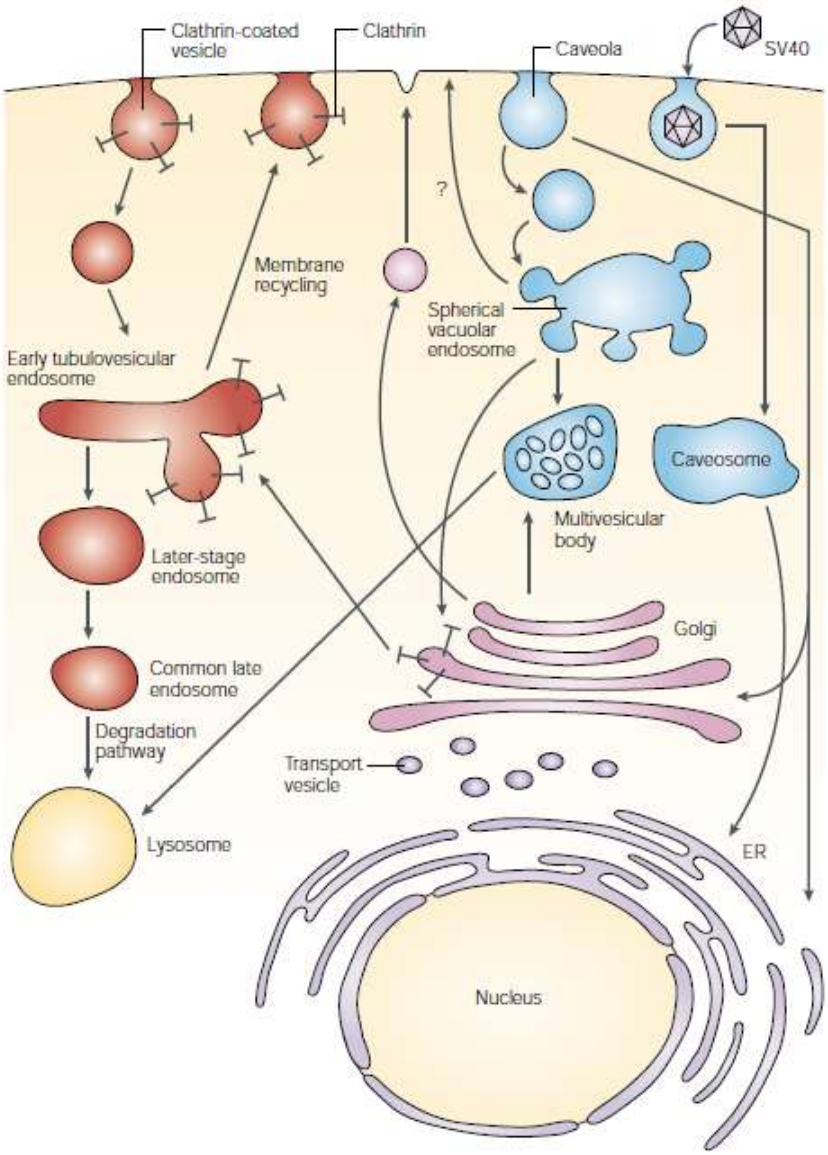


**Figure 1.7** Clathrin-mediated and caveolae-mediated pathway. (Reproduced with permission from reference [Carver, L. A.; Schnitzer, J. E. Nat Rev Cancer 2003, 3, 571-581.]. Copyright [2003] Nature Publishing Group)

In Figure 1.7, after budding from the cellular membrane, clathrin-coated pits are transported to early endosome. Some cargo and proteins would be sent back to cell surface, i.e., exocytosis. Some content would be delivered into late endosome and lysosome for degradation. Alternatively, caveolin-coated vesicles could also internalize foreign content from cell surface, subsequently be delivered to endosomal-like spherical vacuolar compartment. There are pathways available for content to be transported to endosome or lysosome for degradation. Additionally, the cargo could be delivered into endoplasmic reticulum (ER) through Golgi. It is also possible that cargo be directly transported to Golgi or ER though caveolae-mediated endocytosis. Some viruses such as SV40 could enter cells by taking advantage of caveolae.

## 1.4 Reference

1. Watson, J. D.; Crick, F. H. C. *Nature* **1953,** *171*, 737-738.

2. Friedmann, T. *Nat. Genet.* **1992,** *2*, 93-8.

3. Sachidanandam, R.; Weissman, D.; Schmidt, S. C.; Kakoi, J. M.; Stein, L. D.; Marth, G.; Sherry, S.; Mullikin, J. C.; Mortimore, B. J.; Willey, D. L.; Hunt, S. E.; Cole, C. G.; Coggill, P. C.; Rice, C. M.; Ning, Z.; Rogers, J.; Bentley, D. R.; Kwok, P.-Y.; Mardis, E. R.; Yeh, R. T.; Schutlz, B.; Cook, L.; Davenport, R.; Dante, M.; Fulton, L.; Hillier, L.; Waterston, R. H.; McPherson, J. D.; Gilman, B.; Schaffner, S.; Van, E. W. J.; Reich, D.; Higgins, J.; Daly, M. J.; Blumenstiel, B.; Baldwin, J.; Stange-Thomann, N.; Zody, M. C.; Linton, L.; Lander, E. S.; Altshuler, D. *Nature* **2001,** *409*, 928-933.

4. Watson, J. D.; Cook-Deegan, R. M. *FASEB J.* **1991,** *5*, 8-11.

5. Kay, M. A. *Nat. Rev. Genet.* **2011,** *12*, 316-328.

6. Mintzer, M. A.; Simanek, E. E. *Chem. Rev.* **2009,** *109*, 259-302.

7. Naldini, L. *Nat Rev Genet* **2011,** *12*, 301-315.

8. Chou, S.-T.; Leng, Q.; Mixson, A. J. *Drugs Future* **2012,** *37*, 183-196.

9. Sander, J. D.; Joung, J. K. *Nat Biotech* **2014,** *32*, 347-355.

10. Urnov, F. D.; Rebar, E. J.; Holmes, M. C.; Zhang, H. S.; Gregory, P. D. *Nat Rev Genet* **2010,** *11*, 636-646.

11. Mussolino, C.; Cathomen, T. *Curr. Opin. Biotechnol.* **2012,** *23*, 644-650.

12. Sun, N.; Zhao, H. *Biotechnol. Bioeng.* **2013,** *110*, 1811-1821.

13. Pattanayak, V.; Ramirez, C. L.; Joung, J. K.; Liu, D. R. *Nat Meth* **2011,** *8*, 765-770.

14. Shimizu, Y.; Şöllü, C.; Meckler, J. F.; Adriaenssens, A.; Zykovich, A.; Cathomen, T.; Segal, D. J. *Biochemistry* **2011,** *50*, 5033-5041.

15. Guo, J.; Gaj, T.; Barbas Iii, C. F. *J. Mol. Biol.* **2010,** *400*, 96-107.

16. Deng, D.; Yan, C.; Pan, X.; Mahfouz, M.; Wang, J.; Zhu, J.-K.; Shi, Y.; Yan, N. *Science* **2012,** *335*, 720-723.

17. Gaj, T.; Gersbach, C. A.; Barbas Iii, C. F. *Trends Biotechnol.* **2013,** *31*, 397-405.

18. Jinek, M.; Chylinski, K.; Fonfara, I.; Hauer, M.; Doudna, J. A.; Charpentier, E. *Science* **2012,** *337*, 816-821.

19. Mali, P.; Yang, L.; Esvelt, K. M.; Aach, J.; Guell, M.; DiCarlo, J. E.; Norville, J. E.; Church, G. M. *Science* **2013,** *339*, 823-826.

20. Cong, L.; Ran, F. A.; Cox, D.; Lin, S.; Barretto, R.; Habib, N.; Hsu, P. D.; Wu, X.; Jiang, W.; Marraffini, L. A.; Zhang, F. *Science* **2013,** *339*, 819-823.

21. Ran, F. A.; Hsu, P. D.; Lin, C.-Y.; Gootenberg, J. S.; Konermann, S.; Trevino, A. E.; Scott, D. A.; Inoue, A.; Matoba, S.; Zhang, Y.; Zhang, F. *Cell* **2013,** *154*, 1380-1389.

22. Fire, A.; Xu, S.; Montgomery, M. K.; Kostas, S. A.; Driver, S. E.; Mello, C. C. *Nature* **1998,** *391*, 806-811.

23. Wang, J.; Lu, Z.; Wientjes, M. G.; Au, J. L. S. *AAPS J.* **2010,** *12*, 492-503.

24. Tang, G. *Trends Biochem. Sci.* **2005,** *30*, 106-114.

25. Wu, S. Y.; Lopez-Berestein, G.; Calin, G. A.; Sood, A. K. *Sci Transl Med* **2014,** *6*, 240ps7.

26. Davis, M. E.; Zuckerman, J. E.; Choi, C. H. J.; Seligson, D.; Tolcher, A.; Alabi, C. A.; Yen, Y.; Heidel, J. D.; Ribas, A. *Nature* **2010,** *464*, 1067-1070.

27. Tabernero, J.; Shapiro, G. I.; LoRusso, P. M.; Cervantes, A.; Schwartz, G. K.; Weiss, G. J.; Paz-Ares, L.; Cho, D. C.; Infante, J. R.; Alsina, M.; Gounder, M. M.; Falzone, R.; Harrop, J.; White, A. C. S.; Toudjarska, I.; Bumcrot, D.; Meyers, R. E.; Hinkle, G.; Svrzikapa, N.; Hutabarat, R. M.; Clausen, V. A.; Cehelsky, J.; Nochur, S. V.; Gamba-Vitalo, C.; Vaishnaw, A. K.; Sah, D. W. Y.; Gollob, J. A.; Burris, H. A. *Cancer Discov* **2013,** *3*, 406-417.

28. Reineke, T. M.; Grinstaff, M. W. *MRS Bull* **2005,** *30*, 635-639.

29. Robbins, P. D.; Tahara, H.; Ghivizzani, S. C. *Trends Biotechnol.* **1998,** *16*, 35-40.

30. Bouard, D.; Alazard-Dany, N.; Cosset, F. L. *Br. J. Pharmacol.* **2009,** *157*, 153-165.

31. Anderson, W. F. *Nature* **1998,** *392*, 25.

32. Reineke, T. M. *J Polym Sci A Polym Chem* **2006,** *44*, 6895-6908.

33. Prevette, L. E.; Lynch, M. L.; Kizjakina, K.; Reineke, T. M. *Langmuir* **2008,** *24*, 8090-8101.

34. Gonzalez, H.; Hwang, S. J.; Davis, M. E. *Bioconjugate Chem.* **1999,** *10*, 1068-1074.

35. Khalil, I. A.; Kogure, K.; Akita, H.; Harashima, H. *Pharmacol. Rev.* **2006,** *58*, 32-45.

36. Godbey, W. T.; Wu, K. K.; Mikos, A. G. *J. Biomed. Mater. Res.* **1999,** *45*, 268-275.

37. Davis, M. E.; Pun, S. H.; Bellocq, N. C.; Reineke, T. M.; Popielarski, S. R.; Mishra, S.; Heidel, J. D. *Curr. Med. Chem.* **2004,** *11*, 179-197.

38. Liu, Y.; Wenning, L.; Lynch, M.; Reineke, T. M. *J. Am. Chem. Soc.* **2004,** *126*, 7422-7423.

39. Reineke, T. M.; Davis, M. E. *Bioconjugate Chem* **2003,** *14*, 247-254.

40. Reineke, T. M.; Davis, M. E. *Bioconjugate Chem* **2003,** *14*, 255-261.

41. Boussif, O.; Lezoualc'h, F.; Zanta, M. A.; Mergny, M. D.; Scherman, D.; Demeneix, B.; Behr, J. P. *Proceedings of the National Academy of Sciences of the United States of America* **1995,** *92*, 7297-7301.

42. Jones, G. D.; Langsjoen, A.; Neumann, S. M. M. C.; Zomlefer, J. *J. Org. Chem.* **1944,** *09*, 125-147.

43. Brissault, B.; Kichler, A.; Guis, C.; Leborgne, C.; Danos, O.; Cheradame, H. *Bioconjugate Chem.* **2003,** *14*, 581-587.

44. von Harpe, A.; Petersen, H.; Li, Y.; Kissel, T. *J Control Release* **2000,** *69*, 309-322.

45. Suh, J.; Paik, H. J.; Hwang, B. K. *Bioorg Chem* **1994,** *22*, 318-327.

46. Boussif, O.; Lezoualch, F.; Zanta, M. A.; Mergny, M. D.; Scherman, D.; Demeneix, B.; Behr, J. P. *P Natl Acad Sci USA* **1995,** *92*, 7297-7301.

47. Fischer, D.; Li, Y. X.; Ahlemeyer, B.; Krieglstein, J.; Kissel, T. *Biomaterials* **2003,** *24*, 1121-1131.

48. Neu, M.; Fischer, D.; Kissel, T. *J Gene Med* **2005,** *7*, 992-1009.

49. Wightman, L.; Kircheis, R.; Rossler, V.; Carotta, S.; Ruzicka, R.; Kursa, M.; Wagner, E. *J Gene Med* **2001,** *3*, 362-372.

50. Brus, C.; Petersen, H.; Aigner, A.; Czubayko, F.; Kissel, T. *Bioconjugate Chem* **2004,** *15*, 677-684.

51. Mao, S. R.; Neu, M.; Germershaus, O.; Merkel, O.; Sitterberg, J.; Bakowsky, U.; Kissel, T. *Bioconjugate Chem* **2006,** *17*, 1209-1218.

52. Merdan, T.; Kunath, K.; Petersen, H.; Bakowsky, U.; Voigt, K. H.; Kopecek, J.; Kissel, T. *Bioconjugate Chem* **2005,** *16*, 785-792.

53. Godbey, W. T.; Wu, K. K.; Mikos, A. G. *Biomaterials* **2001,** *22*, 471-480.

54. Lee, Y.; Mo, H.; Koo, H.; Park, J. Y.; Cho, M. Y.; Jin, G. W.; Park, J. S. *Bioconjugate Chem* **2007,** *18*, 13-18.

55. Ahn, C. H.; Chae, S. Y.; Bae, Y. H.; Kim, S. W. *J Control Release* **2002,** *80*, 273-282.

56. MacLaughlin, F. C.; Mumper, R. J.; Wang, J.; Tagliaferri, J. M.; Gill, I.; Hinchcliffe, M.; Rolland, A. P. *J Control Release* **1998,** *56*, 259-272.

57. Kiang, T.; Wen, H.; Lim, H. W.; Leong, K. W. *Biomaterials* **2004,** *25*, 5293-5301.

58. Sato, T.; Ishii, T.; Okahata, Y. *Biomaterials* **2001,** *22*, 2075-2080.

59. Germershaus, O.; Mao, S. R.; Sitterberg, J.; Bakowsky, U.; Kissel, T. *J Control Release* **2008,** *125*, 145-154.

60. Wong, K.; Sun, G. B.; Zhang, X. Q.; Dai, H.; Liu, Y.; He, C. B.; Leong, K. W. *Bioconjugate Chem.* **2006,** *17*, 152-158.

61. Kim, Y. H.; Gihm, S. H.; Park, C. R.; Lee, K. Y.; Kim, T. W.; Kwon, I. C.; Chung, H.; Jeong, S. Y. *Bioconjugate Chem.* **2001,** *12*, 932-938.

62. Loretz, B.; Thaler, M.; Bernkop-Schnurch, A. *Bioconjugate Chem.* **2007,** *18*, 1028-1035.

63. Popielarski, S. R.; Mishra, S.; Davis, M. E. *Bioconjugate Chem* **2003,** *14*, 672-678.

64. Kulkarni, R. P.; Mishra, S.; Fraser, S. E.; Davis, M. E. *Bioconjugate Chem* **2005,** *16*, 986-994.

65. Pun, S. H.; Davis, M. E. *Bioconjugate Chem* **2002,** *13*, 630-639.

66. Barbucci, R.; Casolaro, M.; Ferruti, P.; Barone, V.; Lelj, F.; Oliva, L. *Macromolecules* **1981,** *14*, 1203-1209.

67. Franchini, J.; Ranucci, E.; Ferruti, P.; Rossi, M.; Cavalli, R. *Biomacromolecules* **2006,** *7*, 1215-1222.

68. Liu, Y.; Reineke, T. M. *J. Am. Chem. Soc.* **2005,** *127*, 3004-3015.

69. Liu, Y.; Reineke, T. M. *Bioconjug. Chem.* **2005,** *17*, 101-108.

70. Kiely, D. E.; Chen, L.; Lin, T. H. *J Polym Sci Pol Chem* **2000,** *38*, 594-603.

71. Ogata, N.; Hosoda, Y. *J Polym Sci A Polym Chem* **1975,** *13*, 1793-1801.

72. Ogata, N.; Sanui, K.; Hosoda, Y.; Nakamura, H. *J Polym Sci A Polym Chem* **1976,** *14*, 783-792.

73. Viswanathan, A.; Kiely, D. E. *J Carbohydr Chem* **2003,** *22*, 903 - 918.

74. Liu, Y. M.; Reineke, T. M. *Bioconjug. Chem.* **2007,** *18*, 19-30.

75. Liu, Y.; Reineke, T. M. *Biomacromolecules* **2010,** *11*, 316-325.

76. McLendon, P. M.; Fichter, K. M.; Reineke, T. M. *Mol. Pharm.* **2010,** *7*, 738-750.

77. McLendon, P. M.; Buckwalter, D. J.; Davis, E. M.; Reineke, T. M. *Mol. Pharm.* **2010,** *7*, 1757-1768.

78. Fichter, K. M.; Ingle, N. P.; McLendon, P. M.; Reineke, T. M. *ACS Nano* **2012,** *7*, 347-364.

79. Grandinetti, G.; Smith, A. E.; Reineke, T. M. *Mol. Pharm.* **2011,** *9*, 523-538.

80. Srinivasachari, S.; Reineke, T. M. *Biomaterials* **2009,** *30*, 928-938.

81. Ingle, N. P.; Malone, B.; Reineke, T. M. *Trends Biotechnol.* **2011,** *29*, 443-453.

82. Xue, L.; Ingle, N. P.; Reineke, T. M. *Biomacromolecules* **2013,** *14*, 3903-3915.

83. Cherng, J.-Y.; van de Wetering, P.; Talsma, H.; Crommelin, D. A.; Hennink, W. *Pharm. Res.* **1996,** *13*, 1038-1042.

84. van de Wetering, P.; Cherng, J.-Y.; Talsma, H.; Hennink, W. E. *J. Controlled Release* **1997,** *49*, 59-69.

85. van de Wetering, P.; Moret, E. E.; Schuurmans-Nieuwenbroek, N. M. E.; van Steenbergen, M. J.; Hennink, W. E. *Bioconjugate Chem.* **1999,** *10*, 589-597.

86. van de Wetering, P.; Schuurmans-Nieuwenbroek, N. M. E.; Hennink, W. E.; Storm, G. *J Gene Med* **1999,** *1*, 156-165.

87. Jenkins, A. D.; Jones, R. G.; Moad, G. *Pure Appl. Chem.* **2010,** *82*, 483-491.

88. Matyjaszewski, K.; Xia, J. *Chem. Rev.* **2001,** *101*, 2921-2990.

89. Matyjaszewski, K. *Macromolecules* **2012,** *45*, 4015-4039.

90. Moad, G.; Rizzardo, E.; Thang, S. H. *Aust. J. Chem.* **2005,** *58*, 379-410.

91. Ahmed, M.; Narain, R. *Prog Polym Sci* **2013,** *38*, 767-790.

92. Vasilieva, Y. A.; Thomas, D. B.; Scales, C. W.; McCormick, C. L. *Macromolecules* **2004,** *37*, 2728-2737.

93. Scales, C. W.; Huang, F. Q.; Li, N.; Vasilieva, Y. A.; Ray, J.; Convertine, A. J.; McCormick, C. L. *Macromolecules* **2006,** *39*, 6871-6881.

94. Xu, X.; Smith, A. E.; Kirkland, S. E.; McCormick, C. L. *Macromolecules* **2008,** *41*, 8429-8435.

95. York, A. W.; Zhang, Y.; Holley, A. C.; Guo, Y.; Huang, F.; McCormick, C. L. *Biomacromolecules* **2009,** *10*, 936-943.

96. Deng, Z.; Ahmed, M.; Narain, R. *J Polym Sci A Polym Chem* **2009,** *47*, 614-627.

97. Ahmed, M.; Bhuchar, N.; Ishihara, K.; Narain, R. *Bioconjugate Chem.* **2011,** *22*, 1228-1238.

98. Ahmed, M.; Narain, R. *Biomaterials* **2011,** *32*, 5279-5290.

99. Smith, A. E.; Sizovs, A.; Grandinetti, G.; Xue, L.; Reineke, T. M. *Biomacromolecules* **2011,** *12*, 3015-3022.

100. Li, H.; Cortez, M. A.; Phillips, H. R.; Wu, Y.; Reineke, T. M. *ACS Macro Lett.* **2013,** *2*, 230-235.

101. Sizovs, A.; Xue, L.; Tolstyka, Z. P.; Ingle, N. P.; Wu, Y.; Cortez, M.; Reineke, T. M. *J. Am. Chem. Soc.* **2013,** *135*, 15417-15424.

102. Wu, Y.; Wang, M.; Sprouse, D.; Smith, A. E.; Reineke, T. M. *Biomacromolecules* **2014,** *15*, 1716–1726.

103. Convertine, A. J.; Benoit, D. S. W.; Duvall, C. L.; Hoffman, A. S.; Stayton, P. S. *J. Controlled Release* **2009,** *133*, 221-229.

104. Convertine, A. J.; Diab, C.; Prieve, M.; Paschal, A.; Hoffman, A. S.; Johnson, P. H.; Stayton, P. S. *Biomacromolecules* **2010**, null-null.

105. Dufresne, M.-H.; Leroux, J.-C. *Pharm. Res.* **2004,** *21*, 160-169.

106. Ji, W.; Panus, D.; Palumbo, R. N.; Tang, R.; Wang, C. *Biomacromolecules* **2011,** *12*, 4373-4385.

107. He, L.; Read, E. S.; Armes, S. P.; Adams, D. J. *Macromolecules* **2007,** *40*, 4429-4438.

108. Bloomfield, V. A. *Biopolymers* **1997,** *44*, 269-282.

109. Hansma, H. G.; Golan, R.; Hsieh, W.; Lollo, C. P.; Mullen-Ley, P.; Kwoh, D. *Nucleic Acids Res.* **1998,** *26*, 2481-2487.

110. Pack, D. W.; Hoffman, A. S.; Pun, S.; Stayton, P. S. *Nat Rev Drug Discov* **2005,** *4*, 581-593.

111. Won, Y.-Y.; Sharma, R.; Konieczny, S. F. *J. Controlled Release* **2009,** *139*, 88-93.

112. Prevette, L. E.; Kodger, T. E.; Reineke, T. M.; Lynch, M. L. *Langmuir* **2007,** *23*, 9773-9784.

113. Ziebarth, J.; Wang, Y. *J. Phys. Chem. B* **2010,** *114*, 6225-6232.

114. Ziebarth, J.; Wang, Y. *Biophysical Journal* **2009,** *97*, 1971-1983.

115. Amoozgar, Z.; Yeo, Y. *Wiley Interdiscip Rev Nanomed Nanobiotechnol* **2012,** *4*, 219-233.

116. Maeda, H.; Bharate, G. Y.; Daruwalla, J. *Eur J Pharm Biopharm* **2009,** *71*, 409-419.

117. Pun, S. H.; Davis, M. E. *Bioconjugate Chem.* **2002,** *13*, 630-639.

118. Merdan, T.; Kunath, K.; Petersen, H.; Bakowsky, U.; Voigt, K. H.; Kopecek, J.; Kissel, T. *Bioconjugate Chem.* **2005,** *16*, 785-792.

119. Liu, X.-Q.; Du, J.-Z.; Zhang, C.-P.; Zhao, F.; Yang, X.-Z.; Wang, J. *Int J Pharm* **2010,** *392*, 118-126.

120. Venkataraman, S.; Ong, W. L.; Ong, Z. Y.; Joachim Loo, S. C.; Rachel Ee, P. L.; Yang, Y. Y. *Biomaterials* **2011,** *32*, 2369-2378.

121. Tockary, T. A.; Osada, K.; Chen, Q.; Machitani, K.; Dirisala, A.; Uchida, S.; Nomoto, T.; Toh, K.; Matsumoto, Y.; Itaka, K.; Nitta, K.; Nagayama, K.; Kataoka, K. *Macromolecules* **2013,** *46*, 6585-6592.

122. Du, H.; Chandaroy, P.; Hui, S. W. *Biochim. Biophys. Acta, Biomembr.* **1997,** *1326*, 236-248.

123. Ishida, T.; Kiwada, H. *Int. J. Pharm.* **2008,** *354*, 56-62.

124. Kopeček, J.; Kopečková, P. *Adv Drug Deliver Rev* **2010,** *62*, 122-149.

125. Zhang, Z.; Vaisocherová, H.; Cheng, G.; Yang, W.; Xue, H.; Jiang, S. *Biomacromolecules* **2008,** *9*, 2686-2692.

126. Xu, Y.; Takai, M.; Ishihara, K. *Biomaterials* **2009,** *30*, 4930-4938.

127. Ahmed, M.; Jawanda, M.; Ishihara, K.; Narain, R. *Biomaterials* **2012,** *33*, 7858-7870.

128. Mancini, R. J.; Lee, J.; Maynard, H. D. *J. Am. Chem. Soc.* **2012,** *134*, 8474-8479.

129. Ting, S. R. S.; Chen, G.; Stenzel, M. H. *Polym. Chem.* **2010,** *1*, 1392-1412.

130. Low, P. S.; Henne, W. A.; Doorneweerd, D. D. *Acc. Chem. Res.* **2007,** *41*, 120-129.

131. Xia, W.; Low, P. S. *J. Med. Chem.* **2010,** *53*, 6811-6824.

132. Wu, G. Y.; Wu, C. H. *Adv. Drug Delivery Rev.* **1998,** *29*, 243-248.

133. Pathak, A.; Vyas, S. P.; Gupta, K. C. *Int. J. Nanomed.* **2008,** *3*, 31-49.

134. Davis, M. E. *Mol. Pharm.* **2009,** *6*, 659-668.

135. Hoang, B.; Reilly, R. M.; Allen, C. *Biomacromolecules* **2011,** *13*, 455-465.

136. Carver, L. A.; Schnitzer, J. E. *Nat Rev Cancer* **2003,** *3*, 571-581.

137. Rejman, J.; Bragonzi, A.; Conese, M. *Mol. Ther.* **2005,** *12*, 468-474.

138. von Gersdorff, K.; Sanders, N. N.; Vandenbroucke, R.; De Smedt, S. C.; Wagner, E.; Ogris, M. *Mol. Ther.* **2006,** *14*, 745-753.

139. Mukherjee, S.; Ghosh, R. N.; Maxfield, F. R. *Physiol. Rev.* **1997,** *77*, 759-803.

140. Behr, J.-P. *Chimia* **1997,** *51*, 34-36.

141. Sonawane, N. D.; Szoka, F. C.; Verkman, A. S. *J. Biol. Chem.* **2003,** *278*, 44826-44831.

142. Wang, H.-Y.; Chen, J.-X.; Sun, Y.-X.; Deng, J.-Z.; Li, C.; Zhang, X.-Z.; Zhuo, R.-X. *J. Controlled Release* **2011,** *155*, 26-33.

143. Lo, W.-L.; Chien, Y.; Chiou, G.-Y.; Tseng, L.-M.; Hsu, H.-S.; Chang, Y.-L.; Lu, K.-H.; Chien, C.-S.; Wang, M.-L.; Chen, Y.-W.; Huang, P.-I.; Hu, F.-W.; Yu, C.-C.; Chu, P.-Y.; Chiou, S.-H. *Biomaterials* **2012,** *33*, 3693-3709.

# Chapter 2 Experimental Techniques

Chapter two presents the important synthetic and characterization techniques utilized during my graduate study. Reversible deactivation radical polymerization (RDRP), which was employed for the synthesis of cationic copolymers for gene delivery, is briefly discussed in this chapter. Several characterization techniques are also introduced here, including size exclusion chromatography (SEC), dynamic light scattering (DLS), cryogenic transmission electron microscopy (cyroTEM). Detailed experimental procedures will be provided in the following chapters.

## 2.1 Reversible addition-fragmentation chain transfer (RAFT) polymerization

In 1956, Szwarc et al. discovered the first living polymerization techniques.[1] Real living polymerization proceeds without termination or chain transfer reactions. The absence of termination or chain transfer reactions allows for the synthesis of well-defined polymers of controlled molecular weight, narrow molecular weight distributions, and well-tailored architectures. These advanced architectures include statistical[2], alternating[3], AB diblock[4], ABA[5], and ABC triblock[6], tapered block[7], graft,[8] and star[9]structures. However, limited monomer choices and stringent reaction conditions of anionic, cationic, or group transfer polymerization methods, led to the rapid development of reversible deactivation radical polymerization (RDRP)[10].

All of the RDRP techniques include activation and deactivation steps. By utilizing the equilibrium favoring dormant chains over propagating chains, the concentration of active radical species is reduced, thus leading to the low frequency of termination reaction. Although termination still occurs, its contribution would be limited under appropriate conditions. The resulted radical polymerizations behave as controlled system.

RDRP techniques can be classified into two types according to the mechanism by which they activate/deactivate chains. The first type of controlled radical polymerization activates the chain by a reversible termination mechanism, and includes nitroxide mediated polymerization (NMP) or stable free radical polymerization (SFRP)[11], and atom transfer radical polymerization (ATRP)[12]. The mechanism for the second type of RDRP

is degenerate chain transfer process. The example is reversible addition-fragmentation chain transfer (RAFT) polymerization.

RAFT polymerization was first reported by the Commonwealth Scientific and Industrial Research Organization (CSIRO) in 1998.[13-14] The RAFT polymerization method has been the most versatile technique, suitable for almost all classes of vinyl monomers regardless of functionality and a wide range of reaction conditions, including aqueous media.[15]

### 2.1.1 Mechanism of RAFT polymerization

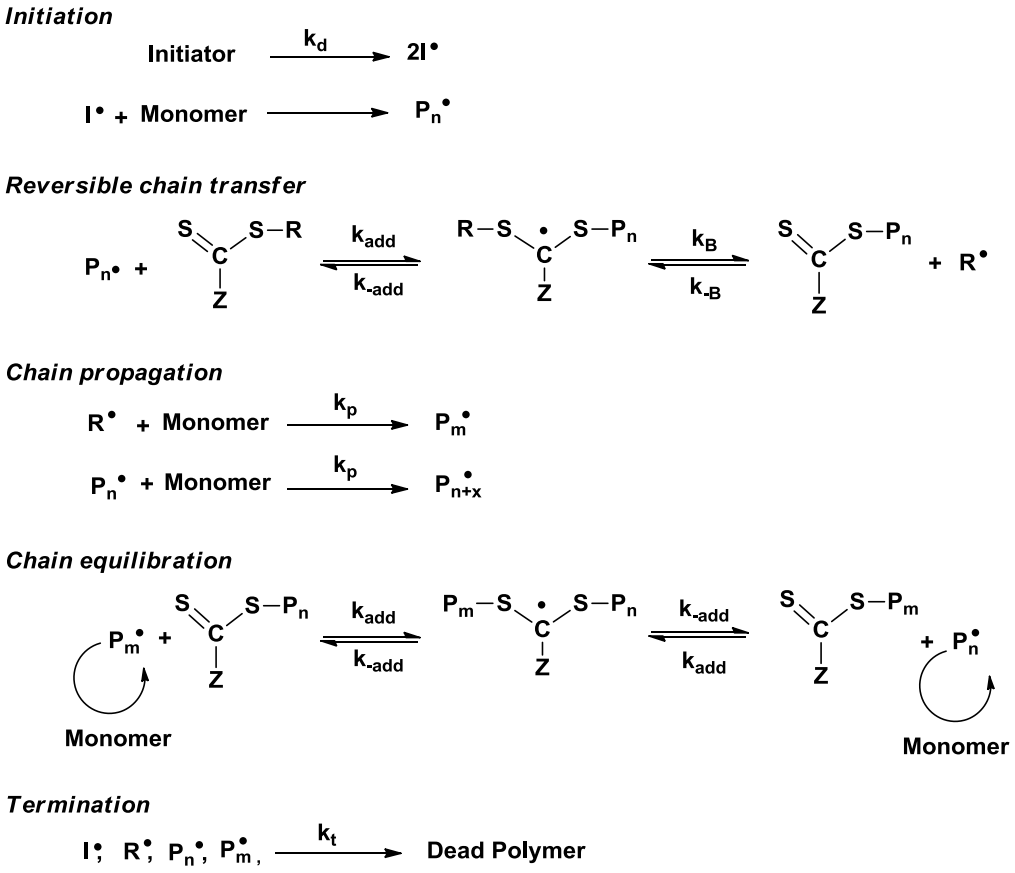


**Scheme 2.1** The accepted RAFT mechanism

Chain propagation in RAFT polymerization is realized by reversible chain transfer reaction (mechanism shown in Scheme 3), different from SFRP and ATRP where reversible deactivation of propagating radical chains controls the propagation[16]. Therefore, RAFT polymerization is actually conventional radical polymerization with a chain transfer agent (CTA), which typically contains thiocarbonylthio moiety. The polymerization is initiated by traditional initiators, including azo compounds, peroxides, redox initiating systems, or photoinitiators. The primary radical (I•) will add to a monomer whose concentration is relatively high before adding to the CTA, unless the CTA is highly reactive. Compared with CTA concentration, the concentration of initiator is mostly kept low to make sure CTAs initiate a majority of the chains, so as to eliminate the initiator-derived chains' negative effect on control of molecular weight. Moreover, the primary radical that is continuously generated will cause bimolecular termination. After the primary radical initiates propagation, the resulting oligomeric chain will react with the CTA to form an intermediate radical. This intermediate radical can yield a macroCTA and one new radical species (R•), or go back to form the starting radical and CTA, dependent on the relative reactivity. Both the radical species produced by intermediate radical can add monomer units, and reversibly add to another thiocarbonylthio group. Eventually the main equilibrium is achieved between the propagating radical and dormant macroCTA. Most monomers will be consumed during the main equilibrium. By minimizing the concentration of active species, irreversible termination can be limited in RAFT polymerization. The termination mechanism of RAFT polymerization could be either coupling or disproportionation, as in conventional

radical polymerization. A high ratio of the concentration of CTAs to that of initiators is utilized to minimize termination[14].

### 2.1.2 The RAFT chain transfer agent

In RAFT polymerization, the chain transfer agent (CTA) is the crucial component to enable control over molecular weight. Families of thiocarbonylthio groups include trithiocarbonates[17-18], dithioesters[19-20], xanthates[21], and dithiocarbamates[22]. For each monomer, the CTA has to be selected carefully to achieve successful RAFT polymerization.[23] The general structure of CTA is RS(=S)Z, and the thiocarbonylthio group is the key feature of the CTA. The Z group is mainly designed to activate the thiocarbonyl double bond for radical addition, and also stabilize the intermediate radical. But over-stabilization will retard the propagation, and even lead to termination. Dithioester and trithiocarbonates are the most reactive RAFT agents, with carbon or sulfur adjacent to the thiocarbonylthio group. RAFT agents such as the O-alkyl xanthates have significantly lower reactivity for radical addition, due to reduced double-bond character caused by resonance between the lone pair and the C=S double bond. The nitrogen lone pair of dithiocarbamates belongs to an aromatic system, thus it is not as available as xanthates. Its reactivity is similar to that of trithiocarbonates.

Monomers with a double bond next to an aromatic ring, a carbonyl group, or a nitrile are considered “more activated”, while those with double bond adjacent to a saturated carbon, an oxygen or nitrogen lone pair, or a heteroatom are generally “less activated”. The propagating radicals generated by more activated monomers are less

reactive toward radical addition; therefore, more active RAFT agents, such as dithioester, are required to achieve good control. "Less activated" monomers are typically polymerized with less active RAFT agents including xanthates. Otherwise, it will lead to retardation or inhibition of the polymerization. Scheme 2.2 shows the general guideline for the selection of Z group.[21]

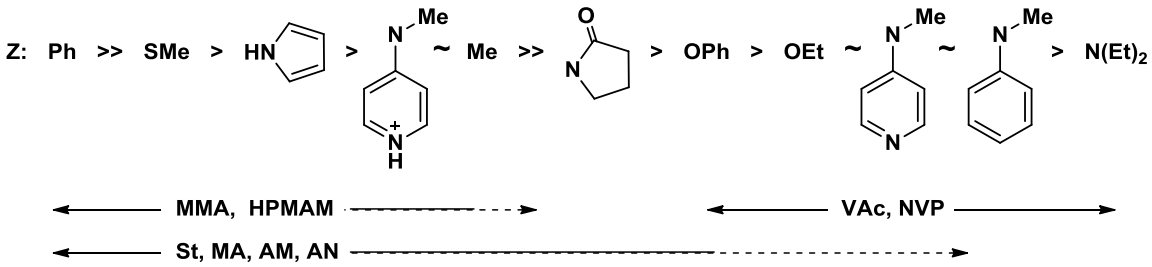


**Scheme 2.2** Guidelines for selection of the Z group of CTA agents (ZC(=S)SR) for polymerization of different monomers. (Reproduced with permission from reference [Keddie, D. J.; Moad, G.; Rizzardo, E.; Thang, S. H. Macromolecules 2012, 45, 5321-5342.]. Copyright [2012] American Chemical Society)

The R group has to be a good leaving group, and able to efficiently initiate the polymerization according to the mechanism of RAFT polymerization. Designing R to be an monomeric analogue of the propagating radical is not always feasible mainly due to penultimate unit effect. Polar effect also plays a significant role in polymerization control process. Electron-withdrawing groups on R reduce the rate of addition to the CTA, but increase the rate of fragmentation. Scheme 2.3 provides the general rule for selecting R group for RAFT polymerization.[21]

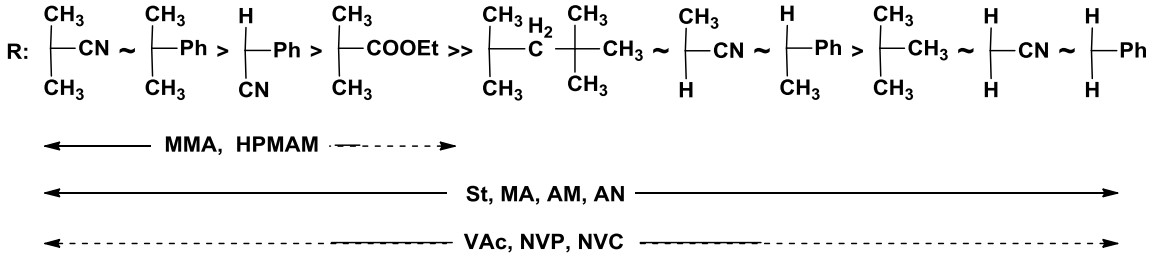


**Scheme 2.3** Guideline for selection of the R group of CTA agent (ZC(=S)SR) for polymerization of different monomers. (Reproduced with permission from reference [Keddie, D. J.; Moad, G.; Rizzardo, E.; Thang, S. H. Macromolecules 2012, 45, 5321-5342.]. Copyright [2012] American Chemical Society)

### 2.1.3 Molecular Weight Control by RAFT Polymerization

To control molecular weight, the RAFT polymerization has to meet some prerequisites, such as high ratio of CTA to initiator and proper choice of CTA. In a RAFT polymerization, if the ratio of CTA to initiator is high enough, and the CTA is proper for the monomer, the molecular weight will simply relate to the concentration of monomers and CTA. The equation for the calculation of theoretical number-average molecular weight is shown below, where $[M]_0$ is the initial concentration of monomer, $M_{MW}$ is the molecular weight of the monomer, ρ is the conversion of monomer, $[CTA]_0$ is the initial concentration of CTA, and $M_{CTA}$ is the molecular weight of CTA.[21]

$$M_{n,th} = \frac{[M]_0 M_{mw} \rho}{[CTA]_0} + M_{CTA} \quad (2.1)$$

The dispersity (Đ) of the obtained polymers could be estimated using the equation shown below, where $[I]_0$, [D] is the concentration of initiator and chain transfer agent, $k_p$

is the rate constant of chain propagation, $k_d$ is the overall rate constant of chain addition to CTA, and p is the conversion of monomer.[24]

$$Đ = \frac{M_w}{M_n} = 1 + \left(\frac{[I]_0 k_p}{k_d[D]}\right)\left(\frac{2}{p} - 1\right) \quad (2.2)$$

## 2.2 Size exclusion chromatography (SEC)

Size exclusion chromatography (SEC) is widely used for the determination of the molecular weights and distributions of polymers.[25] Ideal SEC system requires that analyte has no interaction with the surface of the stationary phase typically packed by polystyrene beads with controlled pore size, and the separation process solely depends upon the volume of the macromolecules. Small molecules can penetrate through most of the region of the stationary phase including both pores and interparticle space, while larger molecules could elute through only relatively larger pore or interparticles space. Therefore, larger molecules elute through the column sooner due to the lower degree of permeation into the porous stationary phase. The eluent is monitored by one or several appropriate detectors for resolving macromolecule solution mixtures as a function of retention time or volume.

### 2.2.1 Molecular weight calculation using polymer standards

Because the retention volume/time is mostly determined by the size of the examined polymers, conventional SEC system determines the molecular weight of sample polymers according to the retention time. In practice, this is usually done through the calibration using polymer standards of known structures and molecular weights.

At certain fraction i, or data point, the concentration of the polymer solution can be determined by the detectors, such as refractive index (RI) detector, connected with SEC system, which signal intensity $Q_i$ is directly proportional to the RI difference between sample solution $n_i$ and solvent $n_0$. The concentration could be calculated using folloing equation 2.3, where $\partial n/\partial c$ is the specific refractive index increment, can be determined using RI detector.

$$Q_i \propto (n_i - n_0) = (\frac{\partial n}{\partial c}) \times c_i \qquad 2.3$$

As the molecular weight is the function of retention time, the molecular weight of the sample eluted out at certain time point (i.e. fraction i) is calculated based upon the calibration curve that created using polymer standards. Combining the equation 2.3, the overall average molecular weight is calculated using following equation 2.4 and 2.5. It should be noted that $M_i$ is only the molecular weight based upon polymer standard relative to the elution time.

$$M_n = \frac{\Sigma c_i}{\Sigma c_i/M_i} = \frac{\Sigma Q_i}{\Sigma Q_i/M_i} \qquad 2.4$$

$$M_n = \frac{\Sigma c_i \times M_i}{\Sigma c_i} = \frac{\Sigma Q_i \times M_i}{\Sigma Q_i} \qquad 2.5$$

### 2.2.2 Molecular weight calculation using static light scattering (SLS) detector

As mentioned, using the polymer standards does not provide the calculation of the true molecular weight of the sample polymers, but is mainly based upon the assumption that sample polymers behave exactly the same as the standard polymers in the SEC systems. Therefore, any difference between sample polymers and standard polymers

could lead to inaccurate calculation, such as solubility difference, different interaction between polymers and stationary phase. To obtain the absolute molecular weight of the sample polymer, static light scattering detector is utilized in the SEC system.

When particles are much smaller than the wavelength of the light, the amount of scattered light at certain angle is directly proportional to the excess Rayleigh ratio R(θ), which is defined as the ratio of the scattered light intensity and incident light intensity. The Rayleigh ratio R(θ) could be expressed using zimm equation 2.6 in static light scattering.

$$I_s(\theta) \propto R(\theta) = K^* McP(\theta)[1 - 2A_2 McP(\theta)] \qquad 2.6$$

In the first term of equation 2.6, M is the weight average molecular weight, c is the concentration of solution, P(θ) is form factor relating to the scattering intensity angular variation. And K* is defined by equation 2.7 below, where $n_0$ is the solvent refractive index, $N_A$ is Avogadro's number, $\lambda_0$ is the wavelength of incident light in vacuum, and $\partial n/\partial c$ is the specific refractive index increment mentioned above. In the second term, $A_2$ is second virial coeffiecient, a measurement of the interaction between polymer solute and solvent. In θ solution, $A_2$ is zero. Positive $A_2$ value means attractive interaction between solute and solvent, while negative value means repulsion between solute and solvent.

$$K^* = \frac{4\pi^2 n_0^2}{N_A \lambda_0^4} \left(\frac{\partial n}{\partial c}\right)^2 \qquad 2.7$$

In the typical instrumentation setup, the in-line static light scattering detector won't be performing conventional Zimm plot to calculate molecular weight of each

fraction of solution ($M_i$), because it doesn't measure a single fraction at various different concentrations. During online data analysis, one of the approach to calculate the molecular weight is to ignore the second virial coefficient, as $A_2$ value is often very low. This will simplify the equation 2.6 to be the equation 2.8. However, this could oversimplify the calculation in some cases, certain instrument software would allow user to enter the $A_2$ value. The overall average molecular weight could still be obtained using equation 2.4 and 2.5, with the molecular weight $M_i$ determined by SLS.

$$R(\theta) = K^* McP(\theta) \qquad 2.8$$

**2.3 Dynamic light scattering**

Dynamic light scattering (DLS) is a technique to determine the size and size distribution of particles in suspension or in solution, typically in the sub micron region.

Brownian motion, which is caused by bombardment by the surrounding solvent molecules, is indirectly proportional to size of particles. The velocity of Brownian motion is defined by the Translational Diffusion Coefficient (*D*). According to Stokes-Einstein equation (2.9) shown below:

$$d_H = \frac{kT}{3\pi\eta D} \qquad 2.9$$

where $d_H$ represents hydrodynamic diameter. It describes how a particle diffuses within a fluid. *D* is translational diffusion coefficient. *k* is Boltzmann's constant. *T* is absolute temperature of solution. And $\eta$ is viscosity of solvent. *k, T,* and $\eta$ are all known in certain experimental condition.

To calculate $d_H$, $D$ is the only unknown parameter. The velocity at which the particles are diffusing is measured in dynamic light scattering. Thus the hydrodynamic diameter will be obtained based upon the equation above.

In an ideal stationary condition, the stable classical speckle pattern from the particles scattering will be seen. The bright blobs of light are caused by the light scattering that arrives at the detector from constructive interference. The dark spots are where the light scattering has destructive interference. But in the system where particles undergo Brownian motion, the phase addition is constantly evolving. So the speckle pattern is also in motion. The intensity of light scattered will fluctuate over time. The rate of the intensity fluctuation depends on the size of particles.

If the intensity of a signal is compared with itself at a particular time point and a time much later, then for a randomly fluctuating signal, the intensities are not going to be related, i.e. there will be no correlation between two signals. However, if the signal at time $t$ is compared with the signal from a very short time later ($t+\delta t$), there will be very strong correlation. If the signal at time $t$ is compared with the signal at time $t+2\delta t$, the correlation will be reduced. Thus, the correlation will decrease over time. The more rapidly particles move, the faster correlation disappears.

In equation, for a large number of monodisperse particles, the correlation function $G(\tau)$ can be calculated as shown below:

$$G(\tau) = A[1 + Bexp(-2\Gamma\tau)] \qquad 2.10$$

where $A$ is the baseline of the correlation function, $B$ is the intercept of the correlation function. And $\Gamma$ is equal to $Dq^2$.

$D$ is the translational diffusion coefficient in Stokes-Einstein equation above. $q$ is equal to $(4\pi n/\lambda_0)\sin(\theta/2)$. Where $n$ is the refractive index of dispersant. $\lambda_0$ is the wavelength of laser, and $\theta$ is scattering angle.

For certain experimental settings, all the parameters are either known, or can be measured, so that $D$ can be solved from this correlation function. Thus, the hydrodynamic diameter ($d_H$) can be calculated according to the Stokes-Einstein equation shown above.

## 2.4 Cryogenic transmission electron microscopy (cryoTEM)

After Knoll and Rusha proposed the idea of electron microscopy in 1932, transmission electron microscopy (TEM) has rapidly developed and become one of the most powerful instruments to imaging nanostructures. Taking advantage of the small de Broglie wavelength of electrons, defined in the equation 2.11, TEM are capable of imaging significantly smaller structure than light microscope.

$$\lambda_e \approx \frac{h}{\sqrt{2m_0E(1+\frac{E}{2m_0C^2})}} \approx \frac{1.22}{E^{1/2}} \qquad 2.11$$

In the equation 2.10, where, h is Planck's constant, $m_0$ is the rest mass of an electron and E is the energy of the accelerated electron. The theoretical smallest distance could be approximately determined using Rayleigh equation 2.12, where $\lambda$ is the wavelength of electron, n is the refractive index of the object material, α is the semi-angular aperture.[26]

$$d = \frac{1.22\lambda}{n\,sin\alpha} \qquad 2.12$$

Despite of the powerful imaging ability, the conventional TEM still has limitation to image in situ microstructure, because it requires solvent removal and staining, which could cause some artifacts such as deformation of objectives, and even undesired interaction between stain and samples.[27] Cryogenic transmission electron microscopy (cryoTEM) extends the capabilities of TEM to capture the in situ morphology of some dedicate structure. Direct imaging of assembled structure in solution is not possible because of the high vacuum in the TEM imaging chamber. During cryoTEM imaging, solution is rapidly vitrified for the physical fixation of assemblies in solution. This enables cryoTEM to direct image the vitrified liquid specimen.

### 2.4.1 CryoTEM sample preparation

CryoTEM sample could be prepared following three steps: 1) loading sample solution onto lacey formvar/carbon copper grid; 2) blotting away extra solution with filter paper, to form a thin liquid film on the grid; 3) Plunging the sample grid rapidly into cryogen reservoir, such as liquid ethane (about -180 ºC). During the preparation process, besides the grid transfer, which is crucial to preserve the quality of the grid, blotting step is very important to control the thickness of the liquid film left on the grid. If the film is too thick, there will not be enough electrons transmitted through the specimen for imaging. If the film is too thin, the relative large structure of objective would be damaged, or only blank film is produced. The procedure is illustrated in the Figure 2.1. Once the aqueous sample is vitrified, the temperature of the sample during storage and

imaging should be kept below -160 ºC to prevent the crystallization, and sublimation in the vacuum TEM chamber during imaging.

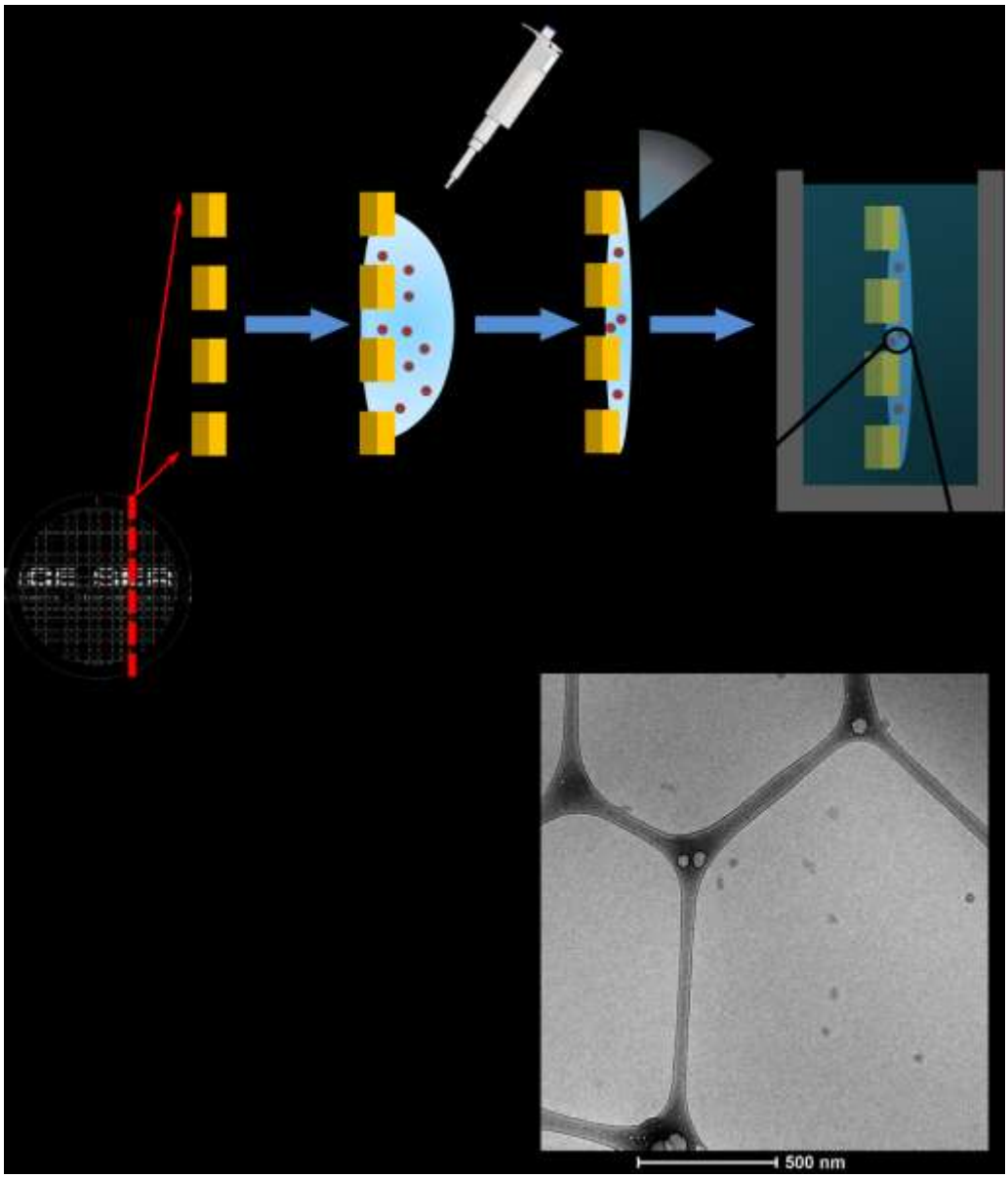


**Figure 2.1** illustration of cryoTEM sample preparation procedure: step 1 loading sample; step 2 removing excess solution; step 3 vitrifying the sample grid in liquid ethane

### 2.4.2 Interaction between electron beam and samples

As high energy electron beam contacts with specimen, several different signals are generated, such as elastically scattered electrons, inelastically scattered electrons, and characteristic X-rays. Among these signals, forward elastic scattering is generally coherent, and occurs at relatively low angles (1-10º).[28] Elastic scattered electrons are the major source for the image contrast in TEM imaging, providing major information to construct the images, while inelastic scattering, which is incoherent and at very low angle (<1º), usually produces background fog.

Contrast in a cryoTEM image is produced by both mass-thickness contrast and phase-contrast.[29] The electron density and thickness of the sample contributes to the mass-thickness contrast. The dense packing of core moieties and the possible presence of heavy atoms, such as sulphur and phosphorus, provides the contrast, which would usually be darker in the image. For example, the packed core of micelle often appears to be dark region, while the well-solvated corona usually is indistinguishable from the background. Mass-thickness contract is often insufficient for imaging, so phase contrast is utilized to obtain better resolved structure. Phase contrast arises from the interference between unscattered electrons and elastically scattered electrons. Under-focusing the objective lense during TEM imaging can enhance the phase contrast. Bright Fresnel ring around darker region is the indicator for under-focus. It should be noted that under-focusing could compromise the resolution of the image, and even lead to distortion of microstructure, which might produce the misrepresentation of the sample.

### 2.4.3 Artifacts observed in cryoTEM

The artifacts observed in cryoTEM can be caused by several reasons: blotting, solvent evaporation, solvent crystallization, shear-induced deformation, confinement of structure into ultrathin ice film,[30] and radiolysis. During blotting to remove the extra solvent, samples are subjective to the deformation by the shear force. Although the shear rate induced by blotting step is inevitable, relaxation over time could help the recovery of the structure to some extent. Solvent evaporation, which could result in the deformation after blotting, could be avoided by preparing the grids in a closed chamber. Preparing samples in "Vitrobot" could somewhat circumvent this issue, but it does also remove certain degree of flexibility during preparation. Ice crystal contamination is the most encountered issue in cryoTEM. The crystallization could damage the assembled structure, and cause optical artifact. Low cooling rate and slow sample transfer are the two major causes for crystallization. Ice crystals could be generally easily identified, as they are often black spots. Additionally, vitrified ice film is kinetically trapped structure, and long exposure to electron beam could lead to the formation of ice cubic crystal as well. Figure 2.2 shows a few examples of artifact observed during our cryoTEM imaging.

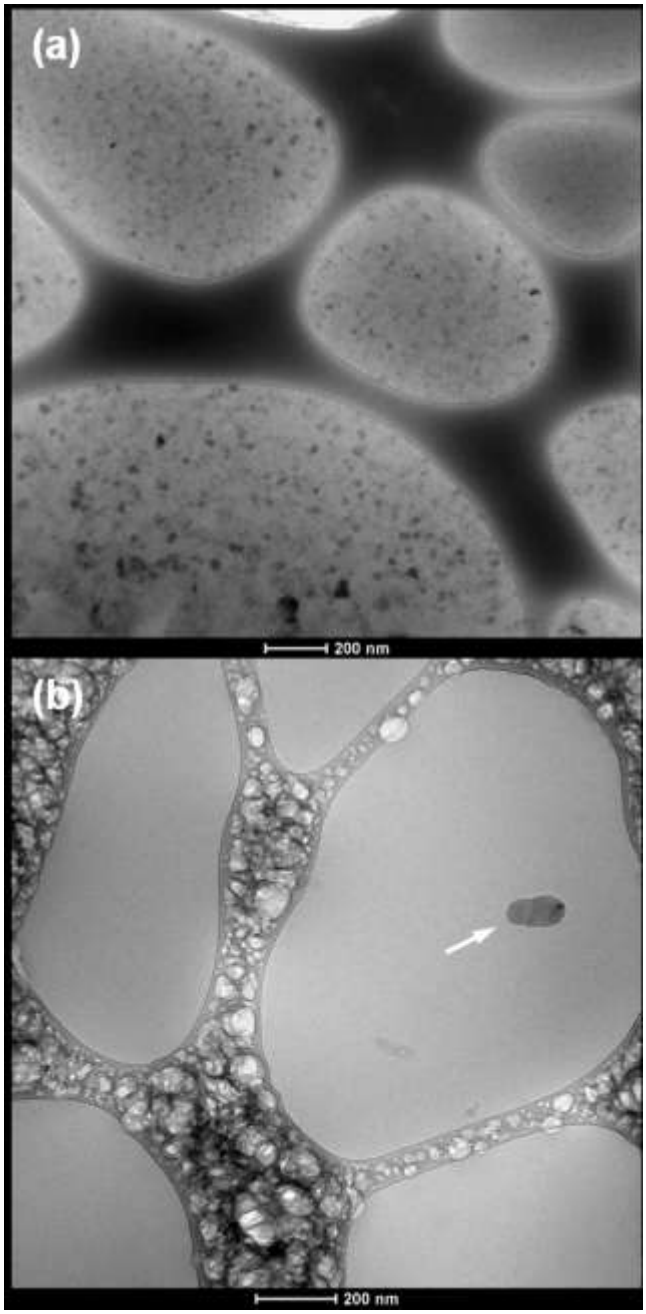


**Figure 2.2** Artifacts observed in cryoTEM: (a) polygonal ice crystals in the film; (b) ice crystals on surface.

The radiolysis of microstructures is resulted from electron interaction with the sample due to the long exposure of high energy electrons, which is often caused by bond breaking through radical reaction. Radiolysis is also often referred to as “beam damage”. Soft materials, such biological samples, are very sensitive and subjective to damage. It is important to reduce the electron exposure time to sensitive samples to preserve the in situ morphology during imaging. Figure 2.3 shows that some complexes between polycation and plasmid DNA were damaged after exposing to high energy electron beam over 30 sec. Low-dose mode could be utilized to avoid overexposing very sensitive samples under electron beam.

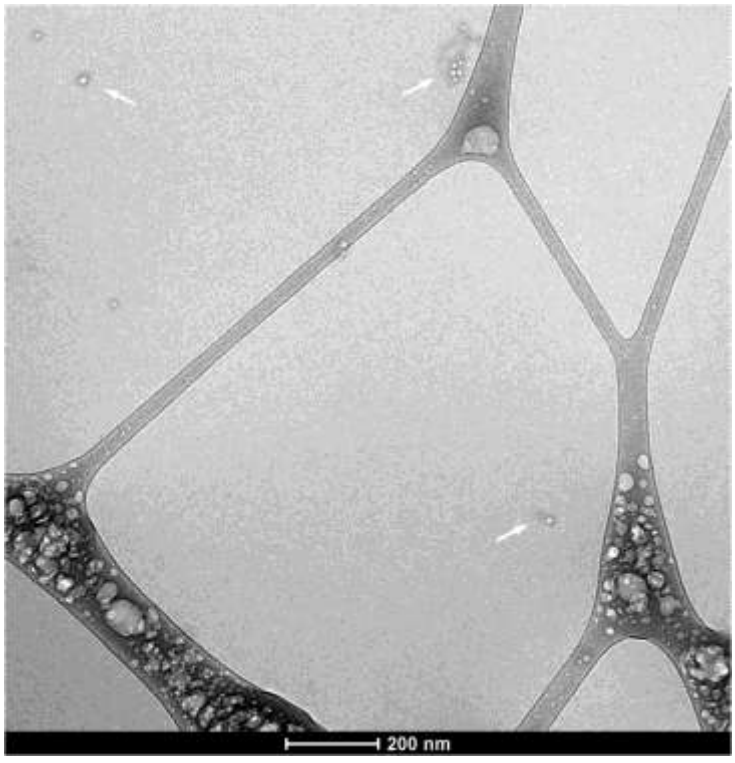


**Figure 2.3** Beam damage observed for polycation/pDNA complex sample.

## 2.5 Reference

1. Szwarc, M.; Levy, M.; Milkovich, R. *J. Am. Chem. Soc.* **1956,** *78*, 2656-2657.

2. Davis, K. A.; Matyjaszewski, K., Statistical, gradient, block, and graft copolymers by controlled/living radical polymerizations. In *Statistical, Gradient, Block and Graft Copolymers by Controlled/Living Radical Polymerizations*, 2002; Vol. 159, pp 1-169.

3. Lutz, J. F.; Kirci, B.; Matyjaszewski, K. *Macromolecules* **2003,** *36*, 3136-3145.

4. Ge, Z.; Cai, Y.; Yin, J.; Zhu, Z.; Rao, J.; Liu, S. *Langmuir* **2007,** *23*, 1114-1122.

5. Bowes, A.; McLeary, J. B.; Sanderson, R. D. *J. Polym. Sci. Polym. Chem.* **2007,** *45*, 588-604.

6. Cao, Y.; Zhu, X. X. *Can. J. Chem.* **2007,** *85*, 407-411.

7. Rivera, M. R.; Rodriguez-Hernandez, A. A.; Hernandez, N.; Castillo, P.; Saldivar, E.; Rios, L. *Ind. Eng. Chem. Res.* **2005,** *44*, 2792-2801.

8. Tsujii, Y.; Ejaz, M.; Sato, K.; Goto, A.; Fukuda, T. *Macromolecules* **2001,** *34*, 8872-8878.

9. Stenzel-Rosenbaum, M.; Davis, T. P.; Chen, V.; Fane, A. G. *J. Polym. Sci. Polym. Chem.* **2001,** *39*, 2777-2783.

10. Jenkins, A. D.; Jones, R. G.; Moad, G. *Pure Appl. Chem.* **2010,** *82*, 483-491.

11. Braunecker, W. A.; Matyjaszewski, K. *Prog. Polym. Sci.* **2007,** *32*, 93-146.

12. Matyjaszewski, K.; Xia, J. *Chem. Rev.* **2001,** *101*, 2921-2990.

13. Chiefari, J.; Chong, Y. K.; Ercole, F.; Krstina, J.; Jeffery, J.; Le, T. P. T.; Mayadunne, R. T. A.; Meijs, G. F.; Moad, C. L.; Moad, G.; Rizzardo, E.; Thang, S. H. *Macromolecules* **1998,** *31*, 5559-5562.

14. Moad, G.; Rizzardo, E.; Thang, S. H. *Aust. J. Chem.* **2006,** *59*, 669-692.

15. McCormick, C. L.; Lowe, A. B. *Acc. Chem. Res.* **2004,** *37*, 312-325.

16. York, A. W.; Kirkland, S. E.; McCormick, C. L. *Adv. Drug Delivery Rev.* **2008,** *60*, 1018-1036.

17. Lai, J. T.; Filla, D.; Shea, R. *Macromolecules* **2002,** *35*, 6754-6756.

18. Wang, R.; Lowe, A. B. *J. Polym. Sci. Polym. Chem.* **2007,** *45*, 2468-2483.

19. Vasilieva, Y. A.; Scales, C. W.; Thomas, D. B.; Ezell, R. G.; Lowe, A. B.; Ayres, N.; McCormick, C. L. *J. Polym. Sci. Polym. Chem.* **2005,** *43*, 3141-3152.

20. Vasilieva, Y. A.; Thomas, D. B.; Scales, C. W.; McCormick, C. L. *Macromolecules* **2004,** *37*, 2728-2737.

21. Moad, G.; Rizzardo, E.; Thang, S. H. *Aust. J. Chem.* **2005,** *58*, 379-410.

22. Schilli, C. M.; Zhang, M. F.; Rizzardo, E.; Thang, S. H.; Chong, Y. K.; Edwards, K.; Karlsson, G.; Muller, A. H. E. *Macromolecules* **2004,** *37*, 7861-7866.

23. Favier, A.; Charreyre, M. T. *Macromol. Rapid Commun.* **2006,** *27*, 653-692.

24. Matyjaszewski, K.; Xia, J. *Chem. Rev.* **2001,** *101*, 2921-2990.

25. Barth, H. G.; Jackson, C.; Boyes, B. E. *Anal. Chem.* **1994,** *66*, 595R-620R.

26. Kohl, H.; Reimer, L., Wave Optics of Electrons. In *Transmission Electron Microscopy*, Springer New York: 2008; Vol. 36, pp 43-74.

27. Nielsen, P. E., In DNA-Protein Interaction, Principles and Protocols. In Moss, T.; Leblanc, B., Eds. Springer: New York, 2009; Vol. 543, pp 87-96.

28. Williams, D. B.; Carter, C. B., *Transmission Electron Microscopy, A Textbook for Materials Science*. Springer: New York, 2009.

29. Cui, H.; Hodgdon, T. K.; Kaler, E. W.; Abezgauz, L.; Danino, D.; Lubovsky, M.; Talmon, Y.; Pochan, D. J. *Soft Matter* **2007,** *3*, 945-955.

30. Danino, D.; Talmon, Y.; Zana, R. *Colloids Surf A Physicochem Eng Asp* **2000,** *169*, 67-73.

# Chapter 3 Characterization of Polyplexes Composed of Cationic Glycopolymers

Chapter three presents our effort to characterize the size and morphology of the polyplexes composed of the cationic block copolymers. The synthesis of the block copolymers with either glucose moieties or trehalose moieties is described in this chapter. The obtained polyplexes are characterized using dynamic light scattering (DLS), and regular transmission electron microscopy (TEM). Additionally, cryoTEM techniques have been explored to capture the in situ morphology of the polyplexes in water.

---



1. Li, H.; Cortez, M. A.; Phillips, H. R.; Wu, Y.; Reineke, T. M. *ACS Macro Lett.* **2013**, *2*, 230-235.
2. Sizovs, A.; Xue, L.; Tolstyka, Z. P.; Ingle, N. P.; Wu, Y.; Cortez, M.; Reineke, T. M. *J. Am. Chem. Soc.* **2013**, *135*, 15417-15424.
3. Wu, Y.; Wang, M.; Sprouse, D.; Smith, A. E.; Reineke, T. M. *Biomacromolecules* **2014**, *15*, 1716–1726.

## 3.1 Introduction

Oppositely charged macromolecules could spontaneously form complexes in solution. The morphologies of the resulted complexes could be affected by the flexibility, charge ratio, charge types, and also the structure of the macromolecules.[1] Nucleic acid and polycations can form polyelectrolyte complexes, i.e. polyplexes. The complexes formation is driven by the decrease of the total electrostatic free energy, loosely considered as the sum of the translational entropy of the polyelectrolyte and the total electrostatic field energy.[2]

The structure of early polycations utilized for gene delivery are relatively simple, like linear polyethyleneimine (PEI), but the resulted polyplexes are susceptible for rapid clearance by reticuloendoethelial system (RES) upon systemic administration due to aggregation and absorption of serum albumin and other negatively charged protein,[3] significantly reducing the efficacy of polyplex delivery. To improve the in vivo transfection efficiency of polyplexes and take advantage of the enhanced permeability and retention (EPR) effect,[4] neutral hydrophilic polymers, such as poly(ethylene glycol) (PEG), have been incorporated into polycation systems to prolong their blood circulation time.[3, 5-8] In addition to the PEG block copolymers, carbohydrate derived polymers have recently been developed as stealth coating for polyplexes.[9-11] The colloidal stability of the polyplexes was attributed to the incorporation of a PMAG block, which is exposed on the surface of the nanocomplexes, which contain a core structure of the polycation block bound to the nucleic acid. Such “core-shell” structures in aqueous salt and serum solutions have

been shown to promote steric shielding of polyplexes to prevent aggregation in biological conditions.[1, 10-12]

Transmission electron microscopy (TEM) has been routinely utilized to characterize the morphology of biomaterials, including polyplexes. The structures of many biological samples are rather fragile, and the removal of aqueous solution could cause deformation. And the subsequent staining process also often cause artifact in some cases.[13] Cryogenic transmission electron microscopy (cryoTEM) provides a mean to directly image the in situ morphology of nanostructures by physical fixation of the liquid sample, i.e. vitrification. There has been significant advance in imaging DNA and liposome-DNA structures using cryoTEM techniques.[14] However, there are still very limited number of literatures to exhibit the in situ morphology of polyplexes, possibly owing to the poor contrast because of its less organized structures and the lack of dense compact cores.[15-16]

Herein, we report the synthesis a series of cationic glycopolymers composed of various types of carbohydrate moieties via RAFT polymerization. The polyplexes formed by the obtained glycopolymers were characterized using dynamic light scattering (DLS), and conventional TEM. Colloidal stability of the polyplexes in serum absent medium was studied via DLS. CryoTEM technique was also employed to reveal the in situ morphology of polyplexes formed by glycopolymers.

## 3.2 Materials and synthesis

### 3.2.1 Materials

All chemicals were purchased from Sigma Aldrich and used without further purification unless specified otherwise. Monomeric aminoethylmethacrylate (AEMT) was purchased from Polysciences (Warrington, PA). *N*-methyl-aminoethylmethacrylate (MAEMT), *N,N*-dimethyl aminoethylmethacrylate (DMAEMT) and *N,N,N*-trimethylammoniumethylmethacrylate (TMAEMT) was prepared by Dr. Haibo Li.[11] 4-cyano-4-(propylsulfanylthiocarbonyl) sulfanylpentanoic acid (CPP) was synthesized according to a previous procedure.[17] N-(2-aminoethyl) methacrylamide hydrochloride (AEMA•HCl) and N-[3-(N,N-dimethylamino)propyl]methacrylamide (DMAPMA) were purchased from Polyscience, Inc. (Warrington, PA), and DMAPMA was purified via vacuum distillation prior to use. 4,4'-Azobis(4-cyanovaleric acid) (V-501) was recrystallized from methanol. 6-methacrylamido-6-deoxy trehalose (MAT) was synthesized by Dr. Antons Sizvos.[18] 2-deoxy-2-methacrylamido glucopyranose (MAG)[19] and the chain transfer agent (CTA) 4-cyano-4-(propylsulfanylthiocarbonyl) sulfanylpentanoic acid (CPP)[17] were synthesized according to previous reports. Cell culture media, Dulbecco's Modified Eagle Medium (DMEM) and Opti-MEM, antibiotic/antimycotic, fetal bovine serum (FBS), phosphate-buffered saline (PBS), and nuclease-free water were purchased from Gibco (Carlsbad, CA).

### 3.2.2 Polymer synthesis

#### 3.2.2.1 The synthesis of PMAG-b-PDMAPMA glycopolymer series

The diblock glycopolymers were synthesized according to similar methods previously published.[10] Typically, to yield PMAG as the macromolecular chain transfer agent (macroCTA), MAG (0.23 g, 0.93 mmol), CPP (1.7 mg, $6.2\times10^{-3}$ mmol), and V-501 (0.17 mg, $6.2\times10^{-4}$ mmol) were dissolved in 2.0 mL of a 4:1 mixture of 0.1 M acetate buffer (pH 5.2) and ethanol. The solution was added to a 5 mL round bottom flask equipped with magnetic stir bar and purged with nitrogen for 50 min before the flask was sealed and placed into a preheated oil bath at 70 ºC. The reaction was then terminated by exposure to air at predetermined time points to yield different lengths of PMAG. The two PMAG macroCTAs were purified by dialysis with 3500 Da molecular weight cut-off dialysis tubing against ultrapure water and lyophilized to dryness. To synthesize the diblock glycopolymers, the macroCTA (100 mg, $3.4\times10^{-3}$ mmol for $PMAG_{118}$; 52 mg, $3.3\times10^{-3}$ mmol for $PMAG_{61}$), AEMA•HCl (33mg, 0.20mmol) or DMAPMA (34 mg, 0.20 mmol), and V-501 (0.21 mg, $7.5\times10^{-4}$ mmol) were dissolved in 1.2 mL 1.0 M acetate buffer (pH 5.2) in a 5 mL round bottom flask. After the solution was purged with nitrogen for 50 min, the polymerization was carried out in a preheated oil bath at 70 ºC. Polymerization was terminated at a predetermined time point to yield different molecular weights by exposing the reaction mixture to air. The final product was purified via extensive dialysis with a 3500 Da molecular weight cut-off membrane against water (pH 5 to 6, pH adjusted by conc. HCl) and lyophilization.

To synthesize homopolymers, the CPP (3.0 mg, $1.1\times10^{-2}$mmol), AEMA•HCl (108.3 mg, 0.66 mmol) or DMAPMA (112.2 mg, 0.66 mmol), and V-501 (0.61 mg, 2.2 $\times10^{-3}$ mmol) were dissolved in 3.29 mL of a 4:1 mixture of 1.0M acetate buffer (pH 5.2) : ethanol in a 5mL round bottom flask. After the solution was purged with nitrogen for 50 min, the polymerization was carried out in a preheated oil bath at 70 ºC for 3 h before termination by exposing the reaction mixture to air. The final product was purified by dialysis with a 3500 Da molecular weight cut-off membrane against water (pH 5 to 6, adjusted with conc. HCl) as described above and white powder was acquired after lyophilization.

### 3.2.2.2 The synthesis of polymethacrylate glycopolymer series

The synthesis was carried out by Dr. Haibo Li. The following is a typical procedure used to prepare the diblock glycopolymers with the various cationic monomers. The PolyMAG macroCTA (0.20 g), MAEMAT chloride (0.278 g, 1.5479 mmol), V-501 (0.87 mg, 0.003096 mmol), and acetate buffer (1.0 M, pH=5.2) (2.40 mL) were added to a 5 mL vial charged with nitrogen gas and a mechanical stirring bar. The mixture was stirred to dissolve the reactants and the solution was purged with nitrogen gas for 30 minutes at room temperature. Next, the reaction mixture was heated to 70 $^{o}$C, and the reaction was stirred for 26 minutes. The solution was then dialyzed against water for three days and lyophilized to yielding 0.23 g of the final glycopolycation final product.

### 3.2.2.3 The synthesis of PMAT-b-PAEMA glycopolymer series

The polymerization studies were performed by Dr. Antons Sizvos. The polymerization kinetics were monitored using $^{1}$H NMR. 6-Methacrylamido-6-deoxy trehalose (MAT) (0.765 g, 1.867 mmol, 65 eq) was dissolved in 7.00 mL of acetate buffer in $D_2O$. CPP (7.97 mg, $2.87x10^{-2}$ mmol, 1 eq) was dissolved in 645 µL of MeOD and added to the solution of MAT, followed by V-501 (0.805 mg, $2.87x10^{-3}$ mmol, 0.1 eq) in 244 µL of MeOD. Finally, 861 µL of MeOD was added to a final volume of 1.75 mL of MeOD in the mixture. The reaction flask was capped with a septum and connected to an NMR tube via cannula. The setup was deoxygenated by bubbling nitrogen through the solution for 45 min. At that time, 0.50 mL of reaction solution was transferred into the NMR tube. Polymerization was conducted in an NMR instrument at 70 °C while spinning the reaction tube at 20 Hz for 9 h. $^{1}$H-NMR spectra were acquired at various time points. The rest of the reaction mixture was kept in the refrigerator overnight.

Once the polymerization kinetics were established, the reaction mixture was removed from the refrigerator and deoxygenated by bubbling nitrogen through the solution for 45 min. The flask was placed in an oil bath pre-heated to 70 $^{o}$C. The reaction was allowed to proceed for 6 h to yield 77% monomer consumption and a targeted degree of polymerization of 50. The reaction was stopped by removing the septum and cooling the reaction mixture on ice. The reaction mixture was then transferred to a dialysis bag having a 3500 Da molecular weight cut-off. It was dialyzed against ultra-pure water acidified to pH 4-5 with HCl. Water changes were performed every 8-10 h. After 3 d of

dialysis, the polymer solution was frozen and lyophilized to yield 490 mg of white, fluffy material.

Polytrehalose (327 mg, $1.56x10^{-2}$ mmol, 1.00 eq) was dissolved in 3.00 mL of acetate buffer and the resulting solution was placed in a flask that contained aminoethylmethacrylamide hydrochloride (AEMA·HCl, 311 mg, 1.89 mmol, 121 eq). To this, 0.780 mL of a solution containing V-501 (0.44 mg, $1.56x10^{-3}$ mmol, 0.10 eq) was added and the flask was sealed. The solution was deoxygenated by bubbling nitrogen for 45 minutes. The flask was placed in an oil bath preheated to 70 $^{o}$C. Two 1.25 mL aliquots were removed with a syringe at 30 min ($PMAT_{51}$-b-$PAEMA_{34}$), 60 min ($PMAT_{51}$-b-$PAEMA_{65}$), and 90 min ($PMAT_{51}$-b-$PAEMA_{34}$). All three samples were dialyzed (3500 Da MWCO) against 3x4L of 0.5 M NaCl solution, followed by 3x4L 0.1 M NaCl and finally 6x4L of ultra-pure water. All dialysis media were acidified with HCl to pH 4-5. Polymer solutions were lyophilized to yield white, flocculent powders.

### 3.2.3 Size exclusion chromatography (SEC)

The number average molecular weight ($M_n$) and dispersity ($M_w/M_n$) for each polycation was determined by size exclusion chromatography (SEC) equipped with Eprogen columns [CATSEC1000 (7 μm, 50 × 4.6), CATSEC100 (5 μm, 250 × 4.6), CATSEC300 (5 μm, 250 × 4.6), and CATSEC1000 (7 μm, 250 × 4.6)], a Wyatt HELEOS II light scattering detector (λ = 662 nm), and an Optilab rEX refractometer (λ = 658 nm). The columns were maintained at 30ºC. An aqueous eluent (0.1M $Na_2SO_4$ / 1 v/v

% acetic acid) was utilized at a flow rate of 0.4 mL/min. And the dn/dc values for each of the polymers were determined offline with the Optilab rEX refractometer.

### 3.2.4 Proton nuclear magnetic resonance spectroscopy

$^1$H NMR measurements for the obtained glycopolymers were performed with a Varian Inova 300 at 70 ºC. Samples were dissolved in $D_2O$ (HOD used as the internal standard), and the block copolymer compositions were determined by calculating the ratio between the integrals of resonances of the PMAG block and those of the PAEMA or PDMAPMA block.

### 3.2.5 Polyplex formation and gel electrophoresis assay

The ability of each polymer to bind with pDNA and form polyplexes was qualitatively determined by gel electrophoresis. pCMV-luc plasmid DNA (1.0 μg, 0.02μg/μL) was mixed with an equal volume of each aqueous polycation solution (which were diluted to form polyplexes at various N/P ratios. The N/P ratio denotes the molar ratio of primary amine or tertiary amine (N) moieties in the amine block to the phosphate (P) groups on the pDNA backbone. After an incubation of 1 h, a 10 μL aliquot was run in a 0.6 % agarose gel containing 6 μg of ethidium bromide / 100 mL TAE buffer (40 mM Tris-acetate, 1 mM ethylenediaminetetraacetic acid (EDTA) for 45 min at 90 V.

### 3.2.6 Dynamic light scattering (DLS) and ζ potential

Polyplex sizes were measured by dynamic light scattering (DLS) at 633 nm with a Malvern Zetasizer Nano ZS. pCMV-luc (1.0 μg, 0.02 μg/μL) was incubated with an equal volume of each polymer at an N/P ratio of 5 and 10 for 1 h to form the subsequent

polyplexes. Thereafter, samples were diluted to 300 μL with either $H_2O$ or Opti-MEM. The samples were measured in triplicate at 25 ºC with a detection angle of 173º. For the study of colloidal stability of the polyplexes in Opti-MEM, samples were measured in triplicate at time intervals of 0, 2 and 4 h after dilution with Opti-MEM.

The ζ potential for each polyplex formulation was measured with the same instrument using a detection angle of 17º. The polyplexes were formed in nuclease-free water according to the aforementioned procedure at an N/P ratio of 5 and 10. After a 1 h incubation time, the polyplex solutions were diluted to 900 μL with nuclease-free water for measurement, and the ζ potential was measured in triplicate.

### 3.2.7 Regular transmission electron microscopy (TEM)

3.0 μL of the polyplexes solutions was applied onto a 300-mesh carbon coated copper grid (Ted Pella, Inc). The excess solution was wiped off with filter paper after 60s. Next a negative stain (3.0 μL 1% uranyl acetate solution) was applied in triplicate to the sample to facilitate visualization of the polyplexes in the TEM image. Imaging was operated in FEI Tecnai$^{TM}$ $G^2$ Spirit BioTWIN transmission electron microscope at 120 kV. Images were recorded using EagleTM 2k CCD camera, and phase contrast was enhanced at 10-12 μm underfocus. Images were saved as TIFF files and analyzed in software ImageJ 1.46r.

### 3.2.8 Cryogenic transmission electron microscopy (cryoTEM)

Polyplex solutions were prepared as described above at an N/P ratio of 5. CryoTEM samples were prepared using Vitrobot Mark IV (FEI). 3.0 μL of polyplex

solution was applied onto a lacey formvar/carbon grid (Ted Pella, Inc.), which was held by a pair of tweezers in humidity controlled (95%) chamber at 22 ºC. After the excess solution was blotted away using filter paper, the grid was quickly plunged into liquid ethane. The vitrified samples were then quickly transferred into liquid nitrogen for storage. For imaging, sample grids were transferred onto a Gatan 626 cryogenic sample holder in liquid nitrogen, and examined in FEI Tecnai$^{TM}$ $G^2$ Spirit BioTWIN $LaB_6$ transmission electron microscope at -178ºC, using an accelerating voltage of 120kV. Images were recorded using Eagle$^{TM}$ 2k CCD camera, and analyzed with FEI TEM Imaging and Analysis (TIA) software. Phase contrast was enhanced by imaging at about 10 μm under focus.

## 3.3 Results and discussion

### 3.3.1 Polymer synthesis and characterization

#### 3.3.1.1 The synthesis of PMAG-b-PDMAPMA glycopolymer series

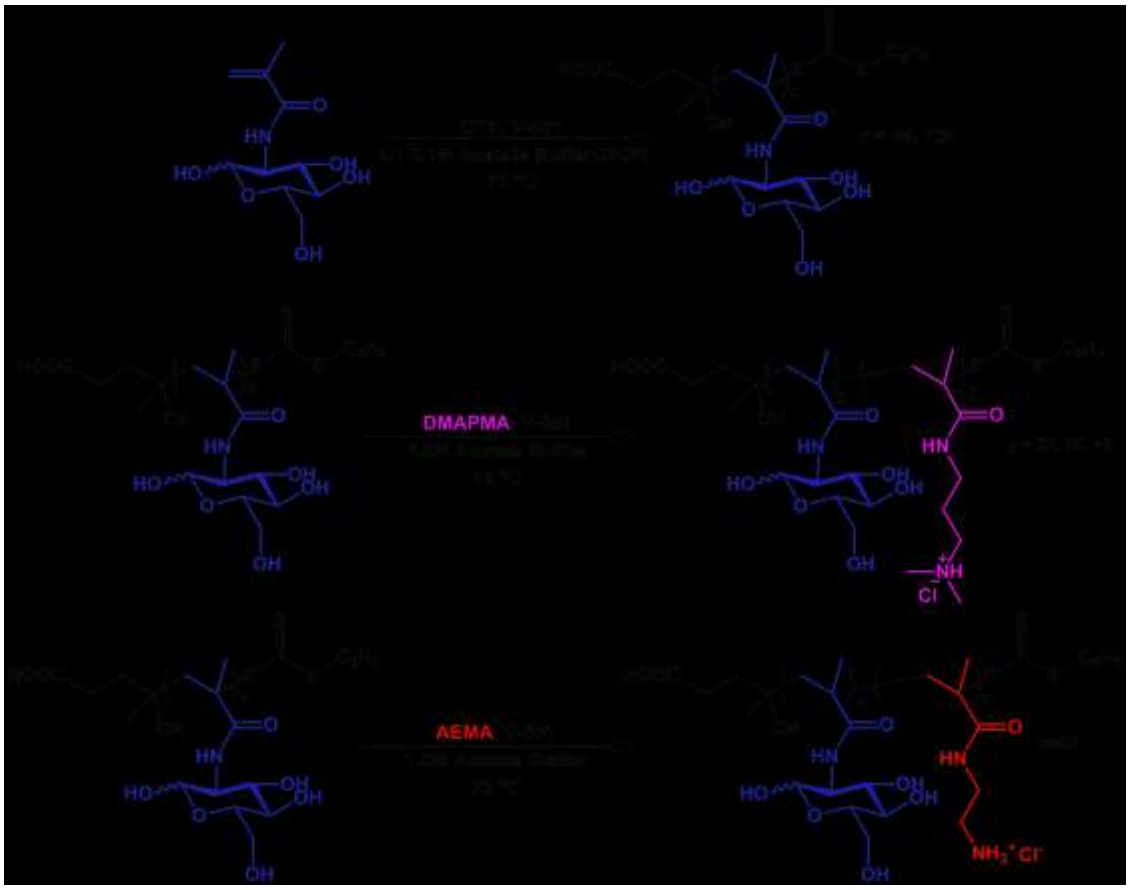


**Scheme 3.1** RAFT Polymerization of $PMAG_x$-b-$PDMAPMA_y$ and $PMAG_x$-b-$PAEMA_z$

Previously, our group reported a series of novel cationic diblock glycopolymers with various chain lengths and charge species as polymeric gene delivery vehicles.[10-11] The polyplexes formed from these series of diblock glycopolymers exhibited colloidal stability in cell media and had relatively low cytotoxicity. Moreover, both amine type and

cationic charge block length were demonstrated to greatly affect transgene expression efficiency *in vitro*.[11] To further understand how polymer structure impacts transgene expression, in particular, the role of the sugar and tertiary amine block length, aqueous RAFT polymerization was employed to synthesize well-defined cationic polymers and their activity was assessed for plasmid DNA delivery. Seven diblock copolymers were synthesized according to Scheme 3.1.

First, the kinetics of the polymerization of MAG was established using $^1$H NMR. 2-deoxy-2-methacrylamido glucopyranose (MAG), CPP, and V-501 (in molar ratio of 1500:10:1) was dissolved in the mixture of $D_2O$ acetate buffer with MeOD. Polymerization was conducted in an NMR instrument at 70 °C. And the data point was collected every 10 mins during polymerization. The seudo-first order kinetics of the monomer consumption rate was established, and shown in figure 3.1, revealing the controlled fashion of the RAFT polymerization of MAG. The polymerization kinetics of the macroCTA was also monitored using $^1$H NMR. Although the polymerization was slower overall, possibly due to the low reactivity of macroCTA, the seudo-first order of polymerization was still achieved over the initial 300 mins. The polymerization significantly slowed down after 300 mins, as shown in figure 3.2.

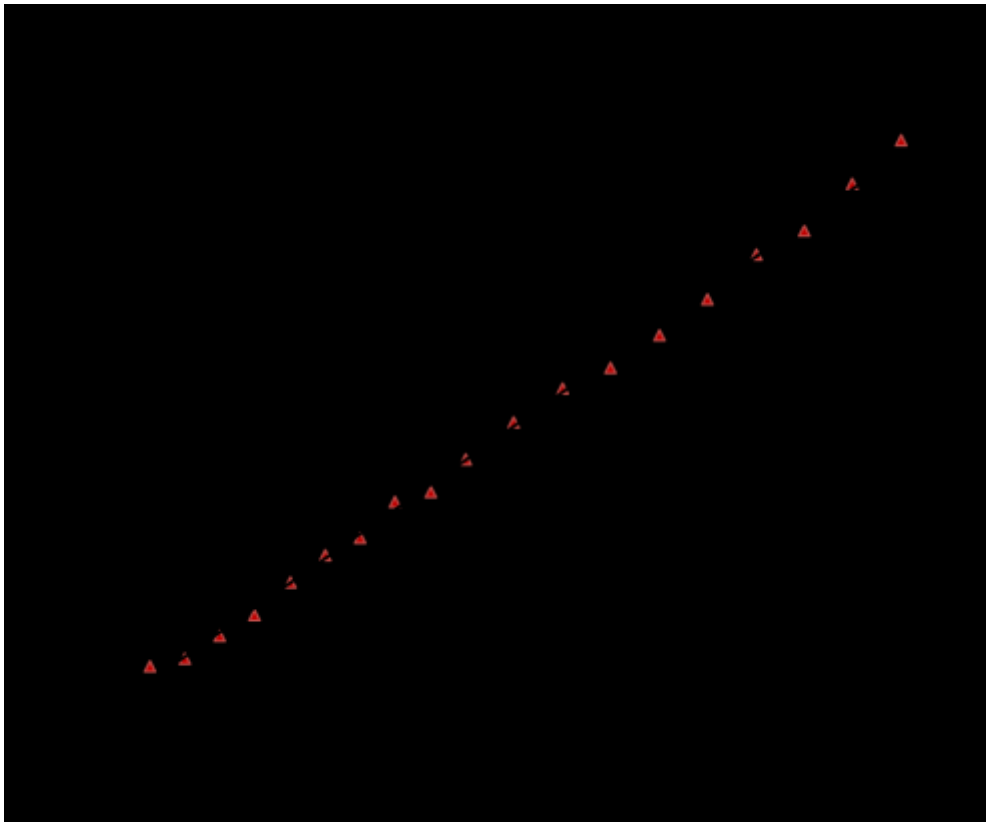

**Figure 3.1** Kinetics of RAFT polymerization of MAG

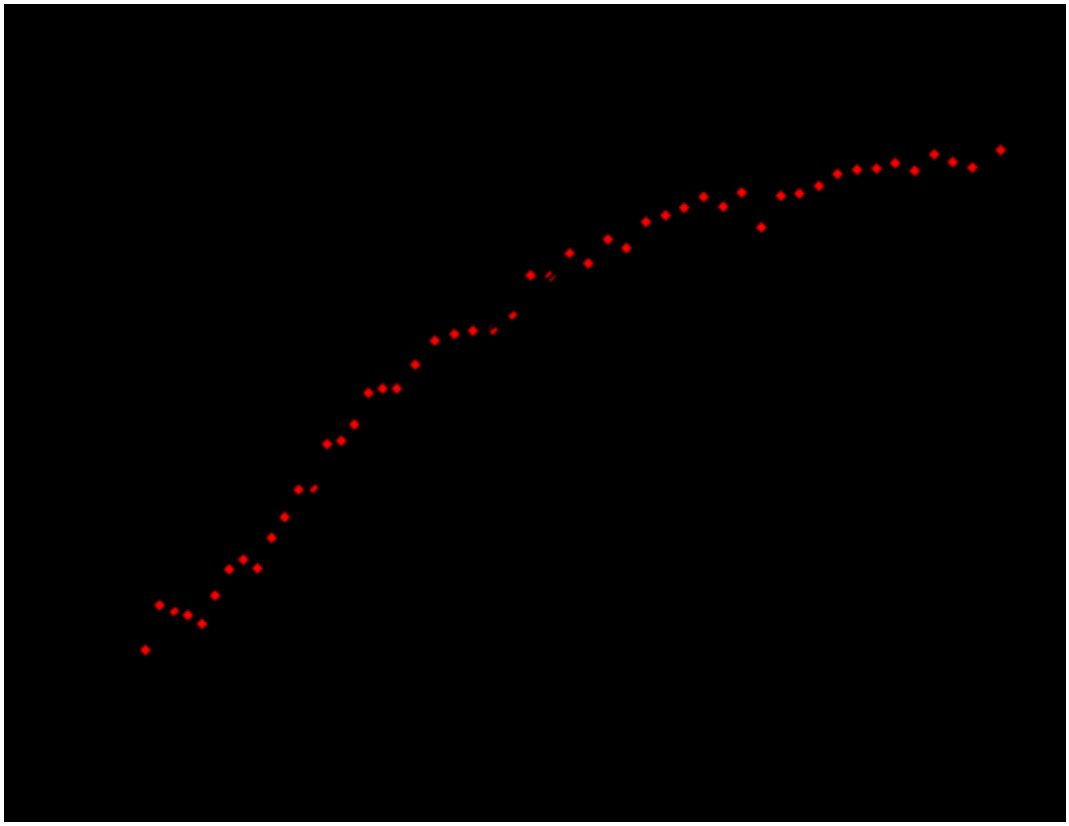

**Figure 3.2** Polymerization kinetics with macroCTA $PMAG_{61}$

Based upon the polymerization kinetics determined by $^{1}H$ NMR, two different lengths of PMAG were obtained (DP = 61 and 118) by quenching the polymerization at predetermined time points, and characterized by SEC (Figure 3.3). Both PMAG derivatives were utilized as a macroCTA for chain extension with either DMAPMA or AEMA to yield the cationic diblock glycopolymers. To prevent the aminolysis of the trithiocarbonate chain end, 1.0 M acetate buffer (pH=5.2) was selected as the reaction solvent. Various block lengths of DMAPMA were acquired by stopping the polymerization at predetermined time points according to the monomer conversion rate. For comparison, AEMA derivatives were synthesized with a block length similar to the

longest DMAPMA block length. The molecular weight and dispersity of all obtained diblock copolymers were determined by SEC chromatography (Figure 3.4). Narrow dispersity ($M_w/M_n \leq 1.1$) of the obtained copolymers indicates a highly controlled polymerization. The composition of the blocks was also confirmed by $^1$H NMR, shown below. Additionally, to probe the importance of the glucose block for our glycopolyplex delivery system, homopolymers of DMAPMA and AEMA were synthesized as controls following the scheme 3.2, for the subsequent studies discussed below. SEC traces of the homopolymers are shown in Figure 3.12 and 3.13. The molecular weight and dispersity of all the polymers are summarized in Table 3.1.

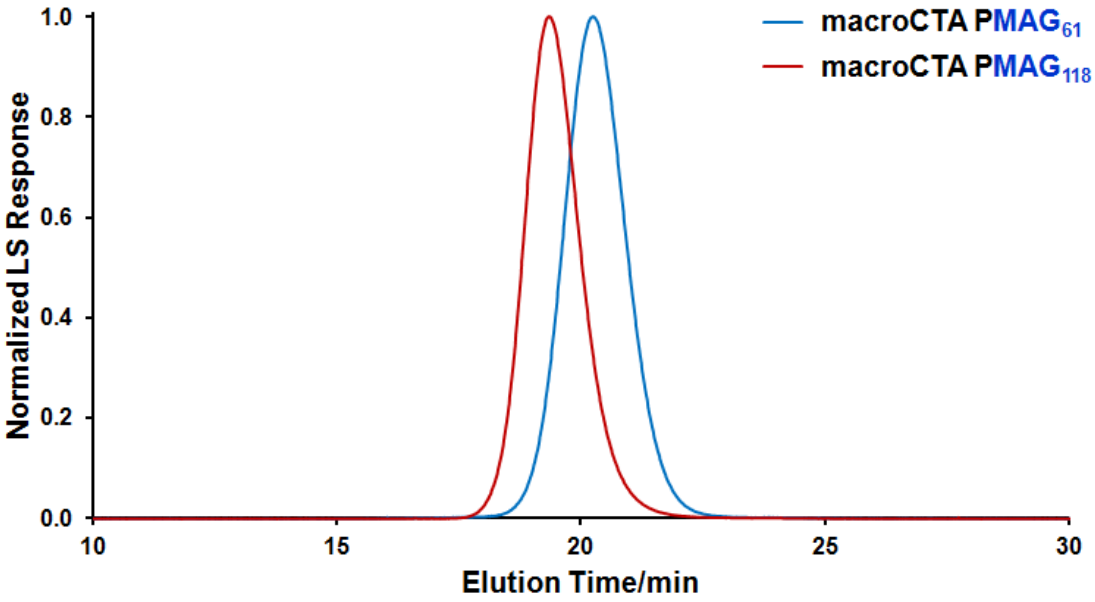


**Figure 3.3** SEC Traces of MacroCTAs

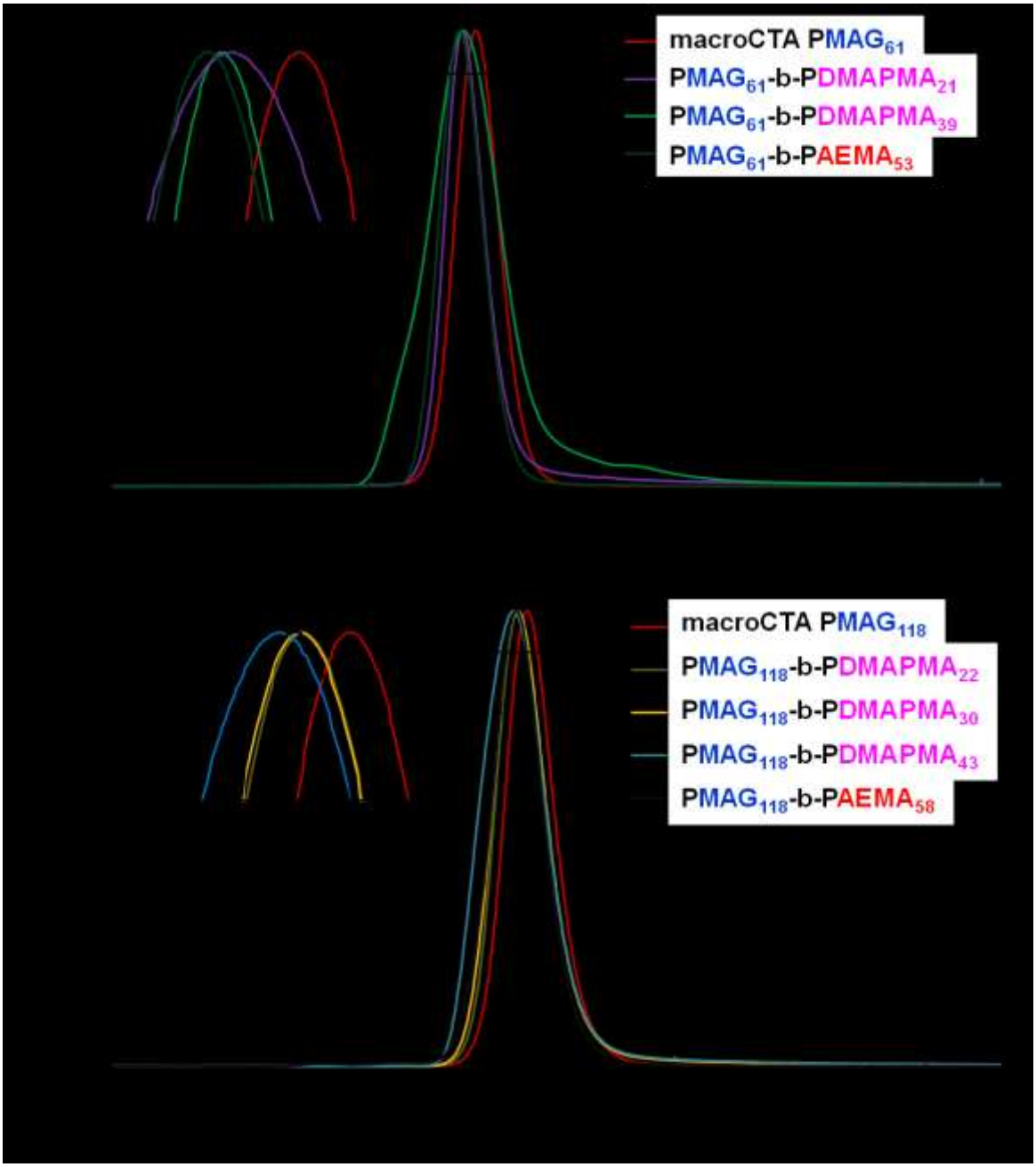


**Figure 3.4** SEC traces for the diblock glycopolymers, (a) $PMAG_{61}$ series; (b) $PMAG_{118}$ series

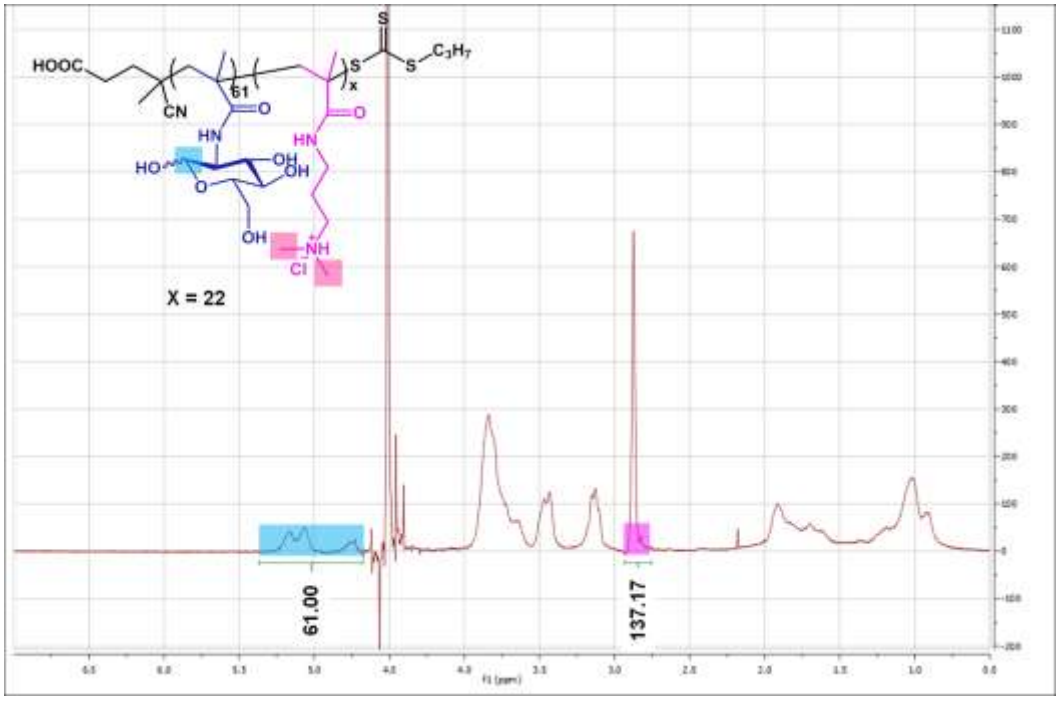


**Figure 3.5** $^{1}$H-NMR Spectra of diblock glycopolymers, $PMAG_{61}$-b-$PDMAPMA_{21}$

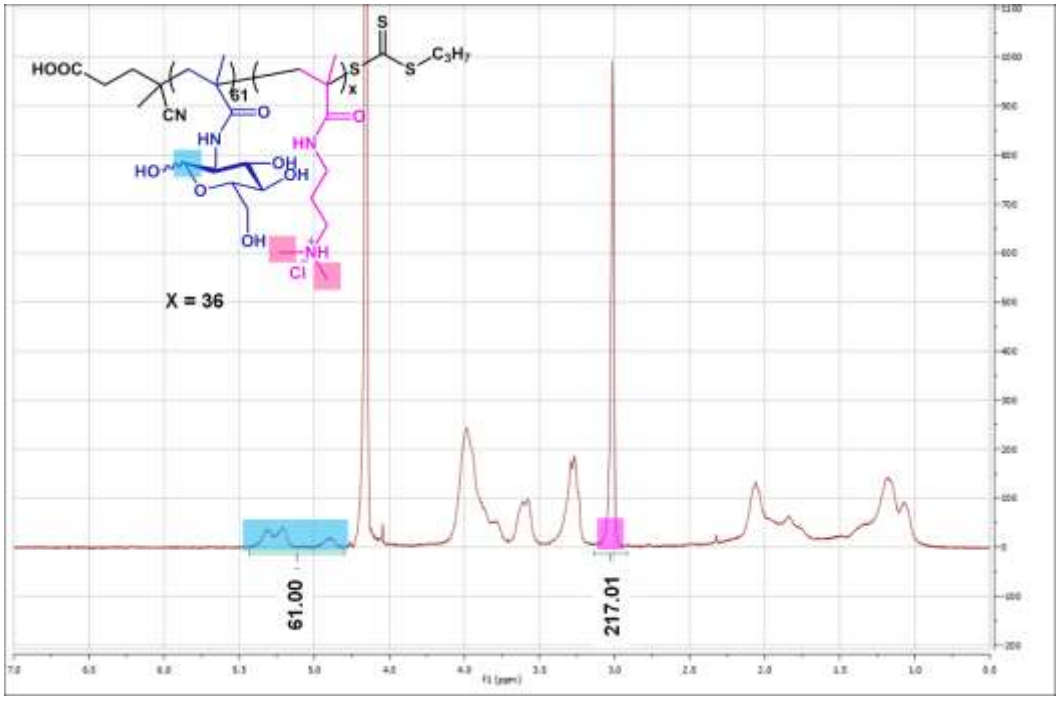


**Figure 3.6** $^{1}$H-NMR Spectra of diblock glycopolymers, $PMAG_{61}$-b-$PDMAPMA_{39}$

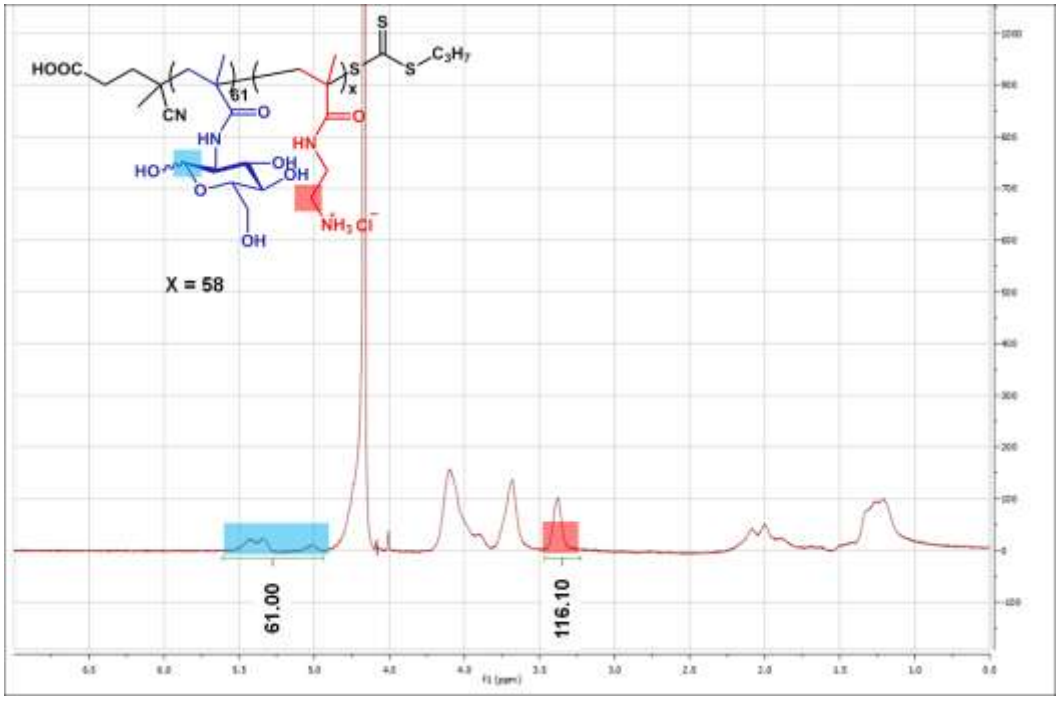


**Figure 3.7** $^{1}$H-NMR Spectra of diblock glycopolymers, $PMAG_{61}$-b-$PAEMA_{53}$

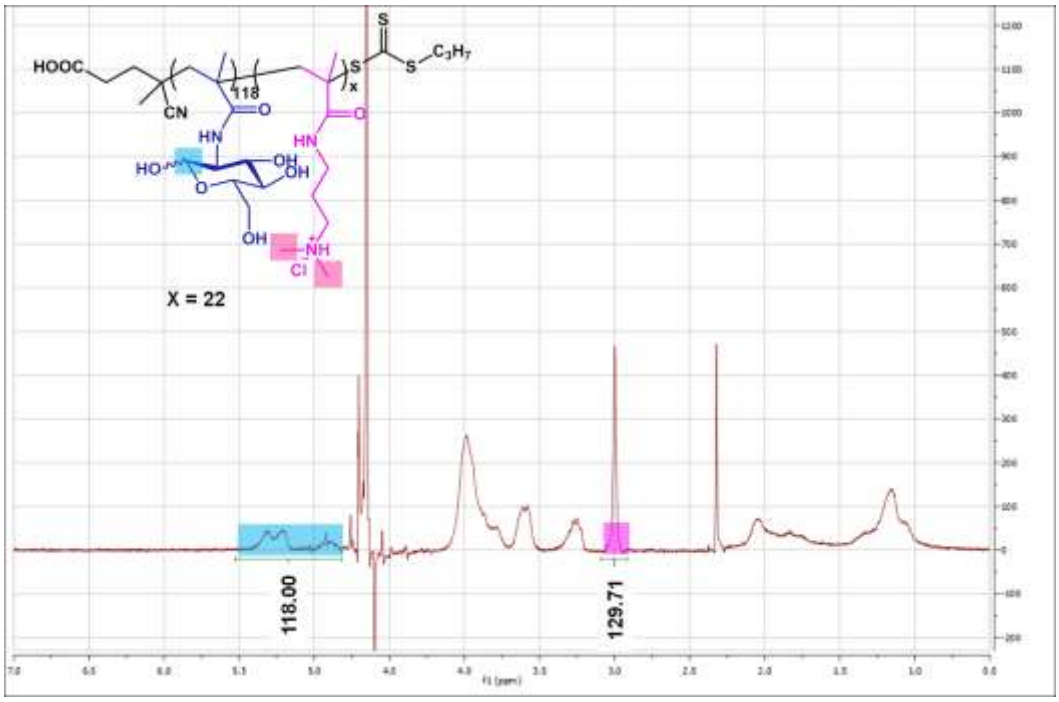


**Figure 3.8** $^{1}$H-NMR Spectra of diblock glycopolymers, $PMAG_{118}$-b-$PDMAPMA_{22}$

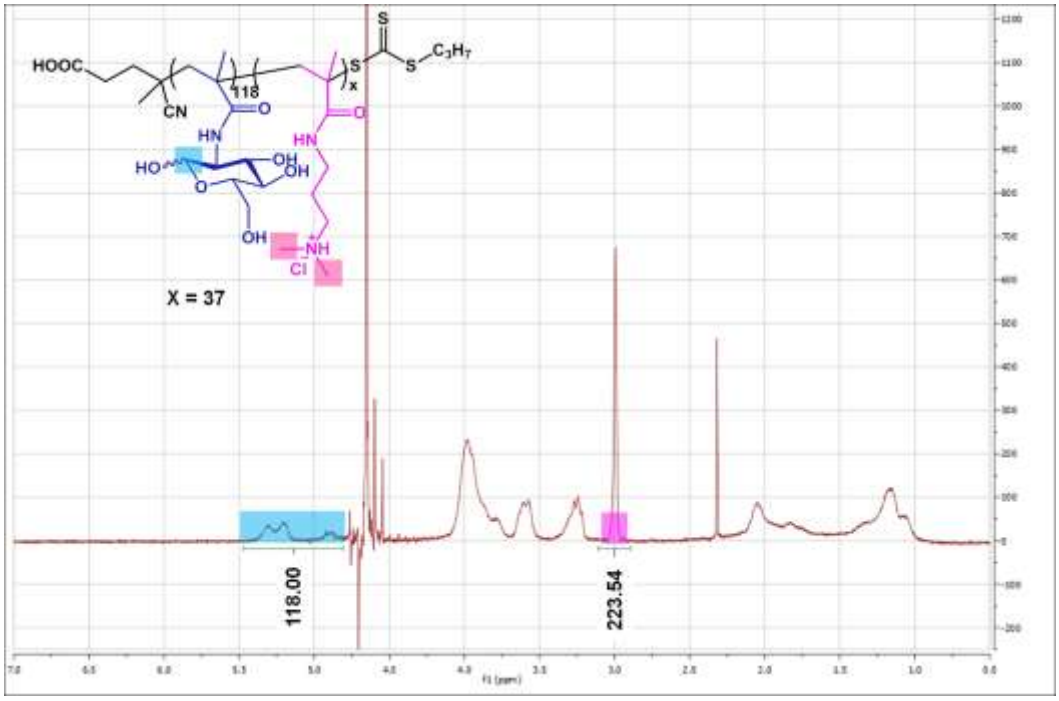


**Figure 3.9** $^{1}$H-NMR Spectra of diblock glycopolymers, $PMAG_{118}$-b-$PDMAPMA_{30}$

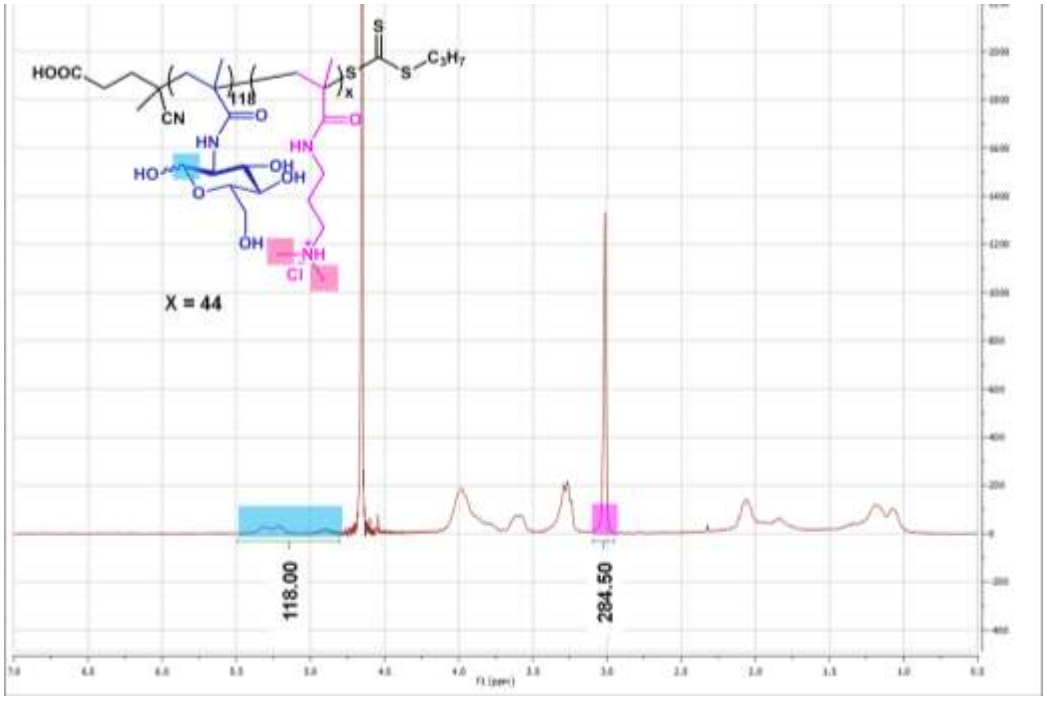


**Figure 3.10** $^{1}$H-NMR Spectra of diblock glycopolymers, $PMAG_{118}$-b-$PDMAPMA_{43}$

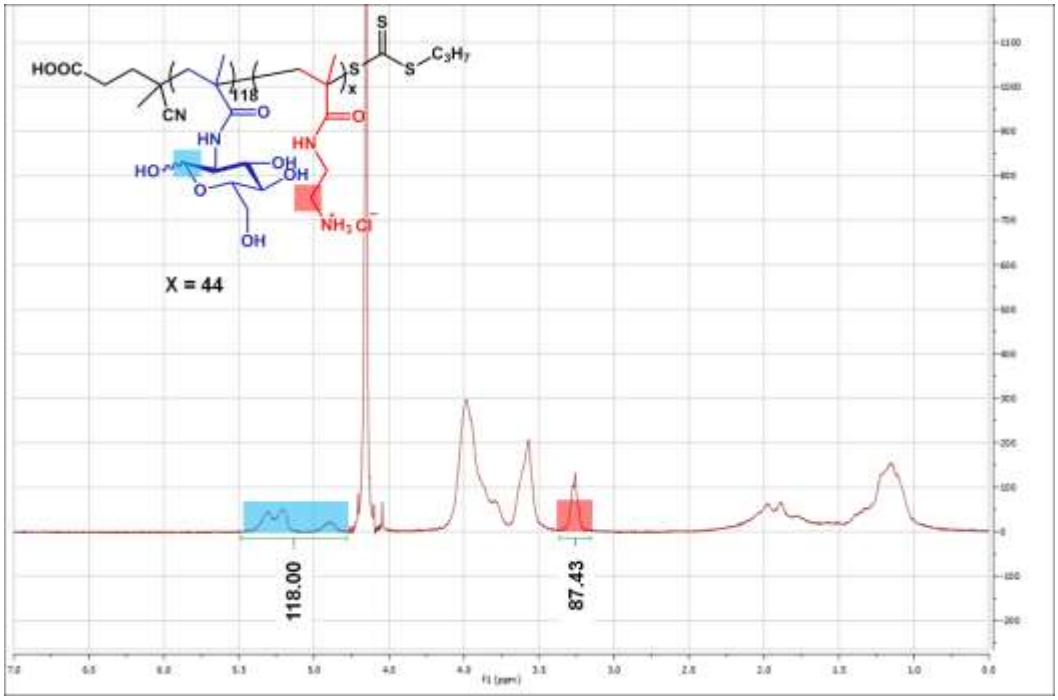


**Figure 3.11** $^{1}$H-NMR Spectra of diblock glycopolymers, $PMAG_{118}$-b-$PAEMA_{58}$

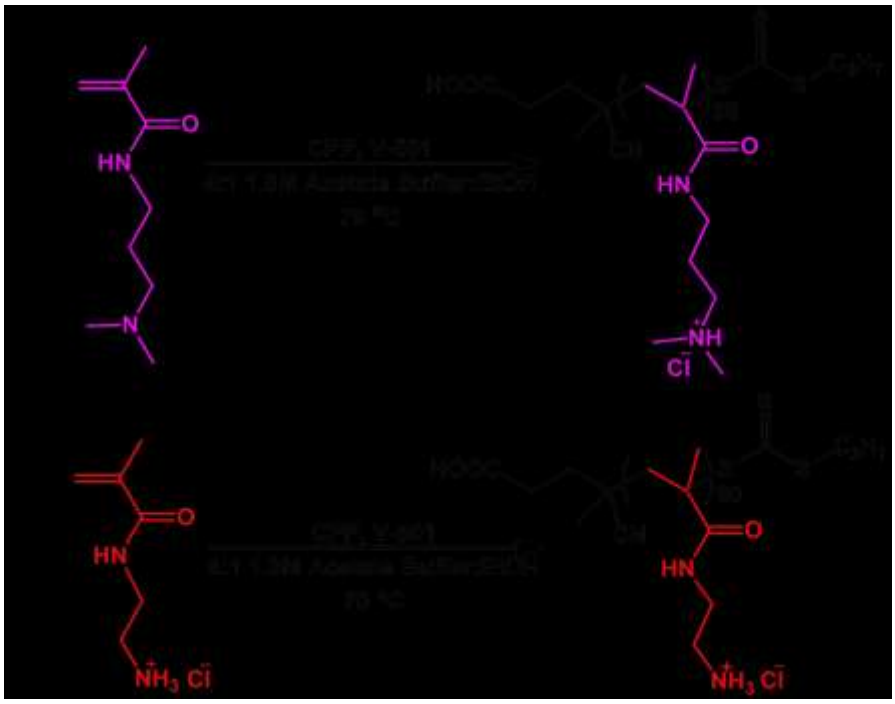


**Scheme 3.2** Polymerization of (a) DMAPMA and (b) AEMA.

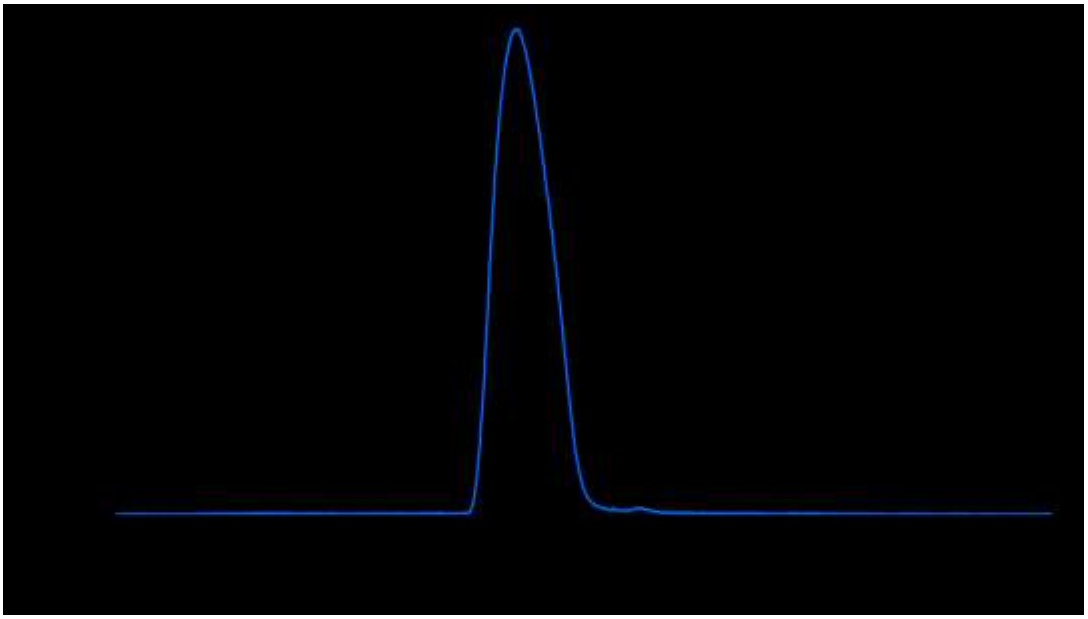

**Figure 3.12** SEC traces of the cationic homopolymers, PAEMA

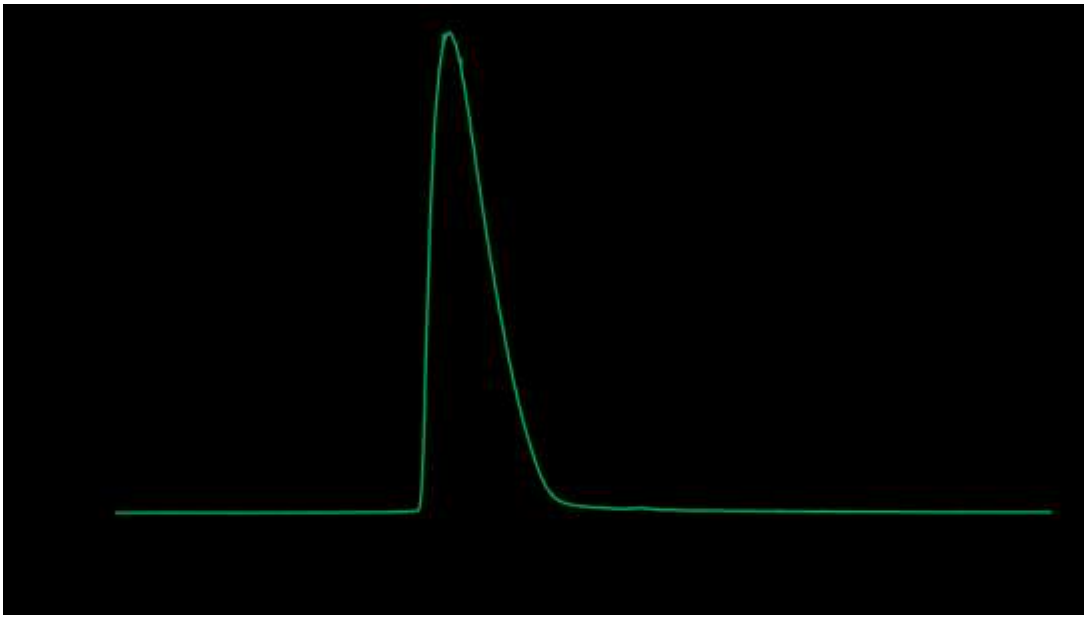

**Figure 3.13** SEC traces of the cationic homopolymers, PDMAPMA

**Table 3.1** Molecular weight, dispersity, and calculated degree of polymerization (DP) of the polymers examined in this study.

| Samples | $M_n$[a]/kDa | $M_w/M_n$[a,c] | MAG DP[a,b] | Amine DP[a,b] |
|---|---|---|---|---|
| $PDMAPMA_{60}$ | 11.4 | 1.41 | | 60 |
| $PAEMA_{58}$ | 7.3 | 1.10 | | 58 |
| $PMAG_{61}$ | 15.6 | 1.01 | 61 | |
| $PMAG_{61}$-b-$PDMAPMA_{21}$ | 19.2 | 1.02 | 61 | 21 |
| $PMAG_{61}$-b-$PDMAPMA_{39}$ | 22.1 | 1.10 | 61 | 39 |
| $PMAG_{61}$-b-$PAEMA_{53}$ | 24.4 | 1.01 | 61 | 53 |
| $PMAG_{118}$ | 29.5 | 1.03 | 118 | |
| $PMAG_{118}$-b-$PDMAPMA_{22}$ | 33.2 | 1.02 | 118 | 22 |
| $PMAG_{118}$-b-$PDMAPMA_{30}$ | 34.6 | 1.01 | 118 | 30 |
| $PMAG_{118}$-b-$PDMAPMA_{43}$ | 36.9 | 1.02 | 118 | 43 |
| $PMAG_{118}$-b-$PAEMA_{58}$ | 39.0 | 1.01 | 118 | 58 |

a. As determined by aqueous SEC using a flow rate of mL/min of 0.1 M $Na_2SO_4$ in 1.0 v% acidic acid, Eprogen CATSEC100, CATSEC300, and CATSEC1000 columns, a Wyatt HELEOS II light scattering detector ($\lambda$ = 662 nm), and an Optilab rEX refractometer ($\lambda$ = 658 nm). b. As confirmed by $^1$H NMR spectroscopy. c. Note: the dispersity was lower than the theoretical value for some samples, possibly due to the dialysis purification method.

### 3.3.1.2 The synthesis of polymethacrylate glycopolymer series

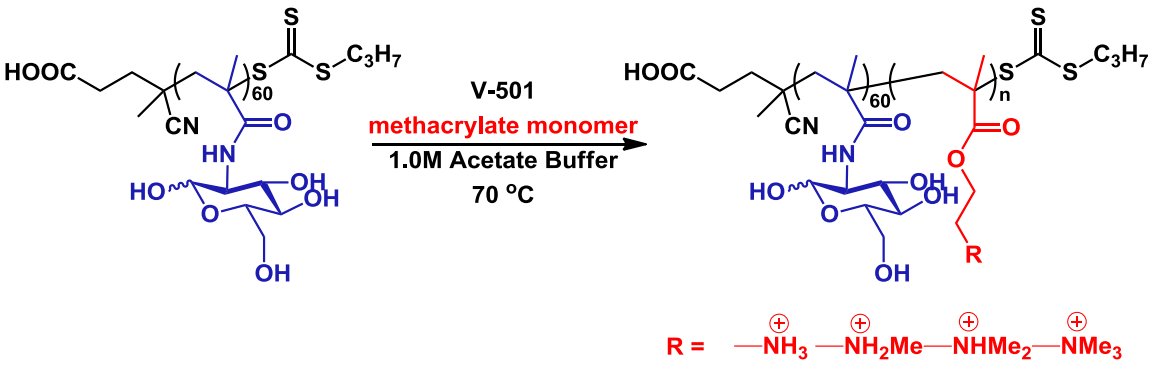


**Scheme 3.3** Preparation of the P(MAG-b-methacrylate) via RAFT polymerization

To further understand the role of charge type and block length of polymer gene delivery vehicles, a family of copolymers was generated comprising polyMAG and polymethacrylates of various block lengths bearing secondary, tertiary, and quaternary amine functionalities. To address the inability of the acrylamide-containing PMAG-b-PAEMA to release its genetic material, polymethacrylates were investigated. In general, methacrylates are more susceptible to hydrolysis than acrylamides, which may result in the destabilization of the polyplexes and allow for the release of genetic material.[20] The methacrylate monomers investigated include aminoethylmethacrylate (AEMT), *N*-methyl aminoethylmethacrylate (MAEMT), *N,N*-dimethyl aminoethylmethacrylate (DMAEMT), and *N,N,N*-trimethylammoniumethylmethacrylate (TMAEMT). It was expected that differing the amine groups and block lengths would create diverse binding capabilities due to the number and nature of the cationic amino/ammonium presented at the electrostatic binding site. Exploring the structural aspects of the cationic block of the glycopolymers may identify a polymer that balances high transfection efficiency with

low toxicity. It should be noted that polymers containing PDMAEMT charge groups have been investigated in the past for nucleic acid delivery and some structural differences have been explored for PDMAEMT and PTMAEMT.[21-23]

Cationic block copolymers of P(MAG-b-methacrylate) were prepared using RAFT polymerization with PMAG as macroCTA. The resulting polymers were purified by dialysis against water and then lyophilized yielding white powder. The $M_n$ and Đ for all of the obtained polymers were low, meaning the polymerizations were well controlled. Detailed characterization information for each polymer can be found in Table 3.2. GPC traces of $PMAG_{51}$-b-$MAEMT_{76}$ and $PMAG_{57}$-b-$TMAEMT_{71}$ are shown below. (Figure 3.14 and Figure 3.15) Three classes of polymers were created that contained PMAG blocks of similar length and charged polymethacrylate blocks (containing secondary, tertiary, and quaternary amines) of three different yet comparable lengths for a systematic comparison of the effects of amine type and block length on the in vitro pDNA delivery capabilities.

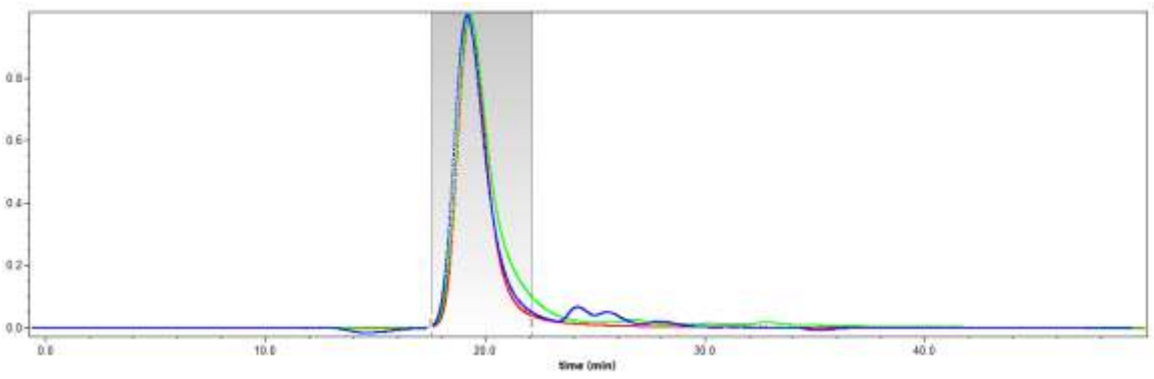


**Figure 3.14** GPC traces for $PMAG_{51}$-b-$PMAEMT_{76}$. (Red trace: light scattering; blue trace: refractive index; Green trace: UV)

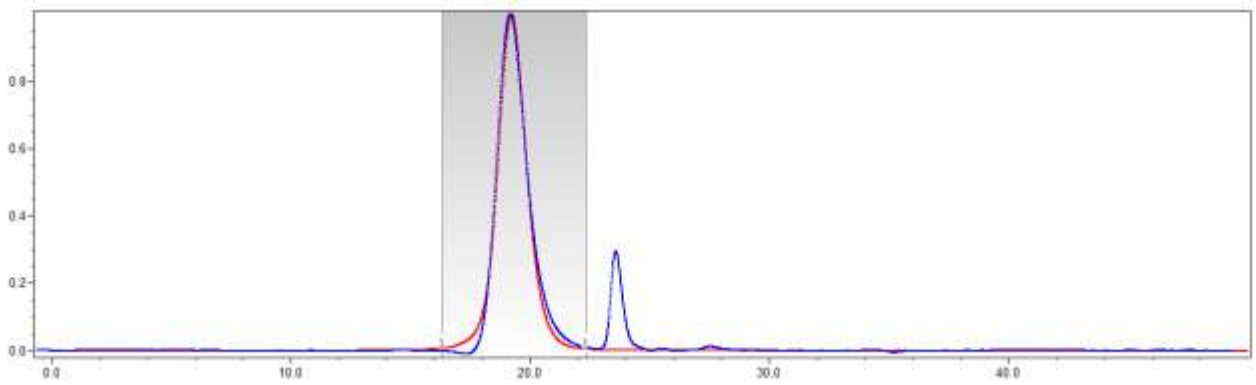


**Figure 3.15** GPC traces for $PMAG_{56}$-b-$PDMAEMT_{71}$. (Red trace: light scattering; blue trace: refractive index)

**Table 3.2** Molecular weight data for P(MAG-b-Methacrylate) containing the indicated charge block

| Samples | $M_n$ /kDa | $M_w/M_n$ | MAG DP | Methacrylate DP |
|---|---|---|---|---|
| $PMAG_{51}$-b-$MAEMT_{30}$ | 18 | 1.02 | 51 | 30 |
| $PMAG_{51}$-b-$MAEMT_{42}$ | 20 | 1.02 | 51 | 42 |
| $PMAG_{51}$-b-$MAEMT_{76}$ | 27 | 1.05 | 51 | 76 |
| $PMAG_{56}$-b-$DMAEMT_{32}$ | 20 | 1.02 | 56 | 32 |
| $PMAG_{56}$-b-$DMAEMT_{53}$ | 24 | 1.02 | 56 | 53 |
| $PMAG_{56}$-b-$DMAEMT_{71}$ | 28 | 1.03 | 56 | 71 |
| $PMAG_{57}$-b-$TMAEMT_{33}$ | 25 | 1.29 | 57 | 33 |
| $PMAG_{57}$-b-$TMAEMT_{48}$ | 29 | 1.06 | 57 | 48 |
| $PMAG_{57}$-b-$TMAEMT_{72}$ | 36 | 1.12 | 57 | 72 |

### 3.3.1.3 The synthesis of PMAT-b-PAEMA glycopolymer series

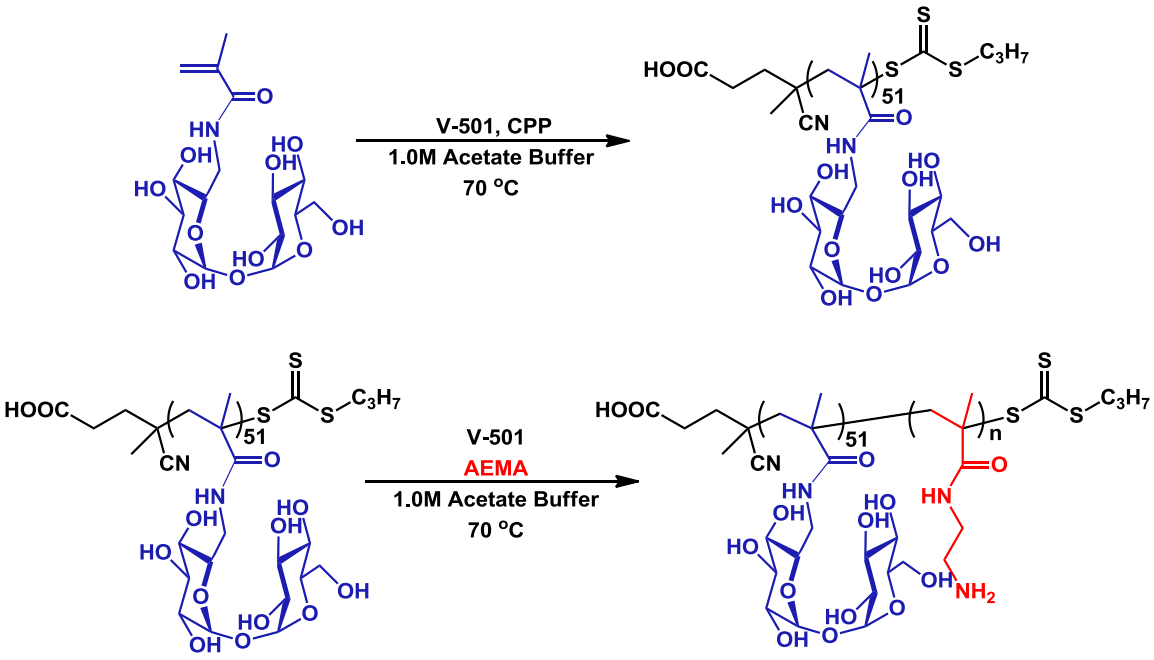


**Scheme 3.4** Preparation of the Polytrehalose macroCTA, and diblock glycopolymer PMAT-b-PAEMA via RAFT polymerization

In addition to glucose, α,α-D-trehalose could be utilized for stealthy coating materials development. This non-reducing disaccharide is composed of two α-1-linked glucose units and is very stable to acidic hydrolysis, even at high temperatures.[24] Trehalose is biosynthesized in many organisms but not in humans; however, the enzyme trehalase is expressed in humans, which promotes metabolism into glucose. Trehalose has also exhibited unique properties in many organisms, protecting cells during oxidative stress[25] and freezing[26]. For example, Selaginalla lepidophylla, whose 90% of the total plant sugar is trehalose, can restore the normal metabolism from desiccated state within

hours upon exposure to water.[27] Our group have shown that step-growth cationic polymers containing alternating units of ethyleneamines and trehalose in their backbones yield high cellular delivery efficiency of pDNA.[28] Tseng et. al. have shown that the presence of free trehalose in cell culture media enhances pDNA delivery by polyethyleneimine (PEI)-based complexes to various cell lines.[29] Wada et al. have demonstrated that a statistical co-polymer of trehalose and acrylamide inhibits the aggregation of amyloid β peptide, associated with Alzheimer's disease.[30] Maynard et al. recently demonstrated that lysozyme covalently attached to p-formylpolystyrene modified with trehalose via an acetonide moiety is capable of imparting both lyo- and heat protectant properties to this enzyme.[31] Herein, we hypothesized that the polytrehalose would impart an increase in the local viscosity on the particle surface, thus enhancing vitrification of the surface-bound water and colloidal stability during lyophilization and resuspension.[32] This poly(trehalose) motif was examined for the colloidal stability of siRNA polyplexes in salt, serum, and especially during the lyophilization process. Polytrehalose and PMAT-b-PAEMA diblock glycopolymers were synthesized via RAFT polymerization following the synthetic scheme 3.4. All polymers were analyzed by size exclusion chromatography equipped with static light scattering detector, exhibiting narrow peaks and expected peak position shift with increase in polymer molecular weight (Figure 3.16). Polymerizations were well controlled providing the final polymers with low dispersity. The molecular weight data was summarized in Table 3.3.

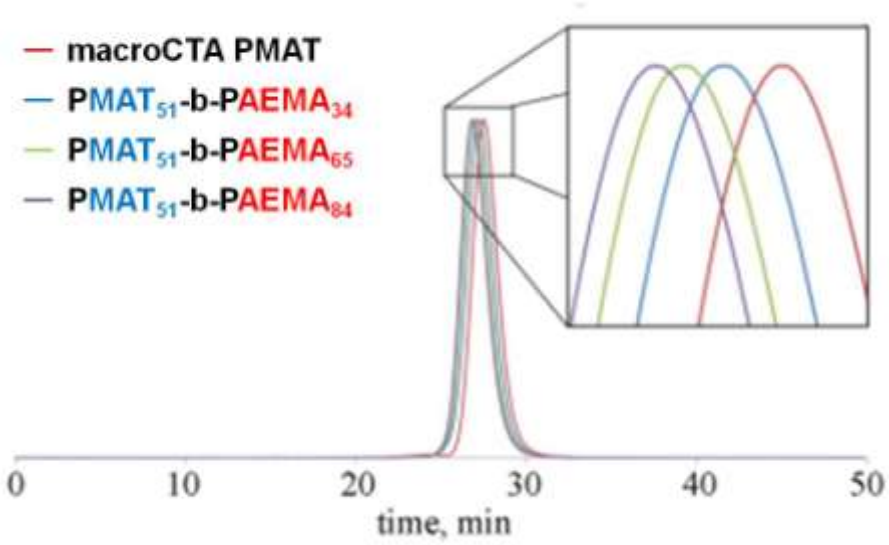


**Figure 3.16** SEC traces for the diblock glycopolymers PMAT-b-PAEMA

**Table 3.3** Molecular weight data for PMAT-b-PAEMA

| Samples | $M_n$ /kDa | $M_w/M_n$ | MAG DP | Amine DP |
|---|---|---|---|---|
| $PMAT_{51}$ | 21.0 | 1.04 | 51 | |
| $PMAT_{51}$-b-$AEMA_{34}$ | 23.4 | 1.04 | 51 | 30 |
| $PMAT_{51}$-b-$AEMA_{65}$ | 29.4 | 1.05 | 51 | 42 |
| $PMAT_{51}$-b-$AEMA_{84}$ | 31.8 | 1.06 | 51 | 76 |

### 3.3.2 The morphology of the glycopolymer polyplexes

#### 3.3.2.1 Gel electrophoresis assay

The nucleic acid binding ability of the obtained glycopolymers was examined through gel electrophoresis shift assays. plasmid DNA was mixed with an equal volume of each aqueous cationic glycopolymers solution at various N/P ratios. Subsequently, the polyplexes were applied into agarose gel, and nucleic acid migration was visualized using ethidium bromide. The gel images of PMAG-b-PDMAPMA pDNA polyplexes at various ratios between 0 and 50 are shown in the Figure 3.17. Figure 3.18 exhibits the gel images of P(MAG-b-methacrylate) series pDNA polyplexes at N/P ratio varying from 0 to 30. The migration of pDNA in the gel was completed hindered at N/P ratios above 4 for all of the samples.

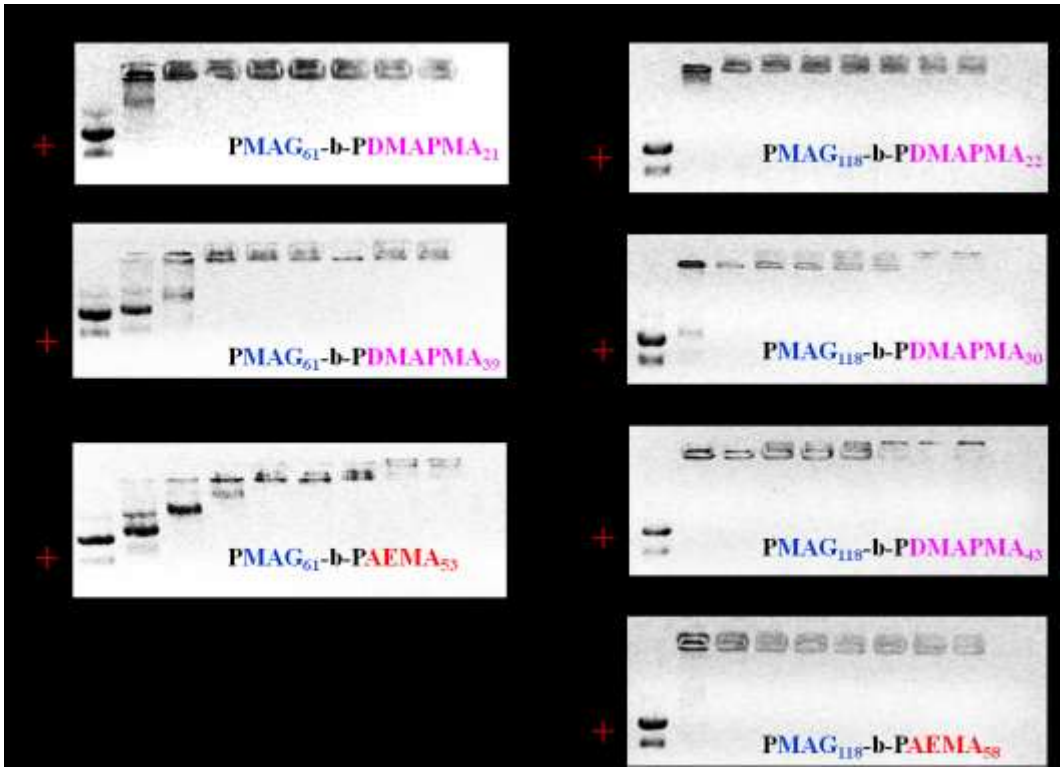


**Figure 3.17** Gel electrophoresis shift assay images of PMAG-b-PDMAPMA series pDNA polyplexes.

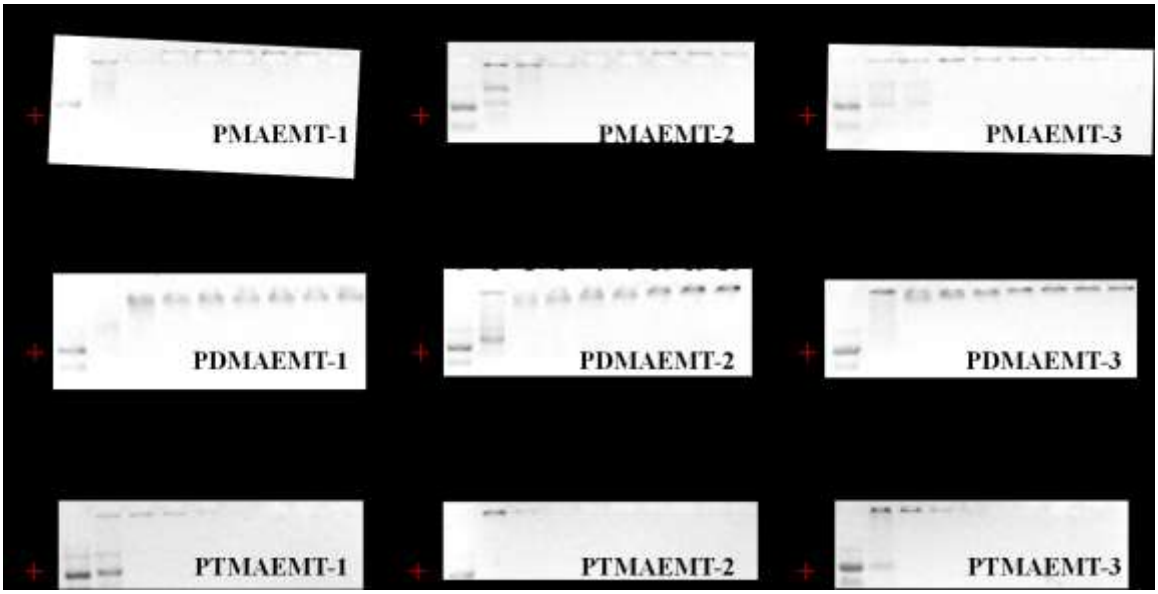


**Figure 3.18** Gel electrophoresis shift assay images of P(MAG-b-methacrylate) series pDNA polyplexes. (Courtesy of Dr. Haibo Li)

The three obtained PMAT-b-PAEMA series were examined for the binding ability to form complex with siRNA at N/P ratio between 0 and 20. Gel electrophoresis image is shown below (Figure 3.19). As evident from gel shift assay data, PMAT-b-PAEMA glycopolymers readily bind siRNA at low N/P ratios (around 3).

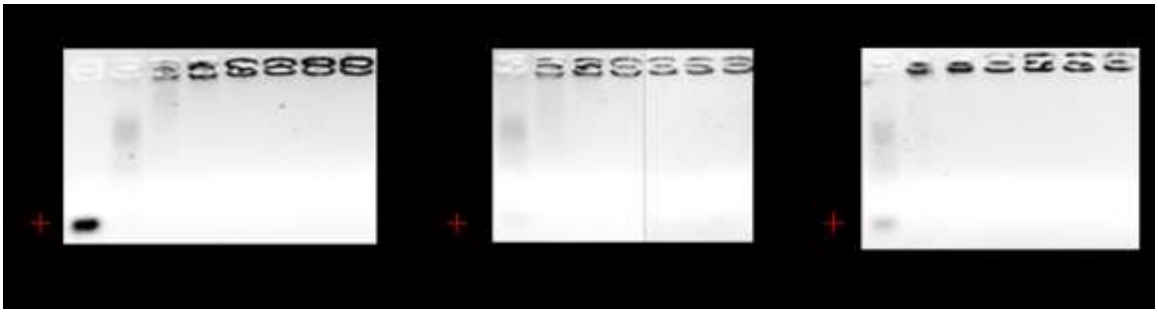

**Figure 3.19** Gel electrophoresis shift assay images of PMAT-b-PAEMA series siRNA polyplexes. (Courtesy of Dr. Antons Sizvos)

### 3.3.2.2 Dynamic light scattering and zeta potential of the obtained polyplexes

The hydrodynamic radius of polyplexes in nuclease-free water was determined to be between 50 and 100 nm via DLS, within the size range for cellular endocytosis. (Figure 3.18) Zeta potential values of the polyplex solutions formulated at N/P ratios of 5 and 10 in nuclease-free water were all between 10 and 40 mV. The positive ζ potentials can enhance nonspecific interaction of polyplexes with the cell membrane to trigger cellular uptake.[33] The zeta potentials of these polyplexes were also measured in Opti-MEM culture medium (Figure 3.19). The values were found to be relatively less positive, ranging from 0 to 10 mV, due to the presence of salt and amino acids in culture medium.

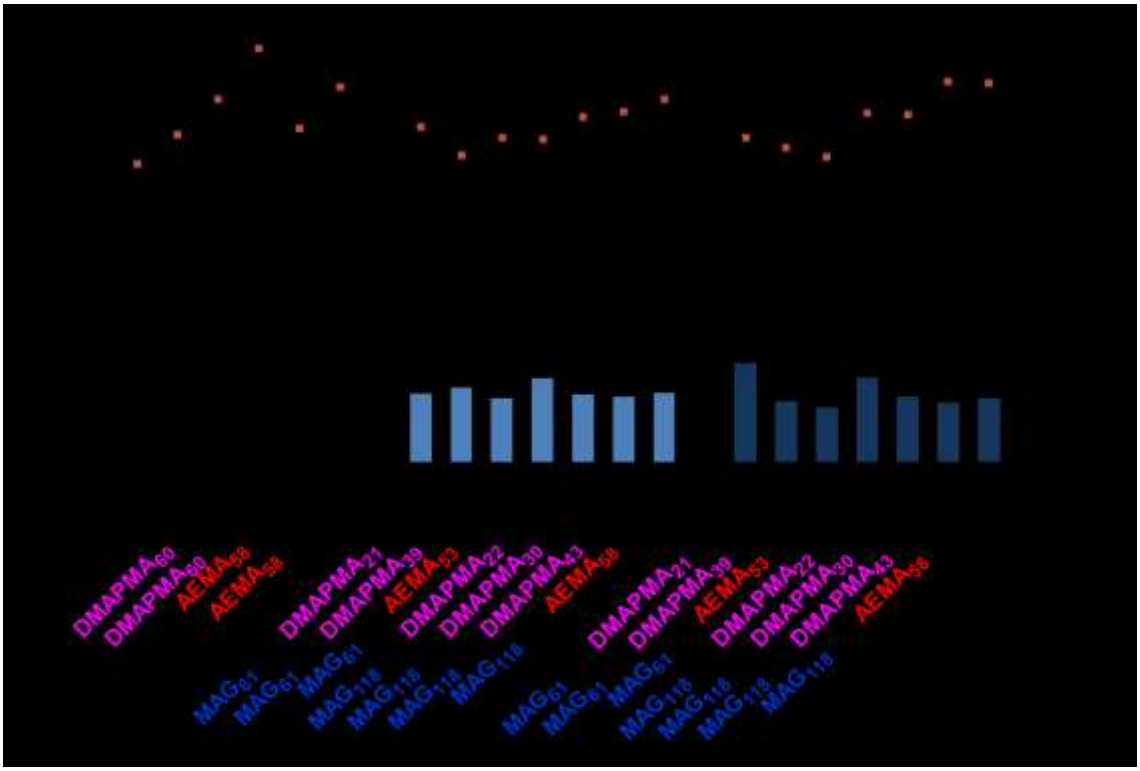


**Figure 3.20** Hydrodynamic radius and zeta potential of polyplex at N/P ratios of 5 and 10 in nuclease free water

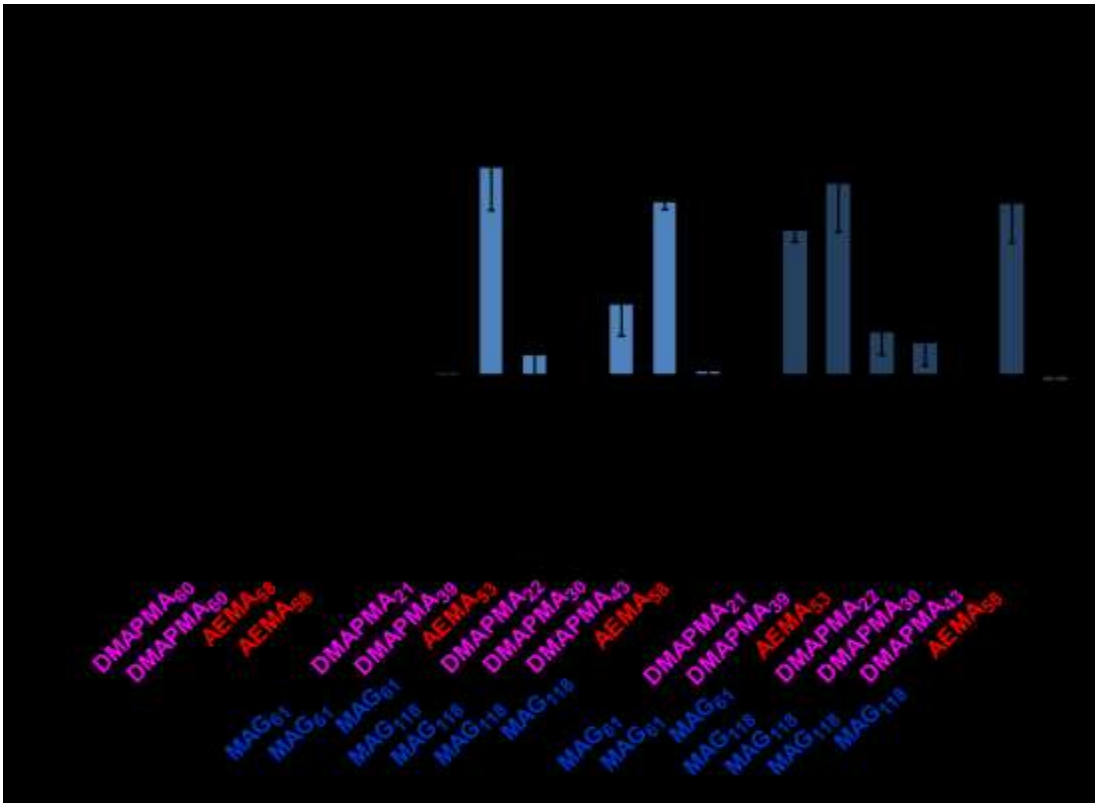


**Figure 3.21** Zeta potential of polyplex at N/P ratios of 5 and 10 in Opti-MEM

### 3.3.2.3 TEM imaging of the glycopolymer polyplexes

The size and morphology of glycopolymer polyplexes was characterized using characterized by TEM. (Figure) The morphology revealed by TEM were spherical, and the diameter of the particles measured from TEM images are typically smaller than those determined by DLS. The difference in size measured in the TEM images as compared to that observed via DLS could be due changes in the corona structure caused by dehydration in TEM sample preparation (DLS measures hydrodynamic radius). Additionally, the negative stain, uranyl acetate, is known to bind to phosphate moieties

on nucleic acids, which may allow visualization of the core only, resulting in observing a smaller polyplex size via TEM.[34]

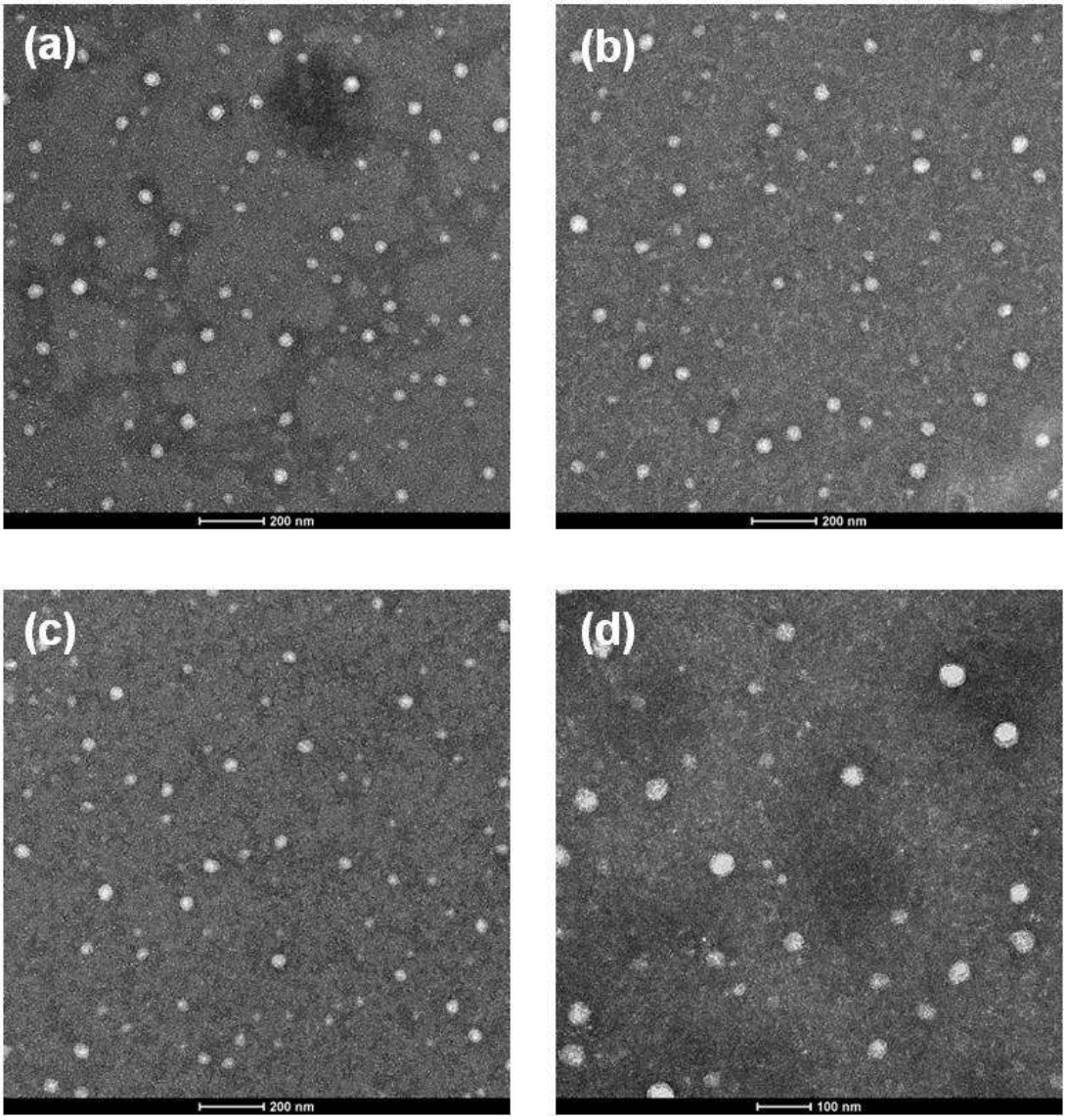


**Figure 3.22** Representative TEM image of pDNA polyplexes composed of (a) $PMAG_{118}$-b-$PDMAPMA_{22}$, (b) $PMAG_{118}$-b-$PDMAPMA_{30}$, (c) $PMAG_{118}$-b-$PDMAPMA_{43}$, (d) $PMAG_{118}$-b-$PAEMA_{58}$, at N/P ratio of 5

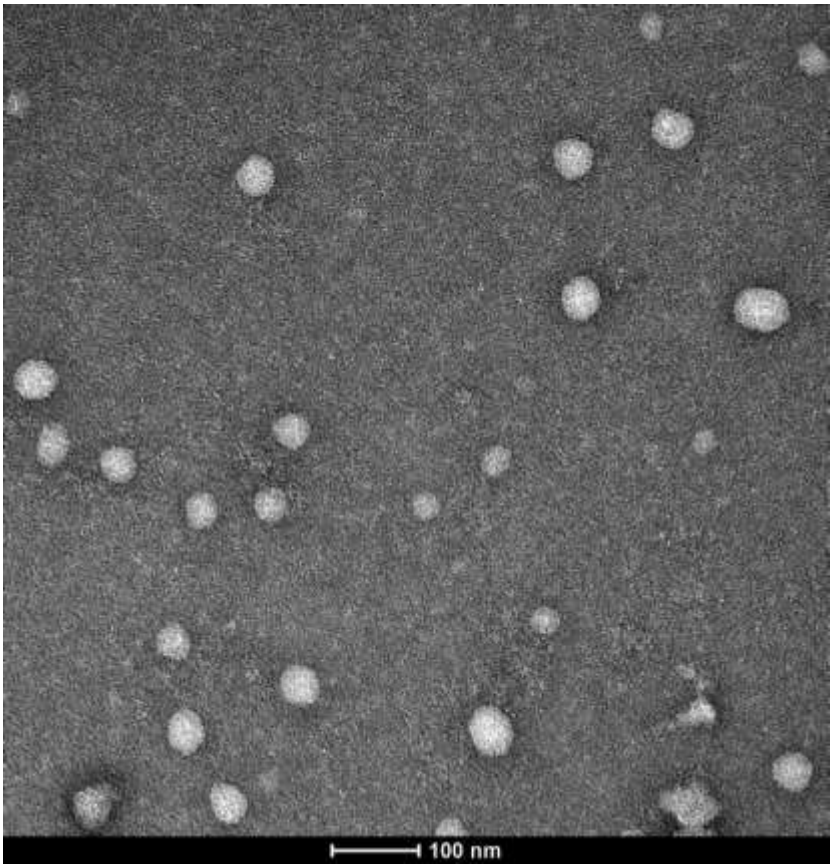


**Figure 3.23** Representative TEM image of pDNA polyplexes composed of $PMAG_{51}$-b-$MAEMT_{76}$ at N/P ratio of 15

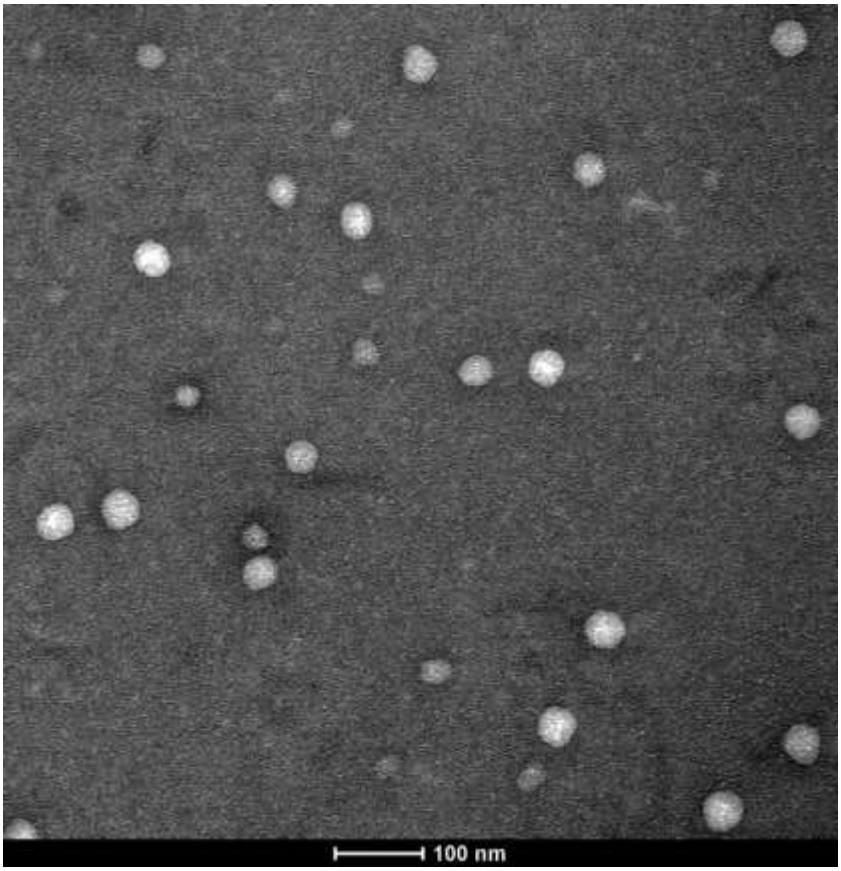


**Figure 3.24** Representative TEM image of pDNA polyplexes composed of $PMAG_{56}$-b-$PDMAEMT_{71}$ at N/P ratio of 15

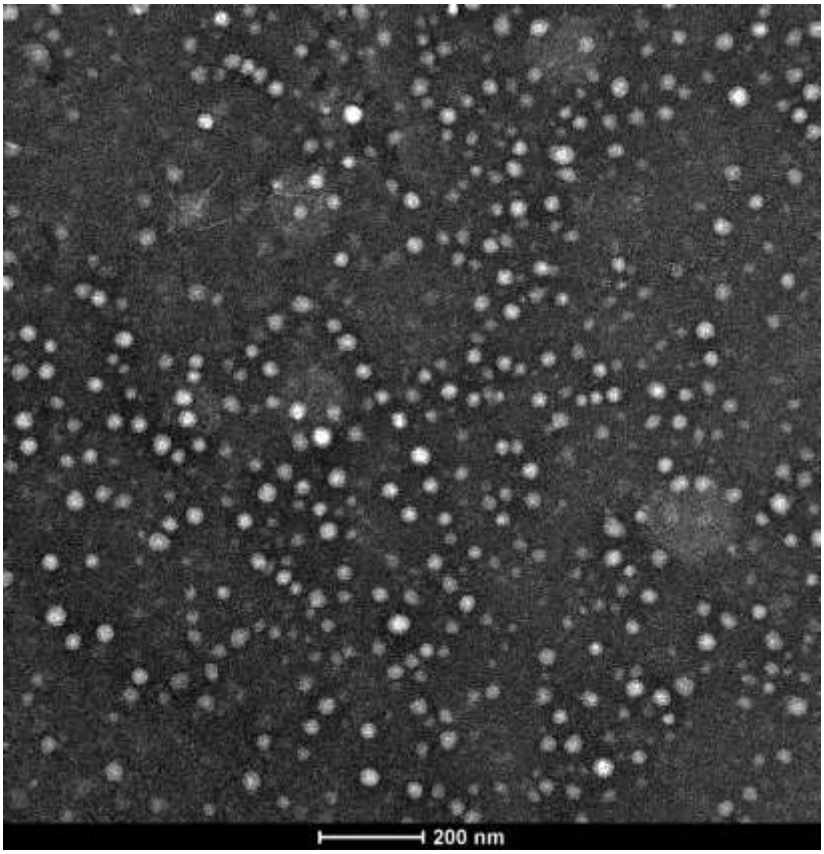


**Figure 3.25** Representative TEM image of siRNA polyplexes composed of $PMAT_{51}$-b-$PMAEMT_{65}$ at the N/P ratio of 10

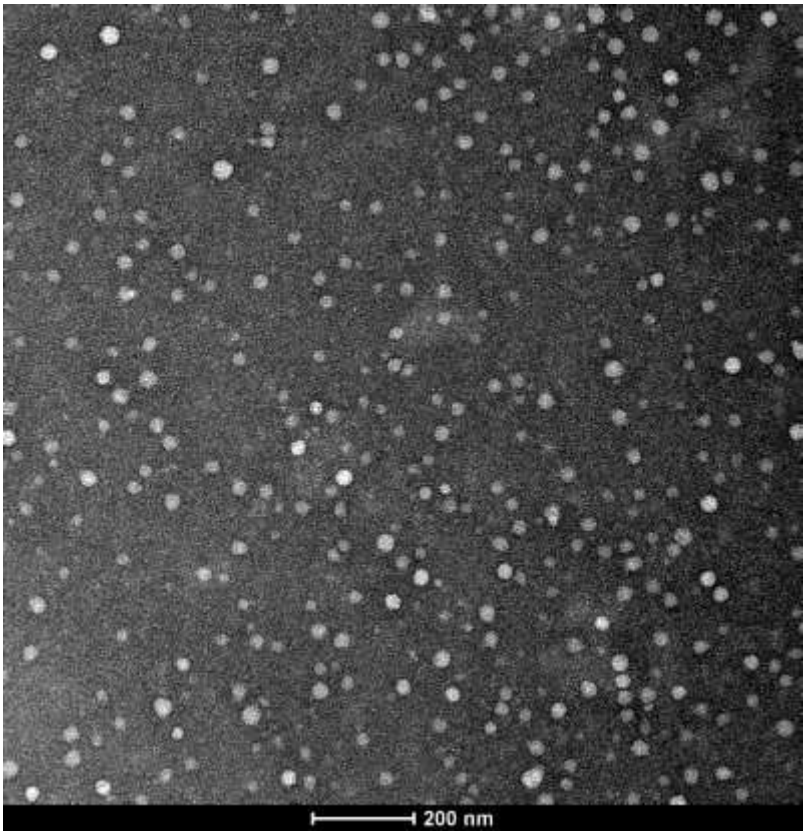


**Figure 3.26** Representative TEM image of siRNA polyplexes composed of $PMAT_{51}$-b-$MAEMT_{84}$ at N/P ratio of 10

### 3.3.2.4 Cryo- and lyo- protective properties of poly(trehalose) for polyplexes

The ability of a nanocarrier system to stabilize various cargo from degradation and aggregation during storage is an important feature for nucleic acid carriers designed for clinical use. For example, Kasper et. al. have shown that PEGylated poly(ethyleneamine) polyplexes containing plasmid DNA can be stabilized from lyophilization and resuspension by creating formulations with excipients such as free trehalose.[35] To demonstrate the cryo- and lyo-protective properties that poly(trehalose) imparts on the polyplexes, lyophilization was performed followed by resuspension of the

polyplex formulas in aqueous conditions. It should be noted that no excipients, nor separate cryo- or lyo-protectants were added to the formulation. After freezing, the polyplex solutions were completely lyophilized to isolate the polyplexes as a white solid (this process also physically aggregates the polyplexes). TEM and DLS was employed to characterize the morphology and size of the polyplexes before and after lyophilization. Remarkably, at both N/P ratios examined (5 and 10), subsequent resuspension of the solid polyplex powder in water yielded isolated nanoparticles that retained their compact size and shape, as determined via TEM imaging (Figure 3.27) and DLS (Figure 3.28). At both N/P ratios, polymer $PMAT_{51}$-b-$PAEMA_{34}$, which has the greatest trehalose content among the three synthesized polymers, appeared to yield optimal results for facilitating the stable resuspension of the polytrehalose-coated polyplexes. TEM imaging, used to visually evaluate the effect of lyophilization on the size and shape of the polytrehalose containing polyplexes made from $PMAT_{51}$-b-$PAEMA_{34}$, revealed visual images of the polyplexes. Following lyophilization and reconstitution, these polyplexes did not change in size and shape. According to TEM, the average core diameter of the polyplexes before lyophilization is 22 ± 4 nm, while the diameter after lyophilization is 31 ± 7 nm, supporting the DLS data in Figure 3.28. It should be noted that the slight difference in size of polyplexes in the TEM images compared that observed via DLS is due to the nature of the sample preparation where complexes are in their dehydrated state in the TEM image as opposed to DLS, where hydrodynamic diameter is observed

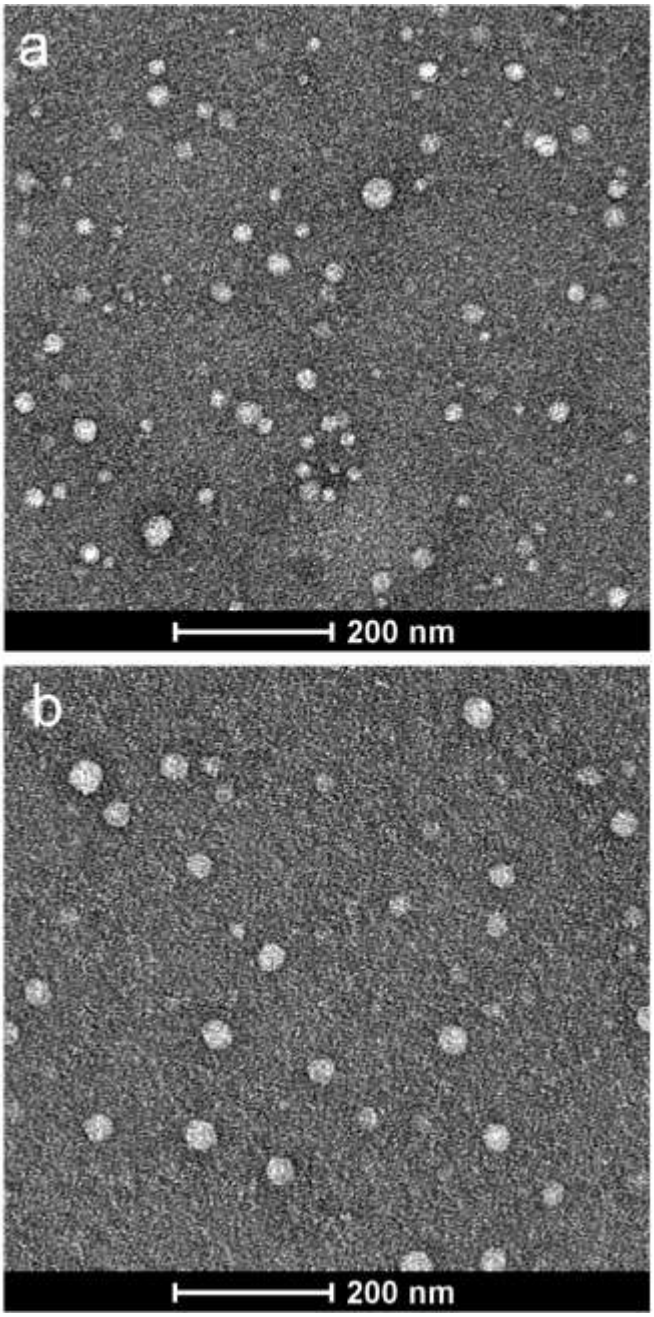


**Figure 3.27** TEM of polyplexes formulated with $PMAT_{51}$-b-$PAEMA_{34}$ and siRNA at an N/P ratio of 10. (a) Image of $PMAT_{51}$-b-$PAEMA_{34}$ polyplexes freshly-prepared in water, and (b) Image of $PMAT_{51}$-b-$PAEMA_{34}$ polyplexes that have been lyophilized to a solid powder and resuspended in water.

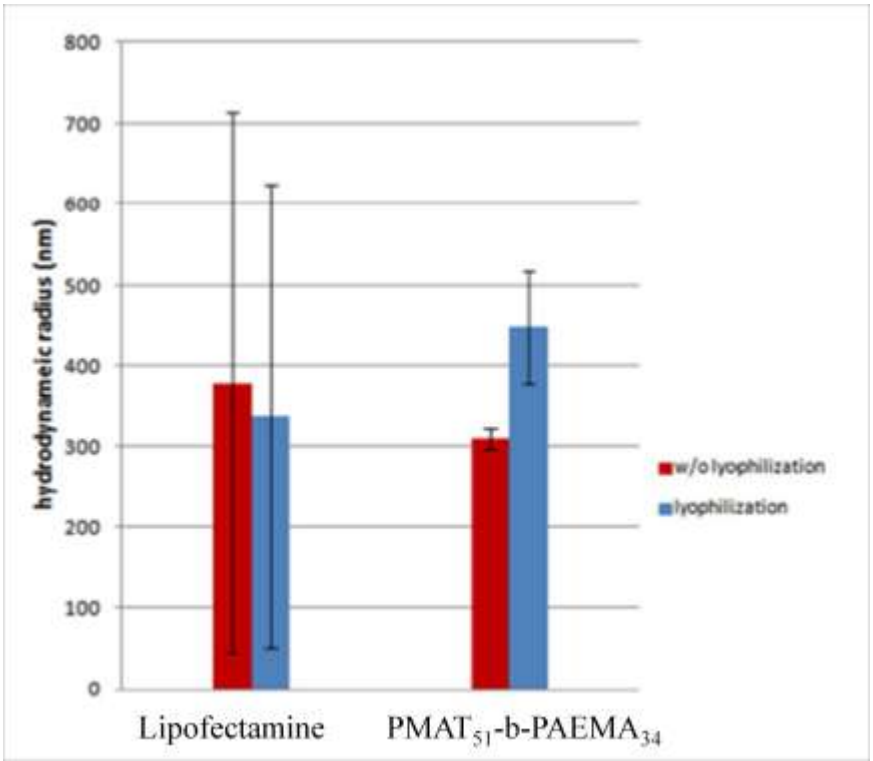


**Figure 3.28** Dynamic light scattering of Lipofectamine siRNA polyplexes and PMAT51-b-$PAEMA_{34}$ before and after lyophilization. Error bars represent the standard deviation of analyzed data from three replicates. (Courtesy of Dr. Zachary P. Tolstyka)

### 3.3.2.5 CryoTEM imaging of the PMAG-b-PDMAPMA pDNA polyplexes

Because of the possibly artifact that could be introduced by negative staining, cryogenic transmission electron microscopy (cryoTEM) was also employed to characterize the native morphology of polyplexes in water. The cryoTEM imaging could reveal the morphology without the impact of the dehydration during sample preparation. During cryoTEM imaging process, it is essential to distinguish the image of samples from the possible background contamination.

To identify whether the particle observed is within the amorphous ice layer, the common procedure is to vary the electron beam focus, from under focus to over focus, which is indicated by Fresnel fringe. Figure 3.29 illustrates the images of polyplexes with different focus. Dark fringe surrounding the lacey structure indicates the image was taken under focus, while bright fringe indicates the over focus imaging. Regardless of the focus level, the bark particles captured in the images did not ‘stand out’ of the surface, confirming that the observed particles are in the sample solution.

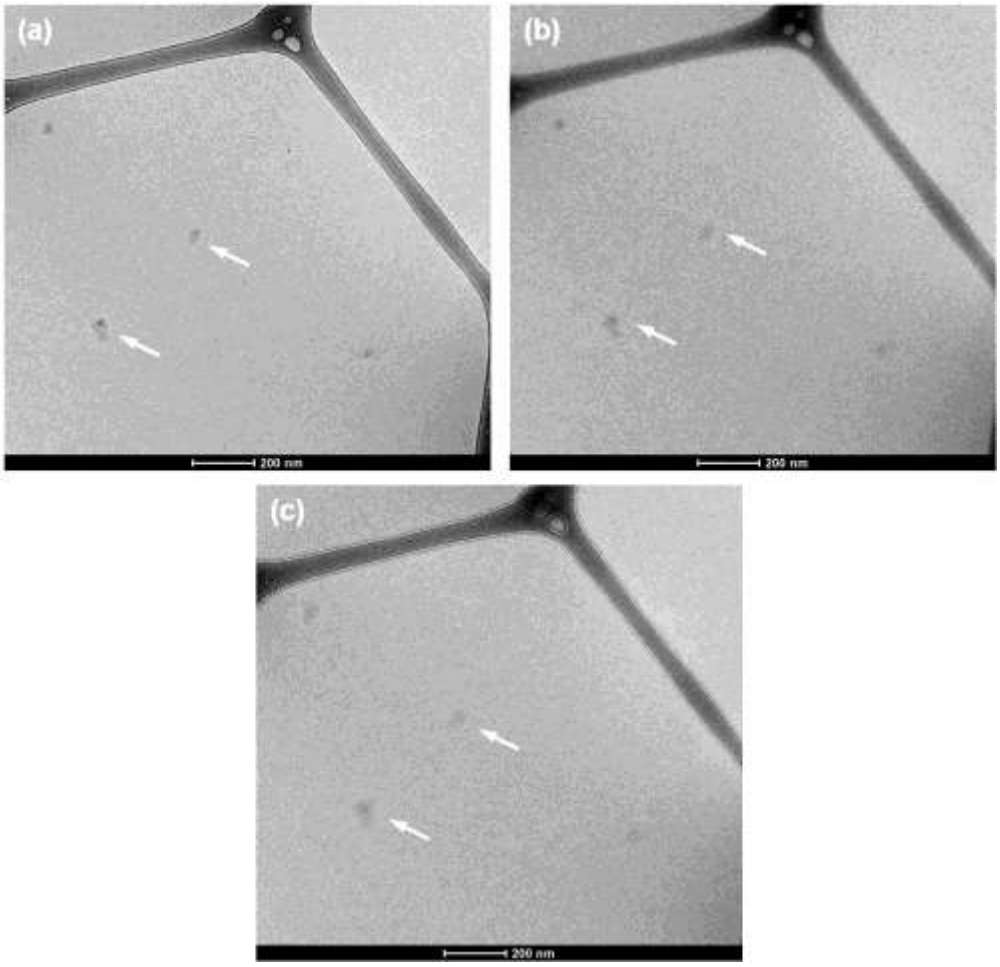


**Figure 3.29** Focus adjustment for cryoTEM of polyplexes: (a) under focus, (b) true focus, (c) over focus

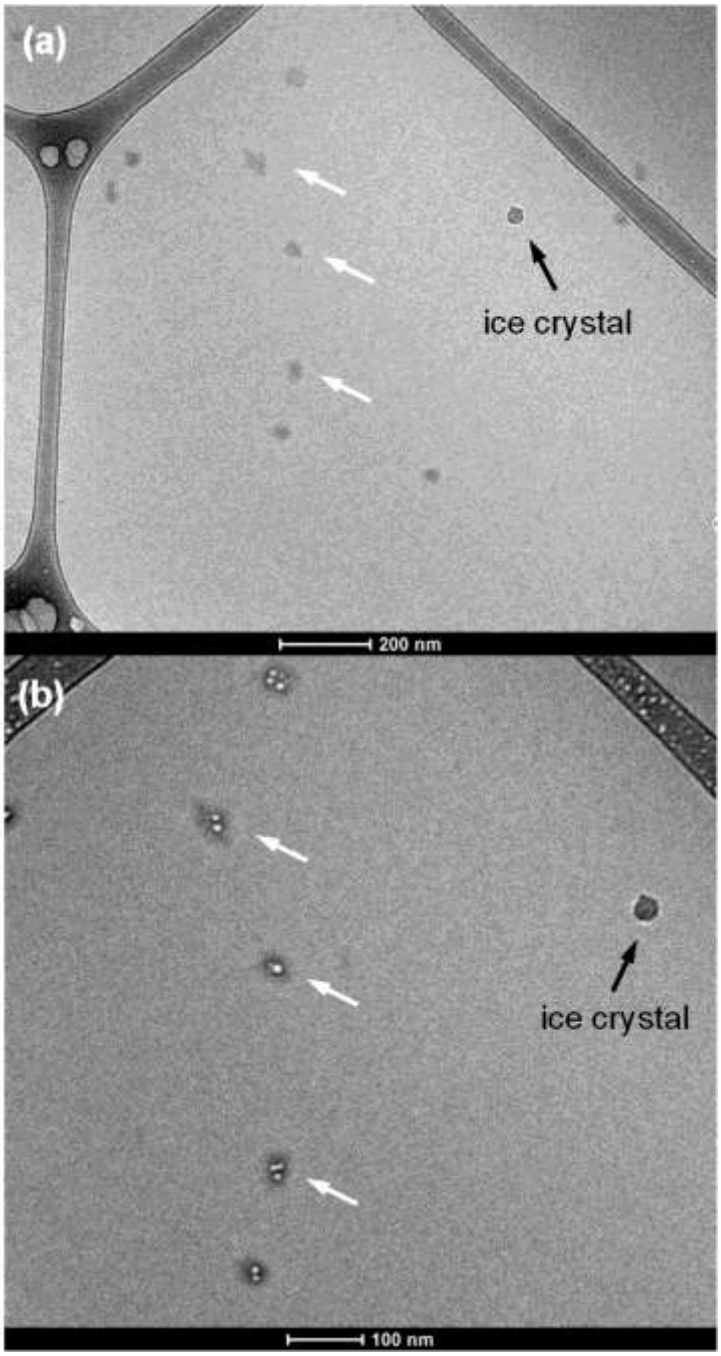


**Figure 3.30** Beam damage in the cryoTEM image of polyplexes (a) initial structure; (b) beam damage caused by long exposure of high energy electrons

One important characteristic of the biological sample is that they are susceptible to beam damage after long exposure to electron beam. Beam damage, i.e. radiolysis, is the specimen structure change caused by the breaking of chemical bonds and ionization by inelastically scattered electrons, through free-radical chain reaction.[13] Radiolysis is especially pronounced for organic compounds, like nucleic acids. Although radiolysis should be avoided while recording image, it still helps sample identification. In Figure 3.30, beam damage is observed for several particles after electron beam was kept on the specific area for over 30 seconds, but the ice crystal on the right edge of the image did not exhibit any structural change. Combined with the previous evidence, it is established that the particles observed are indeed the polyplexes trapped within the amorphous ice layer.

As shown in the representative cryoTEM image (Figure 3.31), polyplexes in pure water appeared have a circular or "speherical" morphology with some irregularities. Levine *et. al*. reported similar polyplex morphologies formed from branched polyethyleneimine (bPEI) in water via cryoTEM.[15] The diameter of the particles of all samples were determined via FEI TEM Imaging and Analysis (TIA) software. The radius of polyplexes revealed by cryoTEM was 26±8 nm, slightly lower than the value measured by DLS (about 50 nm). It was conceived that the glycopolymer vehicles could promote a "core-shell" structure in aqueous solution,[1, 12] where the shell structure might not possess high enough electron density to yield full contrast from that of the amorphous ice. This could cause the discrepancy in size revealed by the cryoTEM data from that revealed via DLS.

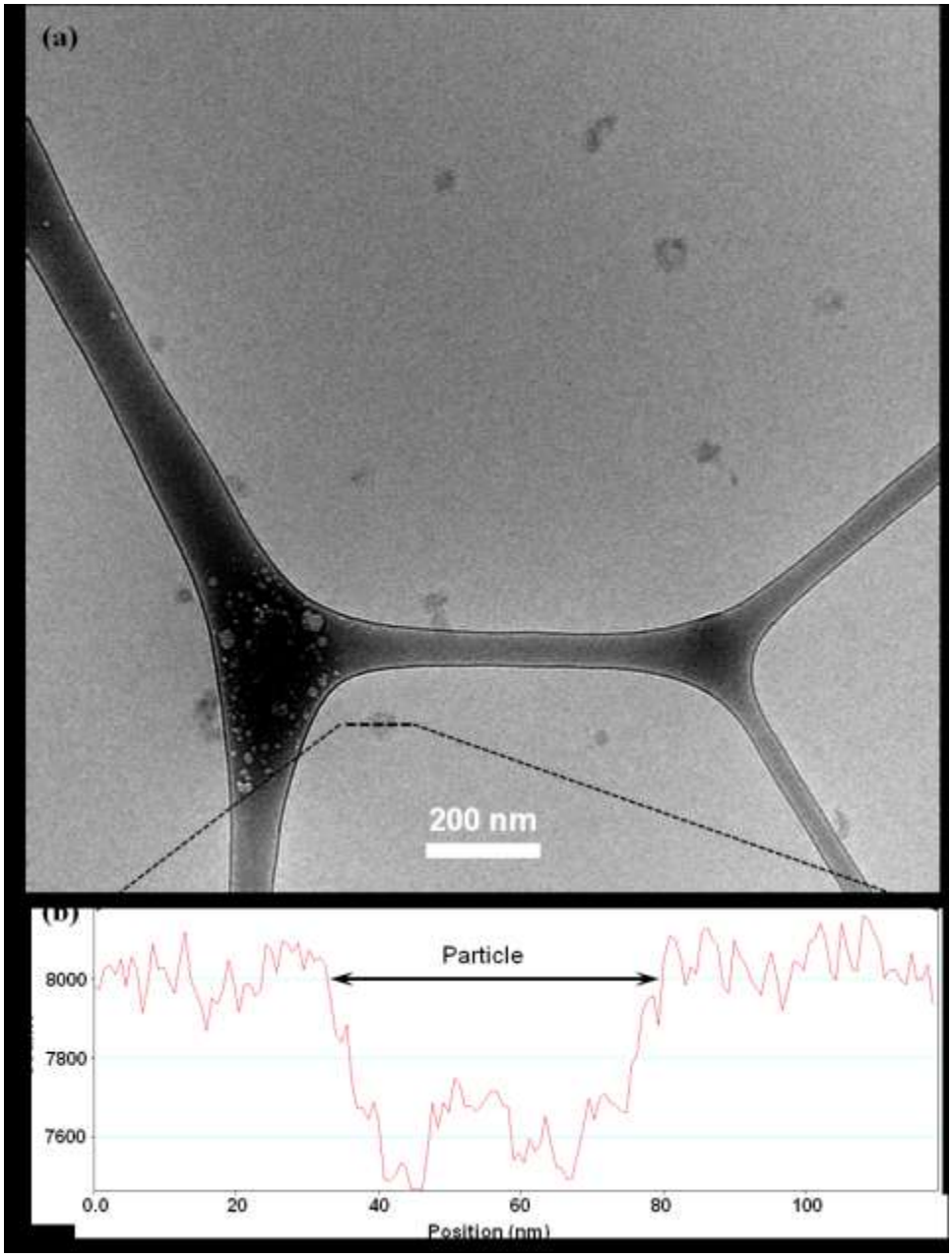


**Figure 3.31** (a) CryoTEM image of a polyplex formed between $PMAG_{61}$-b-$PDMAPMA_{21}$ and pDNA at a N/P ratio of 5; (b) Line profile of counts of electrons vs distance of the polyplex particle highlighted in (a) denoting a diameter of about 45 nm for the polyplex.

### 3.3.3 Enhanced colloidal stability of the glycopolymer polyplexes

To evaluate the colloidal stability of polyplexes in Opti-MEM (contains physiological salt and small molecule nutrients), the sizes of polyplexes were monitored via DLS over the period of 4 h (Figure 3.32). As a comparison, the sizes of polyplexes in nuclease-free water were also measured and reported in the graph. Over the experimental period, the polyplexes formed from JetPEI (N/P ratio = 5) and Glycofect (N/P ratio = 20) aggregated in Opti-MEM with the radius increasing from around 50 nm to over 400 nm. Additionally, polyplexes formed from cationic homopolymers, $PDMAPMA_{60}$ and $PAEMA_{58}$, were found to aggregate in Opti-MEM, which was evident as the radius significantly increased from 50 nm to over 600 nm over a 4 h time period. On the contrary, glycopolymer polyplexes were relatively stable over the 4 h period, with the radius remaining around 50 nm in almost all cases; the size increase of $PMAG_{61}$-b-$PDMAPMA_{39}$ polyplexes was observed at a N/P ratio of 5, probably due to the relatively weak association between pDNA and the tertiary amine block in this analog; interestingly, the aggregation was not as obvious at an N/P ratio of 10. These experimental results are consistent with previous published results, where the polyplexes composed of block glycopolymers exhibited high colloidal stability in cell culture media.[10-11, 36] It is proposed that cationic block copolymers can condense pDNA with a core-shell structure.[1, 12] The stabilization effect is likely attributed to the shell of PMAG, which serves as a bulky hydrophilic coating, preventing the polyplexes from aggregating in Opti-MEM. The protective function of the PMAG block that coats the polyplexes becomes apparent when comparing the stability of glycopolymer polyplexes with that of

polyplexes formed with the cationic homopolymers. As mentioned previously, the hydrodynamic radii of homopolymer-based polyplexes, without the protection of the glucose derived block, increased dramatically in Opti-MEM medium over the experimental period.

Colloidal stability of the polyplexes composed of P(MAG-b-methacrylate) series glycopolymers was also determined by DLS in Opti-MEM. (Figure 3.33) It was observed that the sizes of the ploxplexes stayed within a range of 50-110 nm, and were, in general, stable over a period of 4 hours. The DLS results of these two series of glycopolymers highlighted the importance of PMAG block to prevent polyplexes from aggregation in Opti-MEM.

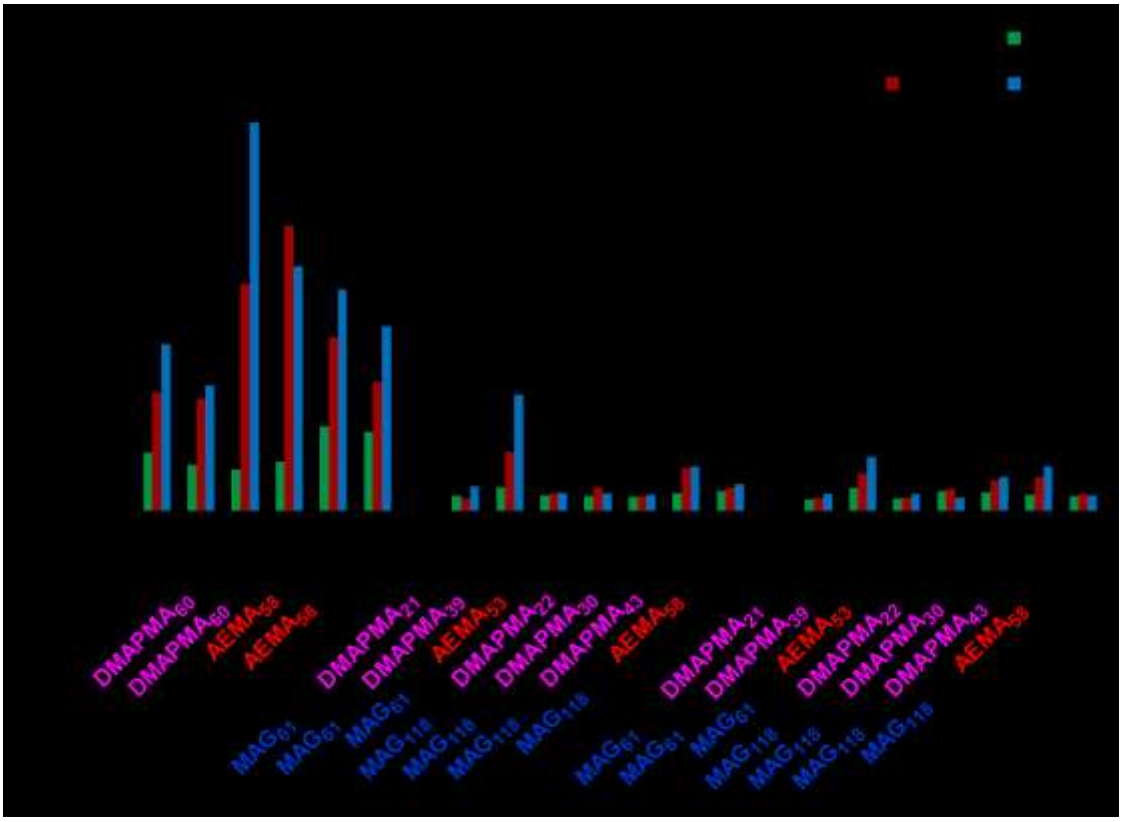


**Figure 3.32** Hydrodynamic radius of polyplexes composed of PMAG-b-PDMAPMA at N/P ratios of 5 and 10 at 0, 2, 4 h after dilution with Opti-MEM. Error bars represent the standard deviation of analyzed data from three replicates.

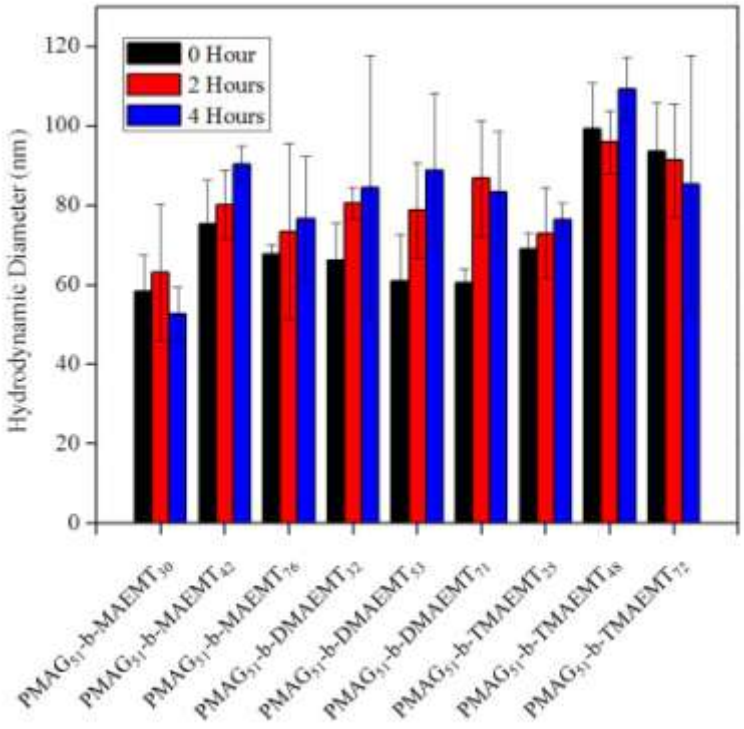


**Figure 3.33** Hydrodynamic radius of polyplexes composed of P(MAG-b-methacrylate) at N/P ratios of 15 at 0, 2, 4 h after dilution with Opti-MEM. Error bars represent the standard deviation of analyzed data from three replicates. (Courtesy of Dr. Haibo Li)

## 3.4 Conclusion

In this chapter, we reported the synthesis of several series of diblock glycopolymers via RAFT polymerization. Two types of carbohydrate moieties, glucosamine and trehalose, were utilized for glycopolymer synthesis. Additionally, both methacrylate based monomers and methacrylamide based monomers were polymerized via aqueous RAFT polymerization with PMAG or PMAT as macroCTA to yield cationic glycopolymers with low dispersity. The obtained PMAG glycopolymers exhibited the ability to bind pDNA at low N/P ratios.

The obtained trehalose containing glycopolymers showed strong binding ability for siRNA. The size and morphology of the polyplexes were characterized using DLS, TEM, and cryoTEM. The diameters of the nanoparticles were determined to be from 50 nm and 100 nm according DLS. TEM showed the spherical morphology; however, the diameters revealed by regular TEM were lower compared to the size measured by DLS, possibly owing to the sample's dehydration state. CryoTEM technique was also employed to characterize the in situ morphology of the polyplexes, which is relatively irregular composed to that revealed by conventional TEM. It was also demonstrated, via TEM and DLS, that poly(trehalose) block could protect the morphology of siRNA polyplexes through lyophilization. Finally, PMAG block could improve the colloidal stability of polyplexes in physiological salt solutions when compared to systems not stabilized by a hydrophilic block.

## 3.5 Reference

1. Ziebarth, J.; Wang, Y. *J. Phys. Chem. B* **2010,** *114*, 6225-6232.

2. de Vries, R.; Cohen Stuart, M. *Curr Opin Colloid Interface Sci* **2006,** *11*, 295-301.

3. Amoozgar, Z.; Yeo, Y. *Wiley Interdiscip Rev Nanomed Nanobiotechnol* **2012,** *4*, 219-233.

4. Maeda, H.; Bharate, G. Y.; Daruwalla, J. *Eur J Pharm Biopharm* **2009,** *71*, 409-419.

5. Pun, S. H.; Davis, M. E. *Bioconjugate Chem.* **2002,** *13*, 630-639.

6. Merdan, T.; Kunath, K.; Petersen, H.; Bakowsky, U.; Voigt, K. H.; Kopecek, J.; Kissel, T. *Bioconjugate Chem.* **2005,** *16*, 785-792.

7. Liu, X.-Q.; Du, J.-Z.; Zhang, C.-P.; Zhao, F.; Yang, X.-Z.; Wang, J. *Int J Pharm* **2010,** *392*, 118-126.

8. Venkataraman, S.; Ong, W. L.; Ong, Z. Y.; Joachim Loo, S. C.; Rachel Ee, P. L.; Yang, Y. Y. *Biomaterials* **2011,** *32*, 2369-2378.

9. Ahmed, M.; Narain, R. *Biomaterials* **2011,** *32*, 5279-5290.

10. Smith, A. E.; Sizovs, A.; Grandinetti, G.; Xue, L.; Reineke, T. M. *Biomacromolecules* **2011,** *12*, 3015-3022.

11. Li, H.; Cortez, M. A.; Phillips, H. R.; Wu, Y.; Reineke, T. M. *ACS Macro Lett.* **2013,** *2*, 230-235.

12. Nakai, K.; Nishiuchi, M.; Inoue, M.; Ishihara, K.; Sanada, Y.; Sakurai, K.; Yusa, S.-i. *Langmuir* **2013,** *29*, 9651–9661.

13. Danino, D. *Curr Opin Colloid Interface Sci* **2012,** *17*, 316-329.

14. Alfredsson, V. *Curr Opin Colloid Interface Sci* **2005,** *10*, 269-273.

15. Levine, R. M.; Pearce, T. R.; Adil, M.; Kokkoli, E. *Langmuir* **2013,** *29*, 9208-9215.

16. Velluto, D.; Thomas, S. N.; Simeoni, E.; Swartz, M. A.; Hubbell, J. A. *Biomaterials* **2011,** *32*, 9839-9847.

17. Xu, X.; Smith, A. E.; Kirkland, S. E.; McCormick, C. L. *Macromolecules* **2008,** *41*, 8429-8435.

18. Sizovs, A.; Xue, L.; Tolstyka, Z. P.; Ingle, N. P.; Wu, Y.; Cortez, M.; Reineke, T. M. *J. Am. Chem. Soc.* **2013,** *135*, 15417-15424.

19. Pearson, S.; Allen, N.; Stenzel, M. H. *J. Polym. Sci., Part A: Polym. Chem.* **2009,** *47*, 1706-1723.

20. van de Wetering, P.; Zuidam, N. J.; van Steenbergen, M. J.; van der Houwen, O. A. G. J.; Underberg, W. J. M.; Hennink, W. E. *Macromolecules* **1998,** *31*, 8063-8068.

21. Zhu, C.; Zheng, M.; Meng, F.; Mickler, F. M.; Ruthardt, N.; Zhu, X.; Zhong, Z. *Biomacromolecules* **2012**.

22. Tang, R.; Palumbo, R. N.; Nagarajan, L.; Krogstad, E.; Wang, C. *J Control Release* **2010,** *142*, 229-237.

23. Li, Z.; Yin, H.; Zhang, Z.; Liu, K. L.; Li, J. *Biomacromolecules* **2012,** *13*, 3162-3172.

24. Teramoto, N.; Sachinvala, N.; Shibata, M. *Molecules* **2008,** *13*, 1773-1816.

25. Benaroudj, N.; Lee, D. H.; Goldberg, A. L. *J. Biol. Chem.* **2001,** *276*, 24261-24267.

26. Hagen, S.; Hofrichter, J.; Eaton, W. *Science* **1995,** *269*, 959-962.

27. Wingler, A.; Fritzius, T.; Aeschbacher, R. A. *Plant Physiol* **2000,** *124*, 105-114.

28. Srinivasachari, S.; Liu, Y.; Zhang, G.; Prevette, L.; Reineke, T. M. *J. Am. Chem. Soc.* **2006,** *128*, 8176-8184.

29. Tseng, W.-C.; Tang, C.-H.; Fang, T.-Y.; Su, L.-Y. *Biotechnol. Prog.* **2007,** *23*, 1297-1304.

30. Wada, M.; Miyazawa, Y.; Miura, Y. *Polym Chem* **2011,** *2*, 1822-1829.

31. Mancini, R. J.; Lee, J.; Maynard, H. D. *J. Am. Chem. Soc.* **2012,** *134*, 8474-8479.

32. Crowe, J. H.; Carpenter, J. F.; Crowe, L. M. *Annu. Rev. Physiol.* **1998,** *60*, 73-103.

33. Liu, Y.; Reineke, T. M. *J. Am. Chem. Soc.* **2005,** *127*, 3004-3015.

34. Nielsen, P. E., In DNA-Protein Interaction, Principles and Protocols. In Moss, T.; Leblanc, B., Eds. Springer: New York, 2009; Vol. 543, pp 87-96.

35. Kasper, J. C.; Schaffert, D.; Ogris, M.; Wagner, E.; Friess, W. *J Control Release* **2011,** *151*, 246-255.

36. Ahmed, M.; Jawanda, M.; Ishihara, K.; Narain, R. *Biomaterials* **2012,** *33*, 7858-7870.

# Chapter 4 Glucose-Containing Diblock Polycations Exhibit Molecular Weight, Charge, and Cell-Type Dependence for pDNA Delivery

Chapter four presents our research effort to study in vitro transfection experiments performed in both HeLa (human cervix adenocarcinoma) cells and HepG2 (human liver hepatocellular carcinoma) cells to examine the role of charge type, block length, and cell type on transfection efficiency and toxicity. These glycopolymers revealed higher cellular uptake and transfection efficiency in HepG2 cells than in HeLa cells, while homopolycations (PAEMA and PDMAPMA) lacking the MAG blocks exhibited the opposite trend signifying that the MAG block could aid in hepatocyte transfection.

---



1. Wu, Y.; Wang, M.; Sprouse, D.; Smith, A. E.; Reineke, T. M. *Biomacromolecules* **2014**, *15*, 1716–1726.

## 4.1 Introduction

Polycations have been extensively studied as macromolecular delivery agents, as they possess the ability to form complexes (i.e. polyplexes) with various polynucleotides (such as plasmid DNA (pDNA), small interfering RNA (siRNA), and microRNA (miRNA)) and to deliver nucleic acids into different cell types.[1-2] For the purpose of therapeutic development, polyplexes need to provide protection from interaction with plasma proteins, aggregation, and clearance by the reticuloendoethelial system (RES) if administered systemically. It becomes apparent that antifouling properties are necessary to achieve successful in vivo delivery.[3-4] Different types of neutral hydrophilic components, such as poly(ethylene glycol) (PEG)[3-5], zwitterion[6-8] and carbohydrates[9-15], have been incorporated into polycation delivery systems and studied as stealth coatings. Despite the wide utilization of these stealth agents, such hydrophilic coatings can sterically hinder the interaction between polyplexes and cellular membranes, resulting in lower transfection efficiency.[4] Additionally, recent studies have found that PEG-containing delivery systems could promote antibody secretion and exhibit clearance from the blood stream after repeated injections under certain conditions.[16-17] These recent findings reinforce the need to design and develop new stealth coatings for drug and gene delivery systems.

Polymeric coatings created from carbohydrates have the ability to improve hydrophilic and steric protective coverage, and may provide the dual benefit of enhancing specific biological interactions through the “glycocluster effect”, which involves binding

between multiple carbohydrate molecules along polymer backbones and membrane receptors.[14, 18] Fernandez-Garcia et. al. demonstrated that amphiphilic di- and triblock glycopolymers are able to self-assemble into micelles in aqueous media and the obtained micelles could bind with Concanavalin A lectin protein through the "glycocluster effect".[19-20] Eun-Ho Song et. al. have also designed glycopolymers with mannose and glucose moieties. By taking advantage of the "glycocluster effect", they established the targeting effect of glycopolymers on alveolar macrophages both in vitro and in vivo, and studied the activation pathways.[21] Cationic block glycopolymers with controlled molecular weights have been designed as gene delivery vehicles by our group and others.[9-13, 15, 22] Owing to these advantages, glycopolymers received significant research interest for delivery vehicle development.

Controlled architecture, molecular weight, and dispersity are essential for thoroughly examining the impact of polymer structure on transfection efficiency. These properties can be achieved with the help of recent progress in reversible-deactivation radical polymerization (RDRP) techniques, such as nitroxide-mediated polymerization (NMP),[23] atom transfer radical polymerization (ATRP),[24] and reversible addition-fragmentation chain transfer polymerization (RAFT).[25] Among these controlled polymerization methods, RAFT polymerization has been widely utilized for the synthesis of drug and polynucleotide vehicles because it is suitable for a variety of solvents, reaction conditions, and monomer functional groups.[22, 26] For example, McCormick and coworkers have designed a series of chain transfer agents (CTAs) for aqueous RAFT (co)polymerization.[27-29] They successfully synthesized a series of cationic copolymers

with N-2-hydroxypropyl methacrylamide (HPMA) and N-[3-(N, N-dimethylamino)propyl]methacrylamide (DMAPMA) for siRNA delivery via aqueous RAFT polymerization, conjugated with folic acid as a targeting moiety. The obtained cationic polymers were evaluated for the ability to deliver siRNA and down regulate the mRNA in cells via the quantitative real-time reverse transcription polymerase chain reaction (qRT-PCR).[30-32]

In this chapter, we report our efforts to synthesize and study a family of block co-glycopolycations consisting of a hydrophilic block, 2-deoxy-2-methacrylamido glucopyranose (MAG), copolymerized with either DMAPMA or N-(2-aminoethyl)methacrylamide (AEMA) for pDNA complexation and delivery. Previously, our group showed that PMAG-b-PAEMAs were able to form polyplexes with pDNA and siRNA, and shield polyplexes from aggregation in physiological salt and serum conditions.[9] The colloidal stability of the polyplexes was attributed to the incorporation of a PMAG block, which is exposed on the surface of the nanocomplexes, which contain a core structure of the polycation block bound to the nucleic acid. Such "core-shell" structures in aqueous salt and serum solutions have been shown to promote steric shielding of polyplexes to prevent aggregation in biological conditions[9-10, 33-34] Herein, seven diblock glycopolymers have been synthesized along with two cationic homopolymer controls lacking a poly(MAG) block, PAEMA and PDMAPMA, to examine the effect of the PMAG and charge block lengths and charge type in pDNA binding and delivery in two cultured cell types both HeLa (human cervix adenocarcinoma) cells and HepG2 (human liver hepatocellular carcinoma) cells. The

current report also concentrates on understanding and comparing the properties between incorporating a primary amine PAEMA block and a tertiary amine PDMAPMA block, along with block length on the complex formation and delivery of nucleic acids.

## 4.2 Materials and experiments

### 4.2.1 Materials

All chemicals were purchased from Sigma Aldrich and used without further purification unless specified otherwise. N-(2-aminoethyl) methacrylamide hydrochloride (AEMA•HCl) and N-[3-(N,N-dimethylamino)propyl]methacrylamide (DMAPMA) were purchased from Polyscience, Inc. (Warrington, PA), and DMAPMA was purified via vacuum distillation prior to use. 4,4'-Azobis(4-cyanovaleric acid) (V-501) was recrystallized from methanol. 2-deoxy-2-methacrylamido glucopyranose (MAG)[35] and the chain transfer agent (CTA) 4-cyano-4-(propylsulfanylthiocarbonyl) sulfanylpentanoic acid (CPP)[29] were synthesized according to previous reports. Cell culture media, Dulbecco's Modified Eagle Medium (DMEM) and Opti-MEM, antibiotic/antimycotic, fetal bovine serum (FBS), phosphate-buffered saline (PBS), and nuclease-free water were purchased from Gibco (Carlsbad, CA). HeLa (Human cervix adenocarcinoma) cells and HepG2 (human liver hepatocellular carcinoma) cells were purchased from ATCC (Rockville, MD). JetPEI was purchased from Polyplus-Transfection Inc. (Illkirch, France). Glycofect was provided by Techulon (Blacksburg, VA) as a gift. 3-[4,5-dimethylthiazol-2-yl]2, 5-diphenyltetrazolium bromide (MTT) was purchased from Molecular Probes (Eugene, Oregon). Luciferase assay kits were purchased from Promega

Corp. (Fitchburg, WI). Protein assay kits were purchased from Bio-Rad Laboratories (Hercules, CA).

### 4.2.2 Polymer synthesis

The diblock glycopolymers were synthesized according to similar methods previously published.[9] Typically, to yield PMAG as the macromolecular chain transfer agent (macroCTA), MAG (0.23 g, 0.93 mmol), CPP (1.7 mg, $6.2\times10^{-3}$ mmol), and V-501 (0.17 mg, $6.2\times10^{-4}$ mmol) were dissolved in 2.0 mL of a 4:1 mixture of 0.1 M acetate buffer (pH 5.2) and ethanol. The solution was added to a 5 mL round bottom flask equipped with magnetic stir bar and purged with nitrogen for 50 min before the flask was sealed and placed into a preheated oil bath at 70 ºC. The reaction was then terminated by exposure to air at predetermined time points to yield different lengths of PMAG. The two PMAG macroCTAs were purified by dialysis with 3500 Da molecular weight cut-off dialysis tubing against ultrapure water and lyophilized to dryness. To synthesize the diblock glycopolymers, the macroCTA (100 mg, $3.4\times10^{-3}$ mmol for $PMAG_{118}$; 52 mg, $3.3\times10^{-3}$ mmol for $PMAG_{61}$), AEMA•HCl (33mg, 0.20mmol) or DMAPMA (34 mg, 0.20 mmol), and V-501 (0.21 mg, $7.5\times10^{-4}$ mmol) were dissolved in 1.2 mL 1.0 M acetate buffer (pH 5.2) in a 5 mL round bottom flask. After the solution was purged with nitrogen for 50 min, the polymerization was carried out in a preheated oil bath at 70 ºC. Polymerization was terminated at a predetermined time point to yield different molecular weights by exposing the reaction mixture to air. The final product was purified via

extensive dialysis with a 3500 Da molecular weight cut-off membrane against water (pH 5 to 6, pH adjusted by conc. HCl) and lyophilization.

To synthesize homopolymers, the CPP (3.0 mg, $1.1\times10^{-2}$mmol), AEMA•HCl (108.3 mg, 0.66 mmol) or DMAPMA (112.2 mg, 0.66 mmol), and V-501 (0.61 mg, 2.2 $\times10^{-3}$ mmol) were dissolved in 3.29 mL of a 4:1 mixture of 1.0M acetate buffer (pH 5.2) : ethanol in a 5mL round bottom flask. After the solution was purged with nitrogen for 50 min, the polymerization was carried out in a preheated oil bath at 70 ºC for 3 h before termination by exposing the reaction mixture to air. The final product was purified by dialysis with a 3500 Da molecular weight cut-off membrane against water (pH 5 to 6, adjusted with conc. HCl) as described above and white powder was acquired after lyophilization.

### 4.2.3 Cellular uptake

Both HeLa cells and HepG2 cells were cultured in high glucose DMEM media with 10 % FBS and 1% antibiotic and antimicrobial in a humidified atmosphere containing 5 % $CO_2$ at 37 ºC, according to the established protocol (ATCC, Rockville, MD).

Cells were seeded in 6-well plates at 250 000 cells/well and incubated for 24 h, as described above. Plasmid DNA was labeled with Cyanine (Cy5) using a Label-IT Cy5 DNA labeling kit (Mirus, Madison, WI) according to the manufacturers protocol. Following the procedure previously described above, 500μL of polyplexes were prepared by combining Cy5-labeled pDNA and each of the polymer samples at an N/P ratio of 5

and 10. JetPEI and Glycofect were both used to prepare polyplexes at N/P ratio of 5 and 20 respectively, as positive controls. 500 μL of polyplex solution was diluted with 1.0 mL of Opti-MEM immediately prior to transfection. Each well of cells was treated with 500 μL of the diluted polyplex solution, followed by 4 h incubation at 37 ºC. Subsequently, the cells were incubated with CellScrub for 5 min after the removal of cell media (to remove surface bound polyplexes), followed by trypsinization, centrifugation, and then suspension in PBS. BD FACSVerse$^{TM}$ flow cytometer (San Jose, CA) equipped with a helium-neon laser to excite Cy5 (633 nm) and BD FACSuite$^{TM}$ software were used for flow cytometry analysis. A total of 10 000 events were collected for each sample well. The positive fluorescence level was established by inspection of the histogram of negative control cells such that <1% appeared in the positive region.

### 4.2.4 Luciferase reporter gene transfection and cell viability

HepG2 or HeLa cells were seeded in 24-well plates at 50 000 cells/well and incubated in supplemented DMEM at 37 ºC and 5% $CO_2$ for 24 h. Prior to transfection, 150 μL gwiz-luc pDNA (0.02 μg/μL) were combined with 150 μL of each polymer solution at a N/P ratio of 5 and 10 to form polyplexes. As positive controls, the same volume of polyplexes formed with JetPEI (N/P = 5) and Glycofect (N/P = 20) were prepared. After mixing with 600 μL of Opti-MEM, the polyplex solution was added onto the cells. Each well of cells were treated with 300 μL mixed solution, followed by the addition of 800 μL of supplemented DMEM after 4 h incubation. The cell media was then replaced with 1 mL supplemented DMEM 24 h after transfection. The luciferase or

MTT assays were carried out 48 h after transfection. For the luciferase assay, each well of cells were washed with PBS and then treated with 100 μL of lysis buffer (Promega, Madison, WI). A 5 μL aliquot of each well of cell lysate was examined on 96-well plates for luciferase activity with a Synergy H1 Hybrid Reader (BioTek, Winooski, VT). The amount of protein in the cell lysates per sample was determined against a standard curve of bovine serum albumin according to the established protocol from Bio-Rad (Hercules, CA) DC protein assay kit.

For the MTT assay, 48 h after transfection, each well of cells was washed with 0.5 mL PBS and then incubated with 1 mL of supplemented DMEM containing 0.5 mg/mL of 3-[4,5-dimethylthiazol-2-yl]2, 5-diphenyltetrazolium bromide (MTT) for 1 h at 37 ºC. Following the removal of the DMEM solution containing MTT, the cells were then washed with PBS, and 600 μL of DMSO was added to each well. The 24-well plates were then placed on a shaker for 20 min for dissolution of the purple formazan. Subsequently, a 200 μL aliquot from each well was added into a 96-well plate and analyzed for absorbance intensity at 570 nm.

### 4.2.5 Asialoglycoprotein (ASGP) Receptor Inhibition experiment

The experimental procedure was adapted from previous publication.[36] Cells were seeded in 24-well plates at 50 000 cells/well in a similar fashion to the previous procedure, and incubated at 37 ºC for 24 h. Polyplex solutions were prepared at an N/P ratio of 5 using aforementioned procedure for transgene expression, and diluted with Opti-MEM prior to transfection. Prior to cellular exposure to the polyplex solutions, each

well of cells was treated with either 200 μL DMEM containing 0.02 μg/μL galactose or 200 μL DMEM for 20 min. Subsequently, the cells were treated with 200 μL of polyplex Opti-MEM solution after the removal of the galactose DMEM solution, and then incubated at 37 ºC for 4 h before 800 μL of supplemented DMEM was added into each well. The cell media was replaced with 1 mL supplemented DMEM 24 h after transfection. A luciferase assay was carried out 48 h after transfection using the same procedure described above.

### 4.2.6 Statistical analysis

All data are presented as the mean ± the standard deviation and each analysis or measurement was performed in triplicate unless otherwise noted. For statistical analysis of the data, the means were compared using a Student's t test with $p < 0.05$ being considered as statistically significant.

## 4.3 Results and discussion

### 4.3.1 The synthesis of diblock glycopolymers

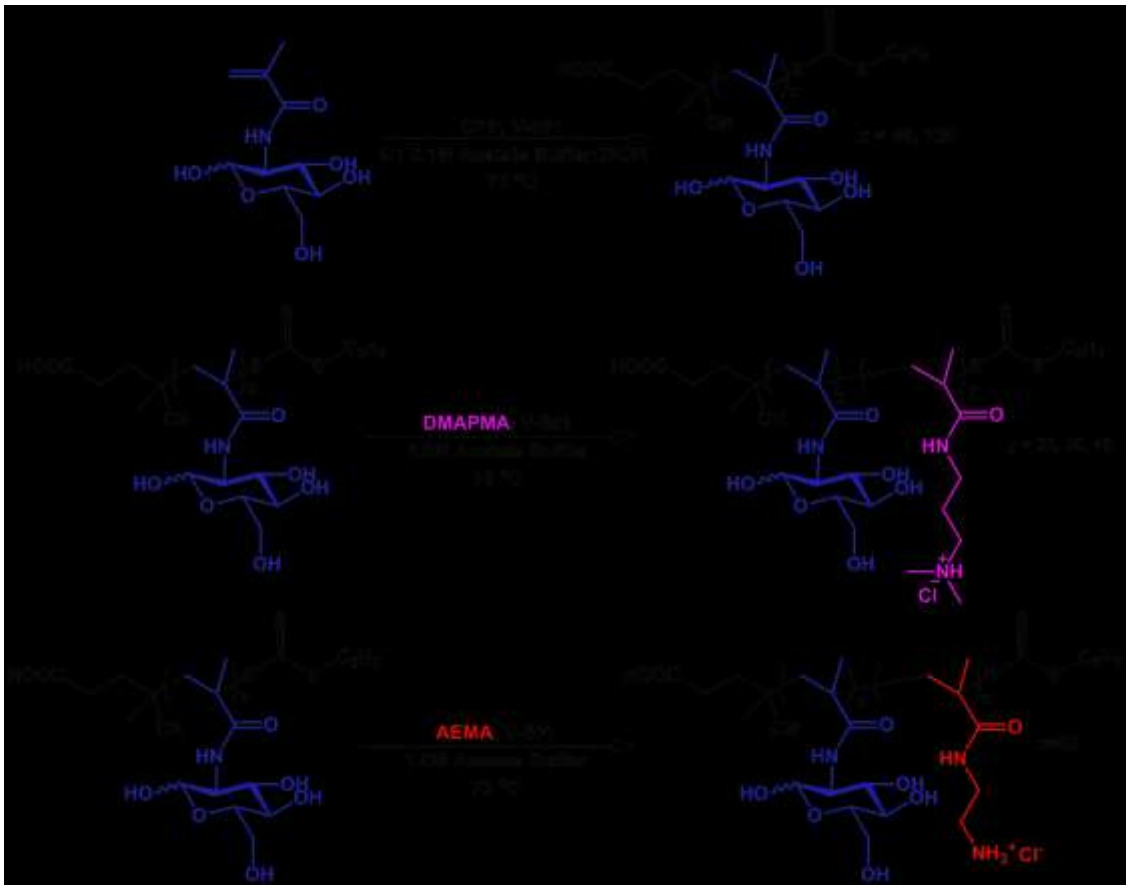


**Scheme 4.1** RAFT Polymerization of $PMAG_x$-b-$PDMAPMA_y$ and $PMAG_x$-b-$PAEMA_z$

Previously, our group reported a series of novel cationic diblock glycopolymers with various chain lengths and charge species as polymeric gene delivery vehicles.[9-10] The polyplexes formed from these series of diblock glycopolymers exhibited colloidal stability in cell media and had relatively low cytotoxicity. Moreover, both amine type and

cationic charge block length were demonstrated to greatly affect transgene expression efficiency *in vitro*.[10] To further understand how polymer structure impacts transgene expression, in particular, the role of the sugar and tertiary amine block length, aqueous RAFT polymerization was employed to synthesize well-defined cationic polymers and their activity was assessed for plasmid DNA delivery. Seven diblock copolymers were synthesized according to Scheme 4.1.

Based upon the polymerization kinetics determined by $^1$H NMR, two different lengths of PMAG were obtained (DP = 61 and 118) by quenching the polymerization at predetermined time points, and characterized by SEC. Both PMAG derivatives were utilized as a macroCTA for chain extension with either DMAPMA or AEMA to yield the cationic diblock glycopolymers. To prevent the aminolysis of the trithiocarbonate chain end, 1.0 M acetate buffer (pH=5.2) was selected as the reaction solvent. Various block lengths of DMAPMA were acquired by stopping the polymerization at predetermined time points according to the monomer conversion rate. For comparison, AEMA derivatives were synthesized with a block length similar to the longest DMAPMA block length. The molecular weight and dispersity of all obtained diblock copolymers were determined by SEC chromatography (Figure 4.1). Narrow dispersity ($M_w/M_n \leq 1.1$) of the obtained copolymers indicates a highly controlled polymerization. Additionally, to probe the importance of the glucose block for our glycopolyplex delivery system, homopolymers of DMAPMA and AEMA were obtained for the subsequent studies discussed below. The molecular weight and dispersity of all the polymers are summarized in Table 4.1.

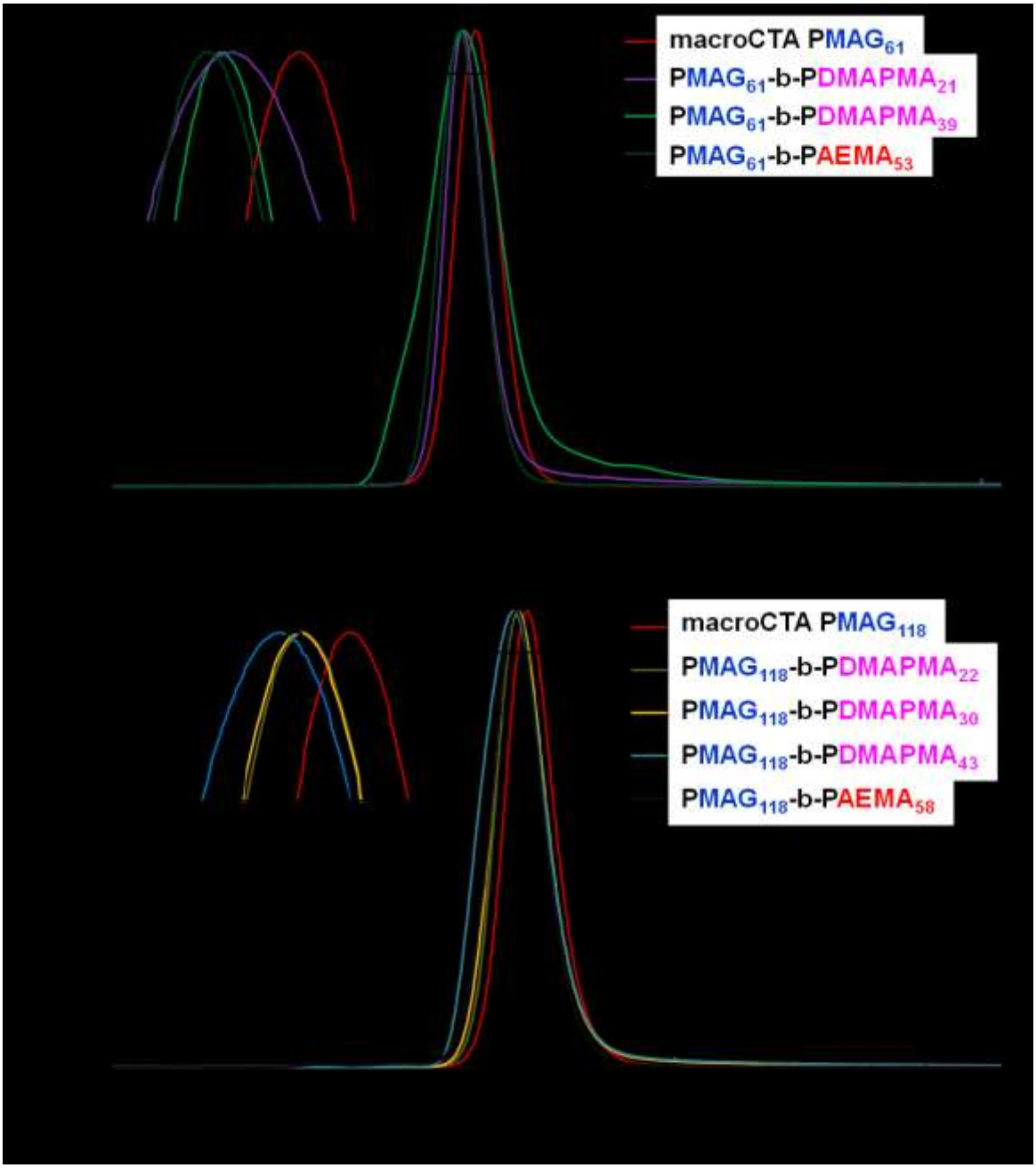


**Figure 4.1** SEC traces for the diblock glycopolymers, (a) $PMAG_{61}$ series; (b) $PMAG_{118}$ series

**Table 4.1** Molecular weight, dispersity, and calculated degree of polymerization (DP) of the polymers examined in this study.

| Samples | $M_n$[a]/kDa | $M_w/M_n$[a,c] | MAG DP[a,b] | Amine DP[a,b] |
|---|---|---|---|---|
| $PDMAPMA_{60}$ | 11.4 | 1.41 | | 60 |
| $PAEMA_{58}$ | 7.3 | 1.10 | | 58 |
| $PMAG_{61}$ | 15.6 | 1.01 | 61 | |
| $PMAG_{61}$-b-$PDMAPMA_{21}$ | 19.2 | 1.02 | 61 | 21 |
| $PMAG_{61}$-b-$PDMAPMA_{39}$ | 22.1 | 1.10 | 61 | 39 |
| $PMAG_{61}$-b-$PAEMA_{53}$ | 24.4 | 1.01 | 61 | 53 |
| $PMAG_{118}$ | 29.5 | 1.03 | 118 | |
| $PMAG_{118}$-b-$PDMAPMA_{22}$ | 33.2 | 1.02 | 118 | 22 |
| $PMAG_{118}$-b-$PDMAPMA_{30}$ | 34.6 | 1.01 | 118 | 30 |
| $PMAG_{118}$-b-$PDMAPMA_{43}$ | 36.9 | 1.02 | 118 | 43 |
| $PMAG_{118}$-b-$PAEMA_{58}$ | 39.0 | 1.01 | 118 | 58 |

a. As determined by aqueous SEC using a flow rate of mL/min of 0.1 M $Na_2SO_4$ in 1.0 v% acidic acid, Eprogen CATSEC100, CATSEC300, and CATSEC1000 columns, a Wyatt HELEOS II light scattering detector ($\lambda$ = 662 nm), and an Optilab rEX refractometer ($\lambda$ = 658 nm). b. As confirmed by $^1$H NMR spectroscopy. c. Note: the dispersity was lower than the theoretical value for some samples, possibly due to the dialysis purification method.

### 4.3.2 Cellular uptake profile of the glycopolymer polyplexes

The *in vitro* internalization profiles of polyplexes formed from Cy5-labeled pDNA and the polymers were examined via flow cytometry 4 hours after cells were exposed to the polyplex formulations. The percentage of Cy5 positive cells in live cells (Figure 4.2) and the mean fluorescence intensity (MFI, Figure 4.3) were determined with a helium-neon laser to excite the Cy5 fluorophore at 633 nm wavelength. The cells only samples were utilized as negative controls to gate out the background fluorescence (<1%). Propidium iodide was also used as the reagent to stain and eliminate unhealthy cells from interfering with the analysis. With both HeLa cells and HepG2 cells, the cationic homopolymers, $PDMAPMA_{60}$ and $PAEMA_{58}$, were successfully internalized by about 95% of cells at N/P ratios of 5 and 10. With polyplexes formed by the PMAG-b-PAEMA series, over 92% of cells in both cell types were Cy5-pDNA positive. However, the polyplexes formulated with glycopolymers containing the DMAPMA blocks exhibited lower cellular internalization levels than that observed with the PMAG-b-PAEMA series at N/P ratios of 5 in HeLa cells. More specifically, the percentage of cells positive for Cy5-pDNA internalization percentage dropped when the DMAPMA block length increased. For example, the uptake level decreased from 77% to 45% when the PDMAPMA block length increased from 22 to 43 repeat units for the $PMAG_{118}$ series of polymers. This uptake percentage decrease was possibly due to the toxicity of the PMAG-b-PDMAPMA copolymers (*vide infra*); the cells that internalized the polyplexes

formed with those block copolymers were found to be positive for propidium iodide staining. The internalization levels for polyplexes formed with the PMAG-b-PDMAPMA polymer series generally improved by increasing the N/P ratio from 5 to 10 in HeLa cells. Interestingly, the polyplexes exhibited different cellular uptake profiles in HepG2 cells from that in HeLa cells. The internalization percentage of the glycopolymer polyplexes was generally comparable to that of the homopolymers in HepG2 cells. Moreover, for the PMAG-b-PDMAPMA polymer series, the Cy5-pDNA internalization percentages were all greater 86 % in HepG2 cells, while the uptake percentage varied from 45% to 84% at an N/P ratio of 5 in HeLa cells. Additionally, the MFI values per cell (fluorescent intensity × uptake percentage) of the polyplexes tested were higher in HepG2 cells than in HeLa cells. This result indicates that more Cy5-pDNA, on average, was internalized by HepG2 cells than by HeLa cells (Figure 4.3). The disparity of the mean intensity between the two cell types could be mainly caused by the inherent nature of these cell types. Although previous research has shown that hydrophilic stabilizing blocks, such as PEG, can hinder the cellular uptake of polyplexes by limiting the interaction between polyplexes and cellular membrane,[37] herein, we did not observe a notable difference in cellular internalization percentages between glycopolymers and the homopolymers, $PAEMA_{60}$ and $PDMAPMA_{58}$, in HepG2 cells. Also, polyplexes formed with the glycopolymers and homopolymers did not exhibit differences in internalization percentages in HeLa cells at an N/P of 10. These results suggested that the presence of the PMAG block coating did not hinder the ability of polyplexes to be internalized by cells.

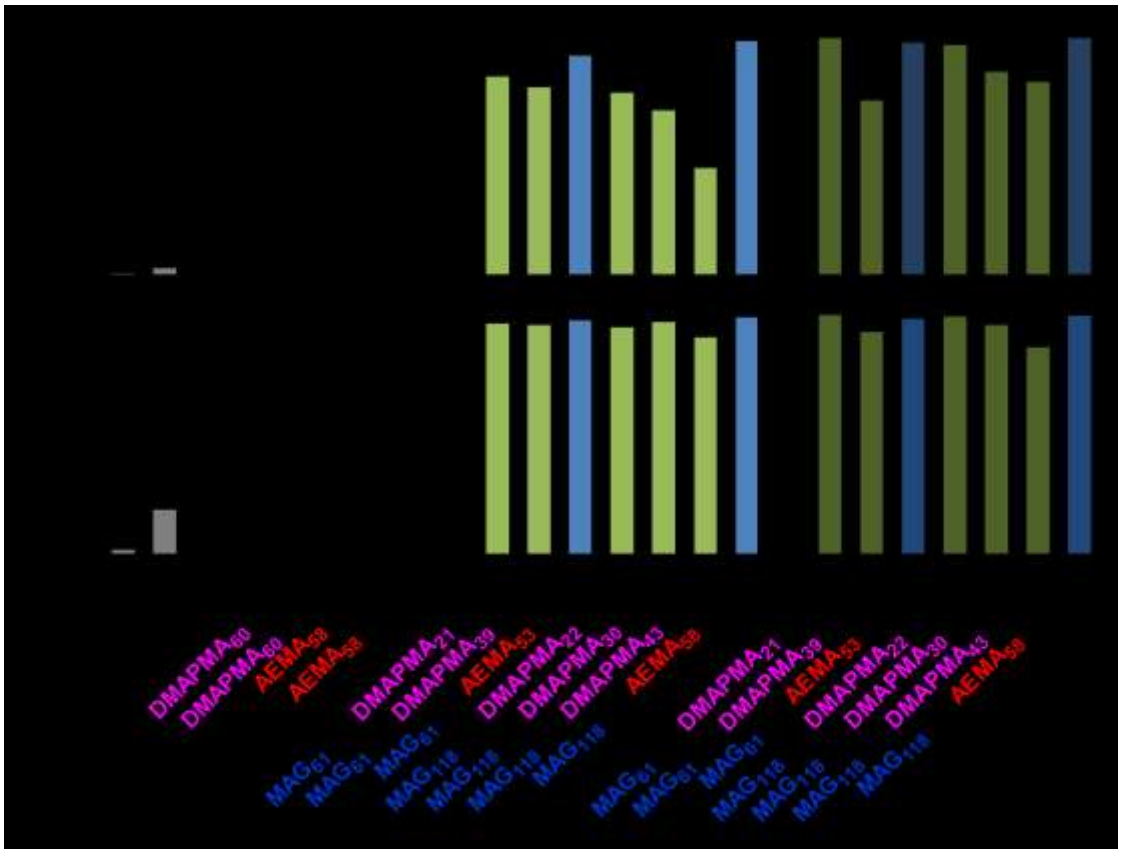


**Figure 4.2** Percentage of Cy5 positive cells 4 h after transfection with polyplexes formed with Cy5-labelled pDNA at N/P ratios of 5 and 10 in (a) HeLa cells (b) HepG2 cells. Error bars represent the standard deviation of analyzed data from three replicates.

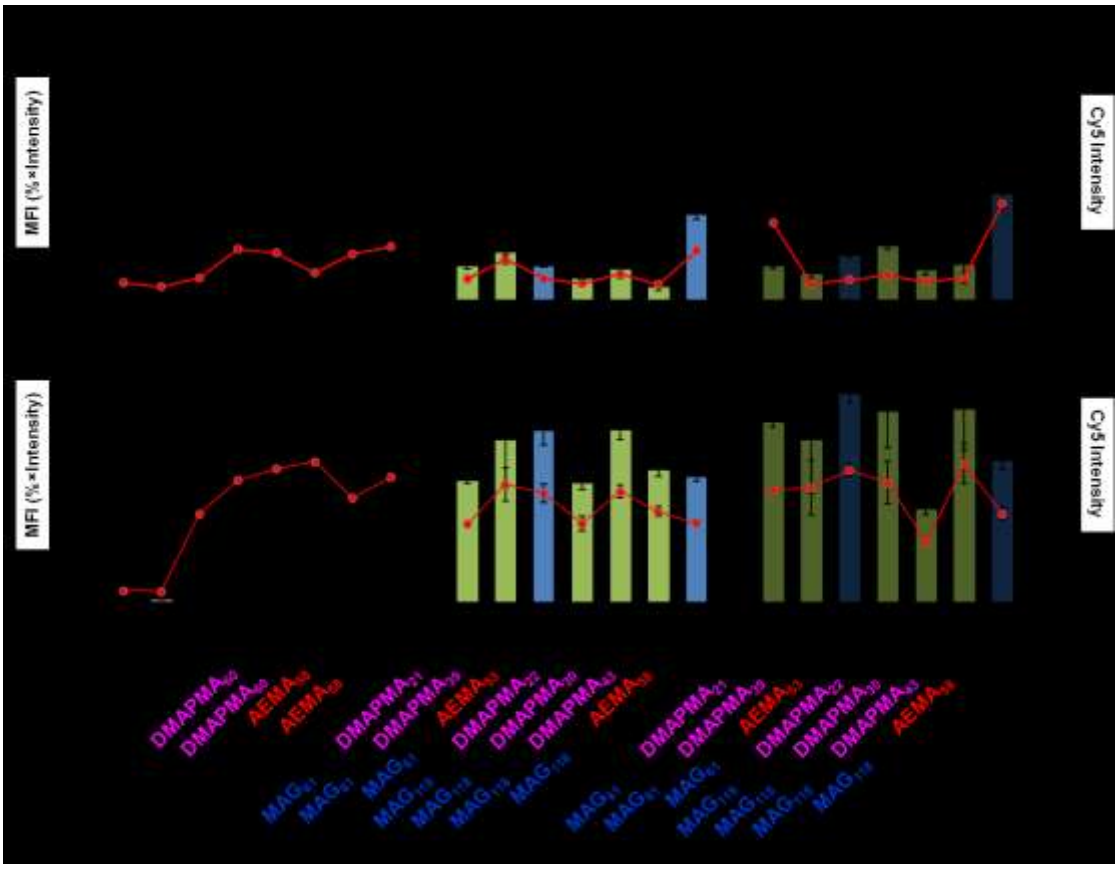


**Figure 4.3** Mean fluorescent intensity (Cy5 positive cell percentage × average Cy5 intensity) (bars, left y axis) and average Cy5 fluorescence intensity (points, right y axis) 4 h after transfection with the indicated polyplexes comprised of Cy5-labeled pDNA in (a) HeLa cells and (b) HepG2 cells.

### 4.3.3 Luciferase assay of the glycopolymer polyplexes

To determine the capability of the polymers to express the delivered pDNA *in vitro*, both HeLa cells and HepG2 cells were treated with polyplexes composed of pDNA encoding firefly luciferase protein at N/P ratios of 5 and 10. A luciferase assay was carried out 48 h after transfection, and the transfection efficiency was quantified by luminescence (relative light units) as a function of total protein expressed (Figure 4.4). In

HeLa cells, glycopolymer polyplexes overall did not exhibit a significant transfection efficiency compared with the commercial reagents, JetPEI ($7.4\times10^8$ RLU/mg) and Glycofect ($5.7\times10^7$ RLU/mg). Polyplexes formulated with the cationic homopolymer, $PAEMA_{58}$, exhibited significantly higher efficiency than polyplexes formulated with $PDMAPMA_{60}$. In addition, the transfection efficiency decreased when the PDMAPMA block length increased for the PMAG-b-PDMAPMA series. For example, at an N/P ratio of 5, the transgene expression level was $5.7\times10^5$ RLU/mg for $PMAG_{118}$-b-$PDMAPMA_{22}$ polyplexes, while the value dropped to $1.1\times10^4$ RLU/mg for $PMAG_{118}$-b-$PDMAPMA_{43}$ polyplexes. The low transfection efficiency of both the $PDMAPMA_{58}$ and PMAG-b-PDMAPMA polyplexes suggested that the PDMAPMA block is not very effective for pDNA delivery and promoting gene expression in HeLa cells. Aside from the toxicity of the PMAG-b-PDMAPMA copolymers playing a role in transfection, it was documented by Palermo *et. al.* that polymers containing primary amines were more capable of binding and disrupting membranes compared to the polymers bearing tertiary amine structures (possibly related to endosomal escape).[38] Palermo et. al. examined the interaction between liposomes formed with the lipid 1-palmitoyl-2-oleoyl-*sn*-glycero-3-phosphocholine (POPC) and three polymethacrylate derivatives consisting of hydrophobic groups and primary, tertiary, or quaternary ammonium salt groups, and demonstrated that primary amine containing polymers achieved the highest dye leakage from liposome vesicles.[38] Interestingly, $PAEMA_{60}$ homopolymers exhibited much higher transfection efficiency than the PMAG-b-PAEMA block copolymers in HeLa cells. At an N/P ratio of 5, the transfection efficiency for polyplexes formulated with $PAEMA_{58}$ was

$8.3\times10^6$ RLU/mg in HeLa cells, while transfection efficiencies of polyplexes formulated with block glycopolymers $PMAG_{61}$-b-$PAEMA_{53}$ and $PMAG_{118}$-b-$PAEMA_{58}$ were $1.1\times10^5$ RLU/mg and $4.3\times10^5$ RLU/mg, respectively. At an N/P ratio of 10, the transfection efficiency increased for $PAEMA_{58}$ polyplexes. While a slight increase was noted in transfection efficiency for both $PMAG_{61}$-b-$PAEMA_{53}$ and $PMAG_{118}$-b-$PAEMA_{58}$ polyplexes at N/P = 10, it was still nearly two orders of magnitude lower than the $PAEMA_{58}$ homopolymer. Several previous reports have demonstrated that PEGylation could hinder the transfection efficiency of PEI due to shielding effects.[39-40] Ahmed *et. al* reported the synthesis of a series of copolymers composed of AEMA and 2-methacryloxyethyl phosphorylcholine (MPC) for pDNA delivery, and the block copolymer $PMPC_{36}$-b-$PAEMA_{40}$ exhibited a lower transfection level than the cationic homopolymer analogue, $PAEMA_{58}$, by about 10 RLU/mg, according to a $\beta$-galactosidase assay.[7] While the hydrophilic block could play some role in decreasing transfection efficiency/gene expression, here in, it is clear that the charge center type plays the largest role in promoting (or suppressing) effective transgene delivery.

In HepG2 cells, the transfection efficiency trend observed for the polyplexes formed with the PMAG-b-PDMAPMA series was similar to that in HeLa cells; as the PDMAPMA block length increased, the transfection efficiency decreased. More specifically, the transfection efficiency was $3.8\times10^6$ RLU/mg for $PMAG_{118}$-b-$PDAMPMA_{22}$ at an N/P ratio of 5, but the value dropped significantly to $3.7\times10^4$ RLU/mg for $PMAG_{118}$-b-$PDAMPMA_{43}$, in HepG2 cells. Additionally, the homopolymers, $PDMAPMA_{60}$, exhibited very low transgene expression levels ($5.3\times10^3$

RLU/mg at an N/P ratio of 5 and had only slightly higher values at an N/P ratio of 10 ($8.5\times10^3$ RLU/mg) in HepG2 cells. These results further suggest that the PDMAPMA blocks did not possess the ability for pDNA delivery in this study. In addition, it was found that the homopolymer $PAEMA_{58}$ did not have the highest transfection efficiency in HepG2 cells. Interestingly, the PMAG-b-PAEMA series yielded the highest transfection efficiency, indicating that this cell type may offer a preference for promoting higher transgene expression for the vehicles containing the MAG blocks.

The direct comparison of the transfection efficiency between cell lines revealed that polyplexes formulated with the block glycopolymers exhibited higher transfection levels in HepG2 cells than in HeLa cells (Figure 4.5). For example, for the copolymer $PMAG_{61}$-b-$PDMAPMA_{21}$, the transfection efficiency at N/P ratio of 5 was $7.4\times10^5$ RLU/mg in HepG2 cells, but $4.2\times10^4$ RLU/mg in HeLa cells. As we established in the cellular uptake experiments, the intensity of Cy5-pDNA was higher in HepG2 cells than in HeLa cells on average (Figure 4.3). Therefore, the higher observed transfection efficiency in HepG2 cells could be, in part, due to the higher cellular internalization. Furthermore, the homopolymers, $PAEMA_{58}$, and the block copolymer PMAG-b-PAEMA series exhibited comparable transfection efficiency in HepG2 cells. At an N/P ratio of 5, the transgene expression level in HepG2 cells for $PAEMA_{58}$ was found to be $1.6\times10^6$ RLU/mg, and the expression levels for $PMAG_{61}$-b-$PAEMA_{53}$ and $PMAG_{118}$-b-$PAEMA_{58}$ were higher ($7.6\times10^6$ RLU/mg and $5.9\times10^6$ RLU/mg, respectively). At the higher N/P ratio of 10, the level of gene expression was similar. Interestingly, as previously mentioned, this trend was not found with HeLa cells; the homopolymer, $PAEMA_{58}$,

exhibited much higher transfection (2 orders of magnitude) than the block copolymers. These results suggested that the PMAG block may have beneficial interactions with HepG2 cells than with HeLa cells, resulting in increased *in vitro* pDNA delivery. These experimental results reveal that the PDMAPMA block was not an ideal charge center structure to promote high transfection efficiency in either cell type. Furthermore, the PMAG block serves as both a hydrophilic coating to prevent colloidal aggregation and appears to also impact the pDNA delivery efficiency in a cell type dependent manner possibly due to the varied interaction between glycopolymer-coated polyplexes and different cellular membranes.

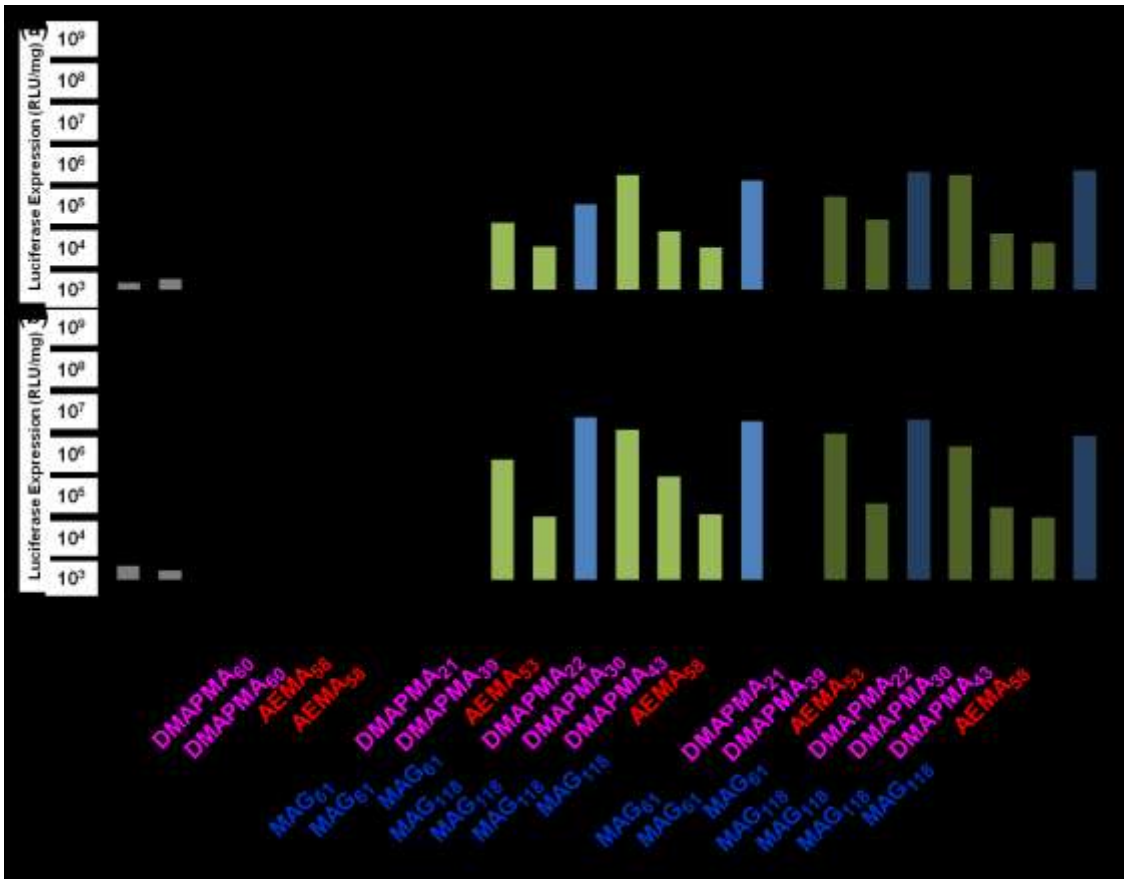


**Figure 4.4** Luciferase gene expression (RLU/mg) 48h after transfection with polyplexes formed at N/P ratios of 5 and 10 in (a) HeLa cells and (b) HepG2 cells.

Error bars represent the standard deviation of analyzed data from three replicates. Measurements found to be statistically significant ($p < 0.05$) compared to cells only are marked with an asterisk. Double asterisks represent the statistically significant difference ($p < 0.05$) between data groups.

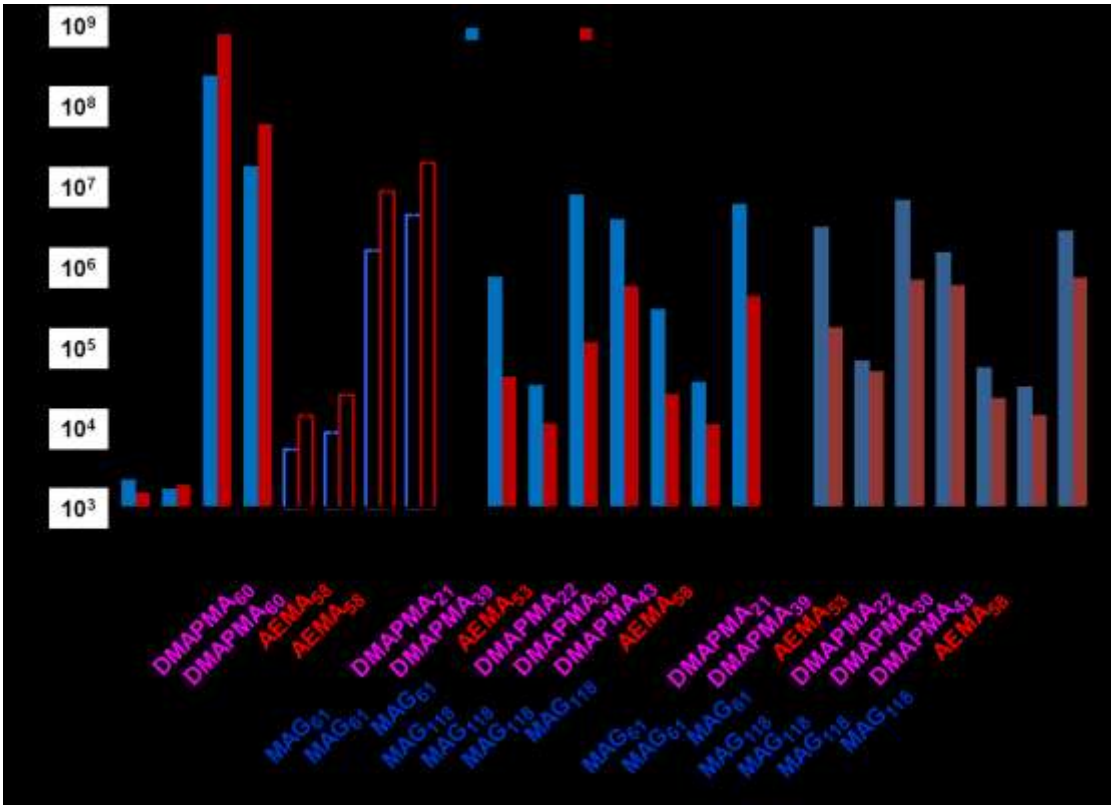


**Figure 4.5** Direct comparison of luciferase gene expression (RLU/mg) of HeLa cells and HepG2 cells treated with glycopolymer/pDNA polyplexes. Error bars represent the standard deviation of analyzed data from three replicates.

### 4.3.4 Asialoglycoprotein (ASGP) Receptor Inhibition

There are approximately 150,000 to 250,000 asialoglycoprotein (ASGP) receptors per cell present on the hepatocellular membrane.[41] The ASGP receptors were discovered to specifically recognize terminal β-linked galactose or N-acetylglucosamine (GlcNAc) residues, and to mediate endocytosis.[41-42] Due to the function of ASGP receptors, they have been heavily exploited for targeted nucleic acid delivery to liver hepatocytes.[41, 43-44] However, ASGP receptors are not present on HeLa cell membranes.[45] The transfection

efficiency comparison between the $PAEMA_{58}$ homopolymer and the PMAG-b-PAEMA glycopolymers revealed that the PMAG block impacted efficiency between the two cell types. The presence of the PMAG block reduced the transfection efficiency in HeLa cells, yet appeared to be beneficial for pDNA delivery in HepG2 cells. As the ASGP receptors are a unique feature of HepG2 cells, it is hypothesized that the PMAG block could interact with ASGP receptors on cellular membrane, and such interaction could facilitate the pDNA delivery for block glycopolymers in HepG2 cells. To test this hypothesis, both HeLa cells and HepG2 cells were treated with a solution of 0.02mg/mL D-(+)-galactose in DMEM for 20 min prior to the exposure to the polyplexes. Owing to the high affinity that the ASGP receptor has for galactose, the carbohydrate binding site of the receptor would be occupied by galactose, it would hence decrease interactions with the glycopolymers after the treatment. DMEM without galactose was also used to treat cells for the same period of time as a control. Figure 5 displays the transfection efficiency of both the control group and the group exposed to galactose (inhibition treatment). For several diblock copolymers ($PMAG_{61}$-b-$PDMAPMA_{21}$, $PMAG_{61}$-b-$PAEMA_{53}$, $PMAG_{118}$-b-$PDMAPMA_{22}$, $PMAG_{118}$-b-$PAEMA_{58}$) the treatment of HepG2 cells with DMEM containing galactose resulted in lower transgene expression. Such a difference in the transfection conditions was not observed in HeLa cells for polyplexes formulated with the diblock glycopolymers. Moreover, galactose containing DMEM treatment did not impact, with either cell line, the transfection efficiency of polyplexes formed with the cationic homopolymers nor the positive controls (commercial reagents). These results indicate that the presence of galactose molecules inhibited pDNA delivery in HepG2 cells

for the block glycopolymer polyplexes. These data reveal that between the two cell types, the polyplexes formulated with the glycopolymers may have an increase in interactions with HepG2 cell membranes. More importantly, such interaction facilitated transgene expression, as the inhibition of this receptor with galactose decreased gene expression with the glycopolymer-based polyplexes in HepG2 cells. These results suggest that the polymerized glucose moieties within the PMAG block facilitates an interaction (potentially with the ASGP receptors) on the HepG2 cell membrane. This premise is further supported by the data showing that the transfection efficiency of the cationic homopolymers, $PDMAPMA_{60}$ and $PAEMA_{58}$, was not altered by the addition of galactose. Additionally, MTT assays revealed that the galactose containing DMEM treatment did not alter the viability of cells exposed to polyplexes throughout the course of the transfection experiment (Supporting Information, Figure S12) . Thus, cell viability was not a factor in the decrease in gene expression for cells treated with galactose, which further supports our hypothesis that the poly(MAG) block aids internalization .

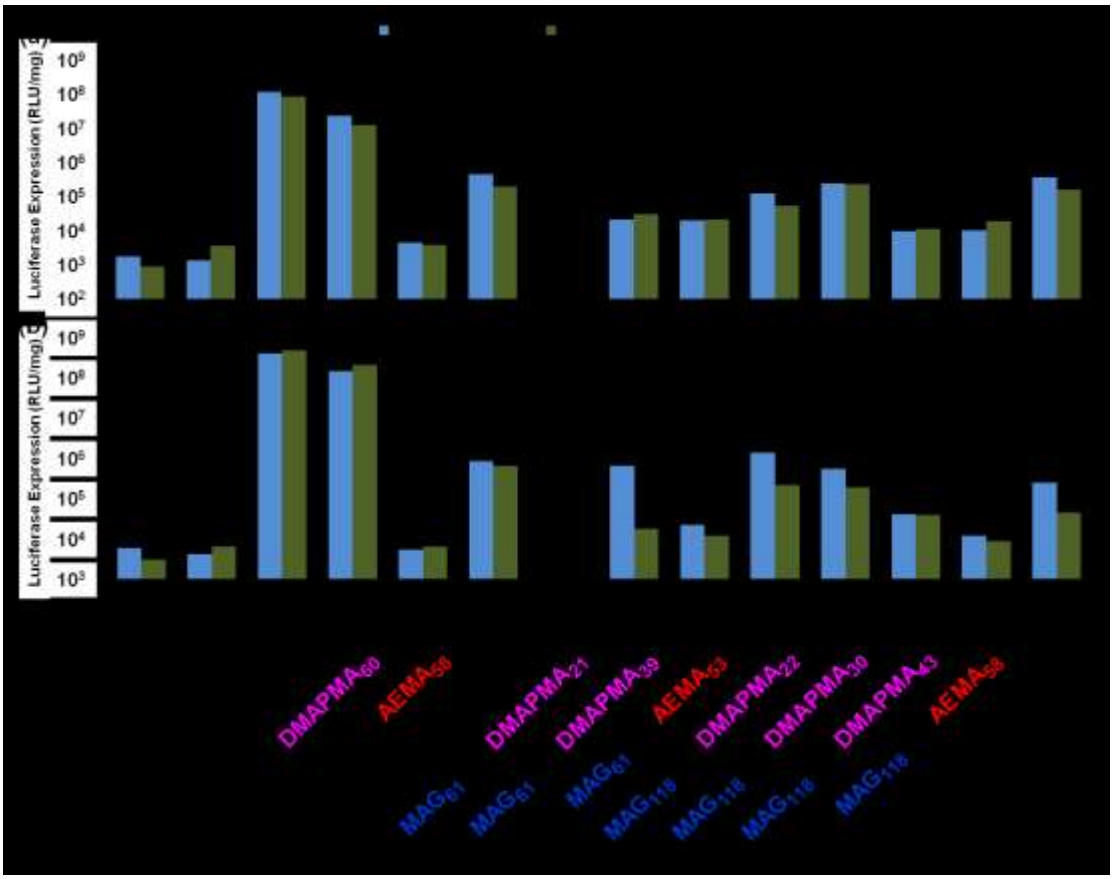


**Figure 4.6** Luciferase gene expression (RLU/mg) 48h after transfection with polyplexes formed at N/P ratios of 5 and 10 in (a) HeLa cells (b) HepG2 cells, treated with and without galactose containing DMEM.

Error bars represent the standard deviation of analyzed data from three replicates. Measurements found to be statistically different ($p < 0.05$) are marked with an asterisk.

### 4.3.5 Cytotoxicity of the glycopolymer polyplexes

The cytotoxicity of the polyplexes was determined through MTT assays with both cell lines (Figure 6). Polyplexes generally exhibited higher cytotoxicity in HeLa cells

than in HepG2 cells. In HepG2 cells, most of the polyplexes exhibited over 80% cell survival 48 h after transfection. It was found that the cytotoxicity of polyplexes increased as both the PDMAPMA block length and the N/P ratio increased in both cell lines. Because the PMAG block alone (no charge block) did not exhibit cytotoxicity according to MTT assays, it can be deduced that the toxic effects stem from the polyamine block. Previous work has demonstrated that the cytotoxicity of polyplexes could be partially caused by nuclear membrane permeation.[46] However, a more in-depth study is needed to determine the major mechanism of toxicity for this series of polymers, in particular, the distinct rationale for the higher toxicity of the PDMAPMA block copolymers.

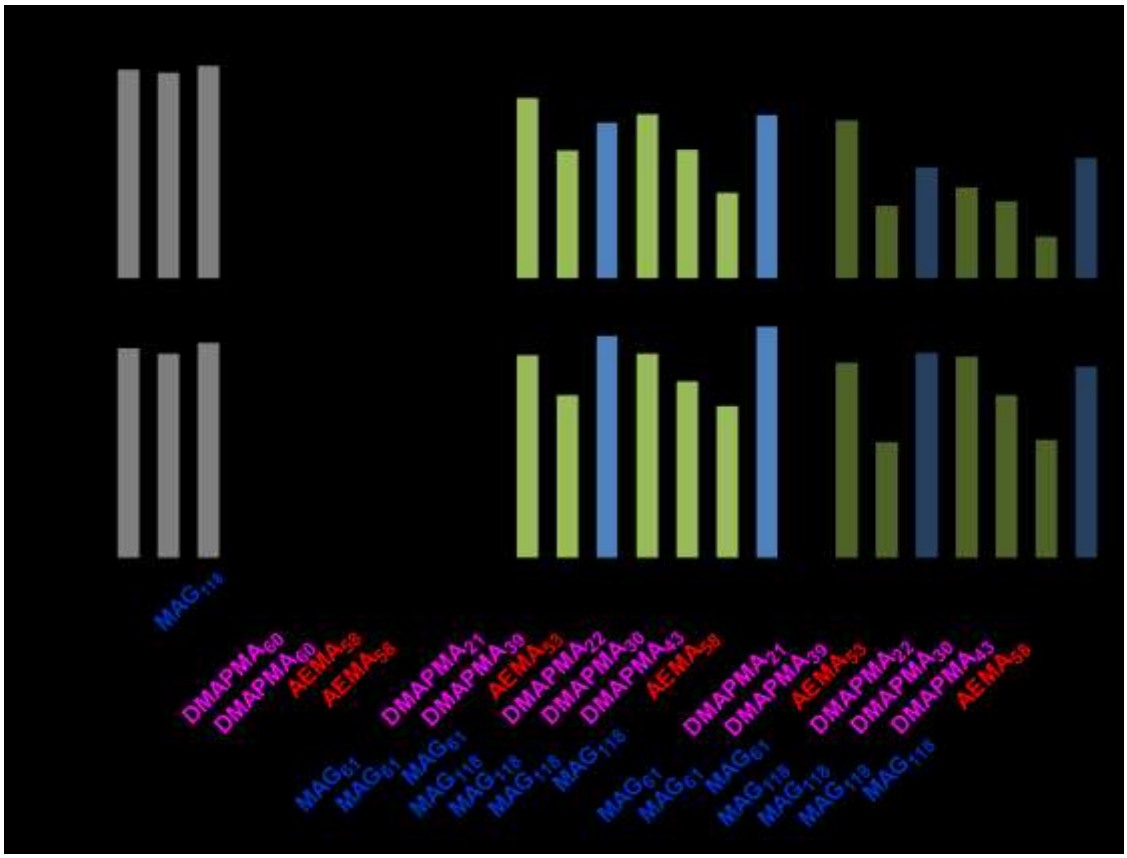


**Figure 4.7** Cell viability 48 h after transfection with glycopolymer/pDNA polyplexes in (a) HeLa cells and (b) HepG2 cells, as determined by an MTT assay.

Error bars represent the standard deviation of the analyzed data from three replicates.

## 4.4 Conclusion

This study reported the synthesis of a series of diblock glycopolymers for pDNA delivery. The glycopolymers exhibited the ability to bind pDNA at low N/P ratios and form polyplexes. The internalization profile, transgene expression efficiency and cytotoxicity of the polyplexes exhibited a large dependency upon the architecture (amine

type and block length) during *in vitro* transfection experiments in both HeLa and HepG2 cells. Generally, polyplexes formed with glycopolymers with a PAEMA block showed higher transfection efficiency than glycopolymers with PDMAPMA block. Moreover, glycopolymers with a longer PDMAPMA block length appeared to be less efficient gene delivery vehicles with higher cytotoxicity. The length of the PMAG block did not show a significant impact on the pDNA delivery in the current study. Interestingly, glycopolymer polyplexes exhibited much higher transfection efficiency in HepG2 cells than in HeLa cells. This was attributed to the ability of HepG2 cells to both internalize more polyplexes and promote higher gene expression, in comparison with the same systems in HeLa cells. Comparing the transfection efficiency between $PAEMA_{58}$ lacking the sugar block and PMAG-b-PAEMA systems in the two cell types, it was revealed that the PMAG block could have interactions with specific receptors on hepatocellular membranes. The interaction between the exposed PMAG block on polyplexes and HepG2 cells could contribute to the increased transfection efficiency in HepG2 cells. The presence of galactose molecules in the media inhibited the transgene expression for some of the glycopolymers in HepG2 cells, potentially indicating that the ASGP receptor could play a role in this enhanced delivery profile. Further studies are needed to explore the intracellular pathways associated with these glycopolymer pDNA delivery systems and the potential mechanism of cytotoxicity associated with the PDMAPMA block.

## 4.5 Reference

1. Kay, M. A. *Nat. Rev. Genet.* **2011,** *12*, 316-328.

2. Mintzer, M. A.; Simanek, E. E. *Chem. Rev.* **2009,** *109*, 259-302.

3. Davis, M. E.; Zuckerman, J. E.; Choi, C. H. J.; Seligson, D.; Tolcher, A.; Alabi, C. A.; Yen, Y.; Heidel, J. D.; Ribas, A. *Nature* **2010,** *464*, 1067-1070.

4. Wang, T.; Upponi, J. R.; Torchilin, V. P. *Int. J. Pharm. (Amsterdam, Neth.)* **2012,** *427*, 3-20.

5. Oba, M.; Miyata, K.; Osada, K.; Christie, R. J.; Sanjoh, M.; Li, W.; Fukushima, S.; Ishii, T.; Kano, M. R.; Nishiyama, N.; Koyama, H.; Kataoka, K. *Biomaterials* **2011,** *32*, 652-663.

6. Xu, Y.; Takai, M.; Ishihara, K. *Biomaterials* **2009,** *30*, 4930-4938.

7. Ahmed, M.; Bhuchar, N.; Ishihara, K.; Narain, R. *Bioconjugate Chem.* **2011,** *22*, 1228-1238.

8. Hemp, S. T.; Smith, A. E.; Bryson, J. M.; Allen, M. H.; Long, T. E. *Biomacromolecules* **2012,** *13*, 2439-2445.

9. Smith, A. E.; Sizovs, A.; Grandinetti, G.; Xue, L.; Reineke, T. M. *Biomacromolecules* **2011,** *12*, 3015-3022.

10. Li, H.; Cortez, M. A.; Phillips, H. R.; Wu, Y.; Reineke, T. M. *ACS Macro Lett.* **2013,** *2*, 230-235.

11. Buckwalter, D. J.; Sizovs, A.; Ingle, N. P.; Reineke, T. M. *ACS Macro Lett.* **2012,** *1*, 609-613.

12. Ahmed, M.; Jawanda, M.; Ishihara, K.; Narain, R. *Biomaterials* **2012,** *33*, 7858-7870.

13. Ahmed, M.; Narain, R. *Biomaterials* **2011,** *32*, 5279-5290.

14. Wang, Y.; Hong, C.-Y.; Pan, C.-Y. *Biomacromolecules* **2013,** *14*, 1444-1451.

15. Ahmed, M.; Narain, R. *Biomaterials* **2012,** *33*, 3990-4001.

16. Knop, K.; Hoogenboom, R.; Fischer, D.; Schubert, U. S. *Angew. Chem., Int. Ed. Engl.* **2010,** *49*, 6288-6308.

17. Barz, M.; Luxenhofer, R.; Zentel, R.; Vicent, M. J. *Polym. Chem.* **2011,** *2*, 1900-1918.

18. Ting, S. R. S.; Chen, G.; Stenzel, M. H. *Polym. Chem.* **2010,** *1*, 1392-1412.

19. Orietta, L.; Alexandra, M.-B.; Vanesa, B.; Manuel, S.-C.; Marta, F.-G. *J. Polym. Sci., Part A: Polym. Chem.* **2011,** *49*, 2627-2635.

20. Alexandra, M.-B.; Orietta, L.; Vanesa, B.; Manuel, S.-C.; Marta, F.-G. *J. Polym. Sci., Part A: Polym. Chem.* **2013,** *51*, 1337-1347.

21. Song, E.-H.; Manganiello, M.; Chow, Y.-H.; Ghosn, B.; Convertine, A.; Stayton, P.; Schnapp, L.; Ratner, D. *Biomaterials* **2012,** *33*, 6889-6897.

22. Smith, D.; Holley, A. C.; McCormick, C. L. *Polym. Chem.* **2011,** *2*, 1428-1441.

23. Hawker, C. J.; Bosman, A. W.; Harth, E. *Chem. Rev. (Washington, DC, U. S.)* **2001,** *101*, 3661-3688.

24. Matyjaszewski, K. *Macromolecules* **2012,** *45*, 4015-4039.

25. Moad, G.; Rizzardo, E.; Thang, S. H. *Aust. J. Chem.* **2005,** *58*, 379-410.

26. Ahmed, M.; Narain, R. *Prog Polym Sci* **2013,** *38*, 767-790.

27. Mitsukami, Y.; Donovan, M. S.; Lowe, A. B.; McCormick, C. L. *Macromolecules* **2001,** *34*, 2248-2256.

28. Convertine, A. J.; Lokitz, B. S.; Vasileva, Y.; Myrick, L. J.; Scales, C. W.; Lowe, A. B.; McCormick, C. L. *Macromolecules* **2006,** *39*, 1724-1730.

29. Xu, X.; Smith, A. E.; Kirkland, S. E.; McCormick, C. L. *Macromolecules* **2008,** *41*, 8429-8435.

30. York, A. W.; Huang, F.; McCormick, C. L. *Polym. Prepr. (Am. Chem. Soc., Div. Polym. Chem.)* **2008,** *49*, 1099-1100.

31. Kirkland-York, S.; Zhang, Y.; Smith, A. E.; York, A. W.; Huang, F.; McCormick, C. L. *Biomacromolecules* **2010,** *11*, 1052-1059.

32. York, A. W.; Huang, F.; McCormick, C. L. *Biomacromolecules* **2010,** *11*, 505-514.

33. Ziebarth, J.; Wang, Y. *J. Phys. Chem. B* **2010,** *114*, 6225-6232.

34. Nakai, K.; Nishiuchi, M.; Inoue, M.; Ishihara, K.; Sanada, Y.; Sakurai, K.; Yusa, S.-i. *Langmuir* **2013,** *29*, 9651–9661.

35. Pearson, S.; Allen, N.; Stenzel, M. H. *J. Polym. Sci., Part A: Polym. Chem.* **2009,** *47*, 1706-1723.

36. Nie, C.; Liu, C.; Chen, G.; Dai, J.; Li, H.; Shuai, X. *J. Biomater. Appl.* **2011,** *26*, 255-275.

37. Gomes-da-Silva, L. C.; Fonseca, N. A.; Moura, V.; Pedroso de Lima, M. C.; Simões, S.; Moreira, J. N. *Acc. Chem. Res.* **2012,** *45*, 1163-1171.

38. Palermo, E. F.; Lee, D.-K.; Ramamoorthy, A.; Kuroda, K. *J. Phys. Chem. B* **2011,** *115*, 366-375.

39. Luo, X.; Feng, M.; Pan, S.; Wen, Y.; Zhang, W.; Wu, C. *J. Mater. Sci.: Mater. Med.* **2012,** *23*, 1685-1695.

40. Sung, S.-J.; Min, S. H.; Cho, K. Y.; Lee, S.; Min, Y.-J.; Yeom, Y. I.; Park, J.-K. *Biol. Pharm. Bull.* **2003,** *26*, 492-500.

41. Wu, G. Y.; Wu, C. H. *Adv. Drug Delivery Rev.* **1998,** *29*, 243-248.

42. Rigopoulou, E. I.; Roggenbuck, D.; Smyk, D. S.; Liaskos, C.; Mytilinaiou, M. G.; Feist, E.; Conrad, K.; Bogdanos, D. P. *Autoimmun. Rev.* **2012,** *12*, 260-269.

43. Pathak, A.; Vyas, S. P.; Gupta, K. C. *Int. J. Nanomed.* **2008,** *3*, 31-49.

44. Fukuma, T.; Wu, G. Y.; Wu, C. H. *Gene Ther. Regul.* **2000,** *1*, 79-93.

45. Pun, S. H.; Davis, M. E. *Bioconjugate Chem.* **2002,** *13*, 630-639.

46. Grandinetti, G.; Smith, A. E.; Reineke, T. M. *Mol. Pharm.* **2011,** *9*, 523-538.

# Chapter 5 Investigating the Impact of Lipophilicity on Polymeric Vehicles for Plasmid DNA Delivery to Multiple Cell Types

This chapter presents our research effort to understand the role of lipophilicity of polycation in in vitro pDNA delivery. The synthesis and characterization of a series of poly(alkylamidoamine) (PAAA) was described. The obtained polymers were examined for their cytotoxicity and transfection efficiency in multiple cell types, including HDFa (human dermal fibroblasts, adult) cells, HeLa (human cervix adenocarcinoma) cells, HMEC (human mammary epithelial cells), and HUVEC (human umbilical vein endothelial cells). How the lipophilic linkers affect pDNA delivery was also studied

## 5.1 Introduction

Gene therapy has recently shown great potential in treating various genetic and infectious diseases; however, the development of safe and efficient nucleic acid delivery vectors is still needed for progress in this area.[1-2] Nonviral vectors have been designed to circumvent several drawbacks involved with viral vectors, including immunogenicity and limited scale-up.[2-5] Among the various classes of synthetic vehicles,[4] polycations and cationic amphiphilic lipids are two of the main classes that have been extensively studied for nucleic acid delivery.[6-7] For example, one of the more popular commercial agents is Lipofectamine 2000,[8] which is comprised of a cationic lipid, 2,3-dioleyloxy-N-[2-(sperminecarboxamido) ethyl]-N, N-dimethyl-1-propanaminium trifluoroacetate (DOSPA), and a neutral lipid, dioleoyl phosphatidylethanolamine (DOPE).[9] While this vehicle forms liposomal vesicles, the electrostatic interaction between cationic groups on the hydrophilic head groups and negatively charged nucleic acid drives lipoplex assembly upon mixing, where the nucleic acid is subsequently associated with either the surface, interior, or both of the liposomal vesicles.[10] The resulting lipoplexes bind to cell membranes mainly via unspecific electrostatic interaction and are then internalized by cells via endocytosis.[10] It is hypothesized that the cationic lipids then destabilize the endosomal membrane, resulting in a flip-flop reorganization of phospholipids and the subsequent release of nucleic acid into cytoplasm.[4] Although Lipofectamine 2000 remains one of the most efficient transfection agents, significant research effort has been devoted to developing more efficient alternative systems to promote nucleic acid delivery.[7, 11-12]

Several research groups have taken advantage of lipophilicity to improve the efficiency of various class of transfection agents, such as polyethylenimine (PEI).[9, 13-14] For example, Bansal et al. have shown that the linear PEI grafted with lipophilic group (4-bromobutyl)triphenylphosphonium bromide (BTP) exhibited the enhanced cellular uptake and transfection level relative to linear PEI in A549 (adenocarcinomic human alveolar basal epithelial cells) and MCF-7 (breast cancer) cells.[13] Valencia-Serna et al. modified branched PEI (2 kDa) with linoleic acid or palmitic acid, and the obtained lipid substituted PEI exhibited exhibited green fluorescent protein (GFP) silencing efficiency comparable to Lipofectamine 2000 for siRNA delivery in K562 (human myelogenous leukemia) cells.[14] Kuchelmeister et al. also attached lipophilic tails (two $C_{18}$ alkyl chains) to the cationic peptidic tweezers, which is composed of two dipeptide arms the basic guanidinocarbonyl pyrrole (GCP) moieties, and the lipophilic modification improved the transfection efficiency of GFP plasmid DNA.[9] Previously, we have developed a library of poly(glycoamidoamine)s (PGAA) and examined their transfection efficiency both in vitro and in vivo.[15-17] PGAA featured various types of carbohydrate group and oligoethyleneamines, and exhibited significantly lower cytotoxicity and similar transfection efficiency as compared to PEI.[15] Here, a family of linear poly(alkylamidoamine) (PAAA) have been created by copolymerizing lipophilic alkyl acid chlorides with a pentaethylenehexamine derivative. It was anticipated that lipophilicity would facilitate the interaction between polyplexes and cellular membrane, and subsequent transfection process.

In this chapter, we reported our effort in synthesizing a series of poly(alkylamidoamine) (PAAA) with various length alkyl linker ($C_3$ to $C_6$), via step-growth polymerization between diacid chloride monomers and diamine monomers. Gel electrophoresis was utilized to examine the pDNA binding ability of the obtained PAAA polymers. The polymer/pDNA complexes, i.e. polyplexes were evaluated for their transfection ability in multiple cell lines, including HDFa (human dermal fibroblasts, adult) cells, HeLa (human cervix adenocarcinoma) cells, HMEC (human mammary epithelial cells), and HUVEC (human umbilical vein endothelial cells). Finally, the molecular weight impact on the transfection was studied.

## 5.2 Materials and experiments

### 5.2.1 Materials

All chemicals were purchased from Sigma Aldrich and used without further purification unless specified otherwise. Pentaethylenehexamine was purchased from Acros Organics and purified via vacuum distillation before use. Cell culture media, Dulbecco's Modified Eagle Medium (DMEM) and Opti-MEM, antibiotic/antimycotic, fetal bovine serum (FBS), phosphate-buffered saline (PBS), and nuclease-free water were purchased from Gibco (Carlsbad, CA). DNase, and RNase free water was from Sigma-Alderich and Cell counting kit-8 (CCK-8) was from Dojindo molecular technologies. GFP plasmid DNA (gwiz-GFP) was obtained from Aldevron. Other reagents used for cell biology experiment, if not specified, were purchased from Life Technologies

### 5.2.2 2,2'-({Ethylenebis[(tert-butoxycarbonyl)imino]}bisc)diethan-1-amine (1)

Compound 1 was synthesized according to our previously reported procedures,[18]. Distilled pentaethylenehexamine (10.0 g, 22.2 mmol, 100 mL of dry dichloromethane (DCM)/dry Methanol (1:1 mixture)) was reacted with ethyl trifluoroacetate (6.6g, 46.7 mmol/100 mL of dry DCM) was then added dropwise over 30 min to selectively protect the terminal primary amines. The resulting mixture was stirred for another 1 h at 0 °C, and for an additional 3 h at room temperature. Di-tert-butyl dicarbonate (Boc) (20.0 g, 91.0 mmol/40 mL of methanol) was then added dropwise over 30 mins into the reaction mixture. The reaction was stirred under room temperature over 24 h to protect the secondary amines. The reaction solvent was then evaporated, the final product was purified and isolated (11.6 g, 63%) via recryslatization using chloroform and filtration. To remove the trifluoroacetyl groups, the product was refluxed in 250 mL of Methanol/water 10:1 with 11 g $K_2CO_3$ for 12 h. Compound 1 was isolated by crystallization in $CHCl_3$. (8.00 g, overall yield 54%).

### 5.2.3 The cationic copolymer synthesis via step-growth polymerization

A solution of diacid chloride monomer (0.10 g, 0.55 mmol/2.50 mL of dry DCM) was added dropwise to a solution of compound 1 (0.35 g, 0.54 mmol/2.50 mL of dry DCM). The mixture was stirred at room temperature for 1 h. After evaporating the DCM, the resultant polymer was stirred with 6 mL of 4 M HCl in dioxane for 4 h to remove the Boc groups, followed by the evaporation of dioxane. The obtained polymer was purified

through dialysis against ultrapure water with 3500 Da MW dialysis tube for 3 days. White solid was yielded after lyophilization.

### 5.2.4 Polymer characterization

The molecular weight, dispersity index (Đ) of all these obtained polymers were characterized by size exclusion chromatography (SEC) equipped with a TSK-GEL $GMPW_{XL}$ column, a Wyatt HELEOS II static light scattering detector ($\lambda$ = 662 nm), and an Optilab rEX refractometer ($\lambda$ = 658 nm), using 0.5 M sodium acetate aqueous solution as mobile phase (pH 5.0) at a flow rate of 0.8 mL/min

### 5.2.5 Polyplex formation and gel electrophoresis assay

The ability of the synthesized polymer to bind with pDNA and form polyplexes was qualitatively determined by gel electrophoresis. plasmid DNA (gwiz-GFP, 1.0 μg, 0.02μg/μL) was mixed with an equal volume of the Opti-MEM solution of each polycation at various N/P ratios (i.e. 5, 10, 25, 50). The N/P ratio signifies the molar ratio of the amine (N) moieties on the polycation to the phosphate (P) groups on the pDNA backbone. After an incubation of 45 mins, a 10 μL aliquot was applied into a 0.6 % agarose gel containing 6 μg of ethidium bromide / 100 mL TAE buffer (40 mM tris-acetate, 1 mM ethylenediaminetetraacetic acid (EDTA), and ran for 45 min at 90 V.

### 5.2.6 Dynamic light scattering (DLS) and ζ potential

Polyplex sizes were measured by dynamic light scattering (DLS) at 633 nm with a Malvern Zetasizer Nano ZS. pDNA gwiz-GFP (1.0 μg, 0.02 μg/μL) was incubated with an equal volume of each polymer at an N/P ratio of 5, 10, 20, 40, 60, 80 for 45 mins to form the

subsequent polyplexes. Thereafter, samples were diluted to 300 μL with Opti-MEM. The samples were measured in triplicate at 25 ºC with a detection angle of 173º.

### 5.2.7 Cell culture experiments

Cells were seeded at 50,000 cells per 24 well and cultured overnight in culture incubator (37°C, 5% $CO_2$). Polyplex solution (PAAA with GFP plasmid) at various predetermined N/P ratios was prepared 45 min before transfection. After 45 min incubation, 100ul of polyplex solution was added to cells in 24 well with 500 μL culture media. The control cells received 100 μL of serum free medium with pDNA only. Transfection with Lipofectamine 2000 reagent was done according to manufacturer's recommendation. Briefly, Lipofectamine 2000 reagent (3 μL per 24 well) was incubated with plasmid DNA in serum free tissue culture medium for 30 min. Subsequently, 100 μL of lipoplex solution was added to cells in 24 well with 500 μl culture medium. Medium with transfection solution was replaced with 1 mL complete medium after 24hr incubation in culture incubator. Cells were then grown overnight, and subjected to cell survival and flow cytometry analysis.

Cells were analyzed on Accuri flow cytometor (Becton Dickinson) for GFP positive cells (488nm laser, FL1: 530nm channel). Negative control cells were used to gated where auto fluorescence was <3% in the FL1 channel.

Cell survival percentages were evaluated by CCK-8 color metric assay kit from Dojindo Molecular Technologies, Inc. Briefly, 48hr after transfection, culture medium was replaced with culture medium with 10% CCK-8 solution. Absorbance at 450 nm was

measured after 90 min (HeLa, HDFa) or 150 min (HMEC, HUVEC) incubation in culture incubator. Absorbance of non-transfected control cells were used as 100% survival. The survival of transfected cells relative to control was expressed as relative cell viability and was calculated by the (Absorbance of transfected) / (Absorbance of control) x 100% formula.

### 5.2.8 Statistical analysis

All data are presented as the mean ± the standard deviation and each analysis or measurement was performed in triplicate unless otherwise noted. For statistical analysis of the data, the means were compared using a Student's t test with $p < 0.05$ being considered as statistically significant.

## 5.3 Results and discussion

### 5.3.1 The synthesis and characterization of polymers

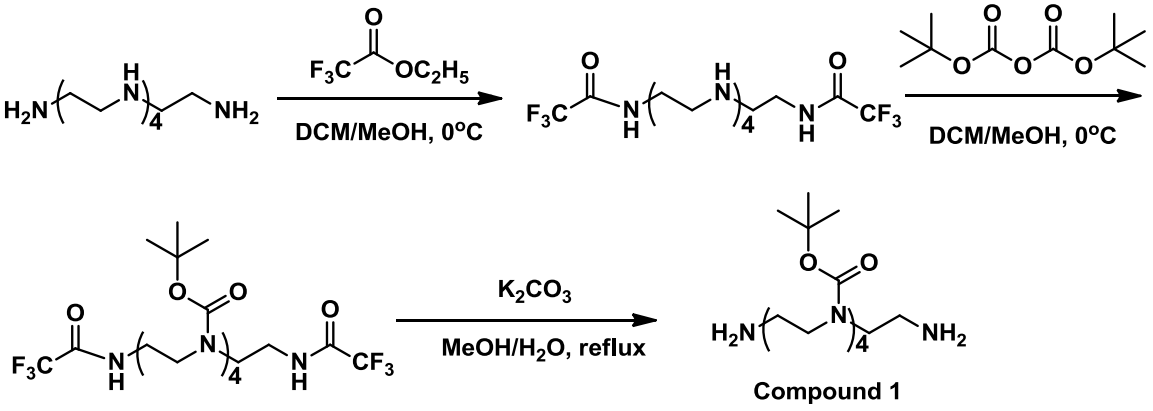


**Scheme 5.1** The synthetic scheme of the compound 1

Our group previously developed a series of PEI-like in vitro transfection agents, poly(glycoamidoamine)s (PGAA), and demonstrated that the carbohydrate type could significantly impact the transfection performance.[15-17] Previous results also showed that the polycation with alkyl linker could deliver pDNA into cells.[18] To systematically evaluate the impact of the length of alkyl linker in polycation on pDNA transfection delivery, we developed a series of poly(alkylamidoamine) (PAAA) by combining compound 1 and diacid chloride monomers with various length of methylene linker. Compound 1 was synthesized following previous published procedure[18]. The protection of primary amine was achieved by using ethyl trifluoroacetate at 0 ºC, followed by Boc protection, and the removal of trifluoroacetate group in basic condition, as shown in scheme 5.1. The final structure of the compound 1 was confirmed via $^1$H NMR (Figure 5.1) and ESI-MS (Figure 5.2).

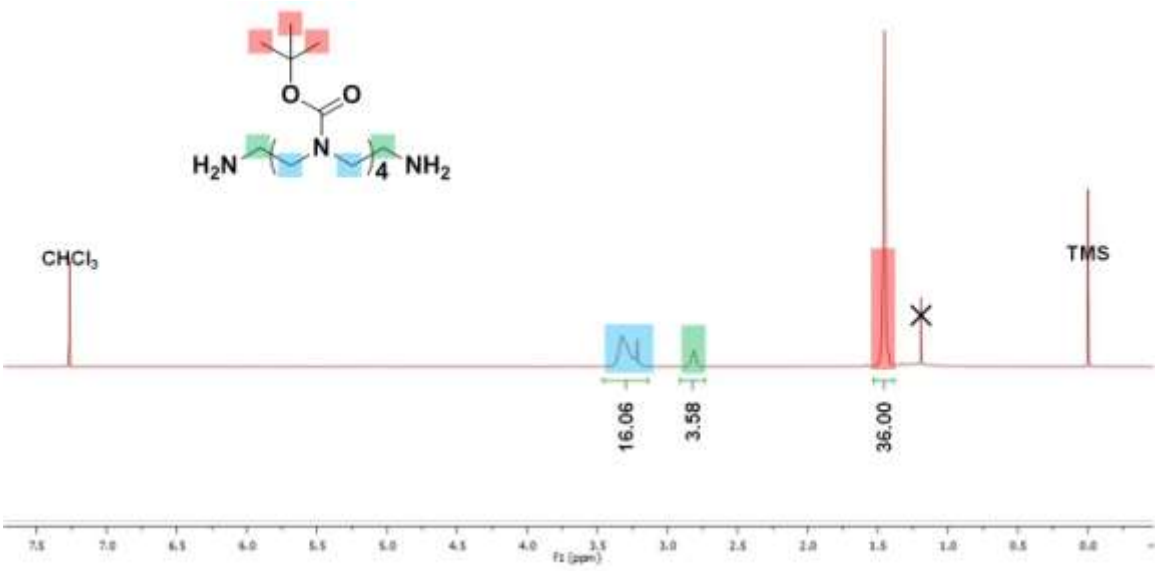


**Figure 5.1** $^1$H NMR spectra of compound 1

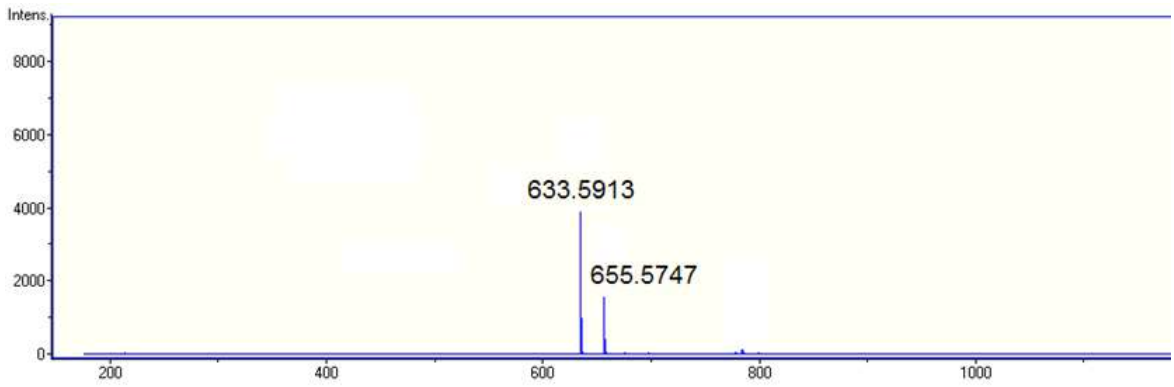


**Figure 5.2** ESI-MS spectra of the compound 1 (calculated $(M+H)^+$: 633.4551; found $(M+H)^+$: 633.5913; $(M+Na)^+$: 655.5747)

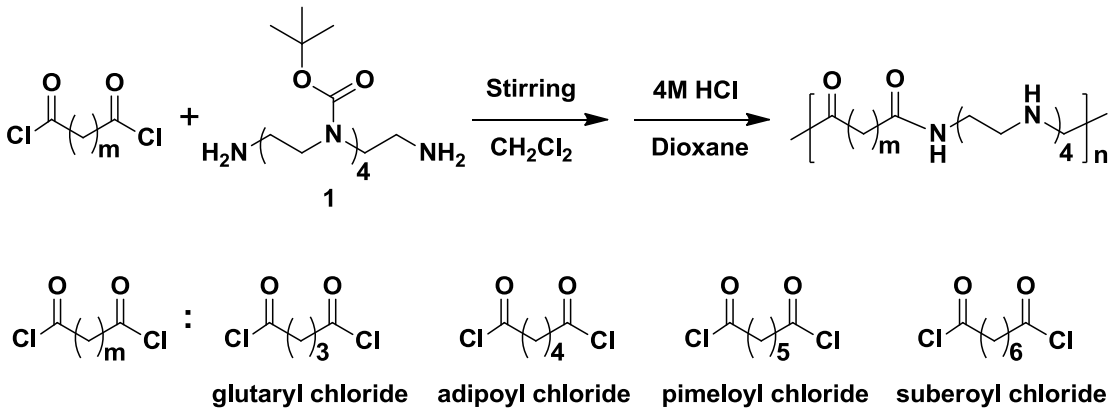


**Scheme 5.2** Synthetic scheme of lipophilic poly(amidoamine) (PAA) via step growth polymerization

The polymerization procedure was adapted from previously published procedure,[15] as shown in the scheme 5.2. A series of alkyl diacid chloride monomers with the number of methylene linker varying from 3 to 6 were utilized for PAAA synthesis (i.e. glutaryl chloride, adipoyl chloride, pimeloyl chloride, suberoyl chloride). Water

soluble PAAA polymers were yielded after the removal of Boc group, poly(glutaramidopentaethylenehexamine) (Glut4), poly(adipamidopentaethylenetetramine) (A4), poly(pimelamidopentaethylenetetramine) (Pim4), and poly(suberamidopentaethylenetetramine) (Sub4). The molecular weight control for step-growth polymerization was achieved by the stoichiometric offset of the feed ratio between diacid chloride monomers and diamine monomers.[19] Additionally, It should be noted that three other more lipophilic diacid chloride monomers were tested for the polymer synthesis as well, including azelaoyl chloride, sebacoyl chloride and dodecanedioyl chloride. However, the polymers synthesized using azelaoyl chloride exhibited poor transfection performance (high toxicity and low transfection efficiecny), and the polymers synthesized from the other two monomer (sebacoyl chloride and dodecanedioyl chloride) exhibited poor water solubility after the removal of Boc protecting group, and hence were excluded from this study.

The molecular weight and dispersity of the obtained polymers were characterized using SEC, and are summarized in Table 5.1. The SEC traces are shown in Figure 5.3. It is worth noting that the relatively low Đ value of all the obtained polymers was possibly due to the dialysis purification process.

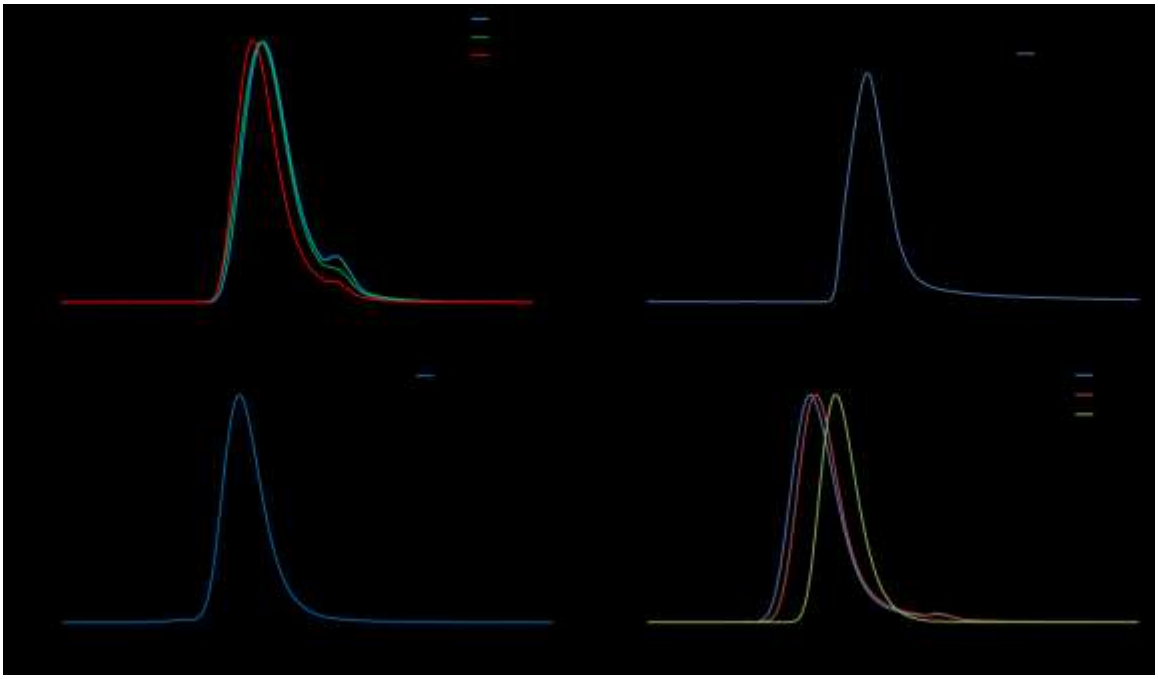

**Figure 5.3** SEC traces of the poly(alkylamidoamine) (PAAA): (a) Glut4 series polymers; (b) A4 polymer; (c) Pim4 polymer; (d) Sub4 series polymers

**Table 5.1** Molecular weight, dispersity, and calculated degree of polymerization (DP) of PAAA polymers examined in this study

| Polymers | Methylene per repeating unit | Mw/kDa | $M_w/M_n$ | DP |
|---|---|---|---|---|
| Glut4-30 | 3 | 9.8 | 1.28 | 30 |
| Glut4-37 | 3 | 12.2 | 1.30 | 37 |
| Glut4-57 | 3 | 18.7 | 1.35 | 57 |
| A4-27 | 4 | 9.2 | 1.40 | 27 |
| Pim4-45 | 5 | 16.0 | 1.18 | 45 |
| Sub4-27 | 6 | 10.0 | 1.17 | 27 |
| Sub4-43 | 6 | 15.9 | 1.25 | 43 |
| Sub4-65 | 6 | 24.1 | 1.25 | 65 |

### 5.3.2 Polyplex formation and gel electrophoresis assay and DLS characterization

Polyplexes were formed by mixing equal volumes of the Opti-MEM solutions of pDNA and PAAA at various N/P ratios The pDNA binding ability of the obtained copolymers in this condition was examined through gel electrophoresis shift assays at various ratios between 0 and 50 (Figure 5.4). Despite of the presence of salt and amino acid in the

serum-free medium, Opti-MEM, pDNA migration in the gel was still retarded at N/P ratios of 5 for all of the examined samples. N/P ratios above 5 were selected for the subsequent study.

The hydrodynamic diameter of polyplexes in Opti-MEM was determined to be around 1000 nm via DLS for all the examined polycation.(Figure 5.5) As the N/P ratio varies from 5 to 20 or 40, the diameter were relatively stable; while higher N/P ratios (above 40) often lead to larger particles size. Overall, the size values are over the size range conventionally considered to be ideal size (30 to several hundred nm)[1]. Our previous published cationic polymers with similar structure were able to form polyplexes with diameter mostly around 200 nm in nuclease-free water.[15] The size increase of the polyplexes in Opti-MEM was contributed to the physiological salt condition of the medium, where the interaction between nucleic acid and polycation was shielded by the surrounding counter ion, resulting in relatively loose complexes. Additionally, aggregation in the medium could in part contribute to the large diameter of the polyplexes. It should be noted that, as the gel images indicates, despite of the salt condition and larger polyplexes size, the polyplexes composed of PAAA still showed stability at a N/P ratio of 5 in most cases, which is important for in vitro nucleic acid delivery[20]. Hence, the polyplexes were utilized for the subsequent in vitro pDNA transfection experiments.

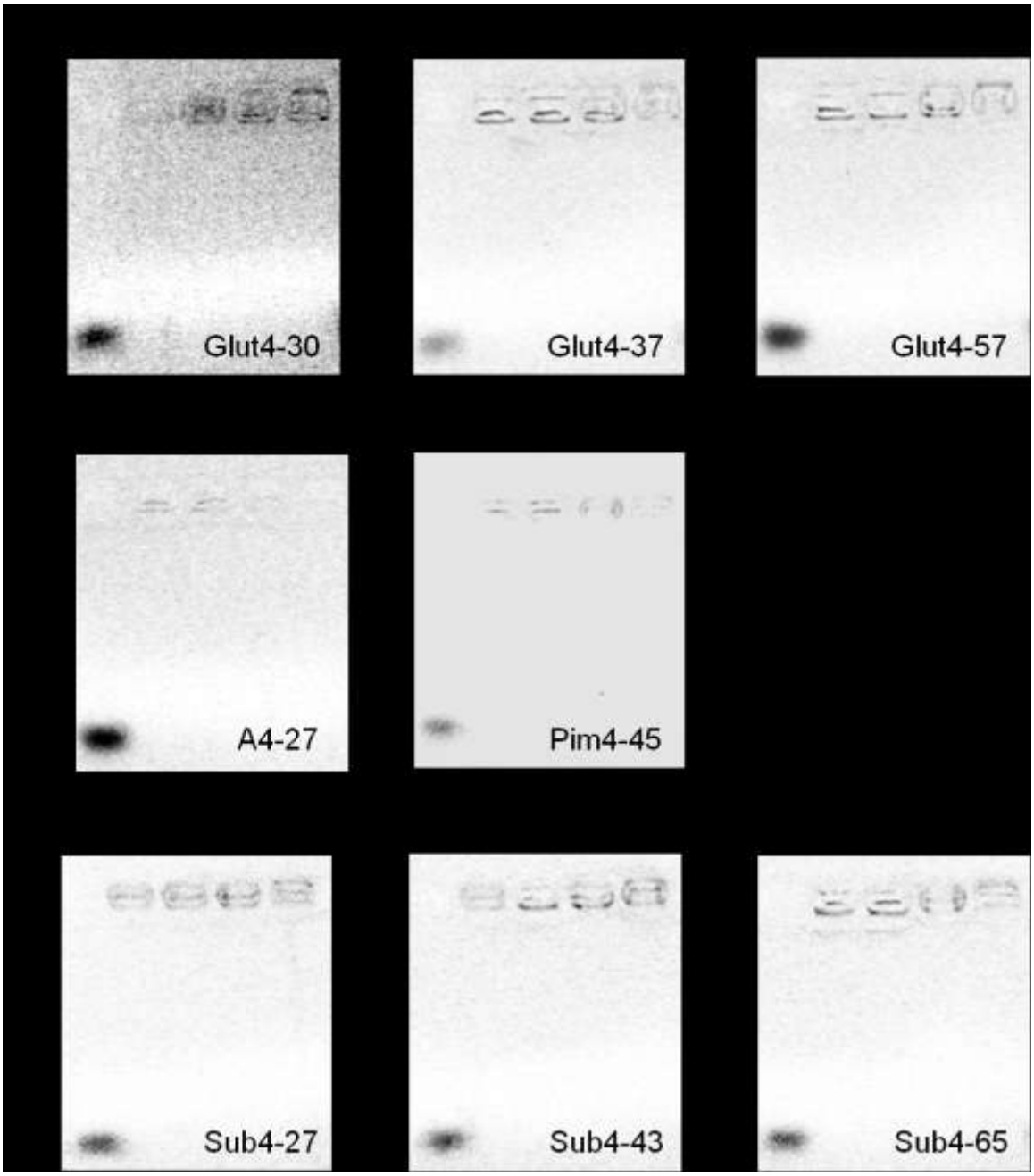


**Figure 5.4** Gel electrophoresis images of the PAAA

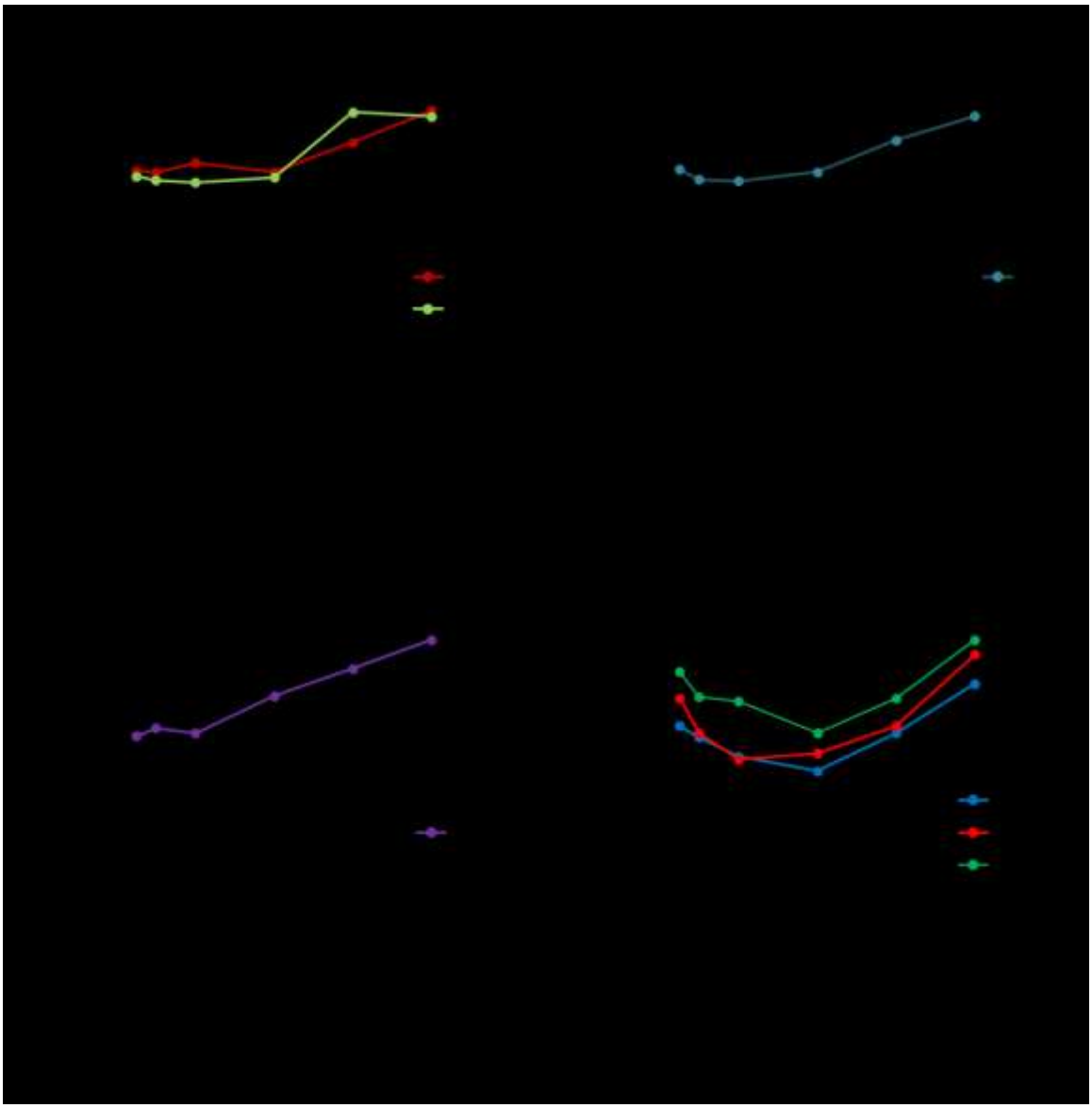

**Figure 5.5** Hydrodynamic diameters of the polyplexes composed of PAAA and gwiz-GFP, formed in OptiMEM. Error bars represent the standard deviation of analyzed data from three replicates.

### 5.3.3 PAAA polyplexes exhibited high transfection efficiency in multiple cell types

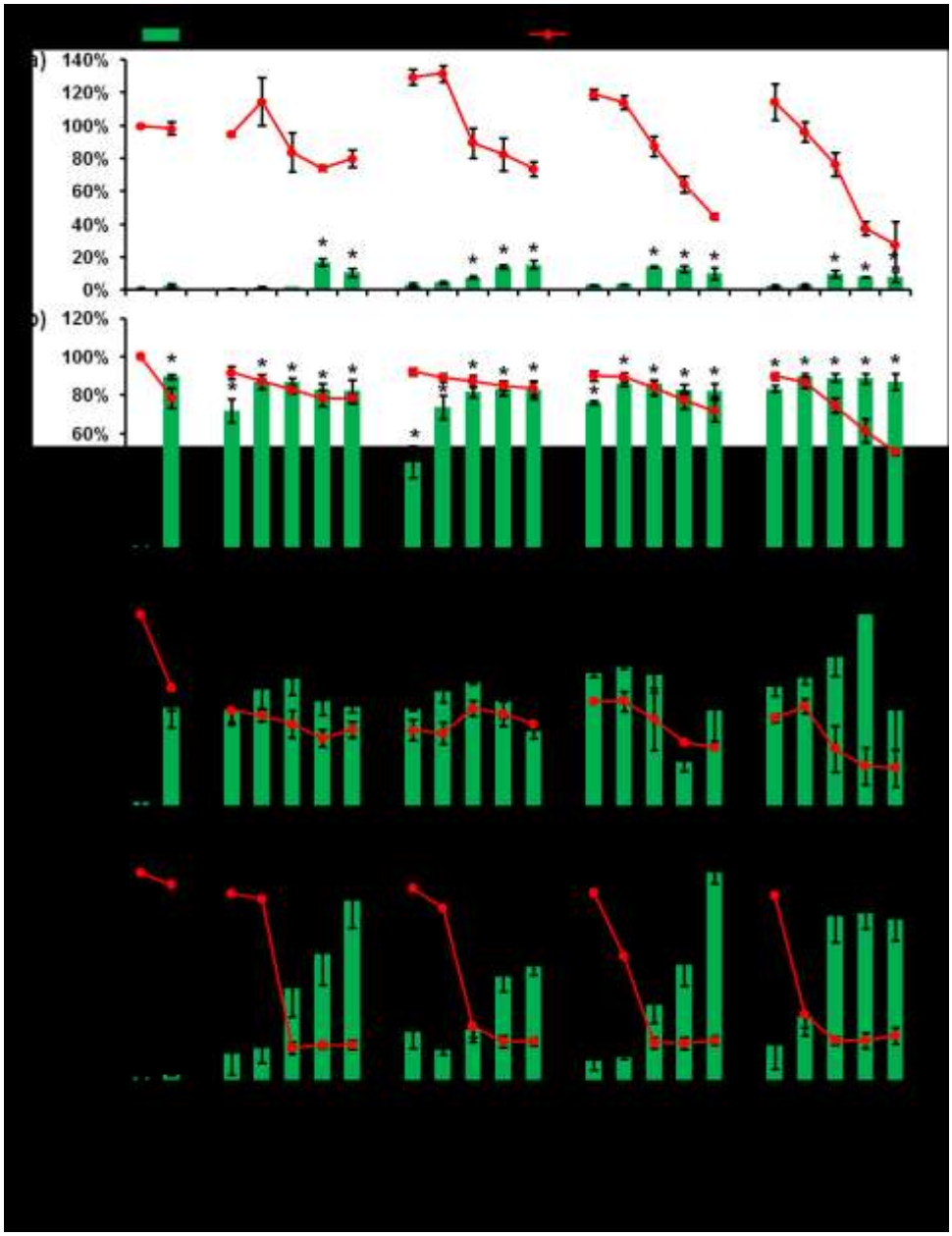


**Figure 5.6** Cytotoxicity (dot-line) and transfection (bar) profiles of Glut4, A4, Pim4, and Sub4 Polymers in various cell types: (a) HDFa; (b) HeLa; (c) HMEC; (d) HUVEC. Error bars represent the standard deviation of analyzed data from three

replicates. Measurements found to be statistically different from control group ($p < 0.05$) are marked with an asterisk

To examine the in vitro pDNA delivery ability of the obtained PAAA, both cytotoxicity and transgene expression were evaluated in multiple cell types, including HeLa (human cervical carcinoma) cells, HDFa (human dermal fibroblasts, adult) cells, HUVEC (human umbilical vein endothelial cell), HMEC (human mammary epithelial cell),. The cytotoxicity profiles of the PAAAs were evaluated with CCK-8 kit 48 h after cells were treated with polyplexes solution. (Figure 5.6, dot-line) Non-transfected cells were used as the 100% survival to normalize the live cell percentage of treated wells. It should be noted different cell types were incubated with CCK-8 solution for different time period (90 min for HDFa and HeLa cells; 150 min for HMEC and HUVEC cells) for optimal results, mainly owing to the difference in cellular metabolism. Lipofectamine 2000 was used as the positive control agent, because of its versatility to transfect multiple cell types. For HeLa cell lines, both Lipofectamine and the PAAA polymers generally exhibited low cytotoxicity. In particular, the PAAA polymers exhibited low toxic effect (around 91% cell survival) at N/P ratio of 10 and 20, while the cytotoxicity of all four PAAA polymers slightly increased at higher N/P ratio. Additionally, longer methylene linker appeared to cause increased toxicity, especially at high N/P ratio. For example, at N/P ratio of 80, Sub4-28 caused nearly 53% cell death, while cells treated with Glut4-37 exhibited about 80% survival. In the other three cell lines, Lipofectamine showed similarly low cytotoxicity; the cytotoxicity generally increased when cells were treated with polyplexes at higher N/P ratio, which is consistent with what is found in HeLa.

However, PAAA polymers exhibited significantly higher cytotoxicity at N/P ratio of 40, 60, and 80 in HDFa and HUVEC. For instance, cell survival percentage at N/P ratio of 10 is close to 100% in HDFa, but the cell survival dropped to about 22% for Sub4-28 polymers. The cytotoxicity profile of Sub4-28 in HUVEC is similar to that in HDFa. In HMEC cells, the PAAA polymers exhibited around 50 % cell survival for most of the N/P ratio tested.

To assess the transfection ability of the obtained PAA polymers, all four cell lines were transfected with plasmid DNA encoded for green fluorescent protein (gwiz-GFP), and the percentage of GFP positive cells were analyzed via flow cytometry. (Figure 5.6, bars) Lipofectamine 2000, the state of the art transfection agent, was selected as positive control. Although the transfection efficiency level varied between cell types, all four analogues exhibited comparable or even superior transfection ability for the cell lines tested, as compared to Lipofectamine 2000. In HeLa cells, the transfection efficiency of Lipofectamine was about 92 %. Most of the polyplexes exhibited similarly high transfection efficiency. At N/P ratio above 20, all the polymers exhibited over 84% transfection efficiency. The impact of N/P ratio increase was not apparent for HeLa cells. Increasing N/P ratio did not lead to apparent increase in transfection efficiency in HMEC cell lines mostly, either. At N/P ratio of 10 and 20, PAAAs and Lipofectamine 2000 achieved similar transfection efficiency (over 50% GFP positive cells). Additionally, for several analogues (A4-27, Pim4-45, and Sub4-28), the drop in transfection efficiency was found for high N/P ratio. For example, the GFP positive cell percentage for Sub4-26 polymers dropped from over 61% over higher at low ratios to about 47% at a N/P ratio of

80 in HMEC. The toxic effect of the PAAA is possibly the cause for decrease in transfection efficiency at high N/P ratio. For HUVEC, and HDFa, negligible level of transfection was achieved by Lipofectamine 2000. However, the PAAA polymers exhibited significantly higher transfection efficiency. In HUVEC cells, despite of the high toxicity effect at high N/P ratio, PAAA polymers exhibited significant level of transfection. The transfection efficiency reached 92%, 58%, 99%, and 79% for Glut4-37, A4-27, Pim4-45, and Sub4-28 at N/P ratio of 80 respectively while Lipofectamine 2000 exhibited negligible level of GFP positive cells percentage. Although the transfection efficiency for PAAA polymers were overall very low (around 20%) in HDFa cells compared to the GFP percentage in other cell types, PAAA polymers still showed higher transfection efficiency at several high N/P ratios (40, 60, and 80) than Lipofectamine did. Overall, the transfection efficiency profiles of the PAAA polymers exhibited apparent cell-type dependence, but the PAAA polymers showed similar or even significantly higher transfection efficiency compared to Lipofectamine 2000. It has been demonstrated that increasing lipophilicity of the synthetic delivery vector could enhance the transfection efficiency for pDNA and siRNA.[13-14, 21-23] Therefore, it is proposed that the synthesized PAAA polymers with lipophilic linker aid in the interaction with lipophilic cellular membrane, and possibly the destabilization of the cellular membrane, which facilitated the nucleic acid delivery for polyplexes.

### 5.3.4 The impact of lipophilicity in PAAA pDNA delivery system

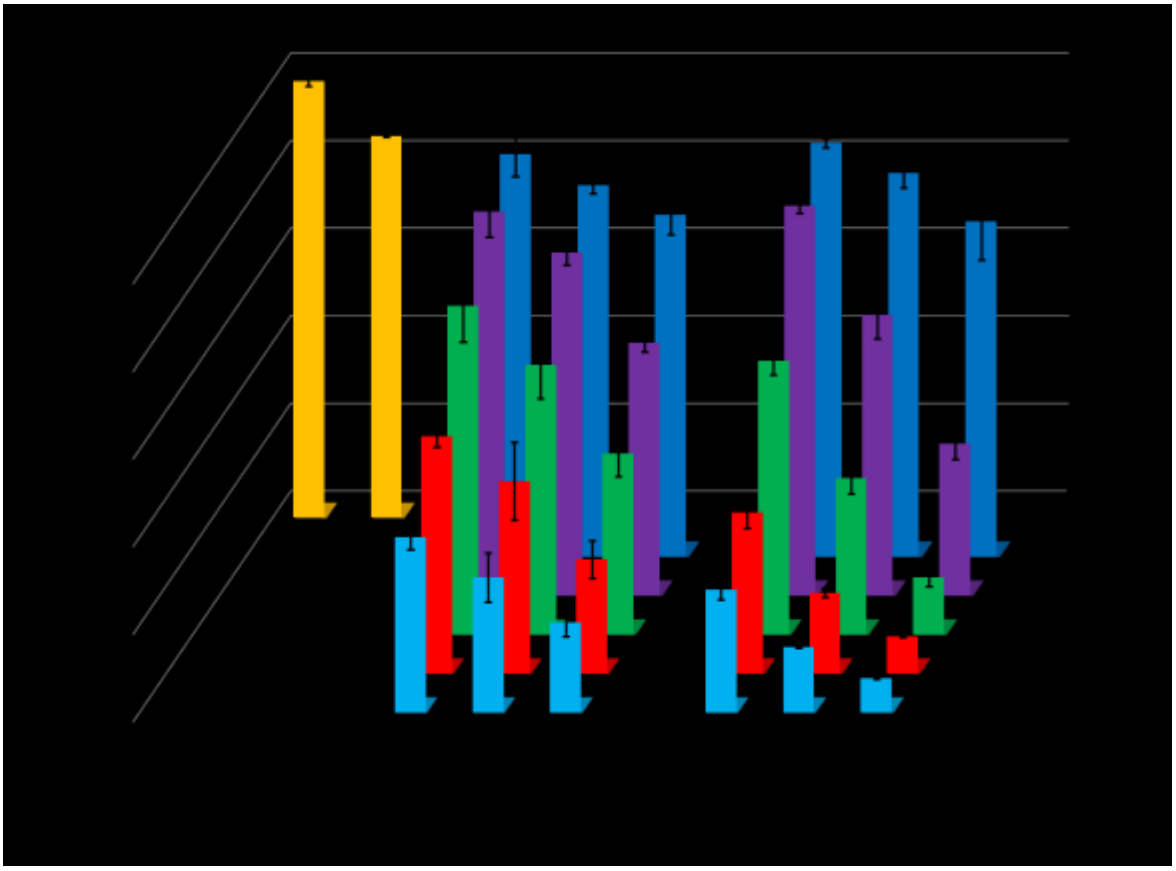

**Figure 5.7** Cytotoxicity profile of Glut4 and Sub4 series of polymers at various N/P ratios in HeLa cells

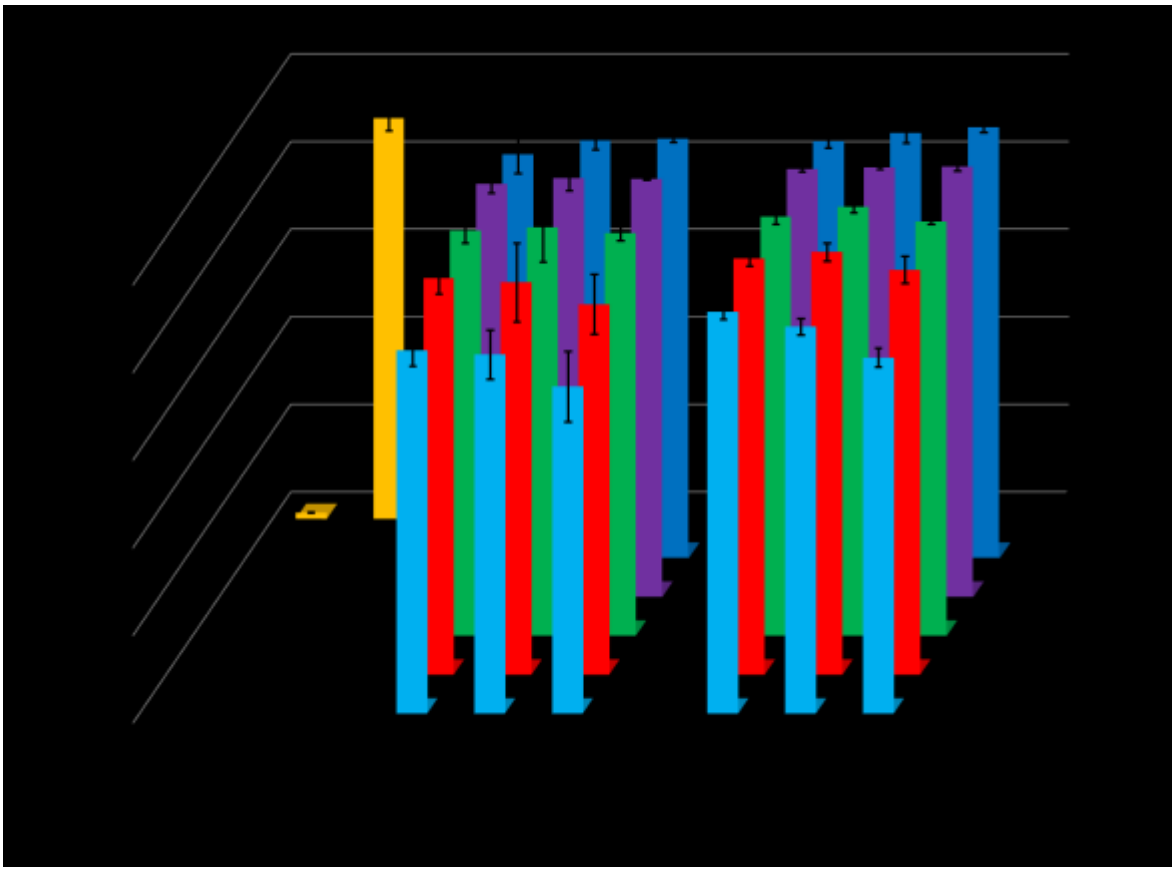

**Figure 5.8** Transfection efficiency of Glut4 and Sub4 series of polymers at various N/P ratios in HeLa cells

To further evaluate the impact of the lipophilic structure, we examined the cytotoxicity and transgene expression efficiency of Glut4 (3 methylene group per repeating unit) and Sub4 (6 methylene group per repeating unit) with similar degree of polymerization at various N/P ratios in HeLa cells.

As shown in Figure 5.7, it is apparent that the toxicity increases as the molecular weight of PAAA increases. Additionally, as the N/P ratio increases, the cell survival percentage drops as well. By comparing the Glut4 series with Sub4 series, it was revealed

that the Sub4 polymers exhibited overall higher cytotoxicity than Glut4 polymers with similar DP at multiple N/P ratios tested. For examples, at N/P raio of 10, both Sub4-43 and Sub4-65 exhibited lower cell survival percentage (63%, 37% respectively) than their Glut4 counterparts (82% for Glu4-40, and 58% for Glut4-57).

The transgene expression results were summarized in Figure 5.8. In HeLa cells, both Glut4 and Sub4 polymers exhibited relatively high transfection efficiency (above 84%) at N/P ratio of 5 and 10. Increasing N/P ratios lead to a slight decrease in transfection efficiency for most polycation examined, and higher molecular weight leads to higher cytotoxicity as well, especially at N/P ratio of 40. The drop in transfection level was mainly contributed to the elevated cytotoxicity. Moreover, at N/P ratio of 30 and 40, Sub4 polymers exhibited higher transfection efficiency than the Glut4 polymers with similar DP did. For example, transfection efficiency for Glut4-30 was 71% at N/P ratio of 40, while Sub4-27 exhibited about 82% transfection efficiency. It was established that lipophilic modification of PEI could enhance the membrane-disruptive properties of the agent, and increase its ability of endosomal escape.[21] Previously, our group demonstrated that the membrane disruption is the main cause for cytotoxicity of PEI reagents. It is hypothesized that lipophilic linker facilitate the interaction with cellular membrane, which possibly leads to membrane disruption, resulting in the increase of cytotoxicity when molecular weight and N/P ratio increased. On the other hand, membrane disruption could also be beneficial for pDNA delivery process, and contribute the relatively high transfection performance in HeLa cells.

## 5.4 Conclusion

In the present chapter, we reported the polymerization of a series of poly(alkylamidoamine) (PAAA) with various length of lipophilic methylene linkers, poly(glutaramidopentaethylenehexamine) (Glut4), poly(adipamidopentaethylenetetramine) (A4), poly(pimelamidopentaethylenetetramine) (Pim4), and poly(suberamidopentaethylenetetramine) (Sub4). All of the obtained polymers were shown to form stable complexes with pDNA in serum reduced medium at about N/P ratio of 5. The toxicity profiles of the PAAA were examined via CCK-5 kit in various cell types, including HDFa, HeLa, HMEC, HUVEC. The cytotoxicity of the polymers were cell type dependent, but toxicity were increased by transfecting cells at higher N/P ratios in all 4 cell types. Interestingly, according to GFP expression assay, all the samples tested exhibited similar transfection efficiency in HeLa and HMEC, compared to Lipofectamine 2000. Moreover, the transfection efficiency of all the polymers were significantly higher than that of Lipofectamine 2000. And it was revealed that, in HeLa cells, longer methylene linker caused higher cytotoxicity, but also higher transfection efficiency by comparing Glut4 polymers with Sub4 polymers with similar DP. These results demonstrate the great potential of the proposed PAAA polymers as in vitro pDNA delivery vectors for multiple cell types.

## 5.5 Reference

1. Pack, D. W.; Hoffman, A. S.; Pun, S.; Stayton, P. S. *Nat Rev Drug Discov* **2005,** *4*, 581-593.

2. Kay, M. A. *Nat. Rev. Genet.* **2011,** *12*, 316-328.

3. Bouard, D.; Alazard-Dany, N.; Cosset, F. L. *Br. J. Pharmacol.* **2009,** *157*, 153-165.

4. Mintzer, M. A.; Simanek, E. E. *Chem. Rev.* **2009,** *109*, 259-302.

5. Guo, X.; Huang, L. *Acc. Chem. Res.* **2012,** *45*, 971-979.

6. Jones, C. H.; Chen, C.-K.; Ravikrishnan, A.; Rane, S.; Pfeifer, B. A. *Mol. Pharm.* **2013,** *10*, 4082-4098.

7. Gomes-da-Silva, L. C.; Fonseca, N. A.; Moura, V.; Pedroso de Lima, M. C.; Simões, S.; Moreira, J. N. *Acc. Chem. Res.* **2012,** *45*, 1163-1171.

8. Dalby, B.; Cates, S.; Harris, A.; Ohki, E. C.; Tilkins, M. L.; Price, P. J.; Ciccarone, V. C. *Methods* **2004,** *33*, 95-103.

9. Kuchelmeister, H. Y.; Karczewski, S.; Gutschmidt, A.; Knauer, S.; Schmuck, C. *Angew. Chem. Int. Ed. Engl.* **2013,** *52*, 14016-14020.

10. Rehman, Z. u.; Zuhorn, I. S.; Hoekstra, D. *J. Controlled Release* **2013,** *166*, 46-56.

11. Mahon, K. P.; Love, K. T.; Whitehead, K. A.; Qin, J.; Akinc, A.; Leshchiner, E.; Leshchiner, I.; Langer, R.; Anderson, D. G. *Bioconjug. Chem.* **2010,** *21*, 1448-1454.

12. Sun, S.; Wang, M.; Knupp, S. A.; Soto-Feliciano, Y.; Hu, X.; Kaplan, D. L.; Langer, R.; Anderson, D. G.; Xu, Q. *Bioconjug. Chem.* **2012,** *23*, 135-140.

13. Bansal, R.; Tripathi, S. K.; Gupta, K. C.; Kumar, P. *J Mater Chem* **2012,** *22*, 25427-25436.

14. Valencia-Serna, J.; Gul-Uludağ, H.; Mahdipoor, P.; Jiang, X.; Uludağ, H. *J. Controlled Release* **2013,** *172*, 495-503.

15. Liu, Y.; Reineke, T. M. *J. Am. Chem. Soc.* **2005,** *127*, 3004-3015.

16. Reineke, T. M. *J Polym Sci A Polym Chem* **2006,** *44*, 6895-6908.

17. Ingle, N. P.; Malone, B.; Reineke, T. M. *Trends Biotechnol.* **2011,** *29*, 443-453.

18. Liu, Y.; Reineke, T. M. *Biomacromolecules* **2010,** *11*, 316-325.

19. Anderson, K.; Sizovs, A.; Cortez, M.; Waldron, C.; Haddleton, D. M.; Reineke, T. M. *Biomacromolecules* **2012,** *13*, 2229-2239.

20. O'Rorke, S.; Keeney, M.; Pandit, A. *Prog Polym Sci* **2010,** *35*, 441-458.

21. Piest, M.; Engbersen, J. F. J. *J. Controlled Release* **2010,** *148*, 83-90.

22. Sunshine, J. C.; Sunshine, S. B.; Bhutto, I.; Handa, J. T.; Green, J. J. *PLoS ONE* **2012,** *7*, e37543.

23. Fortune, J. A.; Novobrantseva, T. I.; Klibanov, A. M. *J Drug Deliv* **2011,** *2011*, 6.

# Chapter 6 Summary

## 6.1 Summary

The overall goal of my project is to understand how polymeric structure impacts the transfection performance, and to develop efficient nonviral nucleic acid delivery vectors accordingly. Currently, numerous structures have been designed to realize efficient gene delivery,[1-3] while the fundamental understanding of the polymeric vector delivery is still lacking behind, especially the intracellular trafficking is still unclear.[4-5] Therefore, without the complete understanding of the transfection process, many researchers have to take the "trial and error" method to design the polymeric structure for better transfection performance. However, the transfection performance of cationic polymeric nucleic acid delivery vector could be affect by a number of different factors, such as charge types, polymer structures (i.e. block, star, or statistical polymer, etc.), molecular weight, targeting moieties, biodegradability, and many others. In this project, we limited our research scope to include a few structural features, such as molecular weight, amine types, lipophilicicty, and examined their effect on the nucleic acid delivery from various aspects.

Reversible-deactivation radical polymerization (RDRP) enables us to synthesize cationic diblock glycopolymers with controlled structure and molecular weight. Among various types of RDRP, reversible addition-fragmentation chain transfer (RAFT) polymerization was employed to synthesize glycopolymers, because of the compatibility with various types monomer with amine group, and aqueous solution. Two types of carbohydrate moieties (glucose and trehalose) were utilized for the synthesis of macroCTA, i.e. poly(2-deoxy-2-methacrylamido glucopyranose) (PMAG) and

poly(methacrylamidotrehalose) (PMAT). The amine containing monomers were incorporated to yield cationic diblock glycopolymers, including PMAG-b-PDMAPMA series,[6] P(MAG-b-methacrylate) series,[7] and PMAT-b-PAEMA series.[8] The obtained glycopolymers were characterized using SEC equipped with SLS detectors. Narrow dispersity was achieved for all the polymers synthesized via RAFT polymerization.

The glycopolymers exhibited the ability to bind nucleic acid at low N/P ratios and form polyplexes. Both PMAG and PMAT block were found to enhance the colloidal stability of polyplexes in physiological salt solutions. Additionally, PMAT block containing glycopolymers exhibited remarkable ability to serve as cryo- or lyo-protectants for the siRNA polyplexes. TEM imaging and DLS revealed that the size and morphology of the polyplexes composed of PMAT-b-PAEMA were not altered by the lyophilization and reconstitution process, while PEG block copolymers were unable to protect the polyplexes. The in situ morphology of the polyplexes composed of PMAG-b-PDMAPMA in aqueous solution was revealed to be relatively irregular “spherical” shape via cryoTEM imaging.

Tertiary amine containing glycopolymers were systematically examined for its pDNA delivery efficiency. The internalization profile, transgene expression efficiency and cytotoxicity of the polyplexes composed of PMAG-b-PDMAPMA or PMAG-b-PAEMA exhibited apparent dependency upon the cell types and polymeric structures (amine type and block length) during in vitro transfection experiments. Overall, PMAG-b-PAEMA showed higher transfection efficiency than PMAG-b-PDMAPMA. Additionally, glycopolymers with a longer PDMAPMA block length appeared to be less

efficient gene delivery vehicles with higher cytotoxicity. The length of the PMAG block did not show a significant impact on the pDNA delivery in the current study. Glycopolymer polyplexes exhibited much higher transfection efficiency in HepG2 cells than in HeLa cells. This was in part attributed to the ability of HepG2 cells to both internalize more polyplexes and promote higher gene expression, in comparison with the same systems in HeLa cells. Comparing the transfection efficiency between homopolymer, $PAEMA_{58}$, and PMAG-b-PAEMA systems in the two cell types, it was demonstrated that the PMAG block could have interactions with specific receptors on hepatocellular membranes. And such interaction was beneficial for the transfection in HepG2 cells using PMAG containing block copolymers. The addition of galactose molecules in the media lead to reduced the transgene expression level for several glycopolymers in HepG2 cells, potentially indicating that the ASGP receptor could play a role in the pDNA delivery process.

Aside from amine types, we also demonstrate the lipophilicity could enhance transfection efficiency of synthetic vectors. A series of poly(alkylamidoamine) (PAAA) with various length of lipophilic linkers, poly(glutaramidopentaethylenehexamine) (Glut4), poly(adipamidopentaethylenetetramine) (A4), poly(pimelamidopentaethylenetetramine) (Pim4), and poly(suberamidopentaethylenetetramine) (Sub4) were synthesized using step-growth polymerization between diamine monomers and diacid chloride monomers. The obtained polymers could form stable complexes with pDNA in serum reduced medium at about N/P ratio of 5 according to gel electrophoresis. The transfection and toxicity profiles of

the PAAA both were examined in multiple cell types, including HDFa, HeLa, HMEC, HUVEC. The cytotoxicity of the polymers were cell-type dependent, but toxicity were increased by transfecting cells at higher N/P ratios in all 4 cell types. According to GFP expression experiment, all the polymers tested exhibited similar transfection efficiency in HeLa and HMEC at most of the N/P ratios, compared to Lipofectamine 2000. Interestingly, the transfection efficiency of all the polymers were significantly higher than that of Lipofectamine 2000 in HDFa and HUVEC cells. It was revealed that, in HeLa cells, increasing the methylene linker length resulted in higher transfection efficiency, but also caused higher percentage of cell death.

In summary, the glycopolymers were able to enhance the colloidal stability of polyplexes in physiological salt condition, and exhibited unique features associated with carbohydrate types. Additionally, tertiary amine was demonstrated to not be an ideal cationic group for plasmid DNA delivery owing to their toxicity and insufficient transfection ability. Lastly, lipophilicity could be utilized to enhance the interaction between polyplexes and cellular membrane, hence facilitate the transfection process.

## 6.2 Reference

1. Ahmed, M.; Narain, R. *Prog Polym Sci* **2013,** *38*, 767-790.

2. Chu, D. S. H.; Schellinger, J. G.; Shi, J.; Convertine, A. J.; Stayton, P. S.; Pun, S. H. *Acc. Chem. Res.* **2012,** *45*, 1089-1099.

3. Xu, F. J.; Yang, W. T. *Prog Polym Sci* **2011,** *36*, 1099-1131.

4. Carver, L. A.; Schnitzer, J. E. *Nat Rev Cancer* **2003,** *3*, 571-581.

5. McLendon, P. M.; Fichter, K. M.; Reineke, T. M. *Mol. Pharm.* **2010,** *7*, 738-750.

6. Wu, Y.; Wang, M.; Sprouse, D.; Smith, A. E.; Reineke, T. M. *Biomacromolecules* **2014,** *15*, 1716–1726.

7. Li, H.; Cortez, M. A.; Phillips, H. R.; Wu, Y.; Reineke, T. M. *ACS Macro Lett.* **2013,** *2*, 230-235.

8. Sizovs, A.; Xue, L.; Tolstyka, Z. P.; Ingle, N. P.; Wu, Y.; Cortez, M.; Reineke, T. M. *J. Am. Chem. Soc.* **2013,** *135*, 15417-15424.

# Bibliography

Ahmed, M.; Bhuchar, N.; Ishihara, K.; Narain, R. *Bioconjugate Chem.* **2011,** *22*, 1228-1238.

Ahmed, M.; Jawanda, M.; Ishihara, K.; Narain, R. *Biomaterials* **2012,** *33*, 7858-7870.

Ahmed, M.; Narain, R. *Biomaterials* **2011,** *32*, 5279-5290.

Ahmed, M.; Narain, R. *Biomaterials* **2012,** *33*, 3990-4001.

Ahmed, M.; Narain, R. *Prog Polym Sci* **2013,** *38*, 767-790.

Ahn, C. H.; Chae, S. Y.; Bae, Y. H.; Kim, S. W. *J Control Release* **2002,** *80*, 273-282.

Alexandra, M.-B.; Orietta, L.; Vanesa, B.; Manuel, S.-C.; Marta, F.-G. *J. Polym. Sci., Part A: Polym. Chem.* **2013,** *51*, 1337-1347.

Alfredsson, V. *Curr Opin Colloid Interface Sci* **2005,** *10*, 269-273.

Amoozgar, Z.; Yeo, Y. *Wiley Interdiscip Rev Nanomed Nanobiotechnol* **2012,** *4*, 219-233.

Anderson, K.; Sizovs, A.; Cortez, M.; Waldron, C.; Haddleton, D. M.; Reineke, T. M. *Biomacromolecules* **2012,** *13*, 2229-2239.

Anderson, W. F. *Nature* **1998,** *392*, 25.

Bansal, R.; Tripathi, S. K.; Gupta, K. C.; Kumar, P. *J Mater Chem* **2012,** *22*, 25427-25436.

Barbucci, R.; Casolaro, M.; Ferruti, P.; Barone, V.; Lelj, F.; Oliva, L. *Macromolecules* **1981,** *14*, 1203-1209.

Barth, H. G.; Jackson, C.; Boyes, B. E. *Anal. Chem.* **1994,** *66*, 595R-620R.

Barz, M.; Luxenhofer, R.; Zentel, R.; Vicent, M. J. *Polym. Chem.* **2011,** *2*, 1900-1918.

Behr, J.-P. *Chimia* **1997,** *51*, 34-36.

Benaroudj, N.; Lee, D. H.; Goldberg, A. L. *J. Biol. Chem.* **2001,** *276*, 24261-24267.

Bloomfield, V. A. *Biopolymers* **1997,** *44*, 269-282.

Bouard, D.; Alazard-Dany, N.; Cosset, F. L. *Br. J. Pharmacol.* **2009,** *157*, 153-165.

Boussif, O.; Lezoualc'h, F.; Zanta, M. A.; Mergny, M. D.; Scherman, D.; Demeneix, B.; Behr, J. P. *Proceedings of the National Academy of Sciences of the United States of America* **1995,** *92*, 7297-7301.

Boussif, O.; Lezoualch, F.; Zanta, M. A.; Mergny, M. D.; Scherman, D.; Demeneix, B.; Behr, J. P. *P Natl Acad Sci USA* **1995,** *92*, 7297-7301.

Bowes, A.; McLeary, J. B.; Sanderson, R. D. *J. Polym. Sci. Polym. Chem.* **2007,** *45*, 588-604.

Braunecker, W. A.; Matyjaszewski, K. *Prog. Polym. Sci.* **2007,** *32*, 93-146.

Brissault, B.; Kichler, A.; Guis, C.; Leborgne, C.; Danos, O.; Cheradame, H. *Bioconjugate Chem.* **2003,** *14*, 581-587.

Brus, C.; Petersen, H.; Aigner, A.; Czubayko, F.; Kissel, T. *Bioconjugate Chem* **2004,** *15*, 677-684.

Buckwalter, D. J.; Sizovs, A.; Ingle, N. P.; Reineke, T. M. *ACS Macro Lett.* **2012,** *1*, 609-613.

Cao, Y.; Zhu, X. X. *Can. J. Chem.* **2007,** *85*, 407-411.

Carver, L. A.; Schnitzer, J. E. *Nat Rev Cancer* **2003,** *3*, 571-581.

Cherng, J.-Y.; van de Wetering, P.; Talsma, H.; Crommelin, D. A.; Hennink, W. *Pharm. Res.* **1996,** *13*, 1038-1042.

Chiefari, J.; Chong, Y. K.; Ercole, F.; Krstina, J.; Jeffery, J.; Le, T. P. T.; Mayadunne, R. T. A.; Meijs, G. F.; Moad, C. L.; Moad, G.; Rizzardo, E.; Thang, S. H. *Macromolecules* **1998,** *31*, 5559-5562.

Chou, S.-T.; Leng, Q.; Mixson, A. J. *Drugs Future* **2012,** *37*, 183-196.

Chu, D. S. H.; Schellinger, J. G.; Shi, J.; Convertine, A. J.; Stayton, P. S.; Pun, S. H. *Acc. Chem. Res.* **2012,** *45*, 1089-1099.

Cong, L.; Ran, F. A.; Cox, D.; Lin, S.; Barretto, R.; Habib, N.; Hsu, P. D.; Wu, X.; Jiang, W.; Marraffini, L. A.; Zhang, F. *Science* **2013,** *339*, 819-823.

Convertine, A. J.; Benoit, D. S. W.; Duvall, C. L.; Hoffman, A. S.; Stayton, P. S. *J. Controlled Release* **2009,** *133*, 221-229.

Convertine, A. J.; Diab, C.; Prieve, M.; Paschal, A.; Hoffman, A. S.; Johnson, P. H.; Stayton, P. S. *Biomacromolecules* **2010**, null-null.

Convertine, A. J.; Lokitz, B. S.; Vasileva, Y.; Myrick, L. J.; Scales, C. W.; Lowe, A. B.; McCormick, C. L. *Macromolecules* **2006,** *39*, 1724-1730.

Crowe, J. H.; Carpenter, J. F.; Crowe, L. M. *Annu. Rev. Physiol.* **1998,** *60*, 73-103.

Cui, H.; Hodgdon, T. K.; Kaler, E. W.; Abezgauz, L.; Danino, D.; Lubovsky, M.; Talmon, Y.; Pochan, D. J. *Soft Matter* **2007,** *3*, 945-955.

Dalby, B.; Cates, S.; Harris, A.; Ohki, E. C.; Tilkins, M. L.; Price, P. J.; Ciccarone, V. C. *Methods* **2004,** *33*, 95-103.

Danino, D. *Curr Opin Colloid Interface Sci* **2012,** *17*, 316-329.

Danino, D.; Talmon, Y.; Zana, R. *Colloids Surf A Physicochem Eng Asp* **2000,** *169*, 67-73.

Davis, K. A.; Matyjaszewski, K., Statistical, gradient, block, and graft copolymers by controlled/living radical polymerizations. In *Statistical, Gradient, Block and Graft Copolymers by Controlled/Living Radical Polymerizations*, 2002; Vol. 159, pp 1-169.

Davis, M. E. *Mol. Pharm.* **2009,** *6*, 659-668.

Davis, M. E.; Pun, S. H.; Bellocq, N. C.; Reineke, T. M.; Popielarski, S. R.; Mishra, S.; Heidel, J. D. *Curr. Med. Chem.* **2004,** *11*, 179-197.

Davis, M. E.; Zuckerman, J. E.; Choi, C. H. J.; Seligson, D.; Tolcher, A.; Alabi, C. A.; Yen, Y.; Heidel, J. D.; Ribas, A. *Nature* **2010,** *464*, 1067-1070.

de Vries, R.; Cohen Stuart, M. *Curr Opin Colloid Interface Sci* **2006,** *11*, 295-301.

Deng, D.; Yan, C.; Pan, X.; Mahfouz, M.; Wang, J.; Zhu, J.-K.; Shi, Y.; Yan, N. *Science* **2012,** *335*, 720-723.

Deng, Z.; Ahmed, M.; Narain, R. *J Polym Sci A Polym Chem* **2009,** *47*, 614-627.

Du, H.; Chandaroy, P.; Hui, S. W. *Biochim. Biophys. Acta, Biomembr.* **1997,** *1326*, 236-248.

Dufresne, M.-H.; Leroux, J.-C. *Pharm. Res.* **2004,** *21*, 160-169.

Favier, A.; Charreyre, M. T. *Macromol. Rapid Commun.* **2006,** *27*, 653-692.

Fichter, K. M.; Ingle, N. P.; McLendon, P. M.; Reineke, T. M. *ACS Nano* **2012,** *7*, 347-364.

Fire, A.; Xu, S.; Montgomery, M. K.; Kostas, S. A.; Driver, S. E.; Mello, C. C. *Nature* **1998,** *391*, 806-811.

Fischer, D.; Li, Y. X.; Ahlemeyer, B.; Krieglstein, J.; Kissel, T. *Biomaterials* **2003,** *24*, 1121-1131.

Fortune, J. A.; Novobrantseva, T. I.; Klibanov, A. M. *J Drug Deliv* **2011,** *2011*, 6.

Franchini, J.; Ranucci, E.; Ferruti, P.; Rossi, M.; Cavalli, R. *Biomacromolecules* **2006,** *7*, 1215-1222.

Friedmann, T. *Nat. Genet.* **1992,** *2*, 93-8.

Fukuma, T.; Wu, G. Y.; Wu, C. H. *Gene Ther. Regul.* **2000,** *1*, 79-93.

Gaj, T.; Gersbach, C. A.; Barbas Iii, C. F. *Trends Biotechnol.* **2013,** *31*, 397-405.

Ge, Z.; Cai, Y.; Yin, J.; Zhu, Z.; Rao, J.; Liu, S. *Langmuir* **2007,** *23*, 1114-1122.

Germershaus, O.; Mao, S. R.; Sitterberg, J.; Bakowsky, U.; Kissel, T. *J Control Release* **2008,** *125*, 145-154.

Godbey, W. T.; Wu, K. K.; Mikos, A. G. *J. Biomed. Mater. Res.* **1999,** *45*, 268-275.

Godbey, W. T.; Wu, K. K.; Mikos, A. G. *Biomaterials* **2001,** *22*, 471-480.

Gomes-da-Silva, L. C.; Fonseca, N. A.; Moura, V.; Pedroso de Lima, M. C.; Simões, S.; Moreira, J. N. *Acc. Chem. Res.* **2012,** *45*, 1163-1171.

Gonzalez, H.; Hwang, S. J.; Davis, M. E. *Bioconjugate Chem.* **1999,** *10*, 1068-1074.

Grandinetti, G.; Smith, A. E.; Reineke, T. M. *Mol. Pharm.* **2011,** *9*, 523-538.

Guo, J.; Gaj, T.; Barbas Iii, C. F. *J. Mol. Biol.* **2010,** *400*, 96-107.

Guo, X.; Huang, L. *Acc. Chem. Res.* **2012,** *45*, 971-979.

Hagen, S.; Hofrichter, J.; Eaton, W. *Science* **1995,** *269*, 959-962.

Hansma, H. G.; Golan, R.; Hsieh, W.; Lollo, C. P.; Mullen-Ley, P.; Kwoh, D. *Nucleic Acids Res.* **1998,** *26*, 2481-2487.

Hawker, C. J.; Bosman, A. W.; Harth, E. *Chem. Rev. (Washington, DC, U. S.)* **2001,** *101*, 3661-3688.

He, L.; Read, E. S.; Armes, S. P.; Adams, D. J. *Macromolecules* **2007,** *40*, 4429-4438.

Hemp, S. T.; Smith, A. E.; Bryson, J. M.; Allen, M. H.; Long, T. E. *Biomacromolecules* **2012,** *13*, 2439-2445.

Hoang, B.; Reilly, R. M.; Allen, C. *Biomacromolecules* **2011,** *13*, 455-465.

Ingle, N. P.; Malone, B.; Reineke, T. M. *Trends Biotechnol.* **2011,** *29*, 443-453.

Ishida, T.; Kiwada, H. *Int. J. Pharm.* **2008,** *354*, 56-62.

Jenkins, A. D.; Jones, R. G.; Moad, G. *Pure Appl. Chem.* **2010,** *82*, 483-491.

Ji, W.; Panus, D.; Palumbo, R. N.; Tang, R.; Wang, C. *Biomacromolecules* **2011,** *12*, 4373-4385.

Jinek, M.; Chylinski, K.; Fonfara, I.; Hauer, M.; Doudna, J. A.; Charpentier, E. *Science* **2012,** *337*, 816-821.

Jones, C. H.; Chen, C.-K.; Ravikrishnan, A.; Rane, S.; Pfeifer, B. A. *Mol. Pharm.* **2013,** *10*, 4082-4098.

Jones, G. D.; Langsjoen, A.; Neumann, S. M. M. C.; Zomlefer, J. *J. Org. Chem.* **1944,** *09*, 125-147.

Kasper, J. C.; Schaffert, D.; Ogris, M.; Wagner, E.; Friess, W. *J Control Release* **2011,** *151*, 246-255.

Kay, M. A. *Nat. Rev. Genet.* **2011,** *12*, 316-328.

Khalil, I. A.; Kogure, K.; Akita, H.; Harashima, H. *Pharmacol. Rev.* **2006,** *58*, 32-45.

Kiang, T.; Wen, H.; Lim, H. W.; Leong, K. W. *Biomaterials* **2004,** *25*, 5293-5301.

Kiely, D. E.; Chen, L.; Lin, T. H. *J Polym Sci Pol Chem* **2000,** *38*, 594-603.

Kim, Y. H.; Gihm, S. H.; Park, C. R.; Lee, K. Y.; Kim, T. W.; Kwon, I. C.; Chung, H.; Jeong, S. Y. *Bioconjugate Chem.* **2001,** *12*, 932-938.

Kirkland-York, S.; Zhang, Y.; Smith, A. E.; York, A. W.; Huang, F.; McCormick, C. L. *Biomacromolecules* **2010,** *11*, 1052-1059.

Knop, K.; Hoogenboom, R.; Fischer, D.; Schubert, U. S. *Angew. Chem., Int. Ed. Engl.* **2010,** *49*, 6288-6308.

Kohl, H.; Reimer, L., Wave Optics of Electrons. In *Transmission Electron Microscopy*, Springer New York: 2008; Vol. 36, pp 43-74.

Kopeček, J.; Kopečková, P. *Adv Drug Deliver Rev* **2010,** *62*, 122-149.

Kuchelmeister, H. Y.; Karczewski, S.; Gutschmidt, A.; Knauer, S.; Schmuck, C. *Angew. Chem. Int. Ed. Engl.* **2013,** *52*, 14016-14020.

Kulkarni, R. P.; Mishra, S.; Fraser, S. E.; Davis, M. E. *Bioconjugate Chem* **2005,** *16*, 986-994.

Lai, J. T.; Filla, D.; Shea, R. *Macromolecules* **2002,** *35*, 6754-6756.

Lee, Y.; Mo, H.; Koo, H.; Park, J. Y.; Cho, M. Y.; Jin, G. W.; Park, J. S. *Bioconjugate Chem* **2007,** *18*, 13-18.

Levine, R. M.; Pearce, T. R.; Adil, M.; Kokkoli, E. *Langmuir* **2013,** *29*, 9208-9215.

Li, H.; Cortez, M. A.; Phillips, H. R.; Wu, Y.; Reineke, T. M. *ACS Macro Lett.* **2013,** *2*, 230-235.

Li, Z.; Yin, H.; Zhang, Z.; Liu, K. L.; Li, J. *Biomacromolecules* **2012,** *13*, 3162-3172.

Liu, X.-Q.; Du, J.-Z.; Zhang, C.-P.; Zhao, F.; Yang, X.-Z.; Wang, J. *Int J Pharm* **2010,** *392*, 118-126.

Liu, Y.; Reineke, T. M. *J. Am. Chem. Soc.* **2005,** *127*, 3004-3015.

Liu, Y.; Reineke, T. M. *Bioconjug. Chem.* **2005,** *17*, 101-108.

Liu, Y.; Reineke, T. M. *Biomacromolecules* **2010,** *11*, 316-325.

Liu, Y.; Wenning, L.; Lynch, M.; Reineke, T. M. *J. Am. Chem. Soc.* **2004,** *126*, 7422-7423.

Liu, Y. M.; Reineke, T. M. *Bioconjug. Chem.* **2007,** *18*, 19-30.

Lo, W.-L.; Chien, Y.; Chiou, G.-Y.; Tseng, L.-M.; Hsu, H.-S.; Chang, Y.-L.; Lu, K.-H.; Chien, C.-S.; Wang, M.-L.; Chen, Y.-W.; Huang, P.-I.; Hu, F.-W.; Yu, C.-C.; Chu, P.-Y.; Chiou, S.-H. *Biomaterials* **2012,** *33*, 3693-3709.

Loretz, B.; Thaler, M.; Bernkop-Schnurch, A. *Bioconjugate Chem.* **2007,** *18*, 1028-1035.

Low, P. S.; Henne, W. A.; Doorneweerd, D. D. *Acc. Chem. Res.* **2007,** *41*, 120-129.

Luo, X.; Feng, M.; Pan, S.; Wen, Y.; Zhang, W.; Wu, C. *J. Mater. Sci.: Mater. Med.* **2012,** *23*, 1685-1695.

Lutz, J. F.; Kirci, B.; Matyjaszewski, K. *Macromolecules* **2003,** *36*, 3136-3145.

MacLaughlin, F. C.; Mumper, R. J.; Wang, J.; Tagliaferri, J. M.; Gill, I.; Hinchcliffe, M.; Rolland, A. P. *J Control Release* **1998,** *56*, 259-272.

Maeda, H.; Bharate, G. Y.; Daruwalla, J. *Eur J Pharm Biopharm* **2009,** *71*, 409-419.

Mahon, K. P.; Love, K. T.; Whitehead, K. A.; Qin, J.; Akinc, A.; Leshchiner, E.; Leshchiner, I.; Langer, R.; Anderson, D. G. *Bioconjug. Chem.* **2010,** *21*, 1448-1454.

Mali, P.; Yang, L.; Esvelt, K. M.; Aach, J.; Guell, M.; DiCarlo, J. E.; Norville, J. E.; Church, G. M. *Science* **2013,** *339*, 823-826.

Mancini, R. J.; Lee, J.; Maynard, H. D. *J. Am. Chem. Soc.* **2012,** *134*, 8474-8479.

Mao, S. R.; Neu, M.; Germershaus, O.; Merkel, O.; Sitterberg, J.; Bakowsky, U.; Kissel, T. *Bioconjugate Chem* **2006,** *17*, 1209-1218.

Matyjaszewski, K. *Macromolecules* **2012,** *45*, 4015-4039.

Matyjaszewski, K.; Xia, J. *Chem. Rev.* **2001,** *101*, 2921-2990.

Matyjaszewski, K.; Xia, J. *Chem. Rev.* **2001,** *101*, 2921-2990.

McCormick, C. L.; Lowe, A. B. *Acc. Chem. Res.* **2004,** *37*, 312-325.

McLendon, P. M.; Buckwalter, D. J.; Davis, E. M.; Reineke, T. M. *Mol. Pharm.* **2010,** *7*, 1757-1768.

McLendon, P. M.; Fichter, K. M.; Reineke, T. M. *Mol. Pharm.* **2010,** *7*, 738-750.

Merdan, T.; Kunath, K.; Petersen, H.; Bakowsky, U.; Voigt, K. H.; Kopecek, J.; Kissel, T. *Bioconjugate Chem.* **2005,** *16*, 785-792.

Merdan, T.; Kunath, K.; Petersen, H.; Bakowsky, U.; Voigt, K. H.; Kopecek, J.; Kissel, T. *Bioconjugate Chem* **2005,** *16*, 785-792.

Mintzer, M. A.; Simanek, E. E. *Chem. Rev.* **2009,** *109*, 259-302.

Mitsukami, Y.; Donovan, M. S.; Lowe, A. B.; McCormick, C. L. *Macromolecules* **2001,** *34*, 2248-2256.

Moad, G.; Rizzardo, E.; Thang, S. H. *Aust. J. Chem.* **2005,** *58*, 379-410.

Moad, G.; Rizzardo, E.; Thang, S. H. *Aust. J. Chem.* **2006,** *59*, 669-692.

Mukherjee, S.; Ghosh, R. N.; Maxfield, F. R. *Physiol. Rev.* **1997,** *77*, 759-803.

Mussolino, C.; Cathomen, T. *Curr. Opin. Biotechnol.* **2012,** *23*, 644-650.

Nakai, K.; Nishiuchi, M.; Inoue, M.; Ishihara, K.; Sanada, Y.; Sakurai, K.; Yusa, S.-i. *Langmuir* **2013,** *29*, 9651–9661.

Naldini, L. *Nat Rev Genet* **2011,** *12*, 301-315.

Neu, M.; Fischer, D.; Kissel, T. *J Gene Med* **2005,** *7*, 992-1009.

Nie, C.; Liu, C.; Chen, G.; Dai, J.; Li, H.; Shuai, X. *J. Biomater. Appl.* **2011,** *26*, 255-275.

Nielsen, P. E., In DNA-Protein Interaction, Principles and Protocols. In Moss, T.; Leblanc, B., Eds. Springer: New York, 2009; Vol. 543, pp 87-96.

O'Rorke, S.; Keeney, M.; Pandit, A. *Prog Polym Sci* **2010,** *35*, 441-458.

Oba, M.; Miyata, K.; Osada, K.; Christie, R. J.; Sanjoh, M.; Li, W.; Fukushima, S.; Ishii, T.; Kano, M. R.; Nishiyama, N.; Koyama, H.; Kataoka, K. *Biomaterials* **2011,** *32*, 652-663.

Ogata, N.; Hosoda, Y. *J Polym Sci A Polym Chem* **1975,** *13*, 1793-1801.

Ogata, N.; Sanui, K.; Hosoda, Y.; Nakamura, H. *J Polym Sci A Polym Chem* **1976,** *14*, 783-792.

Orietta, L.; Alexandra, M.-B.; Vanesa, B.; Manuel, S.-C.; Marta, F.-G. *J. Polym. Sci., Part A: Polym. Chem.* **2011,** *49*, 2627-2635.

Pack, D. W.; Hoffman, A. S.; Pun, S.; Stayton, P. S. *Nat Rev Drug Discov* **2005,** *4*, 581-593.

Palermo, E. F.; Lee, D.-K.; Ramamoorthy, A.; Kuroda, K. *J. Phys. Chem. B* **2011,** *115*, 366-375.

Pathak, A.; Vyas, S. P.; Gupta, K. C. *Int. J. Nanomed.* **2008,** *3*, 31-49.

Pattanayak, V.; Ramirez, C. L.; Joung, J. K.; Liu, D. R. *Nat Meth* **2011,** *8*, 765-770.

Pearson, S.; Allen, N.; Stenzel, M. H. *J. Polym. Sci., Part A: Polym. Chem.* **2009,** *47*, 1706-1723.

Piest, M.; Engbersen, J. F. J. *J. Controlled Release* **2010,** *148*, 83-90.

Popielarski, S. R.; Mishra, S.; Davis, M. E. *Bioconjugate Chem* **2003,** *14*, 672-678.

Prevette, L. E.; Kodger, T. E.; Reineke, T. M.; Lynch, M. L. *Langmuir* **2007,** *23*, 9773-9784.

Prevette, L. E.; Lynch, M. L.; Kizjakina, K.; Reineke, T. M. *Langmuir* **2008,** *24*, 8090-8101.

Pun, S. H.; Davis, M. E. *Bioconjugate Chem.* **2002,** *13*, 630-639.

Pun, S. H.; Davis, M. E. *Bioconjugate Chem* **2002,** *13*, 630-639.

Ran, F. A.; Hsu, P. D.; Lin, C.-Y.; Gootenberg, J. S.; Konermann, S.; Trevino, A. E.; Scott, D. A.; Inoue, A.; Matoba, S.; Zhang, Y.; Zhang, F. *Cell* **2013,** *154*, 1380-1389.

Rehman, Z. u.; Zuhorn, I. S.; Hoekstra, D. *J. Controlled Release* **2013,** *166*, 46-56.

Reineke, T. M. *J Polym Sci A Polym Chem* **2006,** *44*, 6895-6908.

Reineke, T. M.; Davis, M. E. *Bioconjugate Chem.* **2003,** *14*, 247-254.

Reineke, T. M.; Davis, M. E. *Bioconjugate Chem* **2003,** *14*, 255-261.

Reineke, T. M.; Grinstaff, M. W. *MRS Bull* **2005,** *30*, 635-639.

Rejman, J.; Bragonzi, A.; Conese, M. *Mol. Ther.* **2005,** *12*, 468-474.

Rigopoulou, E. I.; Roggenbuck, D.; Smyk, D. S.; Liaskos, C.; Mytilinaiou, M. G.; Feist, E.; Conrad, K.; Bogdanos, D. P. *Autoimmun. Rev.* **2012,** *12*, 260-269.

Rivera, M. R.; Rodriguez-Hernandez, A. A.; Hernandez, N.; Castillo, P.; Saldivar, E.; Rios, L. *Ind. Eng. Chem. Res.* **2005,** *44*, 2792-2801.

Robbins, P. D.; Tahara, H.; Ghivizzani, S. C. *Trends Biotechnol.* **1998,** *16*, 35-40.

Sachidanandam, R.; Weissman, D.; Schmidt, S. C.; Kakoi, J. M.; Stein, L. D.; Marth, G.; Sherry, S.; Mullikin, J. C.; Mortimore, B. J.; Willey, D. L.; Hunt, S. E.; Cole, C. G.; Coggill, P. C.; Rice, C. M.; Ning, Z.; Rogers, J.; Bentley, D. R.; Kwok, P.-Y.; Mardis, E. R.; Yeh, R. T.; Schutlz, B.; Cook, L.; Davenport, R.; Dante, M.; Fulton, L.; Hillier, L.; Waterston, R. H.; McPherson, J. D.; Gilman, B.; Schaffner, S.; Van, E. W. J.; Reich, D.; Higgins, J.; Daly, M. J.; Blumenstiel, B.; Baldwin, J.; Stange-Thomann, N.; Zody, M. C.; Linton, L.; Lander, E. S.; Altshuler, D. *Nature* **2001,** *409*, 928-933.

Sander, J. D.; Joung, J. K. *Nat Biotech* **2014,** *32*, 347-355.

Sato, T.; Ishii, T.; Okahata, Y. *Biomaterials* **2001,** *22*, 2075-2080.

Scales, C. W.; Huang, F. Q.; Li, N.; Vasilieva, Y. A.; Ray, J.; Convertine, A. J.; McCormick, C. L. *Macromolecules* **2006,** *39*, 6871-6881.

Schilli, C. M.; Zhang, M. F.; Rizzardo, E.; Thang, S. H.; Chong, Y. K.; Edwards, K.; Karlsson, G.; Muller, A. H. E. *Macromolecules* **2004,** *37*, 7861-7866.

Shimizu, Y.; Şöllü, C.; Meckler, J. F.; Adriaenssens, A.; Zykovich, A.; Cathomen, T.; Segal, D. J. *Biochemistry* **2011,** *50*, 5033-5041.

Sizovs, A.; Xue, L.; Tolstyka, Z. P.; Ingle, N. P.; Wu, Y.; Cortez, M.; Reineke, T. M. *J. Am. Chem. Soc.* **2013,** *135*, 15417-15424.

Smith, A. E.; Sizovs, A.; Grandinetti, G.; Xue, L.; Reineke, T. M. *Biomacromolecules* **2011,** *12*, 3015-3022.

Smith, D.; Holley, A. C.; McCormick, C. L. *Polym. Chem.* **2011,** *2*, 1428-1441.

Sonawane, N. D.; Szoka, F. C.; Verkman, A. S. *J. Biol. Chem.* **2003,** *278*, 44826-44831.

Song, E.-H.; Manganiello, M.; Chow, Y.-H.; Ghosn, B.; Convertine, A.; Stayton, P.; Schnapp, L.; Ratner, D. *Biomaterials* **2012,** *33*, 6889-6897.

Srinivasachari, S.; Liu, Y.; Zhang, G.; Prevette, L.; Reineke, T. M. *J. Am. Chem. Soc.* **2006,** *128*, 8176-8184.

Srinivasachari, S.; Reineke, T. M. *Biomaterials* **2009,** *30*, 928-938.

Stenzel-Rosenbaum, M.; Davis, T. P.; Chen, V.; Fane, A. G. *J. Polym. Sci. Polym. Chem.* **2001,** *39*, 2777-2783.

Suh, J.; Paik, H. J.; Hwang, B. K. *Bioorg Chem* **1994,** *22*, 318-327.

Sun, N.; Zhao, H. *Biotechnol. Bioeng.* **2013,** *110*, 1811-1821.

Sun, S.; Wang, M.; Knupp, S. A.; Soto-Feliciano, Y.; Hu, X.; Kaplan, D. L.; Langer, R.; Anderson, D. G.; Xu, Q. *Bioconjug. Chem.* **2012,** *23*, 135-140.

Sung, S.-J.; Min, S. H.; Cho, K. Y.; Lee, S.; Min, Y.-J.; Yeom, Y. I.; Park, J.-K. *Biol. Pharm. Bull.* **2003,** *26*, 492-500.

Sunshine, J. C.; Sunshine, S. B.; Bhutto, I.; Handa, J. T.; Green, J. J. *PLoS ONE* **2012,** *7*, e37543.

Szwarc, M.; Levy, M.; Milkovich, R. *J. Am. Chem. Soc.* **1956,** *78*, 2656-2657.

Tabernero, J.; Shapiro, G. I.; LoRusso, P. M.; Cervantes, A.; Schwartz, G. K.; Weiss, G. J.; Paz-Ares, L.; Cho, D. C.; Infante, J. R.; Alsina, M.; Gounder, M. M.; Falzone, R.; Harrop, J.; White, A. C. S.; Toudjarska, I.; Bumcrot, D.; Meyers, R. E.; Hinkle, G.; Svrzikapa, N.; Hutabarat, R. M.; Clausen, V. A.; Cehelsky, J.; Nochur, S. V.; Gamba-Vitalo, C.; Vaishnaw, A. K.; Sah, D. W. Y.; Gollob, J. A.; Burris, H. A. *Cancer Discov* **2013,** *3*, 406-417.

Tang, G. *Trends Biochem. Sci.* **2005,** *30*, 106-114.

Tang, R.; Palumbo, R. N.; Nagarajan, L.; Krogstad, E.; Wang, C. *J Control Release* **2010,** *142*, 229-237.

Teramoto, N.; Sachinvala, N.; Shibata, M. *Molecules* **2008,** *13*, 1773-1816.

Ting, S. R. S.; Chen, G.; Stenzel, M. H. *Polym. Chem.* **2010,** *1*, 1392-1412.

Tockary, T. A.; Osada, K.; Chen, Q.; Machitani, K.; Dirisala, A.; Uchida, S.; Nomoto, T.; Toh, K.; Matsumoto, Y.; Itaka, K.; Nitta, K.; Nagayama, K.; Kataoka, K. *Macromolecules* **2013,** *46*, 6585-6592.

Tseng, W.-C.; Tang, C.-H.; Fang, T.-Y.; Su, L.-Y. *Biotechnol. Prog.* **2007,** *23*, 1297-1304.

Tsujii, Y.; Ejaz, M.; Sato, K.; Goto, A.; Fukuda, T. *Macromolecules* **2001,** *34*, 8872-8878.

Urnov, F. D.; Rebar, E. J.; Holmes, M. C.; Zhang, H. S.; Gregory, P. D. *Nat Rev Genet* **2010,** *11*, 636-646.

Valencia-Serna, J.; Gul-Uludağ, H.; Mahdipoor, P.; Jiang, X.; Uludağ, H. *J. Controlled Release* **2013,** *172*, 495-503.

van de Wetering, P.; Cherng, J.-Y.; Talsma, H.; Hennink, W. E. *J. Controlled Release* **1997,** *49*, 59-69.

van de Wetering, P.; Moret, E. E.; Schuurmans-Nieuwenbroek, N. M. E.; van Steenbergen, M. J.; Hennink, W. E. *Bioconjugate Chem.* **1999,** *10*, 589-597.

van de Wetering, P.; Schuurmans-Nieuwenbroek, N. M. E.; Hennink, W. E.; Storm, G. *J Gene Med* **1999,** *1*, 156-165.

van de Wetering, P.; Zuidam, N. J.; van Steenbergen, M. J.; van der Houwen, O. A. G. J.; Underberg, W. J. M.; Hennink, W. E. *Macromolecules* **1998,** *31*, 8063-8068.

Vasilieva, Y. A.; Scales, C. W.; Thomas, D. B.; Ezell, R. G.; Lowe, A. B.; Ayres, N.; McCormick, C. L. *J. Polym. Sci. Polym. Chem.* **2005,** *43*, 3141-3152.

Vasilieva, Y. A.; Thomas, D. B.; Scales, C. W.; McCormick, C. L. *Macromolecules* **2004,** *37*, 2728-2737.

Vasilieva, Y. A.; Thomas, D. B.; Scales, C. W.; McCormick, C. L. *Macromolecules* **2004,** *37*, 2728-2737.

Velluto, D.; Thomas, S. N.; Simeoni, E.; Swartz, M. A.; Hubbell, J. A. *Biomaterials* **2011,** *32*, 9839-9847.

Venkataraman, S.; Ong, W. L.; Ong, Z. Y.; Joachim Loo, S. C.; Rachel Ee, P. L.; Yang, Y. Y. *Biomaterials* **2011,** *32*, 2369-2378.

Viswanathan, A.; Kiely, D. E. *J Carbohydr Chem* **2003,** *22*, 903 - 918.

von Gersdorff, K.; Sanders, N. N.; Vandenbroucke, R.; De Smedt, S. C.; Wagner, E.; Ogris, M. *Mol. Ther.* **2006,** *14*, 745-753.

von Harpe, A.; Petersen, H.; Li, Y.; Kissel, T. *J Control Release* **2000,** *69*, 309-322.

Wada, M.; Miyazawa, Y.; Miura, Y. *Polym Chem* **2011,** *2*, 1822-1829.

Wang, H.-Y.; Chen, J.-X.; Sun, Y.-X.; Deng, J.-Z.; Li, C.; Zhang, X.-Z.; Zhuo, R.-X. *J. Controlled Release* **2011,** *155*, 26-33.

Wang, J.; Lu, Z.; Wientjes, M. G.; Au, J. L. S. *AAPS J.* **2010,** *12*, 492-503.

Wang, R.; Lowe, A. B. *J. Polym. Sci. Polym. Chem.* **2007,** *45*, 2468-2483.

Wang, T.; Upponi, J. R.; Torchilin, V. P. *Int. J. Pharm. (Amsterdam, Neth.)* **2012,** *427*, 3-20.

Wang, Y.; Hong, C.-Y.; Pan, C.-Y. *Biomacromolecules* **2013,** *14*, 1444-1451.

Watson, J. D.; Cook-Deegan, R. M. *FASEB J.* **1991,** *5*, 8-11.

Watson, J. D.; Crick, F. H. C. *Nature* **1953,** *171*, 737-738.

Wightman, L.; Kircheis, R.; Rossler, V.; Carotta, S.; Ruzicka, R.; Kursa, M.; Wagner, E. *J Gene Med* **2001,** *3*, 362-372.

Williams, D. B.; Carter, C. B., *Transmission Electron Microscopy, A Textbook for Materials Science*. Springer: New York, 2009.

Wingler, A.; Fritzius, T.; Aeschbacher, R. A. *Plant Physiol* **2000,** *124*, 105-114.

Won, Y.-Y.; Sharma, R.; Konieczny, S. F. *J. Controlled Release* **2009,** *139*, 88-93.

Wong, K.; Sun, G. B.; Zhang, X. Q.; Dai, H.; Liu, Y.; He, C. B.; Leong, K. W. *Bioconjugate Chem.* **2006,** *17*, 152-158.

Wu, G. Y.; Wu, C. H. *Adv. Drug Delivery Rev.* **1998,** *29*, 243-248.

Wu, S. Y.; Lopez-Berestein, G.; Calin, G. A.; Sood, A. K. *Sci Transl Med* **2014,** *6*, 240ps7.

Wu, Y.; Wang, M.; Sprouse, D.; Smith, A. E.; Reineke, T. M. *Biomacromolecules* **2014,** *15*, 1716–1726.

Xia, W.; Low, P. S. *J. Med. Chem.* **2010,** *53*, 6811-6824.

Xu, F. J.; Yang, W. T. *Prog Polym Sci* **2011,** *36*, 1099-1131.

Xu, X.; Smith, A. E.; Kirkland, S. E.; McCormick, C. L. *Macromolecules* **2008,** *41*, 8429-8435.

Xu, Y.; Takai, M.; Ishihara, K. *Biomaterials* **2009,** *30*, 4930-4938.

Xue, L.; Ingle, N. P.; Reineke, T. M. *Biomacromolecules* **2013,** *14*, 3903-3915.

York, A. W.; Huang, F.; McCormick, C. L. *Polym. Prepr. (Am. Chem. Soc., Div. Polym. Chem.)* **2008,** *49*, 1099-1100.

York, A. W.; Huang, F.; McCormick, C. L. *Biomacromolecules* **2010,** *11*, 505-514.

York, A. W.; Kirkland, S. E.; McCormick, C. L. *Adv. Drug Delivery Rev.* **2008,** *60*, 1018-1036.

York, A. W.; Zhang, Y.; Holley, A. C.; Guo, Y.; Huang, F.; McCormick, C. L. *Biomacromolecules* **2009,** *10*, 936-943.

Zhang, Z.; Vaisocherová, H.; Cheng, G.; Yang, W.; Xue, H.; Jiang, S. *Biomacromolecules* **2008,** *9*, 2686-2692.

Zhu, C.; Zheng, M.; Meng, F.; Mickler, F. M.; Ruthardt, N.; Zhu, X.; Zhong, Z. *Biomacromolecules* **2012**.

Ziebarth, J.; Wang, Y. *Biophysical Journal* **2009,** *97*, 1971-1983.

Ziebarth, J.; Wang, Y. *J. Phys. Chem. B* **2010,** *114*, 6225-6232.